Conifer Chemical and Structural Defenses Against Pests and Pathogens

by

Colleen E. Fortier

A thesis submitted in partial fulfillment of the requirements for the degree of

Doctor of Philosophy

in

Plant Biology

Department of Biological Sciences
University of Alberta

Abstract

Canada's forests are experiencing unprecedented pest and pathogen outbreaks; such instances are expected to increase under predicted climate change scenarios. A host's ability to mount an effective defense response against pest and pathogen antagonists is dependent on recognition of the antagonist leading to the hormonal induction of molecular and biochemical defenses. Hosts that have a shared history with the antagonist are hypothesized to acquire more finely tuned defense strategies relative to naïve hosts. Defense strategies are further influenced by abiotic stresses such as water deficit, and at different stages of host development, both of which are hypothesized to alter host suitability to the antagonist.

The overall aim of my thesis research was to investigate patterns of chemical and structural plant defenses in the interactions of conifer hosts with a suite of insect and fungal antagonists. To do so, I explored host defense responses at the molecular and biochemical level in two systems: 1) the relationship between mountain pine beetle (*Dendroctonus ponderosae*) and its Ophiostomatoid fungal associate, *Grosmannia clavigera,* in two pine species: lodgepole pine (*Pinus contorta* var. *latifolia*), which has a long-shared history with mountain pine beetle, and jack pine (*Pinus banksiana*), a new host and 2) the relationship between white spruce (*Picea glauca*) and the eastern spruce budworm (*Choristoneura fumiferana*).

In my research, I found that lodgepole pine exhibit more subtle defense responses to *G. clavigera* than jack pine, reflective of differences in their co-evolutionary history with *G. clavigera*. Furthermore, water deficit alters the composition rather than the magnitude of host defense responses to *G. clavigera*, and lodgepole pine defense responses are influenced by water deficit to a greater extent than jack pine defense responses. Hormonal signatures of lodgepole pine defense responses reveal that *G. clavigera* does not contribute to overwhelming host

defenses during mountain pine beetle mass attack, but instead plays a role in the nutrient acquisition of developing mountain pine beetle. Lastly, during white spruce bud burst, foliar toughness is a key factor defining the phenological window of opportunity for spruce budworm feeding. My research has shown that lignin deposition is an important contributor to foliar toughness during white spruce needle development, while cuticular wax deposition is not a reliable predictor of toughness in mature white spruce.

Together, these results demonstrate that conifer defense responses are complex and mediated by several factors. My data sheds some light on how these factors influence host suitability to pest and pathogens, important for predicting future spread and promoting effective pest management strategies within the context of a changing climate.

Preface

Chapters two and three of this thesis include analysis of microarray data generated by members of the Cooke Lab. Plant material for these microarrays was collected from an experiment conducted by Adriana Arango-Velez, Miranda Meents, and Charles Copeland. Adriana Arango-Velez, Miranda Meents, Justin Khunkhun, William Peachman, and Bulcha Dolal extracted RNA. Miranda Meents and Adriana Arango-Velez generated the microarray data. The PtGen2 microarray used for these analyses was provided by Dr. Jeff Dean and Walt Lorenz. Blaire Johnson and Domink Royko performed data extractions. Dominik Royko, Leo Galindo-Gonzalez, and I annotated the differentially expressed sequences, with help from Rhiannon Peery. Walid El Kayal and Chelsea Ju performed the statistical analyses with assistance from Adriana Arango-Velez. Initial mining of the phloem dataset was carried out by Adriana Arango-Velez and Leo Galindo-Gonzalez. Elizabeth Mahon contributed substantially to the *chitinase* heatmap figure, the phloem Venn diagram figure, the tables summarizing enrichment analyses and DE defense sequences, and she generated the hormone heatmap figure in chapter two. I was responsible for additional mining and analysis of the data in chapter two, and for the entirety of the data mining and analysis in chapter three.

Chapter two includes gene expression data for terpene synthases generated by Charles Copeland and for chitinases generated by Elizabeth Mahon. I performed statistical analyses on this data and generated the remaining gene expression data as described in chapter two.

Chapter four describes analysis of a field experiment led by me and Antonia Musso. Irina Zaharia conducted hormone quantification.

Chapter five includes analysis of spruce buds that were collected by Kate St. Onge, Juan Aldana, Marion Mayerhofer, and me. Juan Aldana, Marion Mayerhofer, Kate St. Onge, and Daniel Tucker provided phenotyping data. Bianca Sacchi, Isiah Plouffe, and I did the histology. Juan Aldana performed the toughness measurements. Xu (Sarena) Yang, Kate Stolnikova, and I performed the wax metabolite analysis.

Dedication

"A wizard should know better"

- Treebeard

This thesis is dedicated to the trees – may we honor them by using this knowledge.

Acknowledgements

I respectfully acknowledge that the lands where I live and work are situated on Treaty 6 and Treaty 8 territories, the traditional and unceded lands of the First Nations and Métis people. I acknowledge the privilege that has granted me access to these lands and allowed me to benefit from Indigenous stewardship.

Thank you to my graduate supervisor, Dr. Janice Cooke, who saw something in me and helped me to see it myself. I am forever grateful for her support and guidance. Thank you as well to the members of my supervisory committee, Dr. Jocelyn Hall and Dr. R. Glen Uhrig, for helping to shape my research goals. Thank you to all the past and present members of the Cooke lab, including all the undergraduate students who helped make this research a reality. I am grateful to call many of you friends. Thank you to all the staff in the Department of Biological Sciences, in particular Troy Locke and Arlene Oatway, without whom this research wouldn't look as good. Thank you to Dr. Guanqun (Gavin) Chen and Dr. Yang (Sarena) Xu for all your help with analysis.

I am grateful for all the financial support I have received that has allowed me to put everything I could into this thesis, including funding from the Department of Biological Sciences, NSERC (CGS-M), Alberta Innovates (AITF), the Government of Alberta (QEII), TRIA-Net, and SpruceUp. I am also thankful for the opportunities I was given to participate in conferences and share my work, which was enabled by funding from TRIA-Net, SpruceUp, the Canadian Society of Plant Biologists, the American Society of Plant Biologists, the Department of Biological Sciences, and the Faculty of Graduate and Research Studies at the University of Alberta.

Thank you to all my friends and family who saw me through this. You always believed in me, for which I am so grateful.

Thank you to my chosen family, Ethan, for being my best friend and partner. There is no one else I'd rather share this with.

Table of Contents

List of Figures

List of Abbreviations

ACC	1-aminocyclopropane-1-carboxylate
ANOSIM	analysis of similarities
ANR	anthocyanidin reductase
ANS	anthocyanidin synthase
aRNA	antisense ribonucleic acid
BSTFA	N,O-Bis(trimethylsilyl)trifluoroacetamide
cDNA	complementary deoxyribonucleic acid
CHI	chalcone isomerase
CHS	chalcone synthase
CTI	chitin-triggered immunity
DAD	diode array detector
DAMP	damage-associated molecular pattern
DE	differentially expressed
DFR	dihydroflavonol reductase
DMAPP	dimethylallyl diphosphate
dpi	days post inoculation
dpw	days post wounding
EIN	ethylene insensitive factor
EN	endodermis
EP	epidermis
ERF	ethylene response factor
ET	ethylene
F35H	flavonoid 3,5-hydroxylase
F3H	flavanone 3-hydroxylase
FC	fold change
FLS	flavonol synthase
GC	gas chromatography
GLM	generalized linear model
GLMM	generalized linear mixed model
HAMP	herbivore-associated molecular pattern

HPLC	high performance liquid chromatography
HY	hypodermis
JA	jasmonic acid
JA-Ile	jasmonic acid-isoleucine
JAZ	jasmonate ZIM-domain
LAR	leucoanthocyanidin reductase
LC-MS/MS	liquid chromatography-tandem mass spectrometry
LIMMA	linear models for microarray data
LOX	lipoxygenase
MAPK	mitogen-activated protein kinase
ME	mesophyll
MeJA	methyl jasmonate
MPB	mountain pine beetle
MS	mass spectrometry
MYB	myeloblastosis
MYC	myelocytomatosis oncogene
N-P-K	nitrogen-phosphorous-potassium
NMDS	non-metric multidimensional scaling
NSC	non-structural carbon
OMT	stilbene o-methyltransferase
OPDA	oxo-phytodeinoate
PAL	phenylalanine ammonia lyase
PAMP	pathogen-associated molecular pattern
PMME	pinosylvin monomethyl ether
PP	polyphenolic parenchyma
PR	pathogenesis related
PRRs	pattern recognition receptors
PTI	pattern-triggered immunity
qRT-PCR	quantitative reverse transcription polymerase chain reaction
RNA	ribonucleic acid
SA	salicylic acid

SAR	systemic acquired resistance
SBW	eastern spruce budworm
STS	stilbene synthase
TIF5A	eukaryotic translation initiation factor 5A-1
UBA1	ubiquitin-activating enzyme 1
VB	vascular bundle
VHA-A	vacuolar ATP synthase subunit A
WD	water deficit
WUE	water use efficiency
WW	well-watered
XY	xylem

Chapter 1: Introduction

Over the millennia, trees and plants in general have evolved defense mechanisms to protect against the onslaught of pests, pathogens, and other hurdles faced. While core plant defense strategies are often shared across large groups of species, coexistence of trees with persistent pests has resulted in the specialization and refinement of defense-related responses (Stamp 2003). The long-lived nature of trees is theorized to mean that trees will invest heavily in defenses to manage the many challenges over their lifetime. In this chapter, I will outline several different defense strategies trees employ and summarize current research into the many factors that contribute to how capable a host tree is to defend itself against pests. Lastly, I will introduce two host-pest systems in which I have conducted research into the dynamics of the host defense responses under several conditions.

Antagonistic relationships between insect pests, fungal pathogens, and their plant hosts can be complex and sometimes highly specialized. Differences in structural (physical) and chemical defenses influence host suitability to respective antagonists. Here, I will describe host suitability as the capacity of the pest or pathogen to mount a successful attack, and alternatively from the plant's perspective, the incapacity to contain infection or deter feeding. Additionally, abiotic factors can impact host secondary metabolism (Arango-Velez et al. 2014, 2016) and host phenology (Fuentealba et al. 2017), both of which affect host suitability in plant-antagonist interactions.

Understanding how different factors influence host defenses, and the corresponding role of specialized host defenses in determining host suitability to antagonists, is of growing importance as hosts face greater abiotic stresses under the threat of climate change. In my thesis research, I examined the phenotypic plasticity of host tree chemical and structural defenses

relevant in interactions with two forest insect pest systems that contribute to substantial losses in Canada's forests and that have the greatest potential to negatively impact forest stands in Alberta (Cerezke et al. 2014): (1) mountain pine beetle (MPB, *Dendroctonus ponderosae* Hopkins) – *Grosmannia clavigera* [Robinson-Jeffrey and Davidson] Zipfel, de Beer and Wingfield – lodgepole pine (*Pinus contorta* Dougl. ex Loud. var. *latifolia* Engelm.) and jack pine (*Pinus banksiana* Lamb.), and (2) eastern spruce budworm (SBW, *Choristoneura fumiferana* [Clemens]) – white spruce (*Picea glauca* [Moench] Voss).

1.1 Focal systems for this research

1.1.1 MPB – G. clavigera – lodgepole and jack pine

MPB. MPB is a member of the genus *Dendroctonus* in bark beetle subfamily Scolytinae (Coleoptera: Curculionidae). First described by Hopkins (1902), MPB is distinct from *Dendroctonus brevicomis* (LeConte), with which it overlaps ranges substantially in the United States (Wood 1963), and *Dendroctonus jeffreyi* (Hopkins), with which it is most closely related (Six and Bracewell 2015). MPB's historic range includes south-central British Columbia and much of the western United States (Wood 1963, Six and Bracewell 2015). While *Pinus* spp. are considered the primary host of most *Dendroctonus* bark beetles (Six and Bracewell 2015), MPB has been shown to successfully attack and reproduce in other conifer species, including *Picea abies* (L.) Karst (Furniss and Schenk 1969) and *Picea engelmannii* x *glauca*, also known as interior spruce (Huber et al. 2009).

MPB carries out most of its life cycle within the host, apart from dispersal which typically occurs as adults emerge in July to August (Safranyik and Carroll 2006). MPB is generally univoltine (Safranyik and Carroll 2006, Six and Bracewell 2015), meaning that it produces one generation per year, although divoltine cycles have been observed when conditions

are favourable (Safranyik and Carroll 2006). Mating and oviposition occur following host colonization, and eggs hatch shortly after in August-September (Six and Bracewell 2015, Chiu and Bohlmann 2022). MPB overwinter as third or fourth instar larvae and pupate the following June (Safranyik and Carroll 2006, Chiu and Bohlmann 2022). MPB relies on a mass attack strategy (Figure 1.1) to successfully colonize its host, and a pioneer female will attract additional MPB by releasing aggregation pheromones once a suitable host is selected (Wood 1982, Safranyik and Carroll 2006).

Figure 1.1 Bark removed from a lodgepole pine revealing MPB during mass attack.

Grosmannia clavigera. MPB vectors several Ophiostomatoid (Ascomycota) blue-stain fungi, with the most common associates being *G. clavigera*, *Ophiostoma montium* (Rumbold) von Arx., and *Leptographium longiclavatum* Lee, Kim and Breuil (Roe et al. 2010, Roe, James, et al. 2011). Fungal spores are carried in the MPB gut and in specialized structures called mycangia, thought to have evolved for the purpose of fungal transport (Bleiker et al. 2009, Six 2020a). Unable to degrade lignin and cellulose (Ballard et al. 1984, Six 2020a), these Ophiostomatoids have instead adapted to exploit resources from host parenchyma (Six 2020a). MPB feed on fungi lining the walls of larval galleries, providing nutrients for developing larvae (Ayres et al. 2000, Bentz and Six 2006, Bleiker and Six 2007, Goodsman et al. 2012) and promoting transmission of the fungus by new MPB (Six 2020a).

It is believed that the relationship between MPB and its Ophiostomatoid associates is symbiotic, as both partners have evolved traits which promote the mutualism (Six and Wingfield 2011, Six and Klepzig 2021). Many of these fungal symbionts are virulent to pine hosts and are thought to contribute to MPB colonization by overwhelming host defenses (Lieutier et al. 2009). The most virulent fungal associate, *G. clavigera* (Rice et al. 2007a), is also able to detoxify some host defense compounds (DiGuistini et al. 2011). Furthermore, MPB is unable to reproduce in the absence of fungal associates (Six and Paine 1998), and the fungi are dependent on MPB for transmission (Bleiker et al. 2009, Six 2020a). Because of this close relationship, and because hosts exhibit similar responses to MPB attack and fungal inoculation, inoculation with *G. clavigera* is often used as a proxy for MPB attack (McAllister et al. 2018), particularly in seedling experiments where MPB cannot be introduced.

Lodgepole and jack pine. Lodgepole and jack pine are sister species, believed to have diverged during or before the Pleistocene era (Eckert and Hall 2006). Lodgepole pine's range

extends across British Columbia and western Alberta while jack pine ranges from western Alberta to the east coast of Canada (Critchfield 1985, Cullingham et al. 2011). Despite generally occupying different habitats (Rweyongeza et al. 2007), their distributions overlap and they hybridize readily in central Alberta, northeastern British Columbia, and the southern part of the Yukon (Cullingham et al. 2012, Burns et al. 2019). Lodgepole pine, jack pine, and their hybrids are all potential hosts to MPB (Cullingham et al. 2011).

Current MPB Epidemic. Beginning in the late 1990's, the current MPB outbreak has led to an unprecedented range expansion into the boreal forest of northern Alberta (Cullingham et al. 2011). This range has been shown to include a new host species, jack pine, which has not experienced MPB attack in recorded history (Safranyik et al. 2010, Cullingham et al. 2011). Increased population densities have also shifted host selection behavior of MPB, which can successfully attack larger, healthier, and likely better-defended trees when at epidemic rather than endemic levels (Raffa et al. 2008). If co-evolution of adaptive host strategies between MPB-*G. clavigera*-lodgepole has occurred, then it is theorized that these adaptations would not be present in the evolutionarily naïve host jack pine. Additionally, any pathogen strategies that could have co-evolved in *G. clavigera* during its shared history with lodgepole pine may have different efficacies in jack pine.

1.1.2 SBW – white spruce

SBW. The Lepidopteran SBW moth, a member of the family Tortricidae, was first described in 1865 (Clemens). Its historic range extends from the eastern coast of Canada to the Alberta rocky mountains and north to central Alaska (Marshall and Roe 2021). SBW has a univoltine lifecycle, which begins as adult moths emerge in July and mate shortly after (Mattson et al. 1988). Eggs are deposited within the upper half of the host crown, hatching in late July to

August (Mattson et al. 1988). SBW larvae overwinter as 2nd instars, emerging in May when they begin feeding on host foliage (Mattson et al. 1988). Larvae preferentially feed on expanding foliage during concurrent host bud burst, but early emerging larvae will mine foliage from the previous year and pollen cones until buds begin to swell and developing needles are visible through the bud scales (Fuentealba et al. 2018). Bud scales can protect young, nutritious foliage and provide a barrier to SBW feeding when intact. During this time, SBW may be forced to feed on older, tougher, less nutritious foliage from the previous year's growth. As SBW larvae move along the host branches in search of food, wind may cause dispersal (Mattson et al. 1988) prior to pupation of the 6th instar larvae in July (Marshall and Roe 2021).

SBW Hosts. SBW is considered one of the most important pests affecting spruce and fir (Fuentealba et al. 2017), resulting in defoliation, host growth loss, and large losses of forest products (Fuentealba and Bauce 2016). SBW preferentially feeds on balsam fir (*Abies balsamea* [L.] Mill), but black spruce (*Picea mariana* Mill.), white spruce, and red spruce (*Picea rubens* Sarg.) are all secondary hosts, and exhibit lower levels of defoliation relative to balsam fir (Berguet et al. 2021). Phenological differences between black spruce and balsam fir have been shown to impact feeding behaviour of spruce budworm (Fuentealba et al. 2017). However, in experiments where phenological mismatch was reduced, black spruce and balsam fir were found to be equally suitable hosts (Bellemin-Noël et al. 2021).

White spruce. White spruce is a keystone conifer species in Canada with a transcontinental distribution (Nienstaedt and Zasada 1990) that is nearly continuous across Alberta's boreal forest (Rweyongeza et al. 2011). White spruce is commonly used in pulp and paper production (Duchesne and Zhang 2004), as well as for lumber in construction (Hassegawa et al. 2019). As mentioned above, white spruce hybridizes with Engelmann spruce (*Picea*

engelmannii Parry ex Engelm), as well as with Sitka spruce (*Picea sitchensis* (Bong.) Carr, (Hamilton et al. 2015).

SBW Outbreaks. SBW exhibits periodic outbreaks (Berguet et al. 2021), and dendrochronological records in balsam fir (Bouchard et al. 2006) support current data that outbreaks typically occur every 30 to 40 years (Boulanger and Arseneault 2004). Although SBW range extends throughout the boreal forest, outbreaks are historically most severe in south-eastern Canada (Pureswaran et al. 2015), and past outbreaks which were farther north were of much shorter duration (Gray 2008). However, climate change-related shifts in host and insect phenology have the potential to drive SBW north into regions dominated by black spruce (Pureswaran et al. 2015).

1.2 Host Defense Responses

1.2.1 Constitutive and Induced Defenses

To protect against a wide array of antagonists, plants have adapted a multi-tiered defense strategy comprising numerous defense mechanisms that overlap temporally, spatially, and functionally. Constitutive defenses represent the first tier and are formed prior to interaction with antagonists as part of a host's regular metabolism (Franceschi et al. 2005). These preformed defenses require regular investment of resources but are advantageous in that they are already in place upon invasion (Franceschi et al. 2005). Many constitutive defenses are involved in preventing attack, and function to repel or inhibit the invasion of tissues (Franceschi et al. 2005).

Induced defenses are important for helping to contain and kill invaders and are synthesized following invasion of the host. This strategy can reduce overall resource allocation towards defense, but there is a lag between perception of the antagonist and defense synthesis (Franceschi et al. 2005). Some induced defenses may in fact be more costly as they involve *de*

novo synthesis of new structures or compounds, although they may be fine-tuned in response to attack severity (Franceschi et al. 2005). Many defenses produced constitutively are also inducible, and hosts may exhibit different quantities or chemical compositions following induction. Each plant species employs a unique set of constitutive and induced defenses that are shaped by adaption to specific pests and pathogens (Miresmailli and Isman 2014). These defenses are often categorized as either mechanical (structural) or chemical in nature.

Structural reinforcement of host cells and tissues can provide an effective means of defending against pests and pathogens (Franceschi et al. 2005, Fossdal et al. 2012). In *Arabidopsis thaliana*, lignification is proposed to play a role in plant defense responses triggered by the pathogen *Pseudomonas syringae* (Chezem et al. 2017), while silencing of genes related to monolignol biosynthesis in wheat (*Triticum monococcum*) leads to increased susceptibility to penetration by powdery mildew (*Blumeria graminis* f. sp. *tritici*; Bhuiyan et al. 2009). In conifers, physical obstructions to feeding, such as sclereid stone cells and calcium oxalate crystals have been demonstrated to serve as effective defense mechanisms against herbivores (Hudgins et al. 2003, Whitehill et al. 2016, 2019). Fortification of secondary cell walls by increased lignification in response to herbivory (Wainhouse et al. 1990) and fungal infection (Fossdal et al. 2012) is a commonly observed defense strategy in conifers, and modulation of lignin biosynthesis has been linked to herbivore resistance in wheat to stem rust (Moerschbacher et al. 1990).

Major classes of chemical compounds implicated in plant defense include terpenoids, alkaloids, glucosinolates, and phenolics (Miresmailli and Isman 2014). In angiosperms, alkaloids are nitrogen-containing compounds that have strong toxic effects on mammals and some insects (Mithöfer and Boland 2012). Arabidopsis can synthesize up to 40 glucosinolates (Burow and

Halkier 2017) that form toxic compounds following hydrolysis by myrosinase, released from nearby cells by insect feeding (Hopkins et al. 2009). In angiosperms prone to herbivory of foliage, these compounds will accumulate in leaves. Terpenes and phenolics are prominent conifer defenses (Kolosova and Bohlmann 2012, Krokene 2015) and, as such, are described in more detail below.

1.2.2 Perception of antagonists by host plants

Host plants have also evolved strategies for recognizing invaders so that they can respond more appropriately. Pattern recognition receptors (PRRs) are host receptors on the plant cell surface that can bind small molecules that arise from the antagonist (Zipfel 2014). Chitin, a component of fungal cell walls, can serve as a pathogen-associated molecular pattern (PAMP) detectable by PRRs (Pruitt et al. 2021). Insect oral secretions may be recognized as herbivore-associated molecular patterns (HAMPs), while PRRs can also recognize damage-associated molecular patterns (DAMPs), which are host-derived molecules released during wounding or enzymatic digestion of tissues by pathogens or herbivores (Choi and Klessig 2016). Once a host plant has recognized an antagonist via PRRs, a form of innate (intrinsic) immunity, called pattern-triggered immunity (PTI) may be triggered, conferring broad-spectrum protection to a wide range of antagonists (Wilkinson et al. 2019).

1.2.3 Signaling and Regulation

In Arabidopsis, activation of host immune responses includes initiation of hormone signaling pathways and activation of downstream defenses (Pieterse et al. 2012, Vos et al. 2013). The three hormones primarily involved in host defense responses are salicylic acid (SA), jasmonic acid (JA) and ethylene (ET). SA is typically involved in host defense responses to

biotrophic pathogens (Broekgaarden et al. 2015). SA is also important for activation of systemic acquired resistance (SAR) in tissues distal to the original site of attack (Zhang et al. 2010).

Host perception of DAMPs induces JA synthesis and can also trigger systemic responses following herbivore- or pathogen-related tissue damage (Choi and Klessig 2016). Based on recognition of additional molecular patterns specific to the perceived threat, JA can activate either the myelocytomatosis oncogene (MYC) pathway in response to herbivory or the ethylene response factor (ERF) pathway in response to necrotrophic pathogens (Pieterse et al. 2012, Broekgaarden et al. 2015). This triggers mitogen-activated protein kinase (MAPK) cascades which activate transcription factors that bind and regulate expression of defense-related genes (Broekgaarden et al. 2015). WRKY, NAC, MYB, bZIP, and bHLH factors are all associated with JA signaling (Wasternack and Song 2016, Kundu and Vadassery 2021). Production of ET following necrotrophic infection helps mediate ethylene-related defense genes via signaling involving ERFs and ethylene insensitive (EIN) factors (Broekgaarden et al. 2015, Dolgikh et al. 2019).

1.3 Conifer Protein and Chemical Defenses

1.3.1 Pathogenesis-related (PR) proteins

The PR proteins constitute diverse families of proteins that are all strongly upregulated in response to antagonist attack (Kolosova and Bohlmann 2012, Garcia et al. 2021). PR proteins include chitinases (PR-3, PR-4, PR-8, and PR-11; van Loon et al. 2006), thaumatin-like proteins (PR-5, also called osmotins; Hakim et al. 2018), defensins (PR-12), and peroxidases (PR-9; van Loon et al. 2006). PR-1 proteins, despite their function being unknown, are often a marker of systemic acquired resistance in distal tissues (van Loon, Rep, et al. 2006). Thaumatin-like proteins exhibit anti-fungal activity (Liu et al. 2010), although osmotins are also active in Scots

pine (*Pinus sylvestris* L.) following pine weevil (*Hylobius abietis* L.) feeding (Kovalchuk et al. 2015). Defensins are small antimicrobial peptides that are constitutively found in almost all tissues (Lacerda et al. 2014). Peroxidases are important for maintaining counteracting damaging reactive oxygen species released during tissue damage or accumulated as part of the hypersensitive response (Pan et al. 2018). Peroxidases also play a role in mechanical defenses through their involvement in lignification (Polle et al. 1994, Almagro et al. 2009, Jang et al. 2022).

Of the PR proteins, chitinases appear to play a particularly prominent role in conifer defense. Chitinases comprise two families, glycoside hydrolase family 18 (GH18) and glycoside hydrolase family 19 (GH19; Li and Greene 2010) – members of GH19 but not GH18 are involved in defense (Grover 2012). Chitinases are further classified into seven biochemical classes of enzymes (Grover 2012), of which classes I, II, IV, VI, and VII are GH19 chitinases. However, class VI chitinases have not been identified in conifers (Peery et al. 2021). Apart from class II chitinases which lack a chitin binding domain (Neuhaus 1999, Islam et al. 2011), chitinases are so named for their ability to break down chitin in fungal cell walls (Islam et al. 2011). Chitooligosaccharides released during this process can function as PAMPs or fungal elicitors and indirectly elicit host immune responses (Grover 2012, Dalio et al. 2017) sometimes referred to as chitin-triggered immunity (CTI; Gong et al. 2020). CTI may also trigger upregulation of other chitinases (Rovenich et al. 2014).

Induction of chitinases in response to herbivory was observed in Sitka spruce (*P. sitchensis*, Lippert et al. 2007). Chitinases may also be induced in response to wounding, drought, frost/overwintering, and salt stress (Grover 2012). Galindo-González et al. (2015) observed accumulation of chitinases in white spruce during the transition to dormancy which, in

addition to putative roles as antifreeze proteins, vegetative storage proteins, and proteins involved in cell wall synthesis, may also confer increased protection to biotic stress. The role of chitinases in response to fungal pathogens is well documented in conifers. Previous work from our lab demonstrated that lodgepole and jack activate different patterns across similar classes of chitinases in response to *G. clavigera*, and that both species further utilize different chitinase classes following infection with the biotrophic rust, *Cronartium harknessii* E. Meinecke (Peery et al. 2021). The antifungal activity of some lodgepole pine chitinases, as well as chitinases from interior spruce (*P. glauca x engelmannii*), has additionally been functionally characterized (Kolosova et al. 2014).

1.3.2 Oleoresin and Terpenes

Oleoresin is a hallmark of conifer defense responses – it is a viscous, sticky mixture of mono- and di-terpenes (Keeling and Bohlmann 2006b) that is constitutively synthesized, stored, and secreted in specialized structures called resin ducts (Chiu and Bohlmann 2022). Conifer species possess different types of resin ducts, including axial and radial ducts or resin blisters in the phloem, xylem, and needles (Celedon and Bohlmann 2019, Vázquez-González et al. 2020). Oleoresin is stored under pressure until it is released by the severing of ducts during wounding or herbivory and can act to physically flush out invaders (Huber et al. 2004). Exposed resin will later crystalize, encasing the intruder and acting as a seal to the wound (Franceschi et al. 2005). Concurrently, this releases volatile terpenes which may serve as an indirect defense by attracting predators of the offending insect (Heil 2014).

Terpenes, also called isoprenoids, are present in almost all species of plants but can differ among individuals from the same species (Keeling and Bohlmann 2006a), by chemotype (Kännaste et al. 2018), across different geographical areas (Pureswaran et al. 2004), and under

stress (Kopaczyk et al. 2020). Monoterpenes (C10), sesquiterpenes (C15) and diterpenes (C20) are all formed through condensation of dimethylallyl diphosphate (DMAPP) and further modification by different terpene synthases (Keeling and Bohlmann 2006a). Many terpene synthases can form multiple products (Celedon and Bohlmann 2019) and there exist over 30 000 known terpenes (Keeling and Bohlmann 2006a). In addition to their role as a structural defense as part of oleoresin secretion, many terpenes are toxic at certain concentrations to insects like MPB (Chiu et al. 2017) and spruce beetle (*Dendroctonus rufipennis* Kirby; Davis 2020). However, at lower concentrations, some monoterpenes have been shown to stimulate feeding in SBW (Ennis et al. 2017).

Terpene biosynthesis and biosynthetic gene expression is induced by fungal inoculation (Pollastrini et al. 2015, Arango-Velez et al. 2016) or by insect attack (Faiola et al. 2018, Kopaczyk et al. 2020) in several conifer species. Some conifer species will also develop additional traumatic resin ducts in xylem in response to infection or wounding (Krokene, Nagy, and Krekling 2008). Traumatic resin ducts provide increased resin production (Krokene, Nagy, and Krekling 2008, Vázquez-González et al. 2020) and may be related to resistance in some species. For example, Schiebe et al. (2012) found that Norway spruce trees killed by bark beetle attacks had fewer traumatic resin ducts than controls or individuals that survived attack. The presence of traumatic resin ducts in the dendrochronological records of Engelmann spruce (*P. engelmannii*) have also been identified as indicators of previous spruce beetle outbreaks, and likely a primary defense mechanism contributing to survival of those trees (DeRose et al. 2017).

1.3.3 Phenolics

Phenolics are benzylated compounds with one-to-many hydroxyl groups, produced via the phenolic biosynthesis pathway from the amino acids phenylalanine and tyrosine. Beginning

with phenylpropanoid biosynthesis, the phenolic biosynthesis pathway has many branches leading to more specialized compounds, including lignin. Lignin is an aromatic compound deposited in secondary cell walls to provide fortification and hydrophobicity (Vanholme et al. 2010). A critical component of plant structure under normal growing conditions, lignin is also important as a structural defense (Kolosova and Bohlmann 2012). Lignification of cell walls can alter spruce bark beetle (*Dendroctonus micans* Kugelann) gallery construction (Wainhouse et al. 1990) and limit or prevent enzymatic digestion by pathogens, including Ophiostomatoids (Franceschi et al. 2005, Six 2020a). Lignans are polyphenols derived from phenylalanine with antifungal (Shain and Hillis 1971) and antifeedant (Harmatha and Dinan 2003) properties.

An anatomical feature related to conifer phenolic defenses and specific to Pinaceae (Franceschi et al. 2005) is the constitutive presence of polyphenolic parenchyma (PP) cells located in the phloem tissue that are involved in the storage and synthesis of some phenolic compounds (Li et al. 2012, Nagy et al. 2014). In response to pathogen or insect attack, these cells have been observed to swell and increase in number in some conifer species (Franceschi et al. 2000) and may release phenolic compounds if ruptured by boring insects or fungal hyphae (Franceschi et al. 1998). Phenolics, including lignans, may also accumulate in xylem in reaction zones and lesions formed at the site of infection (Nagy et al. 2012, 2022), and oxidation of these phenolics contributes to discoloration of the wood (Liu et al. 2021). Both natural attack by MPB and accompanying fungal symbionts (including *G. clavigera*), as well as inoculation with *G. clavigera* to simulate attack, cause lesions containing phenolics (Figure 1.2; Shrimpton 1973, Arango-Velez et al. 2016).

Some additional classes of phenolics implicated in conifer resistance are stilbenes and flavonoids, including flavan-3-ols, a subclass of flavonoids. Stilbenes and flavonoids are both

Figure 1.2. Lesion development in mature lodgepole pine at the site of MPB mass attack (left, indicated by knife point) and in lodgepole pine seedlings inoculated with *G. clavigera* (right). In both cases, bark and phloem have been peeled back to reveal the xylem.

synthesized from the same cinnamoyl-CoA precursor via different enzymes and branches of the phenolic biosynthesis pathway. In Norway spruce (*Picea abies*) synthesis of resveratrol, that species' primary stilbene, and flavan-3-ols are linked with resistance to the blue stain fungus *Endoconidiophora polonica* (formerly known as *Ceratocystis polonica* (Siem.) C. Moreau; Evensen et al. 2000, Hammerbacher et al. 2011, 2014), although some strains have evolved detoxification mechanisms (Hammerbacher et al. 2013, Wadke et al. 2016, Zhao et al. 2019). In

Scots pine (*P. sylvestris*), the stilbenes pinosylvin and pinosylvin monomethyl ether (PMME) are major components of lesions induced in response to *Ophiostoma brunneo-cilatum* Math. (Villari et al. 2012) and *Ophiostoma ips* (Rumb.) Nannf (Croisé and Lieutier 1998).

The biochemical environment can also play an important part in determining how phenolic compounds interact with other chemicals and proteins, particularly due to their high oxidation capacity. Phenolic function is also altered by glycosylation (Zhang et al. 2022). For example, two acetophenones in white spruce were found to confer resistance to spruce budworm when present as aglycones but not as glycosides (Delvas et al. 2011, Mageroy et al. 2017). Additionally, many phenolics cause toxicity by the formation of oxygen radicals, however, reducing pH conditions can prevent phenolic oxidation (Appel 1993). Some herbivores are thought to have adapted mechanisms for minimizing phenolic oxidation in their guts by maintaining reducing conditions or by deactivating oxidized phenolics via conjugation (Appel 1993).

1.3.4 Cuticular Waxes

Cuticular wax along the surface of the needle provides an interface for insect interaction and host selection (Riederer and Muller 2006). Optical properties of leaf waxes, including reflectance and absorbance of ultraviolet radiation, can visual influence recognition and landing by approaching insects (Müller and Riederer 2005). Upon landing, phytophagous insects will probe the leaf surface and use cues such as wax structure to determine host suitability (Müller and Riederer 2005). White spruce foliar wax can stimulate spruce budworm oviposition and feeding (Daoust et al. 2010). The presence of soluble terpenes in cuticular wax may add to this attraction (Ennis et al. 2017). Within the wax, chemical composition can impact the morphology, thickness, and reflectance of the cuticle layers (Hanover and Reicosky 1971, Reicosky and

Hanover 1978). Humidity and temperature can also impact cuticle stiffness, in addition to cuticle composition (Domınguez and Heredia-Guerrero 2010).

1.4 Environmental factors Influencing Host Defenses

1.4.1 Seasonal cues: photoperiod and temperature

Plants and insects rely on cues such as photoperiod and temperature to align timing of developmental phases with the season (Bailey and Harrington 2006). I use the term phenology to refer to the alignment of biological phenomena with seasonally associated environmental cues. Phenological synchrony between host and pest can be important for determining host suitability, and there exists a strong selective pressure on insects favoring optimal overlap to maximize fitness (Lawrence et al. 1997). Predicted shifts towards earlier active growth of forest trees due to climate warming are expected to increase phenological synchrony between multiple pests and previously unsuitable host trees (Pureswaran et al. 2015, Fuentealba et al. 2017).

Foliar toughness of mature needles was shown to be a strong predictor of budworm mining success, better than foliar nitrogen content (Fuentealba et al. 2020). Deposition of both lignin and cuticular waxes occurs after growth initiation but before winter conditions (Günthardt-Goerg 1987). The rate at which these changes occur may influence feeding and digestion by a folivore and represent important host qualities marking the end of the window of opportunity.

Seasonal variation in plant metabolism can also impact constitutive chemical defenses, including several defense-associated chitinases (González et al. 2015) and monoterpenes (Kopaczyk et al. 2020). Acetophenone aglycones conferring resistance against spruce budworm were undetectable in white spruce early in the growing season, but levels of these compounds increase later in the season (Mageroy et al. 2017). Lastly, ontogenetic disease resistance, i.e., increased resistance related to age or developmental stage of a plant or its tissues, is compatible

with the idea that repeated exposure to antagonists over time also increases SAR (Bonello et al. 2006).

1.4.2 Abiotic Stresses

Ozone (Percy et al. 1990, Manninen et al. 2002), acidic fog (Lütz et al. 1990, Percy et al. 1990), nitrogen levels (Ghimire et al. 2019), and water availability (Lusebrink et al. 2011, Arango-Velez et al. 2014, 2016) have all been shown to alter levels of defense compounds in conifer tissues. The growth-differentiation balance hypothesis posits that stresses which limit photosynthetic output – such as water deficit – alter allocation of carbon-based resources within a plant and create a trade-off between growth and defense (Herms and Mattson 1992). Trees under water limitation show reduced photosynthesis (Arango-Velez et al. 2014), which can elicit large changes in carbon allocation that can alter secondary metabolism pathways leading to chemical and structural defenses (Massad et al. 2012). Trees under prolonged water deficit potentially undergo seasonal growth cessation sooner (Gruber et al. 2010), triggering phenology-related changes in defenses such as chitinases (González et al. 2015), and terpenes (Staudt et al. 2000, Nealis and Nault 2005), and altering host susceptibility (Krokene et al. 2012).

Generally, water-deficit trees are considered more susceptible to insect attack (Koricheva et al. 1998, Rouault et al. 2006, Netherer et al. 2015) and disease (Desprez-Loustau et al. 2006). Alternatively, a recent study by Netherer et al. (2015) found that while drought decreased Norway spruce resistance to the bark beetle *Ips typographus* L. (Coleoptera: Curculionidae), it also decreased *I. typographus* host acceptance, indicating that drought invokes a change in host suitability. Unpacking the impact of drought on secondary metabolites is not straightforward and appears dependent on the degree and duration of drought (Kolb et al. 2016, Trowbridge et al. 2021). An early study monitoring the effects of water deficit on oleoresin flow in *Pinus taeda* L.

found that lower water availability increased constitutive levels but decreased induced resin flow (Lombardero et al. 2000). However, stress-induced shifts in resource allocation are not consistent across all defenses. Even for monoterpene synthesis, several studies have observed increased total monoterpene levels under water deficit conditions (Lusebrink et al. 2011), while others have decreased (MacAllister et al. 2019) and individual compounds can exhibit different responses (Arango-Velez et al. 2016). Lastly, changes in host volatiles can influence host stand selection (Cardinal et al. 2022), while other host metabolic profiles influence individual host selection and may further compound effects of drought on host suitability.

1.5 Current Study

The overall aim of my thesis research was to investigate patterns of chemical and structural plant defenses in the interactions of conifer hosts with a suite of insect and fungal antagonists. During my thesis, I explored these defense strategies at the molecular and biochemical level. To address my overarching goal, I tested the following hypotheses:

1. A shared evolutionary history between a plant host and pest/pathogen will result in a more effective host defense response.
2. Water limitation will impact host defense responses and ultimately host suitability.
3. Insects and fungi activate different signaling pathways in conifers, eliciting different hormonal signatures of attack.
4. Lignin and cuticle deposition are reliable markers of needle mechanical toughness during needle development and contribute to defining the phenological window of opportunity and host suitability.

To test these hypotheses, I addressed specific objectives in each thesis chapter as follows:

In Chapter 2, I tested hypotheses one and two by addressing the following objectives: a) characterizing differences in expression of defense-related genes, including chitinases, terpene synthases, and phenolics, and differences in phenolic metabolite profiles for lodgepole and jack pine phloem following inoculation with the MPB fungal associate *G. clavigera*, and b) determining if water deficit impacts lodgepole and jack pine phloem defenses, and in particular phloem phenolic defenses, against *G. clavigera*. To do so, I mined existing microarray data for patterns and changes in defense-related genes and conducted additional gene expression profiling of phenolic biosynthesis genes using quantitative reverse transcription PCR (qRT-PCR) from phloem of lodgepole and jack pine seedlings subjected to *G. clavigera* inoculation and/or water deficit. To complement these expression studies, I used high performance liquid chromatography (HPLC) to identify and quantify phenolic metabolite profiles in the same tissues.

In Chapter 3, which largely mirrors Chapter 2 but focuses on xylem rather than phloem, I further tested hypotheses one and two by addressing the following objectives: a) characterizing differences in expression of defense-related genes and differences in phenolic metabolite profiles for lodgepole and jack pine xylem following inoculation with *G. clavigera*, and b) determining if water deficit impacts lodgepole and jack pine xylem defenses, and in particular xylem phenolic defenses, against *G. clavigera*. To do so, I mined existing microarray data for global and specific changes in defense-related gene expression in xylem of lodgepole and jack pine seedlings inoculated with *G. clavigera* under well-watered or water deficit conditions. Additionally, I profiled phenolic biosynthesis gene expression using qRT-PCR and measured phenolic metabolite profiles using HPLC in the same tissues.

In Chapter 4, I tested hypothesis three by addressing the following objectives: a) characterizing differences in defense responses of lodgepole pines attacked by MPB versus

inoculation with *G. clavigera*, and b) determining if *G. clavigera* plays a role in induction of host defenses during MPB mass attack. To do so, I conducted a large-scale field experiment to generate experimental materials enabling a comparison of lodgepole pine defense responses to MPB and *G. clavigera*. In phloem and xylem collected from this experiment, I quantified hormone levels using HPLC-mass spectrometry (MS). Additionally, I examined phenolic biosynthesis gene expression using qRT-PCR and phenolic metabolite profiles using HPLC in the same tissues.

In Chapter 5, I tested hypothesis four by addressing the following objectives: a) determining the temporal and spatial deposition of structural defenses such as lignin and epicuticular waxes relative to needle maturation during white spruce bud flush, and b) determining whether changes in lignin and cuticular wax are related to changes in foliar toughness during the phenological window of opportunity for SBW feeding. To do so, I conducted two independent experiments, in which I monitored changes in buds and expanding foliage of white spruce seedlings during bud burst. I similarly monitored changes in buds and expanding foliage of mature white spruce trees during bud burst. For each experiment, I measured lignin and cuticular wax deposition in developing needles using multiple histochemical methods. I also extracted and quantified cuticular wax from buds and expanding foliage and measured wax metabolite profiles using gas chromatography-mass spectrometry (GC-MS). Lastly, I compared this data to additional measurements of mechanical toughness of the same expanding foliage.

In Chapter 6, I summarize the findings of my thesis research in the context of the hypotheses that I tested and describe how this work has contributed to an improved understanding of conifer defenses.

Chapter 2: Water deficit accentuates pre-existing differences in phloem defense strategies of lodgepole and jack pine to challenge with *Grosmannia clavigera*

2.1 Introduction

The current mountain beetle (MPB, *Dendroctonus ponderosae* Hopkins) outbreak is estimated to have caused large-scale mortality of approximately 27 million ha. Of pine forests in western North America, including more than 20 million ha. In the Canadian provinces of British Columbia and Alberta (Hart et al. 2015, Hodge et al. 2017). Over the course of the outbreak, MPB has undergone large-scale range expansion from south and central British Columbia, where it has historically attacked lodgepole pine (*Pinus contorta* Dougl. ex Loud. var. *latifolia* Engelm.), eastwards into the boreal forests of Alberta. Here, MPB has encountered a novel host, jack pine (*Pinus banksiana* Lamb.; Cullingham et al. 2011), which represents a potential gateway into eastern Canada.

MPB is associated with several Ophiostomatoid fungal species, which are assumed to assist in attack by weakening tree host defenses while also providing a nutritional source for MPB through acquisition of resources such as nitrogen from the pine host (Six and Wingfield 2011, Goodsman et al. 2012). While the role of fungal associates in MPB mass attack is not yet understood, their introduction to pine hosts by MPB nonetheless contributes to eventual tree host mortality by growing into host sapwood tissue and blocking transport of water through occlusion of ray parenchyma and tracheids (Ballard et al. 1982, Solheim and Krokene 1998, Lee et al. 2006). *Grosmannia clavigera* [Robinson-Jeffrey and Davidson] Zipfel, de Beer and Wingfield is considered one the most virulent MPB fungal associates (Rice et al. 2007a) and is capable of killing pine in the absence of MPB (Yamaoka et al. 1995).

Conifer trees rely on a wide array of constitutive and induced defenses to defend against MPB and its fungal associate *G. clavigera*. The presence of chemical defenses such as phenolic and terpenoid compounds can act to contain or impede movement of invaders, and expression of pathogenesis response (PR) proteins such as chitinases, osmotins and defensins all play important anti-microbial roles contributing to tree host defense response (Neuhaus 1999, Keeling and Bohlmann 2006a). Previous research has shown that lodgepole pine and jack pine differ in monoterpene profiles (Clark et al. 2014, Cale et al. 2017) and induction of monoterpenes in response to *G. clavigera* (Arango-Velez et al. 2016). Composition of defense metabolites, both constitutive and induced, can influence host quality and is an important factor for predicting MPB selection and reproductive success in novel hosts (Krokene 2015, Raffa et al. 2016, Biedermann et al. 2019). Induction of host defenses is initiated through hormonal signalling following invasion, and the ethylene-JA pathway is generally invoked in response to challenge by necrotrophic pathogens (Glazebrook 2005, de Vries et al. 2018). We have previously demonstrated that *in vivo* levels of JA-Ile increase in both lodgepole and jack pine seedlings in response to challenge by *G. clavigera,* providing evidence that *G. clavigera* is a necrotrophic pathogen (Arango-Velez et al. 2016). Additionally, exogenous application of JA has been associated with the induction of anatomical and chemical defenses such as the formation of traumatic resin ducts and accumulation of terpenoid compounds in conifers (Hudgins and Franceschi 2004, Krokene, Nagy, and Solheim 2008, Lundborg et al. 2019), similar to pine defenses observed in response to MPB and *G. clavigera*.

Ecological studies suggest that trees subjected to abiotic stresses such as drought are more susceptible to MPB attack, particularly at sub-epidemic populations (McDowell et al. 2008, Breshears et al. 2009, Safranyik et al. 2010), as drought-induced stomatal closure can deplete

carbohydrate stores and limit resources for carbon-based defenses (Stamp 2003). Higher densities of attacking MPB are required to overcome the critical threshold of resistance in healthy and vigorously growing tree hosts, whereas lower densities are sufficient to overcome resistance of physiologically stressed trees (Berryman 1982, Boone et al. 2011). Several regions of North America, including northern Alberta where the MPB epidemic is still active, have experienced periods of drought over the past two decades (Hogg and Michaelian 2015), and it is expected that many trees in these regions are experiencing water deficit conditions as a result.

Lodgepole and jack pine are often found in areas with contrasting climate moisture indices (Cullingham et al. 2012), with jack pine generally occupying drier, more sandy sites than lodgepole pine (Lotan and Critchfield 1990, Rudolph and Laidly 1990, Rweyongeza et al. 2007). Differences in adaptive water strategies between species may influence resource allocation to defense during periods of drought (Stamp 2003). Our previous studies revealed that water-limited lodgepole pine seedlings exhibit more conservative water use strategies than water-limited jack pine (Arango-Velez et al. 2016). Molecular studies have shown that water deficit conditions influence the defense response of lodgepole x jack pine hybrids to *G. clavigera*, attenuating some induced defenses while increasing some constitutive defenses, altering the transcript abundance of biotic stress response genes and reducing the number traumatic resin ducts appearing in xylem tissue (Arango-Velez et al. 2014). Further studies have also shown that water deficit conditions influence monoterpene levels and abundance of resin ducts differently between lodgepole and jack pine seedlings (Arango-Velez et al. 2016).

Understanding how molecular responses of lodgepole pine and jack pine hosts differ to *G. clavigera* challenge when faced with water deficit conditions can provide much-needed insight on the mechanisms by which drought impacts host quality both across and between

species. In this study, we use transcriptomics together with quantification of phenolic defenses in lodgepole pine and jack pine seedlings subjected to differential water availability and pathogen challenge to test the hypotheses that (1) lodgepole pine and jack pine display quantifiably different responses to *G. clavigera* challenge; (2) induced defense responses will be attenuated under water deficit conditions in both species; and (3) water deficit will exert a greater effect on induced responses of lodgepole pine than jack pine, given that jack pine shows greater adaptation to habitats with lower water availability.

2.2 Materials and Methods

2.2.1 Plant Material

Two independent experiments were conducted for this study, following essentially the same experimental design and methods. Experiment 1, used to generate materials for microarray and quantitative RT-PCR (qRT-PCR) analyses, has been described in detail in Arango-Velez et al. (2016). This experiment was conducted with lodgepole pine seedlings originating from a west central Alberta provenance and jack pine seedlings originating from an Ontario provenance. Experiment 2 was used to generate materials for physiological and metabolite analyses. Experiment 2 was conducted with lodgepole pine seedlings originating from the same west-central Alberta provenance and jack pine seedlings originating from a central Saskatchewan provenance. Seedlings were obtained as dormant one year old material and transplanted into 3.78 L pots (Beaver Plastic Ltd, Acheson, Alberta, Canada) with Sunshine Mix #4 growing media (Sun Gro Horticulture, Seba Beach, Alberta Canada), and grown in controlled environment growth rooms with 19 °C (day/night) temperature, 20-35% relative humidity, 16 h day/ 8 h night photoperiod, and ca. 200 µmol photosynthetically active radiation. Seedlings were watered twice a week and fertilized once a week to field capacity with a 500 mg L^{-1} solution of 20-20-20 (N-P-

K) fertilizer (Plant Products Ltd, Brampton, Ontario, Canada). Once seedlings were approximately two months into their second growth cycle, the most vigorously growing seedlings were selected for the experiments and randomly assigned into treatment groups. For both Experiment 1 and 2, full factorial experiments were carried out with (a) two species, lodgepole and jack pine; (b) two levels of water availability, well-watered (>50% relative water content, RWC_{soil}) or water deficit (approximately 20% RWC_{soil}); (c) three inoculation treatments, untreated control, mechanically wounded (i.e., mock-inoculated), or *Grosmannia clavigera*-inoculated; and (d) four time points, 1, 7, 14 and 28 days post-inoculation (dpi), using a complete randomized block experimental design. The unit of replication was defined as the individual, independent seedling. Because provenance materials were used for these experiments, there is a low probability of kinship between individual seedlings.

Differential water availability treatments were applied to plants one week in advance of inoculation treatments as described in Arango-Velez et al. (2016). Soil relative water content was measured using a time domain reflectometer (Tektronix 1502B Cable TDR Cable Tester, Tektronix, Inc., Scarborough, Ontario, Canada) and values calculated according to (Arango-Velez et al. 2011).

Fungal culturing and inoculation was performed as outlined in Arango-Velez et al. (2016). In brief, a *G. clavigera* spore suspension of approximately 140 spores μL^{-1} suspended in deionized water was prepared from the isolate M001-03-03-07-UC04DL09 described in Roe et al. (2010), originally cultured from a host located near Fox Creek, Alberta (54°24'N, 116°48'W). Spores were injected into the cambial region of inoculated seedlings using a 23GI PrecisionGlide™ needle (Becton, Dickinson and Company Mississauga, Ontario) at 3-4cm intervals along the stem. Mechanical wounding (mock inoculation) was performed using the

same syringe procedure but without inoculation with the spore suspension, while control trees were both unwounded and uninoculated.

At each time point, bark was collected from treatment seedlings by peeling it away from the xylem at the cambial zone along the regions of the stem that were *G. clavigera*- or mock-inoculated, or along the equivalent region for control seedlings, and flash frozen in liquid nitrogen before transferring to -80ºC for long term storage. Because most of the living tissue within the bark of these trees in their second growth cycle comprises secondary phloem, these bark samples are referred to as phloem through the remainder of the paper.

2.2.2 RNA Extractions

Frozen tissue samples were ground to a fine powder using a Retsch Mixer Mill (Verder Scientific, Newtown, PA, USA). Total RNA was extracted from ~100 mg frozen tissue according to Pavy *et al*. (2008), quantified using a NanoQuant 200 (Tecan Infinite® Morrisville NC, USA) and assessed with a 2100 Bioanalyzer (Agilent, Mississauga, ON, Canada).

2.2.3 cDNA Microarray Transcript Profiling

Transcriptome analyses of lodgepole and jack pine samples harvested at 1 dpi and 7 dpi were carried out using loblolly pine heterologous cDNA microarrays. The use of heterologous arrays enabled analysis of transcriptomes from both lodgepole pine and jack pine with a single array, which in turn enabled inferences about putative orthologous sequences. Probe preparation, microarray hybridizations and data extraction were carried out essentially as described in El Kayal et al. (2011). Two micrograms of total RNA were used for amino allyl antisense RNA (aRNA) amplification procedures following the manufacturer's protocol (Superscript Indirect RNA Amplification System, Invitrogen, Carlsbad, CA, USA), followed by direct labelling of 5 µg aRNA with Alexa Fluor® 555 or 647 dyes (Invitrogen). Labelled probes were hybridized

according to Pavy *et al*. (2008) to PtGen2 loblolly pine cDNA microarrays (Lorenz *et al.* 2009, 2011). Each array contained 26,946 total spots (minus buffer blanks and duplicate spots), including 25,848 loblolly pine cDNAs generated from root, stem, and needle tissues (Lorenz *et al.* 2009, 2011). *G. clavigera*-inoculated samples were co-hybridized either with the corresponding mock-inoculated sample or control untreated samples. Mock-inoculated samples were also co-hybridized with corresponding control untreated samples. Four independent biological replicates were hybridized for each treatment, with two biological replicates used in reciprocal dye swaps.

Microarray images were obtained using a GenePix 4000B microarray scanner and data extracted with GenePix Pro 6.0 software using the adaptive circle method (Axon Instruments, Sunnyvale, CA, USA) according to El Kayal *et al.* (2011). Following filtering of low quality signals, background removal, within-array normalization and multiple quality inspection checks as described in El Kayal *et al.* (2011), statistically differentially expressed (DE) sequences were determined using the linear models for microarray data (LIMMA; Smyth 2005) and exploratory analysis for two-colour spotted microarray data (marray; Yang and Paquet 2005) packages from BioConductor (Gentleman et al. 2005) in R v3.0.2 (R Core Team 2013), using a Benjamini-Hochberg adjusted *p*-value of 0.05 (Benjamini and Hochberg 1995). Statistically DE sequences were further filtered to include only sequences with fold change values greater than 1.5 or smaller than 0.6.

Lodgepole and jack pine transcriptomes (Hall *et al.* 2013) were mapped to the microarray by using BLASTx (Camacho *et al.* 2009) to identify the lodgepole and jack pine contigs with the highest similarity to the loblolly pine probe sequences represented on the array. A total of 11,032 loblolly pine probe sequences showed high similarity to at least one lodgepole and/or jack pine

contig, of which one for each species was designated as the putatively orthologous sequence to the loblolly pine probe. The putatively orthologous lodgepole and jack pine sequences were then annotated using the NCBI nr database (https://www.ncbi.nlm.nih.gov/nucleotide), and TAIR 7.0 (The Arabidopsis Information Resource, Berardini *et al*. 2015). Functional categories or 'bins' were assigned using the Mercator Automated Sequence Annotation Pipeline for the loblolly pine sequences, and these data were used to visualize functional categorization of differentially expressed genes using MapMan (Usadel et al. 2009, Lohse et al. 2014).

Gene enrichment analyses using a hypergeometric distribution statistic with a Bonferroni correction to obtain adjusted *p*-values were performed according to Galindo González *et al.* (2012) by comparing MapMan categories of gene subsets to the categories of all lodgepole and jack pine sequences represented on the PtGen2 array. Select sequences were further characterized using manual annotation and phylogenetic analyses. Lodgepole and jack pine sequences were translated into amino acid sequences based on the longest open reading frame using the NCBI ORFfinder (www.ncbi.nlm.nih.gov/orffinder/), and aligned with amino acid sequences of functionally characterized genes from other species with the MAFFT server auto alignment function (v7; https://mafft.cbrc.jp/alignment/server/, Katoh et al. 2019). Amino acid substitution models and bootstrap consensus trees were calculated using the IQ Tree web server (http://iqtree.cibiv.univie.ac.at/; Trifinopoulos et al. 2016, Kalyaanamoorthy et al. 2017) using default auto calculation options and Bayesian (BIC) selection criterion. Dendrograms were visualized in Geneious 2021.1.1 (www.geneious.com). Heatmaps were generated using R v4.0.3 (R Core Team 2020), RStudio v1.4.1106 (RStudio Team 2020) and the gplots package v3.1.1 (Warnes et al. 2020). R files are available at https://github.com/c4tier.

2.2.4 qRT-PCR

Total RNA was treated with DNase I (New England Biolabs, Whitby, ON, Canada) prior to cDNA synthesis using Invitrogen™ Superscript™ II Reverse Transcriptase (Thermo Fisher Scientific, Mississauga, ON, Canada), following the manufacturers' protocols. qRT-PCR primers (Supplemental Table 1) were designed using Primer Express 3.0 (Applied Biosystems, Thermo Fisher Scientific). qRT-PCR reactions and standard curve quantification were performed essentially according to El Kayal *et al*. (2011), with six biological replicates and two technical replicates for each treatment. *Eukaryotic translation initiation factor 5A-1* (*TIF5A*; accession number KF322083), which had been previously tested and validated for *G. clavigera*-challenged lodgepole x jack pine (Arango-Velez et al. 2014) was validated as an appropriate reference gene for the experimental material used in this study (Appendix 1 Figure 1).

Statistical analyses were performed using R v4.0.3 (R Core Team 2020) and RStudio v1.4.1106 (RStudio Team 2020). Normalized data for each gene were fit to a generalized linear model; formulas used for each dataset are summarized in Appendix 1. Assumptions of normality and homoscedascity were assessed visually as well as with Shapiro-Wilks and Bartlett tests. Analysis of deviance, including Wald's chi square test statistics and Pearson's error estimate, was calculated from GLMs using the car package v3.0-11 (Fox and Weisberg 2019). Estimated marginal means were calculated to determine significant differences between modeled groups using the emmeans package v1.5.3 (Lenth 2020), and letters were assigned using the multcomp package v1.4-15 (Hothorn et al. 2008). Datasets were visualized using the ggplot2 v3.3.3 (Wickham 2016) and cowplot v1.1.1 (Wilke 2020) packages. R files are available at https://github.com/c4tier.

2.2.5 Metabolite Profiling

Approximately 100 mg of ground phloem tissue was extracted using 1 mL HPLC-grade methanol (Thermo Fisher Scientific). Tissue was suspended by vortexing, then shaking, covered, and incubated at 4ºC for 1 h. Twenty-five microlitres of 4 mg/mL gallic acid monohydrate (Sigma-Aldrich Cat. 398225) was added as an internal standard prior to centrifuging for 15 minutes at 22,000 g. The supernatant was collected, and the pellet re-extracted three times, with the four resulting supernatants pooled prior to evaporating to dryness under nitrogen. Residues were stored at -20ºC for up to one month prior to analyses. Residues were resuspended in 200 uL methanol, vortexed, and filtered through an Ultrafree-MC 0.2 µm PTFE centrifugal filter (EMD Millipore Cat. UFC30LG25).

Ten microlitres of filtered sample were injected onto a Luna 5 µm C18(2) 100 Å 250 x 4.6 mm column (Phenomenex Cat. 00G-4252-E0) and separated using an Agilent 1200 series HPLC. Mobile phase flow rate was 1 mL min^{-1} and column temperature maintained at 25°C (± 8°C). Extracts were separated using a gradient modified from Lin and Harnly (2012), where formic acid (0.2%, v/v, in HPLC-grade water, Thermo Fisher Scientific) and acetonitrile (Thermo Fisher Scientific) represent mobile phases A and B, respectively, in the following elution profile: 0 to 35 min, 5% to 20% B in A; 35 to 65 min, 20% to 65% B; 65 to 80 min, 79% B; 80 to 90 min, 100% B; 95 to 100 min, 0% B to recover column. Eluting compounds were measured by diode array detector (Agilent G1315C) at 270 nm.

The following standards (Sigma-Aldrich) were used for identification based on retention time similarity: coniferyl alcohol (Cat. 223735), dihydromyrcetin (Cat. SML0295), taxifolin (Cat. 78666), pinoresinol (Cat. 40674), p-coumaroyl alcohol (Cat. PHL82506), pinosylvin (Cat. 56297), (±)-dihydrokaemperol (Cat. 91216), kaempferol 3-glucoside (Cat. 04500585), trans-cinnamic acid (Cat. C80857), p-coumaric acid (Cat. C9008), dihydromyricetin (Cat. SML0295),

coniferyl alcohol (Cat. 223735), matairesinol (Cat. 40043), and quercetin 3-glucoside (Cat. 16654). Additionally, (+)-catechin hydrate (Fisher Cat C07051G) was included as a standard.

Metabolite data analysis was carried out using R v4.0.3 (R Core Team 2020) and RStudio v1.4.1106 (RStudio Team 2020). Peaks with sufficient resolution and consistency between technical replicates that were detectable in at least three out of four biological replicates and in at least one treatment were selected for further analysis (Appendix 1 Figure 2). Non-metric multidimensional scaling (NMDS) was run using the vegan package v2.5-7 (Oksanen et al. 2020). Ordination plots were generated using the ggplot2 v3.3.3 (Wickham 2016) and ggord v1.1.5 (Beck 2020) packages, and statistical differences between treatments were determined using the analysis of similarities (ANOSIM) test (Clarke 1993) within the vegan package. Individual compound data were fit to generalized linear models, and formulas for each compound are summarized in Appendix 1. Total phenolics were calculated as the sum of all compounds selected for ordination. Models were analyzed using the same methods as the qRT-PCR data and visualized using the same packages. R files are available at https://github.com/c4tier.

2.3 Results

2.3.1 Effect of water availability on pine physiology

Consistent with our previous findings in which we showed a significant effect of the imposed water deficit treatment from Experiment 1 on parameters such as photosynthesis, stomatal conductance, and water use efficiency (WUE) in lodgepole and jack pine seedlings (Arango-Velez et al. 2016), the degree of water deficit imposed in Experiment 2 was sufficient to impact WUE in both lodgepole and jack pine relative to well-watered conditions (Appendix 1 Figure 3). WUE increased significantly in water deficit jack pine seedlings compared to well-

watered control trees at 7 dpi (uninoculated control z = -3.91, $p < 0.001$; *G. clavigera*-inoculated z = -3.24, $p = 0.001$) and well-watered *G. clavigera*-inoculated trees at 35 dpi (z = -3.23, $p = 0.001$). WUE of water deficit lodgepole pine seedlings significantly increased in trees that were also inoculated with *G. clavigera* at 7 dpi (z = -2.629, $p = 0.009$) and 35 dpi (z = -2.79, $p = 0.005$), but not at 14 dpi (z = -1.44, $p = 0.15$). Furthermore, WUE of *G. clavigera*-inoculated lodgepole pine trees was significantly higher than controls under well-watered and water deficit conditions at 35 dpi (well-watered z = -2.29, $p = 0.02$; water deficit z = -3.51, $p < 0.001$), while no significant differences in WUE were observed between inoculation treatments in jack pine (Appendix 1 Figure 3).

2.3.2 Transcriptome profiling of lodgepole and jack pine gene expression in response to G. clavigera *and water availability*

Several experimental optimizations, together with data quality checks, were performed to ensure that labelled lodgepole and jack pine probes hybridized with consistency to the loblolly pine cDNA heterologous microarray, and that there were no systemic biases in labelling or hybridization efficiencies between treatments or species. Given that no or very few DE sequences were detected between untreated control versus mock-inoculated (wounded) samples for any treatment combination, and that *G. clavigera*-inoculated versus untreated control and *G. clavigera*-inoculated versus mock-inoculated comparisons for any treatment combination yielded essentially the same significantly DE sequences, only *G. clavigera*-inoculated *versus* untreated control comparisons are presented.

Enrichment analyses using MapMan functional classes annotated using Mercator revealed statistical overrepresentation of DE sequences for a small number of bins in both lodgepole and jack pine (Figure 2.1). Sequences associated with secondary metabolism were

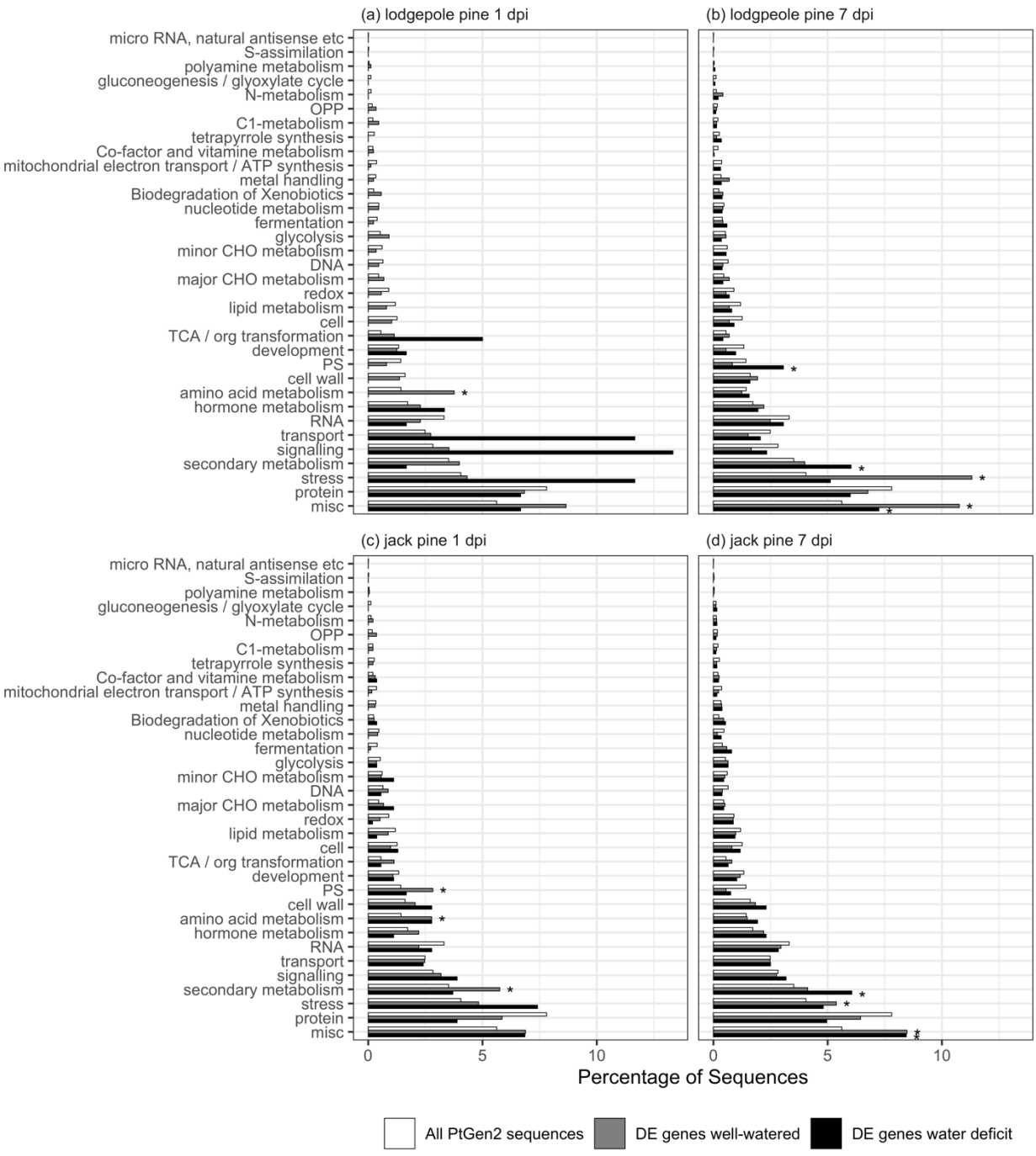

Figure 2.1. Enrichment analyses of sequences DE in response to *G. clavigera* inoculation in lodgepole pine (a, b) and jack pine (c, d) show enrichment of secondary metabolism and stress annotations under water deficit and well-watered conditions, respectively. DE sequences were annotated into functional categories using Mercator. Asterisks (*) represent significant over-representation of categories of DE sequences relative to all sequences on the array, based on a hypergeometric distribution probability statistic (adjusted $p < 0.001$).

significantly enriched in both *G. clavigera*-inoculated lodgepole and jack pine under water deficit conditions at 7 dpi, whereas in jack pine, sequences associated with secondary metabolism in 1 dpi well-watered samples were also significantly enriched. At 7 dpi, both lodgepole and jack pine stress-related annotations were enriched under well-watered conditions (Figure 2.1).

Venn diagrams were used to identify overlapping and distinct sets of DE sequences between species and water availability conditions at 1 and 7 dpi (Figure 2.2). In these analyses, lodgepole and jack pine sequences hybridizing to the same spotted cDNA probe on the microarray were inferred to be putative orthologues. Over half of the sequences that were DE at 1 and/or 7 dpi under well-watered conditions were unique to jack pine, while a sizeable proportion of the remaining DE sequences were putative orthologues that were DE in both lodgepole and jack pine (Figure 2.2a). A similar number of putative orthologues were DE in both species under water deficit and well-watered conditions, including many defense-related sequences DE in both species at 7 dpi (Appendix 1 Table 2). However, under water deficit, far fewer sequences were uniquely DE in *G. clavigera*-inoculated jack pine seedlings, and far more sequences were uniquely DE in *G. clavigera*-inoculated lodgepole pine relative to well-watered conditions.

Four-way Venn diagrams further revealed that, in lodgepole pine, approximately half (53%) of sequences were DE at 7 dpi under well-watered conditions (Figure 2.2b), while this proportion increased to 88% of DE sequences in *G. clavigera*-inoculated seedlings under water deficit (Figure 2.2c). In contrast, jack pine exhibited fewer DE sequences at 7 dpi under water deficit relative to well-watered conditions (Figure 2.2d), and a much larger number of sequences DE across water treatments compared to lodgepole pine seedlings (Figure 2.2e).

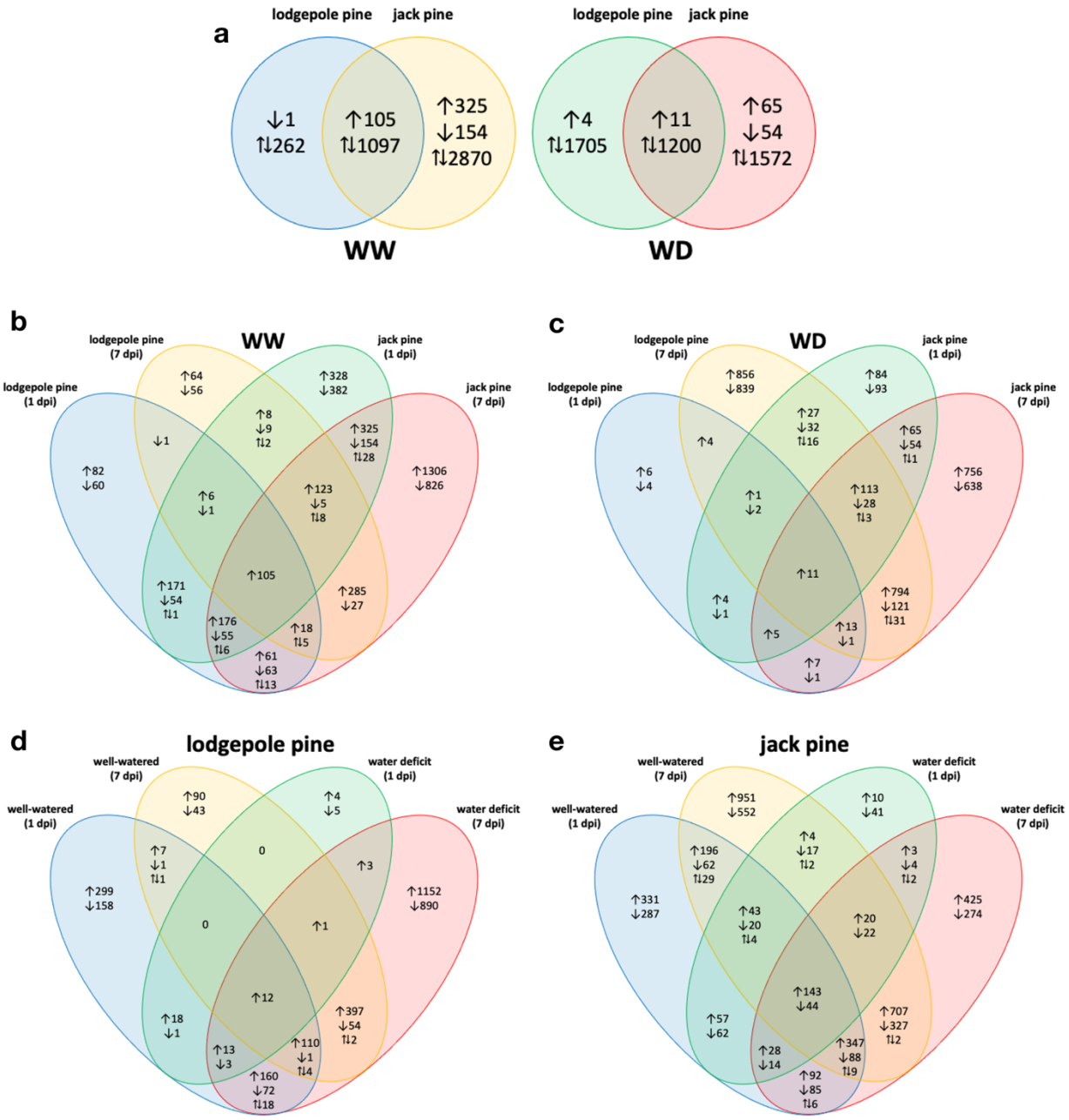

Figure 2.2. Venn diagrams illustrating shared and unique DE sequences in *G. clavigera*-challenged lodgepole and jack pine. a Comparison of sequences DE at 1 dpi and/or 7 dpi between lodgepole and jack pine. **b,c** Shared and distinct DE sequences between lodgepole and jack pine under well-watered (WW; **a**) or water deficit (WD; **c**) conditions. **d,e** Shared and distinct DE sequences in lodgepole pine (**d**) or jack pine (**e**) under well-watered vs water deficit conditions. Up arrows indicate significant upregulation relative to controls; down arrows indicate

significant downregulation relative to controls. A combination of up plus down arrows indicates sequences that showed different regulation at 1 and 7 dpi.

Secondary metabolism annotations were significantly enriched in many of the Venn diagram comparisons in Figure 2.2, including in lodgepole and jack pine sequences DE only in water deficit conditions (Appendix 1 Table 3). Given the possibility of redundancy in cDNA probe sequences on the array, the number of non-redundant annotations related to flavonoid, isoprenoid, and phenylpropanoid biosynthesis was determined by choosing a single representative sequence from the PtGen2 array for DE sequences with identical annotations and expression profiles (Appendix 1 Table 4). Under well-watered conditions, most flavonoid, isoprenoid or phenylpropanoid biosynthesis DE sequences were DE only in *G. clavigera*-inoculated jack pine, whereas under water deficit conditions, a greater proportion of sequences were DE in both lodgepole and jack pine (Appendix 1 Table 4).

To better understand how *G. clavigera* challenge and water deficit altered the composition of defense responses in lodgepole vs. jack pine, we looked further at the timing of differential expression for defense-related sequences. These included pathogenesis-related (PR) proteins such as chitinases, secondary metabolism including flavonoid and isoprenoid biosynthesis, ethylene and jasmonic acid signalling genes and defense-associated transcription factors (Appendix 1 Tables 5-6). Under well-watered conditions, several osmotins were DE earlier in lodgepole pine than in jack pine (Appendix 1 Tables 5), while a collection of dirigent-like, chitinase, and isoprenoid sequences were DE earlier in jack pine than lodgepole pine under well-watered and water deficit conditions (Appendix 1 Tables 6). Most defense-related sequences that were DE later under water deficit relative to well-watered conditions were also DE in either lodgepole or jack pine rather than DE in both species (Appendix 1 Table 7).

2.3.3 Influence of G. clavigera *and water availability on expression of key defense-associated genes*

Building upon these global assessments of water deficit-modulated changes to lodgepole and jack pine gene expression responses to *G. clavigera* challenge, we next mined the transcriptome data for gene families associated with three important components of the conifer defense arsenal – chitinases, terpenoids and phenolics – to ascertain whether expression profiles for these genes showed an overall pattern of reduced *G. clavigera* induction in water-deficit plants. Lodgepole and jack pine putative orthologues having annotations associated with one of these three categories were further characterized using phylogenetic analyses and diagnostic motif identification to provide additional confidence in the BLAST annotations. Quantitative RT-PCR was used both to validate microarray expression profiles for subsets of these sequences (Appendix 2 Figure 2) as well as to develop more detailed transcript abundance profiles of constitutive and *G. clavigera*-induced expression for these genes by including mock-inoculated samples and additional time points.

Microarray data mining revealed that several class I, IV and VII chitinase sequences were significantly upregulated in both lodgepole and jack pine in response to *G. clavigera* inoculation, particularly at 7 dpi (Figure 2.3). A greater proportion of chitinases were significantly DE at 1 dpi in jack pine relative to lodgepole pine, with several of these being significantly upregulated only under well-watered conditions (Figure 2.3). All chitinase sequences that were significantly DE at 1 dpi were also significantly DE at 7 dpi: most were significantly DE under both well-watered and water-deficit conditions.

Consistent with the microarray data, qRT-PCR analyses for a subset of lodgepole and jack pine chitinases showed significant upregulation of Class I and Class IV chitinases in

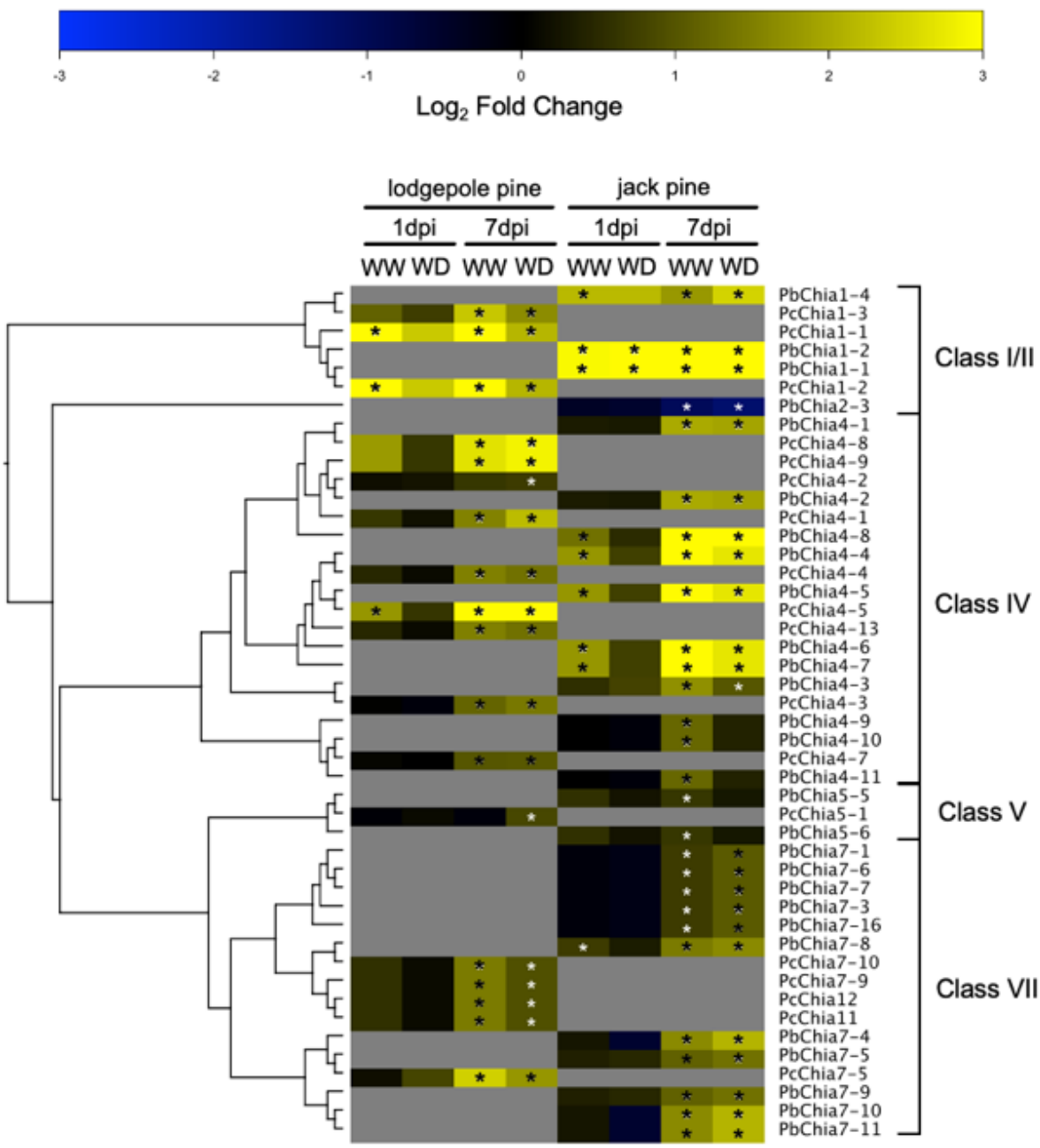

Figure 2.3. Transcript abundance profiles of chitinases (*Chia*) using microarrays illustrate strong increases in transcript abundance in response to *G. clavigera* challenge at 7 dpi for several classes of chitinases under well-watered (WW) and water deficit (WD) conditions. Lodgepole (Pc) and jack pine (Pb*)* chitinases DE in at least one treatment are ordered along the Y-axis of the heatmap based upon phylogenetic relationships determined by maximum likelihood analysis. Yellow and blue indicate higher or lower transcript abundance in *G. clavigera*-challenged seedlings relative to controls, respectively, depicted on a $\log_2$ scale. Asterisks (*) mark sequences significantly DE between *G. clavigera*-inoculated and control

samples (adjusted $p < 0.05$, n = 4). Since transcript abundance data for a given chitinase of only one species is indicated in each row of the heat map, grey shading is used as counterbalance for the other species.

response to *G. clavigera* inoculation at 1, 7, 14 and/or 28 dpi relative to control untreated samples (Figure 2.4). Overall patterns of chitinase gene expression in response to *G. clavigera* and water availability were similar between putative lodgepole and jack pine orthologues, although in many cases the magnitude of transcript abundance was greater for jack pine than for lodgepole pine. Class II chitinases showed limited response to *G. clavigera* inoculation, and Class VII chitinases did not respond significantly to *G. clavigera* inoculation. While Class I chitinases showed significant upregulation in response to *G. clavigera* across all or nearly all time points including 1 dpi, Class IV chitinases showed significant upregulation only by 7 dpi, and in some cases expression levels returned to levels comparable to control samples by 28 dpi. Class I chitinases were also significantly upregulated by the mock (wounding only) treatment at 1 dpi, while Class IV chitinases were not responsive to mock inoculation. In several cases, *G. clavigera*-induced increases in chitinase transcript abundance under water deficit conditions were less than that under well-watered conditions, but apart from *PcChia4-1,* the differences were not statistically significant (Appendix 1 Table 9).

Given the established importance of terpenoid biosynthesis to conifer defense against pests and pathogens (Kolosova and Bohlmann 2012), and given the prominence of isoprenoid-related annotations in our global analyses (Appendix 1), we next mined expression profiles for DE terpene synthases. Putative sesquiterpene and diterpene synthase sequences showed similar expression profiles in both lodgepole and jack pine seedlings; most of these sequences were strongly upregulated at 7 days post-inoculation regardless of water treatment (Figure 2.5). A subset of sesquiterpenes synthases, and all pinene synthases, were upregulated in jack pine at 1

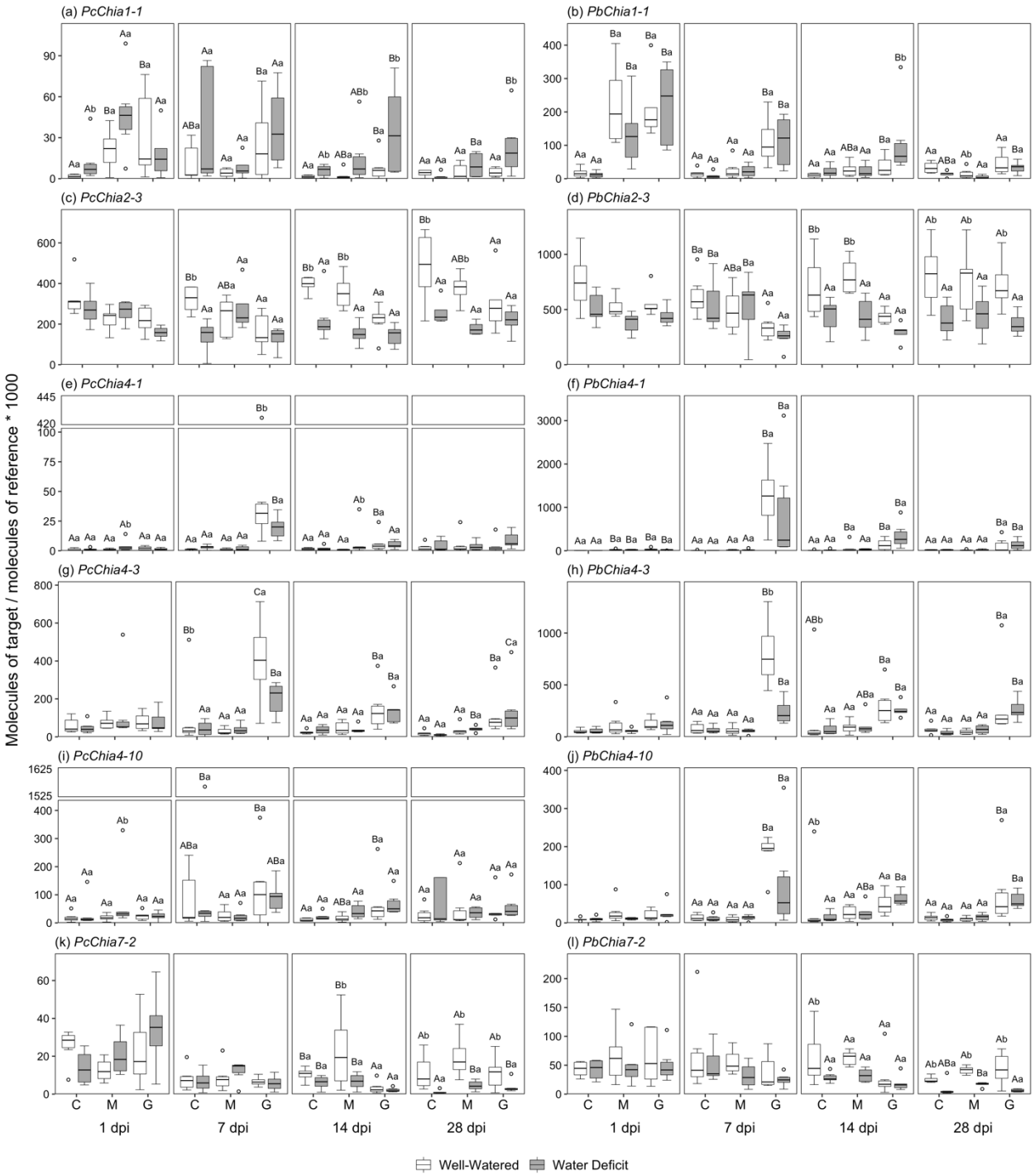

Figure 2.4. qRT-PCR transcript profiling reveals several chitinases (*Chia*) that respond to G. clavigera inoculation, with water availability modulating expression of a subset of these chitinases. Chitinase expression profiles of well-watered (white boxes) and water deficit (grey boxes) lodgepole (*Pc*) and jack pine (*Pb*) seedlings, grouped by uninoculated control (C), mock inoculation (M), or *G. clavigera* inoculation (G). Within each time point, capitalized letters

indicate significant differences between inoculation treatments, while lower-case letters indicate differences between water treatments (adjusted $p < 0.05$, n = 5-6).

dpi in well-watered trees only. A few pinene synthases were also upregulated in well-watered lodgepole pine at 1 dpi or at 7 dpi in water deficit but were generally not differentially expressed in *G. clavigera*-challenged lodgepole pine (Figure 2.5).

Quantitative RT-PCR profiling of two pairs of putative α-pinene synthase orthologues revealed limited significant differences in transcript abundance between controls and *G. clavigera*-inoculated seedlings, largely due to high levels of variance between individuals (Figure 2.6). Jack pine *(-)-α-pinene synthase* and *(+)-α-pinene synthase* both exhibited reduced transcript abundance in response to *G. clavigera*-inoculation at 28 dpi. Although the decrease in *Pb(+)-α-pinene synthase* was not statistically significant under well-watered conditions (z = 1.33, $p = 0.38$), the effect of inoculation on both *a-pinene-synthase* genes was significant in jack pine only (*Pb(+)-a-pinene synthase* $\chi^2 = 14.57$, d.f. = 2, $p < 0.001$; *Pb(-)-a-pinene synthase* $\chi^2 = 15.93$, d.f. = 2, $p < 0.001$; Appendix 1 Table 10). Transcript abundances of *Pc(-)-α-pinene synthase* and *Pc(+)-α-pinene synthase* were significantly reduced at 14 dpi under water deficit, relative to well-watered trees inoculated with *G. clavigera* (*Pc(-)-α-pinene synthase* z = 3.06, $p = 0.002$; *Pc(+)-α-pinene synthase* z = 2.10, $p = 0.04$; Figure 2.6). In contrast, transcript abundances of *Pb(-)-α-pinene synthase* and *Pb(+)-α-pinene synthase* in trees inoculated with *G. clavigera* under water deficit were significantly lower than well-watered trees at 28 dpi (*Pb(-)-α-pinene synthase* z = 2.63, $p = 0.009$; *Pb(+)-α-pinene synthase* z = 2.40, $p = 0.02$; Figure 2.6)

Genes putatively involved in phenolic biosynthesis were profiled using the microarray data and overlaid with the biosynthetic pathway to visualize changes that may indicate shifts in flux though these pathways to change the phenolic compound profiles of the phloem (Figure

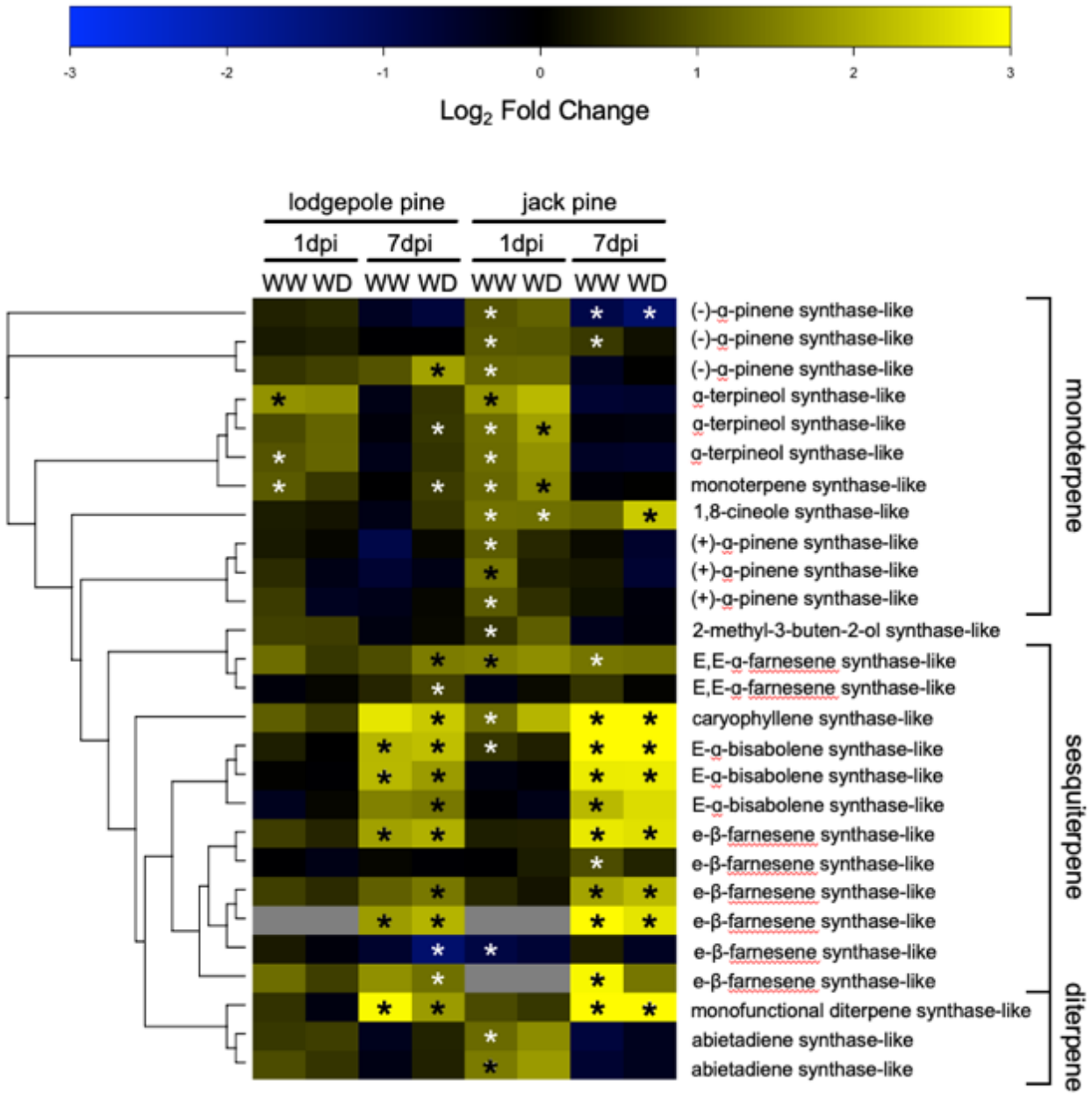

Figure 2.5. Microarray expression profiles of terpene synthases demonstrate different regulation patterns of monoterpene biosynthesis in lodgepole and jack pine seedlings inoculated with *G. clavigera* under well-watered (WW) or water deficit (WD). Terpene synthases DE in at least one treatment are ordered along the Y-axis of the heatmap based upon phylogenetic relationships determined by maximum likelihood analysis. Yellow and blue indicate higher or lower transcript abundance in *G. clavigera*-inoculated seedlings relative to controls, respectively, depicted on a $\log_2$ scale. Asterisks (*) mark transcripts significantly DE between control and inoculated samples (adjusted $p < 0.05$, n = 4). Since transcript abundance

data for a given chitinase of only one species is indicated in each row of the heat map, grey shading is used as counterbalance for the other species.

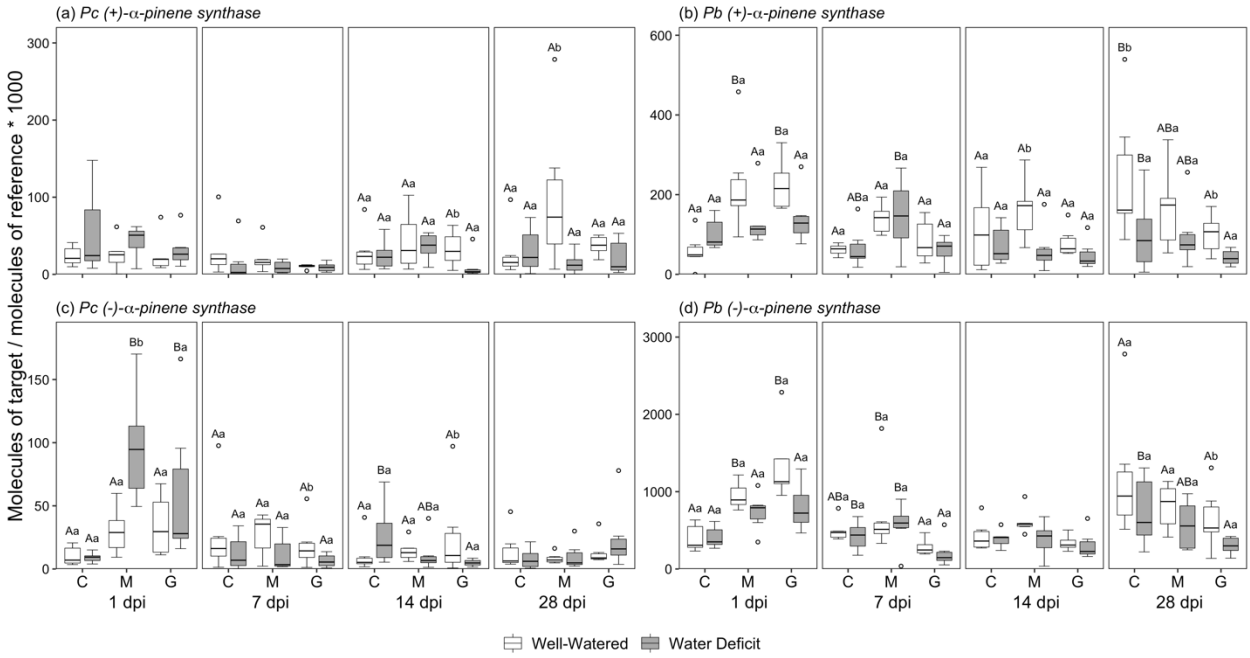

Figure 2.6. qRT-PCR transcript profiling of α-pinene synthases in lodgepole (*Pc*) and jack pine (*Pb*) seedlings inoculated with *G. clavigera* indicate more of an effect of water deficit on jack pine than lodgepole pine *a-pinene synthases*. Expression profiles of seedlings under well-watered (white boxes) and water deficit (grey boxes) conditions are grouped by control (C), mock-inoculation (M), or *G. clavigera*-inoculation (G) for each time point. Within each time point, capitalized letters indicate significant differences between estimated marginal means of inoculation treatments while lower-case letters indicate differences between water treatments (adjusted $p < 0.05$, n = 5-6).

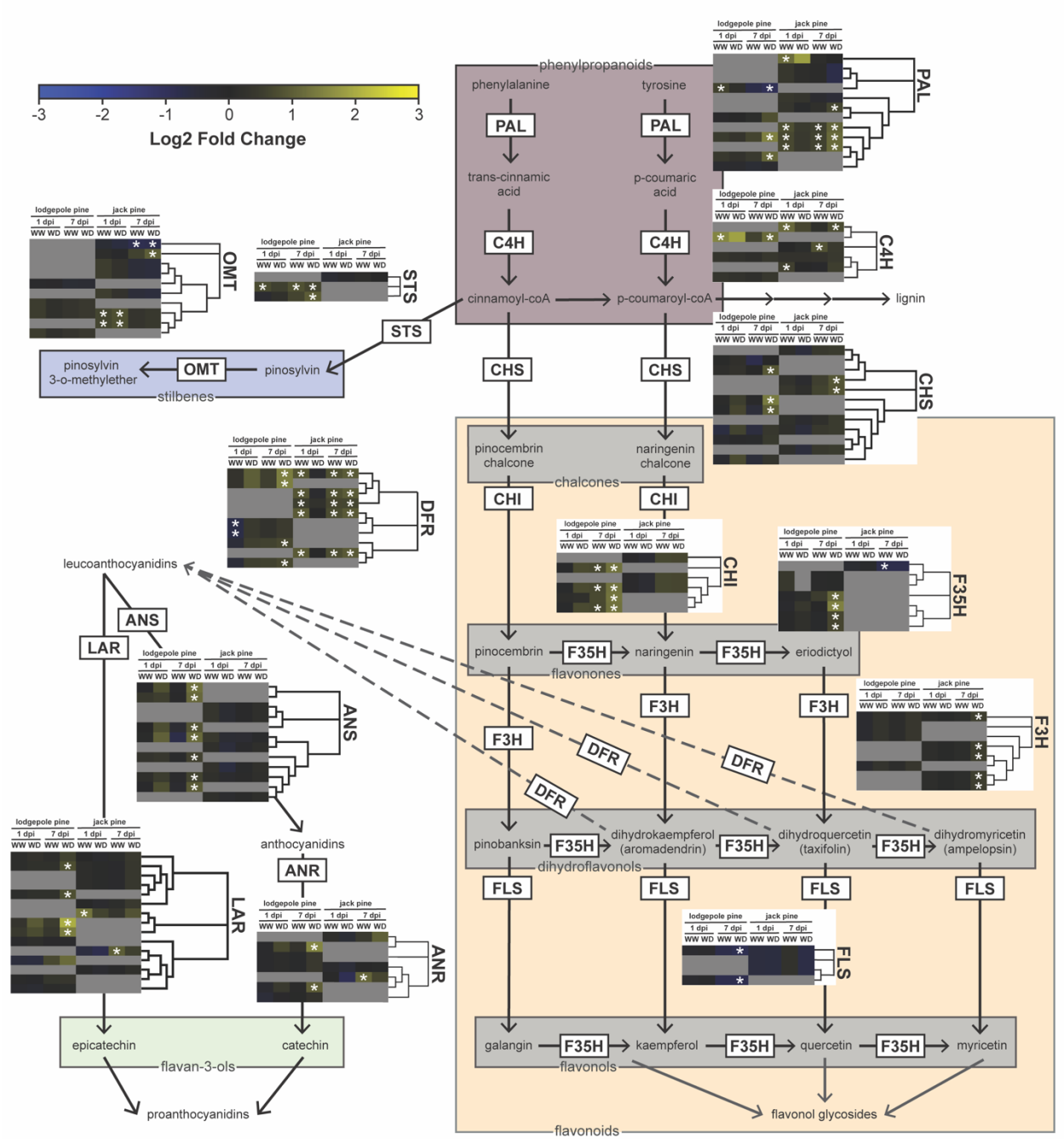

Figure 2.7. Expression of phenolic biosynthesis genes measured by microarray reveals shared and distinct responses to *G. clavigera* in lodgepole (*Pc*) and jack pine (*Pb*) seedlings, modulated by water deficit (WD). Sequences putatively encoding enzymes involved in phenolic biosynthesis are ordered along the Y-axis of the heatmap according to the phylogenetic relationship determined by maximum likelihood analysis. Yellow and blue indicate higher or lower transcript abundance in seedlings inoculated with *G. clavigera* relative to controls, respectively, depicted on a $\log_2$ scale. Asterisks (*) mark transcripts significantly DE between

control and inoculated samples (adjusted $p < 0.05$, n = 4). Since transcript abundance data for a given phenolic biosynthesis gene corresponding to only one species is indicated in each row of the heat map, grey shading is used as counterbalance for the other species. Enzymes include phenylalanine ammonia lyase (PAL), cinnamate 4-hydroxylase (C4H), stilbene synthase (STS), stilbene o-methyltransferase (OMT), chalcone synthase (CHS), chalcone isomerase (CHI), flavanone 3-hydroxylase (F3H), flavonoid 3,5-hydroxylase (F35H), flavanol synthase (FLS), anthocyanidin synthase (ANS), anthocyanidin reductase (ANR), leucoanthocyanidin reductase (LAR), dihydroflavonol reductase (DFR). WW = well-watered.

2.7). Mining of the transcriptomic data showed that many lodgepole and jack pine sequences encoding enzymes involved in key steps of the core phenylpropanoid, flavonoid, and stilbene biosynthetic pathways exhibited significant upregulation in response to *G. clavigera* inoculation at 7 dpi, mainly under water deficit conditions. A smaller number of sequences were DE at 1 dpi. There were notable differences in expression profiles of sequences encoding several phenolic biosynthesis enzymes between lodgepole and jack pine. For example, sequences encoding *flavonoid 3,5-hydroxylase (F35H)*, *anthocyanidin synthase (ANS)*, *chalcone isomerase (CHI)*, and *stilbene synthase (STS)* only showed significant upregulation in lodgepole pine, while *flavanone 3-hydroxylase (F3H)* and *stilbene o-methyltransferase (OMT)* sequences only showed significant upregulation in jack pine.

Expression profiles for select genes encoding enzymes at key branch points in these pathways were further examined using qRT-PCR (Figure 2.8). Quantitative RT-PCR transcript profiles largely reflected microarray transcript profiles (Appendix 1 Figure 4), although in some cases the changes in transcript abundance measured using qRT-PCR were not significant, potentially because different biological replicates were used. *G. clavigera* inoculation had a significant effect on *STS* expression in both lodgepole and jack pine relative to mock-inoculation, particularly under well-watered conditions (*PcSTS* 7 dpi well-watered $z = -4.79$, $p < 0.001$;

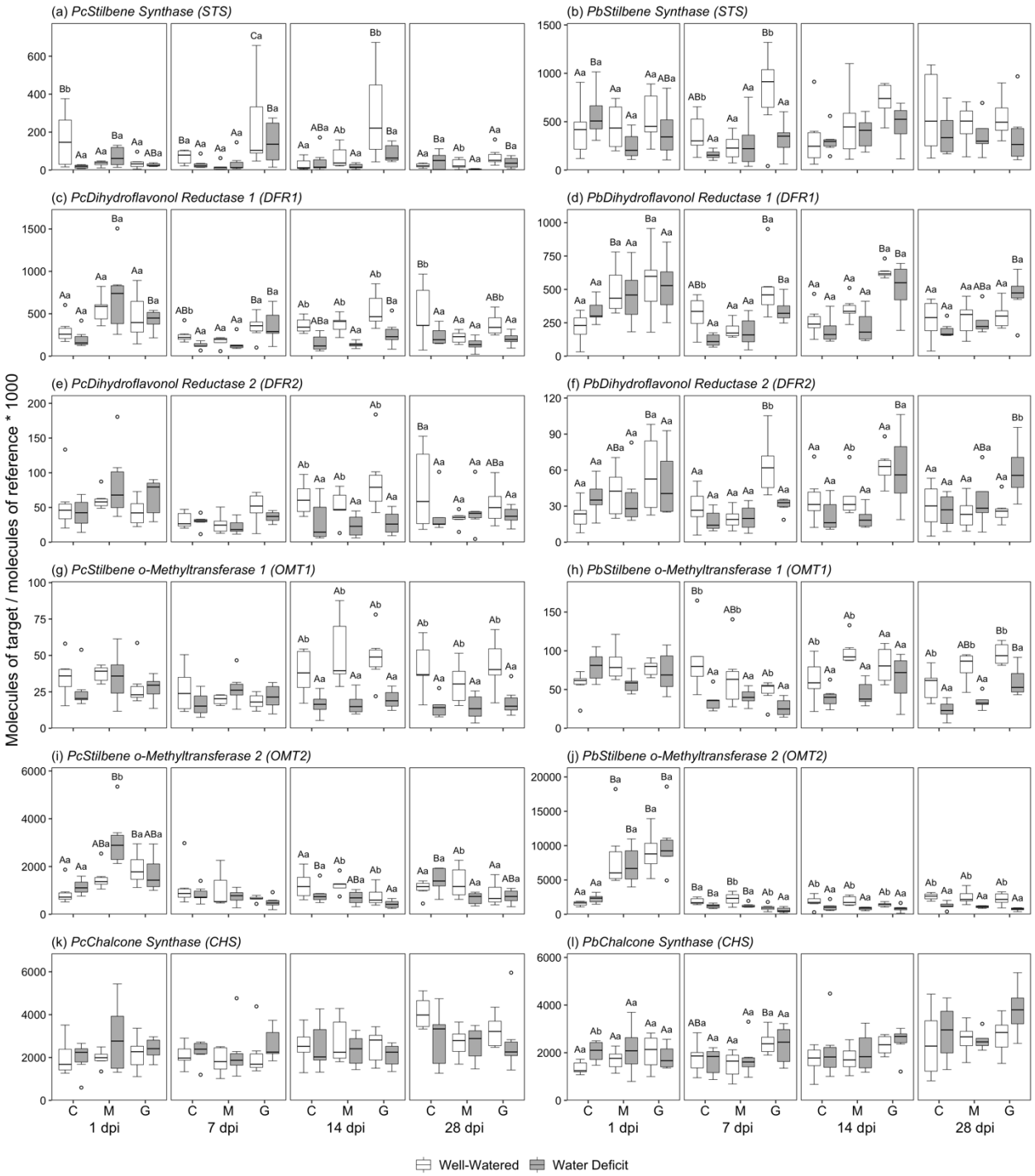

Figure 2.8. qRT-PCR transcript profiling indicates different phenolic biosynthesis genes respond to *G. clavigera*-challenge between lodgepole (*Pc*) and jack pine (*Pb*). Phenolic biosynthesis gene expression of well-watered (white boxes) and water deficit (grey boxes) seedlings are grouped by control (C), mock-inoculation (M), or *G. clavigera*-inoculation (G) for each time point. Within each time point, capitalized letters indicate significant differences

between estimated marginal means of inoculation treatments while lower-case letters indicate differences between water treatments (adjusted $p < 0.05$, n = 5-6).

PcSTS 7 dpi water deficit z = -2.64, $p = 0.02$; *PcSTS* 14 dpi well-watered z = -2.79, $p = 0.01$; *PcSTS* 14 dpi water deficit z = -3.03, $p = 0.007$; *PcSTS* 28 dpi water deficit z = -4.50, $p < 0.001$; *PbSTS* 7 dpi well-watered z = -3.51, $p = 0.001$; Figure 2.8). Several genes, including *DFR1*, *DFR2*, and *OMT1,* exhibited increased transcript abundance in response to *G. clavigera* inoculation in jack pine (*PbDFR1* 7 dpi well-watered z = -3.94, $p < 0.001$; *PbDFR1* 7 dpi water deficit z = -2.62, $p = 0.02$; *PbDFR1* 14 dpi well-watered z = -2.39, $p = 0.04$; *PbDFR1* 14 dpi water deficit z = -3.44, $p = 0.002$; *PbDFR2* 7 dpi well-watered z = -4.02, $p < 0.001$; *PbDFR2* 14 dpi water deficit z = -3.72, $p < 0.001$; *PbOMT1* 28 dpi water deficit z = -2.59, $p = 0.03$), but that were not observed in lodgepole pine or to a lesser extent. Decreases to constitutive and *G. clavigera*-induced expression of both *DFR* and *OMT* genes, and for *STS* at some time points, were observed in both lodgepole and jack pine, although these changes were occasionally observed earlier in jack pine (Figure 2.8).

2.3.4 Influence of G. clavigera *and water availability on phenolic metabolite profiles*

Terpenoid specialized metabolism has been extensively studied in relation to pine defenses against insect pests and fungal pathogens, including lodgepole and jack pine responses to *G. clavigera* challenge (Kolosova and Bohlmann 2012, Burke and Carroll 2016, Arango-Velez et al. 2016, Six et al. 2021). In contrast, phenolic specialized metabolism has received considerably less attention. Based upon the transcript profiles for sequences encoding enzymes of the stilbene and flavonoid pathways reported in the previous section, we conducted phenolic metabolite profiling to determine whether these changes in gene expression reflected changes in steady state metabolite levels for the phenolic compounds associated with these enzymes. A

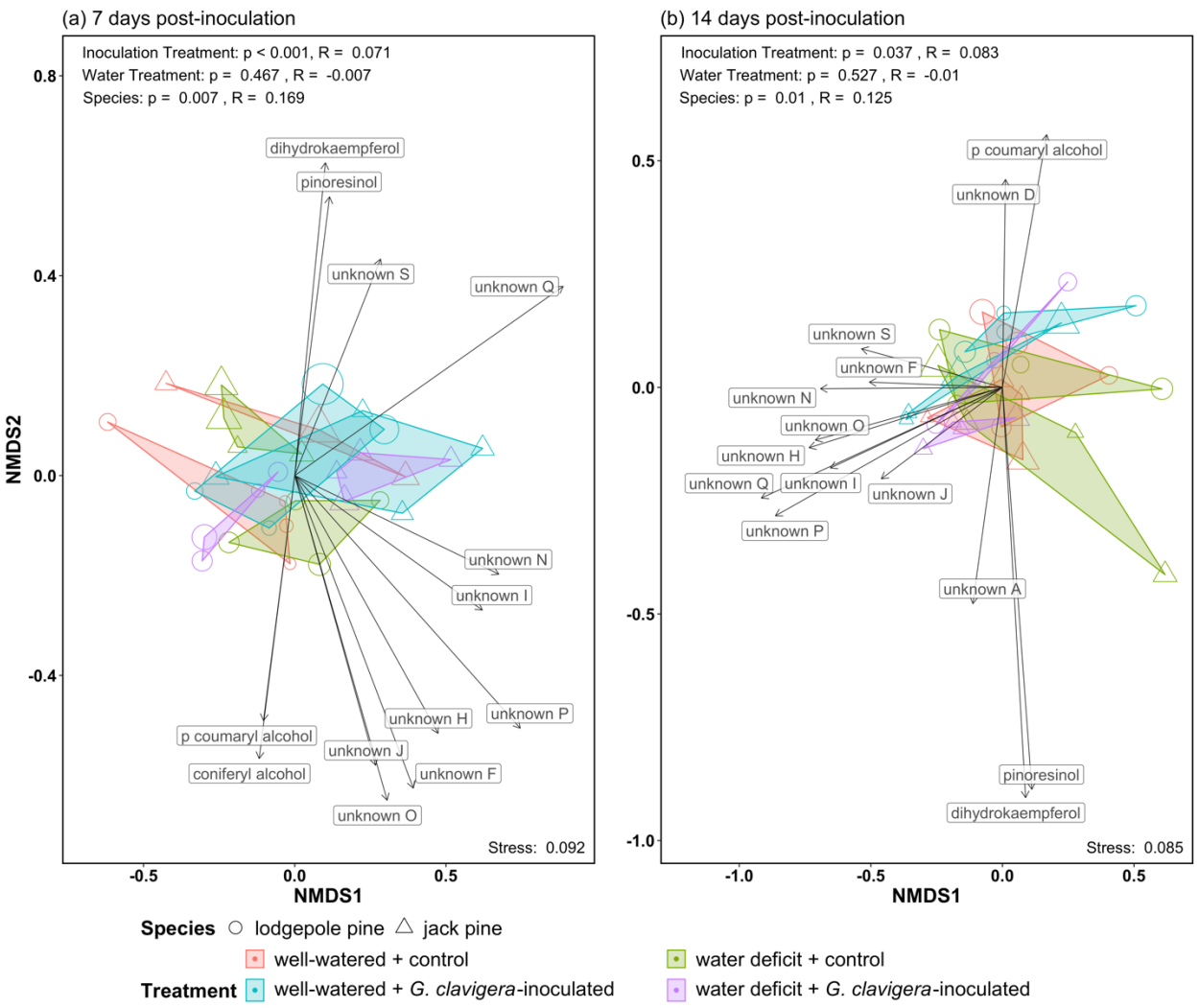

Figure 2.9. Phenolic profiles of secondary phloem are not substantively altered by *G. clavigera* challenge in either lodgepole or jack pine. Non-metric multidimensional scaling (NMDS) indicates that secondary phloem phenolic compounds are primarily influenced by species at 7 (a) and 14 (b) days post-inoculation with *G. clavigera*. Point shape indicates species, point color indicates treatment, and point size is proportional to sample goodness of fit. Phenolic compounds identified as significantly contributing to differences in phenolic profiles between groups are included ($P < 0.05$); arrows represent the strength and direction of each predictor. Stress values indicate the fit of the ordination model; values less than 0.2 are considered a good fit. ANOSIM values indicate the influence of treatment or species on the phenolic profiles; *p*-values represent the significance of each factor while R values represent the similarity of phenolic profiles within a factor (R values of 1 indicate that samples are identical).

subset of phenolic compounds quantified using HPLC-DAD were successfully identified based on comparison of retention times to authenticated standards. Additional unidentified compounds were also included in ordination analysis. NMDS stress values were less than 0.1 for both the 7 and 14 dpi ordination models, indicating a good fit of the model to the ordination data (Figure 2.9). ANOSIM values indicated that phenolic profiles differed significantly between inoculation treatments at both 7 dpi ($p < 0.001$, R = 0.071) and 14 dpi ($p = 0.037$, R = 0.083). Phenolic profiles were also significantly different between species at both 7 dpi ($p = 0.007$, R = 0.169) and 14 dpi ($p = 0.01$, R = 0125; Figure 2.9).

Several compounds were revealed as significant predictors of differences among phenolic profiles of lodgepole and jack pine seedlings, including *p*-coumaryl alcohol and coniferyl alcohol (lignin precursors), pinoresinol (a lignan), and dihydrokaempferol (a flavonoid). Ten unidentified compounds were also found to be significant predictors. Closer examination of a subset of these phenolic compounds, as well as total phenolics, revealed that in jack pine coniferyl alcohol was only detectable under water deficit (Figure 2.10d). As a result, this data set did not meet the assumptions of our GLM and we were unable to further compare differences between inoculation treatments under water deficit conditions, although the treatments appear to have similar coniferyl alcohol levels in jack pine. In contrast, water availability did not appear to affect coniferyl alcohol in lodgepole pine, yet levels were significantly decreased following *G. clavigera*-inoculation at 14 dpi (well-watered z = 2.61, $p = 0.04$; water deficit z = 2.86, $p = 0.02$; Figure 2.10c). Lastly, dihydrokaempferol was significantly lower in *G. clavigera*-inoculated jack pine at 14 dpi, but only under well-watered conditions (Figure 2.10f). This is consistent with increased *PbDFR2* expression we observed under the same conditions at 7 dpi (Figure 2.8f), for which dihydrokaempferol is a possible substrate.

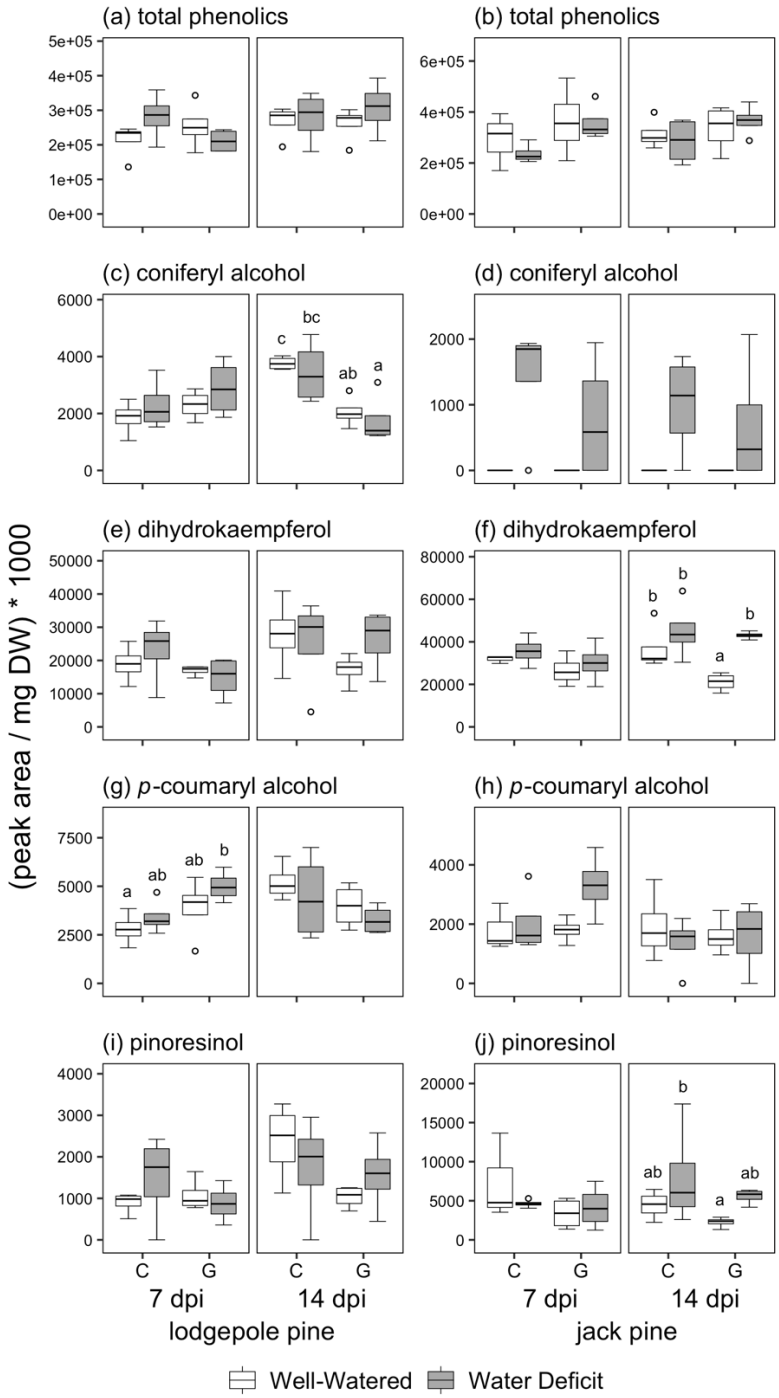

Figure 2.10. Individual phenolic compounds exhibit different responses to *G. clavigera* inoculation and water deficit conditions in lodgepole pine versus jack pine. Metabolite measurements are grouped by control (C) or *G. clavigera*-inoculation (G) for each time point. Within each time point, capitalized letters indicate significant differences between estimated marginal means of inoculation treatments while lower-case letters indicate differences between water treatments (adjusted $p < 0.05$, n = 4).

2.3.5 **G. clavigera** *induction of the JA/ethylene signaling pathway in lodgepole and jack pine*

Given our earlier finding that *G. clavigera* challenge led to elevated *in vivo* levels of JA and JA-Ile in both lodgepole and jack pine (Arango-Velez et al. 2016), we mined the transcriptome datasets for DE sequences associated with JA signalling. Genes putatively involved in biosynthesis of JA such as *lipoxygenase* (*LOX*) and *oxo-phytodeinoate* (*ODPA*)-*reductase* were significantly upregulated at 1 dpi in both lodgepole and jack pine. A subset of these genes was also significantly upregulated under water deficit conditions. Putative members of the *JAZ-like* transcription factor family were also significantly upregulated in both lodgepole and jack pine inoculated with *G. clavigera* (Figure 2.11).

In angiosperms, ethylene also plays an important role in plant responses to necrotrophic pathogens (van Loon, Rep, et al. 2006). Accordingly, we also mined the transcriptome datasets for DE sequences associated with ethylene signalling. Genes determined to be putatively involved in the biosynthesis of ethylene also displayed upregulation in both lodgepole and jack pine, particularly at 7 dpi (Figure 2.11). Fold change increases in transcript abundance for inoculated vs. control samples were particularly high for several *ACC oxidase* sequences and a subset of putative *ERF-like* sequences in 7 dpi lodgepole pine under water deficit conditions (Figure 2.11).

2.4 Discussion

2.4.1 **G. clavigera** *elicits a core transcriptomic response in lodgepole and jack pine, mediated by JA and ethylene signaling*

The first objective of this study to was to determine the extent to which lodgepole and jack pine exhibit similar vs. distinct defense responses to *G. clavigera* inoculation at the molecular level. Comparison of sequences differentially expressed following *G. clavigera*

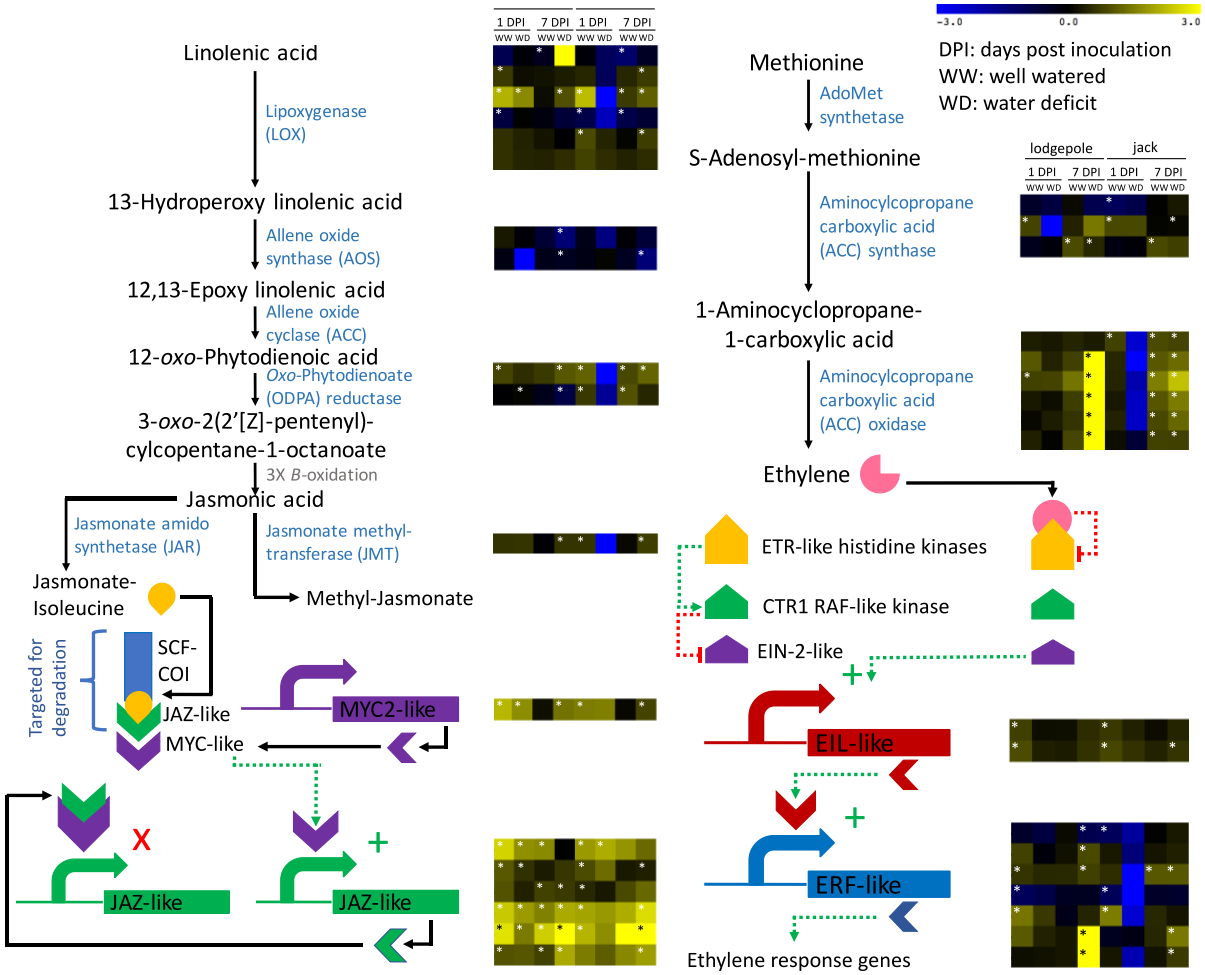

Figure 2.11. Microarray expression profiles of lodgepole and jack pine jasmonic acid (left) and ethylene (right) biosynthesis and signaling genes show strong regulation following inoculation with *G. clavigera*. Yellow and blue indicate higher or lower transcript abundance in *G. clavigera*-challenged seedlings relative to controls, respectively, depicted on a log2 scale, with asterisks (*) marking significantly DE transcripts (adjusted $p < 0.05$, n = 4).

inoculation revealed a core set of genes that were invoked in the response of both lodgepole and jack pine to this pathogen. These include putative orthologues classically associated with defense responses, such as chitinases and other PR proteins, terpene synthases, and genes involved in phenolic biosynthesis. Several sequences putatively encoding transcription factors that play well-known roles in regulating expression of defense-associated genes, such as *MYBs* and *WRKYs*, were also DE in both lodgepole and jack pine. Our results suggest that JA and ethylene are involved in mediating early responses to *G. clavigera* infection in both lodgepole and jack pine. This response is consistent with previous work reporting increased *in vivo* levels of JA and JA-Ile in lodgepole and jack pine seedlings inoculated with *G. clavigera*, and the contribution of ET further supports classification of *G. clavigera* as a necrotrophic pathogen (Arango-Velez et al. 2016). In conifers, exogenous application of JA has been reported to induce an array of terpene-related defense responses (Franceschi et al. 2002, Lundborg et al. 2016, 2019).

In contrast, much less work has been carried out on the role of ethylene in the defense response of conifers. Accumulation of *ACC oxidase* was reported in Douglas-fir (*Pseudotsuga menziesii* Mirb.) treated with both MeJA and wounding, suggesting that in the presence of JA, ethylene biosynthesis is induced and the resulting increase in ethylene promotes downstream defenses such as formation of traumatic resin ducts and accumulation of polyphenolic cells (Hudgins and Franceschi 2004). These reports support the model that in conifers, like angiosperm systems, ethylene works in concert with JA to mediate the inducible defense response of lodgepole and jack pine to *G. clavigera*. An important next step will be to measure *in vivo* levels of ethylene or ethylene precursors such as ACC in *G. clavigera*-challenged pines to determine whether these transcript abundance patterns reflect *in planta* hormone levels.

2.4.2 Jack pine molecular responses to **G. clavigera** *invokes more genes and earlier timing of defense-associated gene expression relative to lodgepole pine*

A larger set of defense-related sequences were uniquely DE in *G. clavigera*-challenged jack pine under well-watered conditions, suggesting that although jack pine and lodgepole pine share a core defense strategy, jack pine also invokes different or additional strategies to respond to the necrotrophic pathogen *G. clavigera*. For example, while the majority of chitinases exhibited similar temporal profiles of transcript abundance between species, we identified a subset of class IV chitinases that were DE earlier in jack pine than in lodgepole pine. Studies have shown a correlation between earlier induction of PR proteins such as chitinases in pine to resistant genotypes, and later induction of the same proteins to susceptible genotypes (Davis et al. 2002, Hietala et al. 2004).

Consistent with this pattern, several *monoterpene synthases* were also found to exhibit significant upregulation earlier in jack pine than lodgepole pine. While previous work by Lusebrink et al. (2011) and Arango-Velez et al. (2016) showed that lodgepole pine exhibited greater induction of several monoterpenes following *G. clavigera* inoculation, other monoterpene compounds such as 3-carene and α-pinene were constitutively higher in the monoterpene profiles of jack pine seedlings (Lusebrink et al. 2011, Arango-Velez et al. 2016). While patterns of transcript abundance do not always predict metabolite levels, our data suggest that these differences in terpene synthase gene expression patterns between lodgepole and jack pine could further compound differences in oleoresin composition, which in turn could influence host interactions with *G. clavigera* or its MPB vector. Host (-)-α-pinene can serve as the precursor for female MPB production of the aggregation pheromone (-)-*trans*-verbenol (Chiu et al. 2019, Chiu and Bohlmann 2022), and increases in emission of (-)-α-pinene could increase MPB mass attack

numbers. Additionally, work has shown that higher levels of α-pinene like those observed in jack pine following fungal inoculation significantly reduce *G. clavigera* growth, while levels found in lodgepole pine did not have a significant effect (Cale et al. 2017). As *G. clavigera* plays an important role in MPB growth and development (Bleiker and Six 2007, Myrholm and Langor 2016), the interaction between host α-pinene levels and fungal growth could further influence MPB success and ultimately host survival.

Similarly, lodgepole and jack pine exhibited differences in phenolic gene expression and phenolic metabolite levels following inoculation with *G. clavigera* relative to controls. *DFR1* and *DFR2* are key enzymes involved in the shift of flavonoid substrates towards anthocyanin-derived products. Both genes were strongly upregulated in *G. clavigera*-inoculated jack pine but not lodgepole pine and corresponded to decreased levels jack pine levels of DFR-precursor dihydrokaempferol at 14 dpi. Flavan-3-ols and proanthocyanidins (condensed tannins) were reported to increase in Norway spruce (*Picea abies* (L.) Karst) following inoculation with *Endoconidiophora polonica* (formerly known as *Ceratocystis polonica* (Siem.) C. Moreau), and *E. polonica* growth is slowed on flavan-3-ol supplemented media (Hammerbacher et al. 2014). While toxicity of these compounds has not yet been tested on *G. clavigera,* these studies with other conifer – bark beetle-vectored pathogenic fungi pathosystems suggest that the phenolic composition of jack pine phloem may alter *G. clavigera* colonization and/or growth rates following MPB attack.

The differences in defense responses to *G. Clavigera* we observed between lodgepole and jack pine could be indicative that both species may have co-evolved different strategies of pest/pathogen detection and defense responses relevant to their different life histories. Lodgepole pine is a historic host of MPB and its Ophiostomatoid associates, including *G. clavigera*, while

jack pine is considered a novel host (Safranyik et al. 2010, Cullingham et al. 2011). It is possible that lodgepole pine may have evolved specialized defense strategies against *G. clavigera*, while jack pine would then be theorized to rely on more general necrotrophic-related defenses. Alternatively, it is also possible that *G. clavigera* has evolved mechanisms which allow it to evade or contend with host defenses, like the ability to detoxify some monoterpenes (DiGuistini et al. 2011). Our hormone expression data indicate that both species likely detect *G. clavigera* at similar times. The slower, more subtle response of lodgepole pine to *G. clavigera*, relative to the jack pine response, could be indicative of a more strategic defense response that may utilize specific, specialized defenses against *G. clavigera*, rather than a resource-heavy bombardment of non-specific defenses.

2.4.3 At the level of gene expression, water deficit has a greater effect on composition of induced defenses than magnitude

The second objective of this study was to determine the effect of water deficit on induced defenses of lodgepole and jack pine to *G. clavigera.* Globally, water deficit led to increased expression of many defense-related genes in both species that were not DE under well-watered conditions, including many genes putatively involved in secondary metabolism. Previous studies have suggested that water limitation increases constitutive expression of defenses in conifers and attenuates induced defenses (Lorio et al. 1995, Lombardero et al. 2000), including our previous studies demonstrating that total monoterpene levels and levels of several specific monoterpenes increased in control lodgepole and jack pine under water deficit (Lusebrink et al. 2011, Arango-Velez et al. 2016). In contrast, other studies have also shown the constitutive resin flow in Norway spruce decreased under water deficit (Netherer et al. 2015). Our global transcriptome analyses in this present study indicated that the effects of water deficit on induced defenses at the

level of gene expression are more nuanced than a concerted lack of increased transcript abundance corresponding to large numbers of defense-associated genes in response to *G. clavigera* challenge. Rather, water deficit appears to affect subsets of defense-associated genes by either attenuating their increased expression in *G. clavigera*-challenged trees or delaying their upregulation. We did not find evidence for wholesale upregulation of entire groups of genes involved in metabolic networks synthesizing classes of defense-associated secondary metabolites such as terpenoids or phenolics. These transcriptome profiles are consistent with the metabolite profiling for phenolic compounds that we conducted as part of this study, and the previously published studies examining monoterpene profiles mentioned above. Similarly, only a subset of chitinases that we examined showed attenuated induced expression in response to *G. clavigera* challenge. Therefore, while these global patterns of gene expression provide some support for the hypothesis that water deficit attenuates induced defenses, our transcriptome analyses more strongly suggest that at the level of gene expression, water deficit influences the composition of the induced defense arsenal invoked in response to invasion by a necrotrophic fungal pathogen more than the overall magnitude of this defense.

2.4.4 Lodgepole and jack pine defense gene induction patterns are modified by water availability

Our third and final objective of this study was to determine whether the effects of water deficit were greater on defenses of the more drought-sensitive lodgepole pine relative to jack pine. Whereas lodgepole pine exhibits classic isohydric responses to water deficit and is adapted to more mesophytic conditions, jack pine exhibits near-isohydric behaviours and is adapted to more xerophytic conditions (Cullingham et al. 2012, Arango-Velez et al. 2016). Consistent with our findings reported in Arango-Velez et al. (2016), we observed in this study that WUE showed

greater increases in response to water deficit conditions in lodgepole pine than in jack pine. We have also observed that while lodgepole pine hydraulic conductivity is significantly reduced by *G. clavigera*-induced tracheid cavitation, jack pine hydraulic conductivity is unaffected despite *G. clavigera*-induced tracheid cavitation, suggesting that jack pine exhibits compensatory mechanisms to maintain water transport despite loss of functional tracheary conduits (Arango-Velez et al. 2016). Transcriptome profiling in this study supports the notion that water deficit has a greater impact on lodgepole pine responses at the level of gene expression to *G. clavigera* challenge than on jack pine responses, perhaps reflecting the more drought-tolerant nature of jack pine. However, these differences at the level of gene expression may not translate into meaningful differences in the phloem chemical defense arsenal of lodgepole and jack pine at the degree of water stress that was imposed in this study. We observed, for example, a greater overall number of DE genes in *G. clavigera*-inoculated lodgepole pine than *G. clavigera*-inoculated jack pine under water deficit, whereas the inverse was true under well-watered conditions. Of note was the increased expression of specific phenolic biosynthesis genes only under water deficit conditions in *G. clavigera*-inoculated lodgepole pine than jack pine, although these differences in transcript profiles made only modest differences to the overall phenolic profiles of *G. clavigera*-inoculated lodgepole and jack pine. Some phenolic compounds, such as coniferyl alcohol, showed distinct responses to water deficit conditions in lodgepole and jack pine: whereas coniferyl alcohol levels were significantly lower in *G. clavigera*-inoculated lodgepole pine regardless of water treatment, levels were significantly higher in jack pine regardless of inoculation status. These compositional differences in the phenolic profiles between species and in response to fungal challenge or water availability could perhaps modulate overall defense efficacy. Similarly, a subset of terpene synthases were upregulated more quickly in jack

pine under well-watered versus water deficit conditions, but these shifts in gene expression were largely not reflected in the phloem monoterpene profiles reported in Arango-Velez et al. (2016).

Interestingly, while expression profiles were similar for JA biosynthesis and signalling genes in *G. clavigera*-inoculated lodgepole pine and jack pine under well-watered and water deficit conditions, we observed that upregulation of a set of ACC oxidase and ethylene response genes was substantially greater in *G. clavigera* lodgepole pine under water deficit than under well-watered conditions, or in jack pine under both well-watered and water deficit conditions. This finding leads to the testable hypothesis that enhanced ethylene biosynthesis in the more drought sensitive lodgepole pine may contribute to shifts in defense-associated gene expression under water deficit that we noted in this study.

2.5 Conclusion

Initially, we hypothesized that lodgepole and jack pine would exhibit different responses to *G. clavigera*, reflective of their evolutionary differences and life histories. We found that while these sister pine species share a core set of molecular defense responses, lodgepole and jack pine exhibit largely different strategies based on the timing and composition, and to a lesser extent magnitude, of their induced defenses. Our gene expression data largely supports similar trends that have been observed in defense metabolites like monoterpenes. These differences in induced defenses likely compound with differences in constitutive defenses observed between species to influence fungal growth. While the more moderate response of the co-evolved host lodgepole pine could be reflective of more strategic and efficient defenses against *G. clavigera*, jack pine's naïve but massive defense response could prove to be more effective.

We also hypothesized that water deficit would alter host defenses, but to a greater extent in lodgepole pine. Water deficit appeared to have a mixed effect on some defense responses,

primarily altering defense composition, but did not trigger any global changes to defense gene expression. Furthermore, water deficit had very little effect on jack pine defense responses, likely reflective of jack pine's more conservative water use strategy. Our results suggest that lodgepole pine host quality is modulated under water deficit while jack pine host quality is not, although the extent to which this will influence fungal growth remains unclear. If changes under water deficit reduce lodgepole pine's specialized defenses, then we would anticipate water deficit lodgepole pine, but not water deficit jack pine, to be more susceptible to *G. clavigera* and mountain pine beetle attack.

Chapter 3: Phenolics are a major component of the pine defense response to *Grosmannia clavigera* in xylem

3.1 Introduction

Mountain pine beetle (*Dendroctonus ponderosae* Hopkins; MPB) is a bark beetle that attacks multiple pine species found in western North America, including lodgepole pine (*Pinus contorta* Dougl. ex Loud. var. *latifolia* Engelm.) and jack pine (*Pinus banksiana* Lamb.). During the current outbreak of MPB, lodgepole pine has been the main host for MPB. Over the course of the outbreak, MPB has undergone range expansion and has been found to have successfully attacked a new host, jack pine (Cullingham et al. 2011), introducing the possibility for further expansion of MPB eastward into Canada's boreal forest.

Ophiostomatoid fungal species play a symbiotic role in the life history of MPB (Six and Paine 1998, Six and Wingfield 2011). The most virulent of these Ophiostomatoid fungal associates of MPB is *Grosmannia clavigera* [Robinson-Jeffrey and Davidson] Zipfel, de Beer and Wingfield (Rice et al. 2007a). These fungi are introduced into the phloem by MPB during attack and colonization (Ballard 1982), and quickly spread into xylem tissue as a means of nutrient resource acquisition (Ballard et al. 1982, 1984, Six 2020a). Host deposition of tyloses, originating from nearby cells, block water transport in the tracheids (De Micco et al. 2016), as will the eventual growth of fungal hyphae. Continual fungal growth and deposition contribute to lost conductivity in the host and eventual mortality (Yamada 2001).

Another common mechanism that pine hosts have evolved to contain invading pests and pathogens is the development of lesions that are characterized by the accumulation of secondary metabolites (Yamada 2001, Franceschi et al. 2005, Witzell and Martín 2008). Lodgepole and jack pine form distinctive lesions in response to attack by MPB and the fungal associates that

they vector (Safranyik and Carroll 2006), as well as following manual inoculation with *G. clavigera* and other Ophiostomatoid fungi (Rice et al. 2007b, 2007a, Arango-Velez et al. 2016). Because of this similarity, as well as the shared history of association between *G. clavigera* and MPB, inoculation with *G. clavigera* is often used as a proxy for MPB attack in seedlings (McAllister et al. 2018).

The arsenal of defenses that are induced by MPB and/or their Ophiostomatoid fungal associates differ between pine species (Arango-Velez et al. 2016, Pimentel et al. 2017, Kichas et al. 2021), and are also influenced by abiotic stress such as drought (Öhrn et al. 2021, Trowbridge et al. 2021, Lusebrink et al.). Several studies have reported increased incidence of disease following periods of low precipitation (Desprez-Loustau et al. 2006) and it is believed that stressed trees may be more susceptible to infection (Klutsch et al. 2017, Trowbridge et al. 2021). However, several theories posit that moderate drought may temporarily enhance defenses, as growth is paused and those resources are reallocated to defense (Herms and Mattson 1992, Lorio et al. 1995, Kolb et al. 2016).

Most studies that have examined pine responses to MPB and their Ophiostomatoid fungal associates have focused on the responses that take place in the bark, since the bark is the primary point of host-antagonist interactions during the attack phase (Goodsman et al. 2012, Six 2020a). Given that the Ophiostomatoid fungi colonize the xylem, and that this colonization is a key contributor to host mortality, it is also important to know how xylem responds to fungal colonization, and how abiotic stressors affect this response. However, little research has been carried out to examine xylem responses to attack by MPB Ophiostomatoid fungal associates, particularly at the molecular and biochemical level. The present study addresses two objectives aimed at filling this knowledge gap: 1) to compare lodgepole and jack pine xylem defense

responses to *G. clavigera* and 2) to determine the effect of water deficit on these defense responses. Understanding similarities and differences in how these two pine species defend themselves against *G. clavigera* is important for predicting further spread of MPB and its fungal associates. We hypothesize that water deficit will cause a shift in resource allocation towards storage of carbon for induced defenses, enhancing host defenses responses to *G. clavigera*, at least until reserves become depleted. We also hypothesize that lodgepole and jack pine will exhibit different degrees of phenotypic plasticity under water deficit conditions, reflecting differences in their water use strategies. Lodgepole and jack pine occupy not only different geographical regions, but also different elevations and climates, with lodgepole typically found on more mesic clay soils and bogs while jack pine is found on more xeric sandy sites (Yeatman 1967, Rweyongeza et al. 2007). We predict that lodgepole pine will be less drought-tolerant, and therefore more sensitive to changes under water deficit and more likely to exhibit enhanced defense responses, than jack pine.

To test these hypotheses, we used transcriptomic data to examine global effects of *G. clavigera* and water availability on gene expression of xylem in lodgepole and jack pine seedlings, and the interaction between these biotic and abiotic stressors. We also examine gene expression and metabolite profiles for phenolic biosynthesis – a major component of the lesions that include many compounds with oxidative and phytochemical properties – to determine how the interaction of these stressors impacts this component of the pine defense arsenal.

3.2 Materials and Methods

3.2.1 Plant Material

Experimental conditions for seedlings used to generate material for microarray, quantitative RT-PCR (qRT-PCR), physiological and metabolite analyses are described in

Arango-Velez et al. (2016) and in Chapter 2. Lodgepole pine seedlings originating from a west central Alberta provenance and jack pine seedlings originating from an Ontario provenance were received as dormant one year old seedlings following growth at the same facility. Seedlings were transplanted into 3.78 L pots (Beaver Plastic Ltd, Acheson, Alberta, Canada) in Sunshine Mix # 4 growing media (Sun Gro Horticulture, Seba Beach, Alberta, Canada). Growth rooms were maintained at a temperature of 19 °C (day/night), relative humidity of 20-35%, 16 h day/ 8 h night photoperiod, and 200 μmol photosynthetically active radiation. Trees were watered twice weekly prior to drought treatment and fertilized once a week using a 500 mg L^{-1} 20-20-20 (N-P-K) fertilizer solution (Plant Products Ltd, Brampton, Ontario, Canada). After approximately two months of growth, healthy seedlings were selected and randomly assigned to a treatment group.

Treatment groups consisted of a full factorial design with (a) two levels of water availability, well-watered (>50% relative water content, RWC_{soil}) or water deficit (approximately 20% RWC_{soil}), (b) three levels of inoculation treatments, untreated control, mechanical wounding (i.e., mock-inoculation), or inoculation with *G. clavigera*, as well as (c) two species, lodgepole and jack pine, and (d) four time points, 1-, 7-, 14- and 28-days post inoculation (dpi). Treatments were implemented using a randomized block design and independent individual seedlings were used as the unit of biological replication. There is a low likelihood of kinship expected between individuals since seedlings originated from provenances, rather than clonal or pedigree material.

Water availability conditions were differentially applied to seedlings one week prior to inoculation treatments. A time domain reflectometer (Tektronix 102B Cable TDR Cable Tester, Tektronix, Inc., Scarborough, Ontario, Canada) was used to measure relative soil water content

based on calculations outlined in Arango-Velez et al. (2011), and water content criteria used for well-watered and water deficit treatments are defined in detail in Arango-Velez et al. (2016).

Details regarding fungal culturing and inoculation with *G. clavigera* are outlined in Arango-Velez et al. (2016) and in Chapter 2. Approximately 140 spores μL^{-1} of *G. clavigera* isolate M001-03-03-07-UC04DL09 (described in Roe et al. 2010), originally from Fox Creek, Alberta (54°24'N, 116°48'W) were suspended using deionized water and injected into the cambial region with a 23GI PrecisionGlide™ needle (Becton, Dickson and Company, Mississauga, Ontario). Injections were made along the stem at 3-4 cm intervals, and mock inoculation was performed using the same procedure without application of the spore suspension. Control trees remained uninoculated.

Entire stem sections were collected at each timepoint (1-, 7-, 14-, and 28-days post inoculation) along the region of inoculation, or the equivalent region in control seedlings. Following removal of the bark, remaining portions of stem were quickly chopped and flash frozen in liquid nitrogen prior to long term storage at -80ºC. These stem samples are referred to as xylem throughout the remainder of the paper.

3.2.2 RNA Extractions

Frozen samples were ground to a powder consistency using a Retsch Mixer Mill (Verder Scientific, Newton, PA, USA). Extraction of total RNA was performed as described in (Pavy et al. 2008), using ~100 mg of ground frozen tissue and quantified with a NanoQuant 200 (Tecan Infinite® Morrisville, NC, USA). RNA quality was assessed using a 2100 Bioanalyzer (Agilent, Mississauga, ON, Canada) prior to microarray profiling.

3.2.3 cDNA Microarray Transcript Profiling

Lodgepole and jack samples were collected at 7 and 28 dpi and used to generate transcriptome analyses. Microarray probe preparation, hybridization, and data extraction were completed as outlined in (El Kayal et al. 2011). Amino allyl antisense RNA (aRNA) was amplified from 2 µg of total RNA following the manufacturer's protocol (Superscript Indirect RNA Amplification System, Invitrogen, Carlsbad, CA, USA) and 5 µg aRNA was labeled directly with Alexa Fluor® 555 or 647 dyes (Invitrogen) before hybridization to PtGen2 loblolly pine cDNA microarrays (Lorenz et al. 2009, 2011). Arrays consisted of 26,946 total spots, not including buffer blanks and duplicate spots, of 25,848 cDNAs from loblolly root, stem, and needle tissues (Lorenz et al. 2009, 2011). Samples from seedlings inoculated with *G. clavigera* were co-hybridized with corresponding mock-inoculated or control untreated samples, and mock-inoculated samples were independently co-hybridized with control untreated samples. For each treatment, four replicates from independent individuals were hybridized, and two replicates were used as reciprocal dye swaps.

Microarray hybridizations were imaged using a GenePix 4000B microarray scanner and data extraction completed using the GenePix 6.0 software (Axon Instruments, Sunnyvale, CA, USA) adaptive circle method outlined in El Kayal *et al.* (2011). Low quality signal filtering, removal of background noise, normalization within-array and multiple quality checks were performed as described in El Kayal *et al.* (2011). Sequences with statistically differentially expression (DE) were identified in R v3.0.2 (R Core Team 2013) with the linear models for microarray data (LIMMA, Smyth 2005) and exploratory analysis for two-color spotted microarray data (marray, (Yang and Paquet 2005) packages available from BioConductor (Gentleman et al. 2005). DE sequences were filtered based on a Benjamini-Hochberg adjusted *p*-

value of less than 0.05 (Benjamini and Hochberg 1995), and fold change values greater than 1.5 or less than 0.6.

Lodgepole and jack pine transcriptome assemblies (Hall et al. 2013) were used to BLASTx (Camacho *et al.* 2009) loblolly pine cDNA from the microarray and a total of 11,032 sequences were identified as putatively orthologous with lodgepole and/or jack pine transcripts. The matching lodgepole and jack pine sequences were then annotated using the NCBI nr (https://www.ncbi.nlm.nih.gov/nucleotide) and TAIR 7.0 (The Arabidopsis Information Resource; Berardini et al. 2015) databases and MapMan functional annotation categories were assigned to the orthologous loblolly pine sequences using the Mercator annotation pipeline (Usadel et al. 2009, Lohse et al. 2014). Gene enrichment of MapMan categories within subsets was determined using a hypergeometric distribution statistic and Bonferroni correction as described in (Galindo González et al. 2012), relative to representation of categories across all 11,032 orthologous sequences represented on the PtGen2 array.

Manual annotation of select lodgepole and jack pine sequences was completed using phylogenetic analyses. Translated amino acid sequences of the longest open reading frame, as determined by the NCBI ORFfinder (www.ncbi.nlm.nih.gov/orffinder/), were aligned with functionally characterized genes from other species using the MAFFT server auto alignment function (v7; https://mafft.cbrc.jp/alignment/server/, Katoh et al. 2019). The IQ Tree web server (http://iqtree.cibiv.univie.ac.at/; Trifinopoulos et al. 2016, Kalyaanamoorthy et al. 2017) was used to identify the best amino acid substitution model and generate bootstrap consensus trees for each alignment using auto calculation options and Bayesian (BIC) selection criterion. Dendrograms were visualized using Geneious 2021.1.1 (www.geneious.com). Heatmaps of microarray profiles were created using R v4.0.3 (R Core Team 2020), RStudio v1.4.1106

(RStudio Team 2020) and the gplots package v3.1.1 (Warnes et al. 2020). R files are available at https://github.com/c4tier.

3.2.4 qRT-PCR

Prior to cDNA synthesis, total RNA was treated with Dnase I (New England Biolabs, Whitby, ON, Canada) using Invitrogen™ Superscript™ II Reverse Transcriptase (Thermo Fisher Scientific, Mississauga, ON, Canada), according to the manufacturers' protocols. qRT-PCR primers (Supplemental Table 1) were designed using Primer Express 3.0 (Applied Biosystems, Thermo Fisher Scientific). qRT-PCR reactions and standard curve quantification were performed essentially according to El Kayal *et al*. (2011), with six biological replicates and two technical replicates for each treatment. Target gene data was normalized to the arithmetic mean of *Vacuolar ATP synthase subunit A* (*VHA-A;* accession GT257942.1) and *Ubiquitin-activating enzyme 1* (*UBA1;* accession GT229647.1) for both lodgepole and jack pine. This was determined to be a suitable reference gene combination using Normfinder (Andersen et al. 2004), BestKeeper (Pfaffl et al. 2004), GeNorm2 (Vandesompele et al. 2002), and by GLMM (Appendix 2 Figure 1).

Statistical analyses of qRT-PCR data was performed using R v4.0.3 (R Core Team 2020) and Rstudio v1.4.1106 (RStudio Team 2020). Normalized data for each gene was fit to a generalized linear model with the following formula: normalized transcript abundance ~ time point * water treatment * inoculation treatment, family = Gamma (link = log). Assumptions of normality and homoscedascity were assessed visually as well as with Shapiro-Wilks and Bartlett tests. Analysis of deviance, including Wald's chi square test statistics and Pearsons' error estimate, was calculated from GLM models using the car package v3.0-11 (Fox and Weisberg 2019). Significant differences between modeled groups were determined from estimated

marginal means using the emmeans package v1.5.3 (Lenth 2020), and letters were assigned using the multcomp package v1.4-15 (Hothorn et al. 2008). Visualizations were prepared using the ggplot2 v3.3.3 (Wickham 2016) and cowplot v1.1.1 (Wilke 2020) packages. R files are available at https://github.com/c4tier.

3.2.5 Metabolite Profiling

Ground xylem (~100 mg) was extracted using 1 mL HPLC-grade methanol (Thermo Fisher Scientific). Tissue was vortexed to suspend then shaken, covered, at 4ºC for one hour. Prior to centrifuging for 15 minutes at 22,000 g, 25µL of 4 mg/mL gallic acid monohydrate (Sigma-Aldrich Cat. 398225) was added as an internal standard. Samples were re-extracted three times and four supernatants pooled and evaporated to dryness under nitrogen. Residues were stored at -20ºC for up to one month before resuspension in 200 µL methanol, vortexed, and filtered through an Ultrafree-MC 0.2 µm PTFE column (EMD Millipore Cat. UFC30LG25) for analysis.

Filtered sample (10 µL) was injected into a Luna 5 µm C18(2) 100 Å 250 x 4.6 mm column (Phenomenex Cat. 00G-4252-E0) attached to a Agilent 1200 series HPLC. Mobile phase flow rate was 1 mL min^{-1} and column temperature maintained at 25°C (± 8°C). Peaks were separated along a gradient modified from Lin and Harnly (2012) where formic acid (0.2%, v/v, in HPLC-grade water, Thermo Fisher Scientific) and acetonitrile (Thermo Fisher Scientific) represent mobile phases A and B, respectively, in the following elution profile: 0 to 35 min, 5% to 20% B in A; 35 to 65 min, 20% to 65% B; 65 to 80 min, 79% B; 80 to 90 min, 100% B; 95 to 100 min, 0% B to recover column. Eluting compounds were measured by diode array detector (Agilent G1315C) at 270 nm.

The following standards (Sigma-Aldrich) were used for identification based on similarity of retention times: coniferyl alcohol (Cat. 223735), dihydromyrcetin (Cat. SML0295), taxifolin (Cat. 78666), pinoresinol (Cat. 40674), p-coumaroyl alcohol (Cat. PHL82506), pinosylvin (Cat. 56297), (±)-dihydrokaemperol (Cat. 91216), kaempferol 3-glucoside (Cat. 04500585), trans-cinnamic acid (Cat. C80857), p-coumaric acid (Cat. C9008), dihydromyricetin (Cat. SML0295), coniferyl alcohol (Cat. 223735), matairesinol (Cat. 40043), and quercetin 3-glucoside (Cat. 16654). Additionally, (+)-catechin hydrate (Fisher Scientific Cat C07051G) was included as a standard.

Metabolite data was analyzed using R v4.0.3 (R Core Team 2020) and Rstudio v1.4.1106 (RStudio Team 2020). Peaks with sufficient resolution and consistency between technical replicates and that were detectable in most biological replicates in at least one treatment were selected for further analysis (Appendix 2 Figure 2). Non-metric multidimensional scaling (NMDS) was run using the vegan package v2.5-7 (Oksanen et al. 2020). The packages ggplot2 v3.3.3 (Wickham 2016) and ggord v1.1.5 (Beck 2020) were used to generate ordination plots, and analysis of similarities (ANOSIM) tests within the vegan package were used to determine statistical differences between treatments. R files are available at https://github.com/c4tier.

3.3 Results

3.3.1 Physiological responses of lodgepole and jack pine to G. clavigera and water deficit

Relative water content (% RWC) was maintained at significantly lower levels in water deficit seedlings throughout the course of the experiment ($p < 0.05$; Appendix 2 Figure 3). Seedlings under water deficit conditions significantly increased water use efficiency (WUE) across species and inoculation treatments at 28 dpi ($p < 0.05$; Appendix 2 Figure 4).

3.3.2 Changes in lodgepole and jack transcriptomes following inoculation with **G. clavigera** *under different water treatments*

We examined global gene expression changes at 7 and 28 dpi to compare early and advanced host responses to fungal challenge with *G. clavigera* between lodgepole and jack pine. Secondary metabolism sequences were significantly enriched at both time points under well-watered and water deficit conditions in jack pine, but only under water deficit at 7 dpi in lodgepole pine (Figure 3.1). In contrast, stress annotations were statistically enriched in lodgepole pine under both water conditions at 7 and 28 dpi, but only at 28 dpi in jack pine. Lastly, hormone metabolism was statistically over-represented in lodgepole pine only at 7 dpi under well-watered and water deficit conditions (Figure 3.1).

Putatively orthologous DE sequences were further compared across timepoints, water conditions, and species using Venn diagrams (Figure 3.2). Orthology was inferred for lodgepole and jack pine sequences which hybridized to the same cDNA probe of the PtGen2 microarray. Two-way Venn diagrams revealed that the majority of sequences DE under well-watered conditions were unique to jack pine, four times greater than the number of DE sequences unique to lodgepole under the same water treatment (Figure 3.2a). Within this group, enrichment analysis indicated that secondary metabolism annotations were statistically over-represented ($p < 0.001$; Appendix 2 Table 2). In contrast, most sequences that were DE under water deficit conditions were DE in both species, although the number of DE sequences unique to jack pine was still double those unique to lodgepole pine (Figure 3.2A).

Further in-depth comparison across time points using four-way Venn diagrams revealed that for both lodgepole and jack pine, most sequences were DE at 7 dpi, with some overlap at 28 dpi (Figure 3.2B). Under water deficit conditions, a large portion of sequences that were DE in

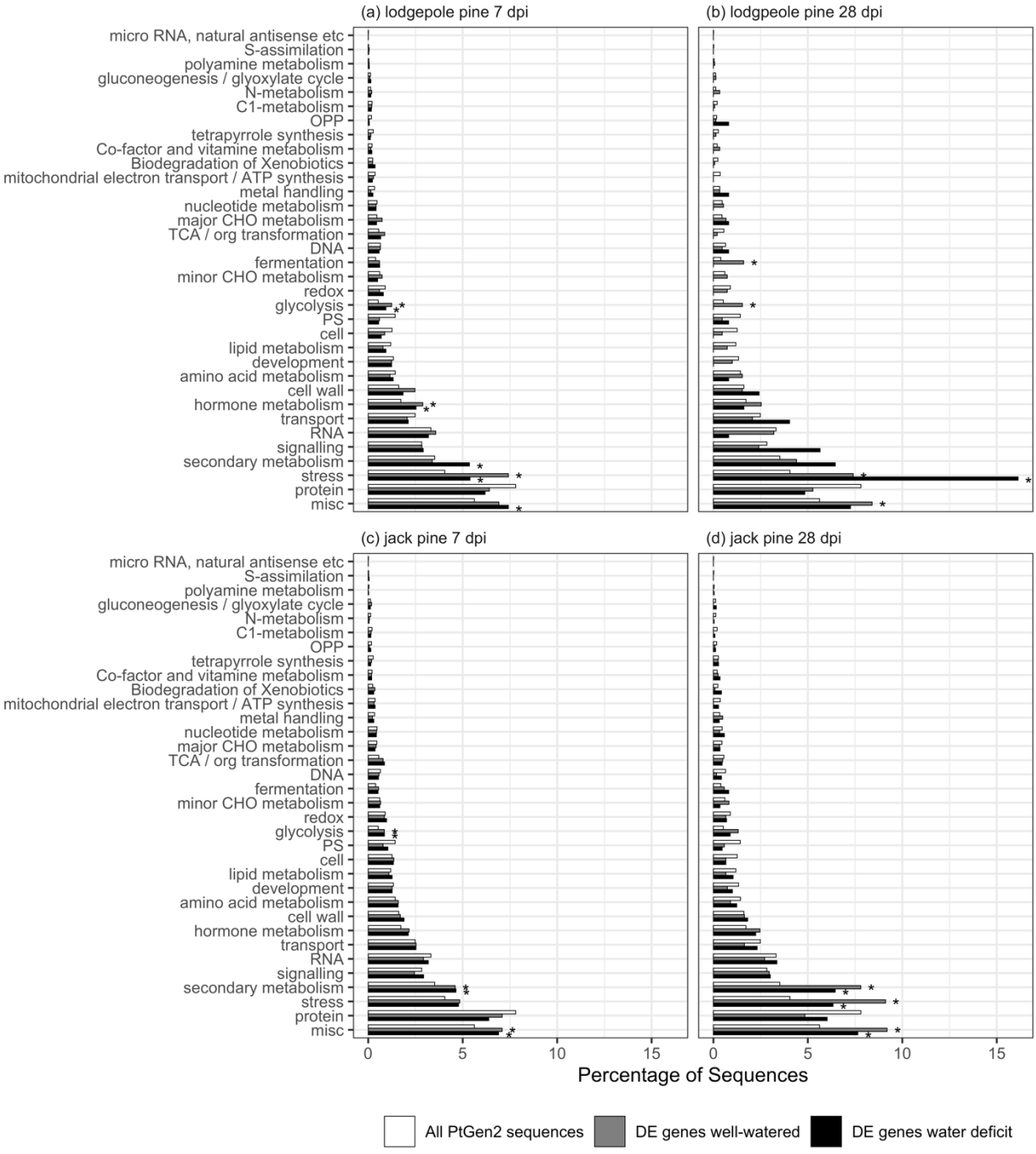

Figure 3.1. Secondary metabolism and stress annotations are statistically over-represented in DE sequences of lodgepole **(a,b)** and jack pine **(c,d)** seedlings inoculated with *G. clavigera*, under well-watered (grey bars) and water deficit (black bars) conditions. Asterisks (*) represent significant enrichment of categories of DE sequences relative to all PtGen2 sequences (white bars), based on a hypergeometric distribution probability statistic (adjusted $p < 0.001$).

Figure 3.2. More sequences are significantly DE in jack pine seedlings inoculated with *G. clavigera,* relative to controls, than are differentially expressed in *G. clavigera*-inoculated lodgepole pine seedlings under the same conditions. A Comparison of sequences that were DE in lodgepole and/or jack pine under well-watered (WW) or water deficit (WD) conditions. Both 7 dpi and 28 dpi data were combined for these analyses **b,c** Comprehensive comparison of sequences that were DE between species and timepoints under each water condition. **D,e** Contrast of sequences that were DE between water conditions and timepoints with a species.

Single up or down arrows indicate sequences with significant up- or down-regulation across comparisons, respectively, and combination arrows indicate sequences with variable regulation across comparisons.

lodgepole pine only at 7 dpi were DE at both 7 and 28 dpi in jack pine (Figure 3.2C). Additionally, several sequences were DE earlier in lodgepole pine under water deficit conditions (Figure 3.2D), which was not observed in jack pine (Figure 3.2E). Stress annotations were statistically over-represented in both lodgepole and jack pine sequences that were DE at 7 dpi and/or 28 dpi under well-watered and water deficit (Appendix 2 Table 2) conditions. Hormone metabolism was statistically over-represented in lodgepole pine sequences DE under both water treatments and secondary metabolism was statistically enriched under the same conditions, but only for jack pine sequences (Appendix 2 Table 2). Secondary metabolism was also found to be over-represented in lodgepole pine only under water deficit conditions (Appendix 2 Table 2).

As secondary metabolism appeared to constitute a large proportion of DE sequences, we further compared these annotations across biosynthesis groups (flavonoids, phenylpropanoids, and isoprenoids) in Appendix 2 Table 3. Most sequences in each biosynthesis group were DE exclusively in jack pine under well-watered conditions, while a larger proportion were DE in both species under water deficit (Appendix 2 Table 3). Only a small proportion of DE secondary metabolism-associated sequences were unique to lodgepole under well-watered or water deficit conditions (Appendix 2 Table 3).

3.3.3 Effect of **G. clavigera** *and water availability on expression of common defense-associated genes*

Chitinases are commonly associated with defense against fungal pathogens, whose cell walls contain chitin (Grover 2012). To compare chitinase expression across treatments, we mined the microarray data using chitinase-like sequences previously identified from lodgepole

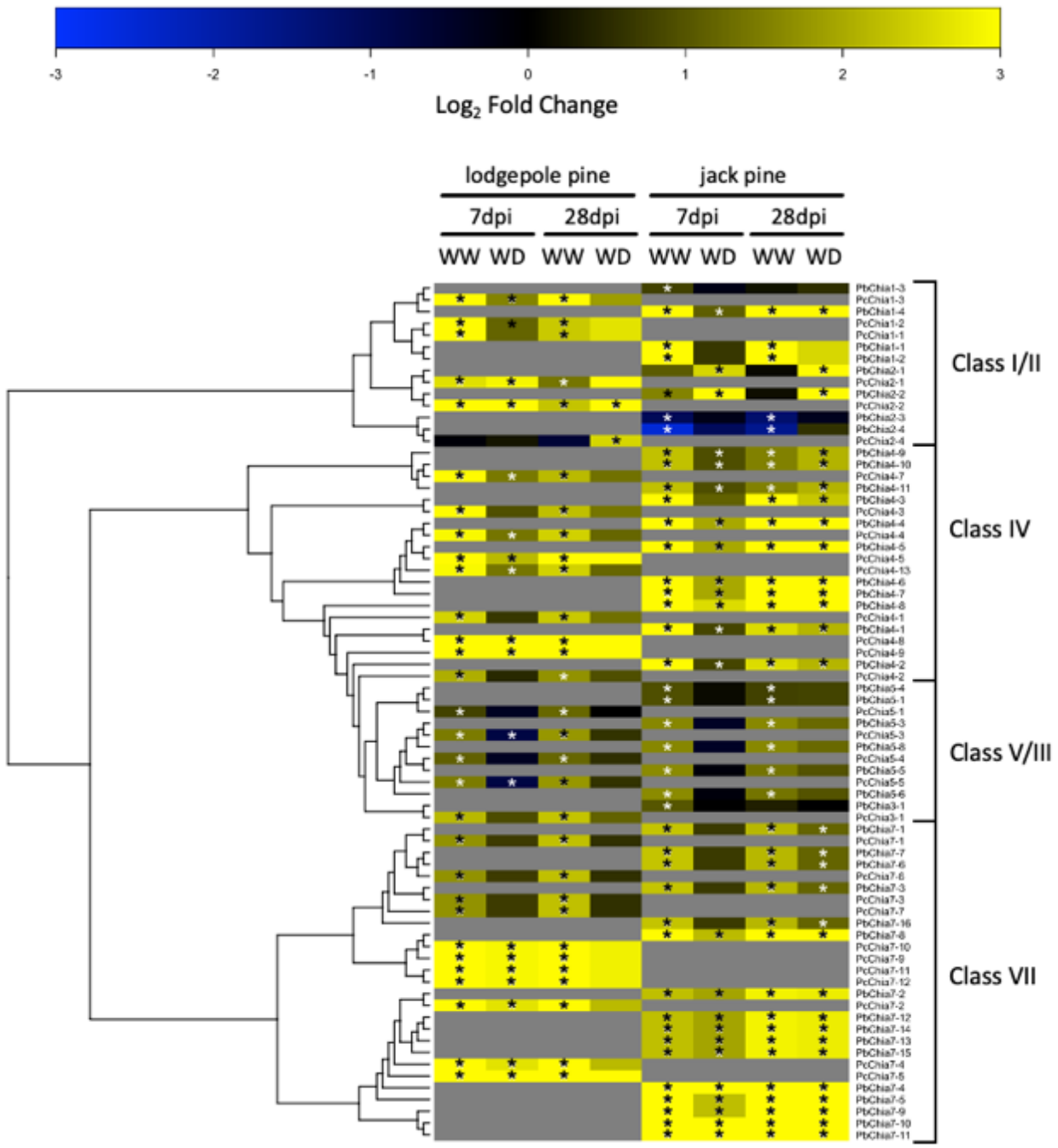

Figure 3.3. Strong upregulation of class I, II, IV, and VII chitinase *(Chia)* expression is apparent in both lodgepole (Pc) and jack pine (Pb) seedlings inoculated with *G. clavigera* at 7 dpi and 28 dpi but is less persistent over time in lodgepole pine under water deficit (WD) conditions. Chitinases differentially expressed in at least one treatment are ordered along the Y-axis of the heatmap based upon phylogenetic relationships determined by maximum likelihood analysis. Yellow and blue indicate higher or lower transcript abundance in *G. clavigera*-challenged seedlings relative to controls, respectively, depicted on a $\log_2$ scale. Asterisks (*)

mark sequences that were significantly DE between control and inoculated samples under well-watered (WW) or water deficit conditions (adjusted $p < 0.05$, n = 4). Grey spaces were used where microarray comparisons did not match the species of a given chitinase gene.

and jack pine EST resources (Hall et al. 2013). Of chitinases that were found to be DE under at least one treatment, almost all were significantly upregulated in response to inoculation with *G. clavigera*, particularly at 7 dpi (Figure 3.3). Class IV and VII chitinases exhibited mostly similar expression patterns between species, except under water deficit conditions at 28 dpi when several chitinases were no longer DE in lodgepole pine only (Figure 3.3).

Terpenes are an important component of resin production and sapwood defenses (Celedon and Bohlmann 2019, Chiu and Bohlmann 2022). We similarly mined the microarray data for terpene synthase-like sequences that were DE under at least one treatment. DE sequences that were annotated as belonging to the terpene synthases included primarily monoterpene synthases, as well as a few diterpene and sesquiterpene synthases (Figure 3.4). Two sequences, *monofunctional diterpene synthase-like* and *caryophyllene synthase-like*, were strongly upregulated in both species. Most monoterpene and diterpene synthase-like sequences were down-regulated, but more were significantly down-regulated in jack pine than lodgepole pine, particularly under well-watered conditions.

In addition to evidence that phenolics accumulate in *G. clavigera*-inoculated xylem (Arango-Velez et al. 2016), phenolic biosynthesis genes represented a large section of secondary metabolism genes DE in our previous analyses. As such, we mined the microarray data for genes putatively involved in phenolic biosynthesis and profiled gene expression across the phenolic biosynthesis pathway to compare how DE might influence phenolic metabolite profiles (Figure 3.5). Many genes putatively involved in flavonoid and anthocyanin biosynthesis exhibited strong

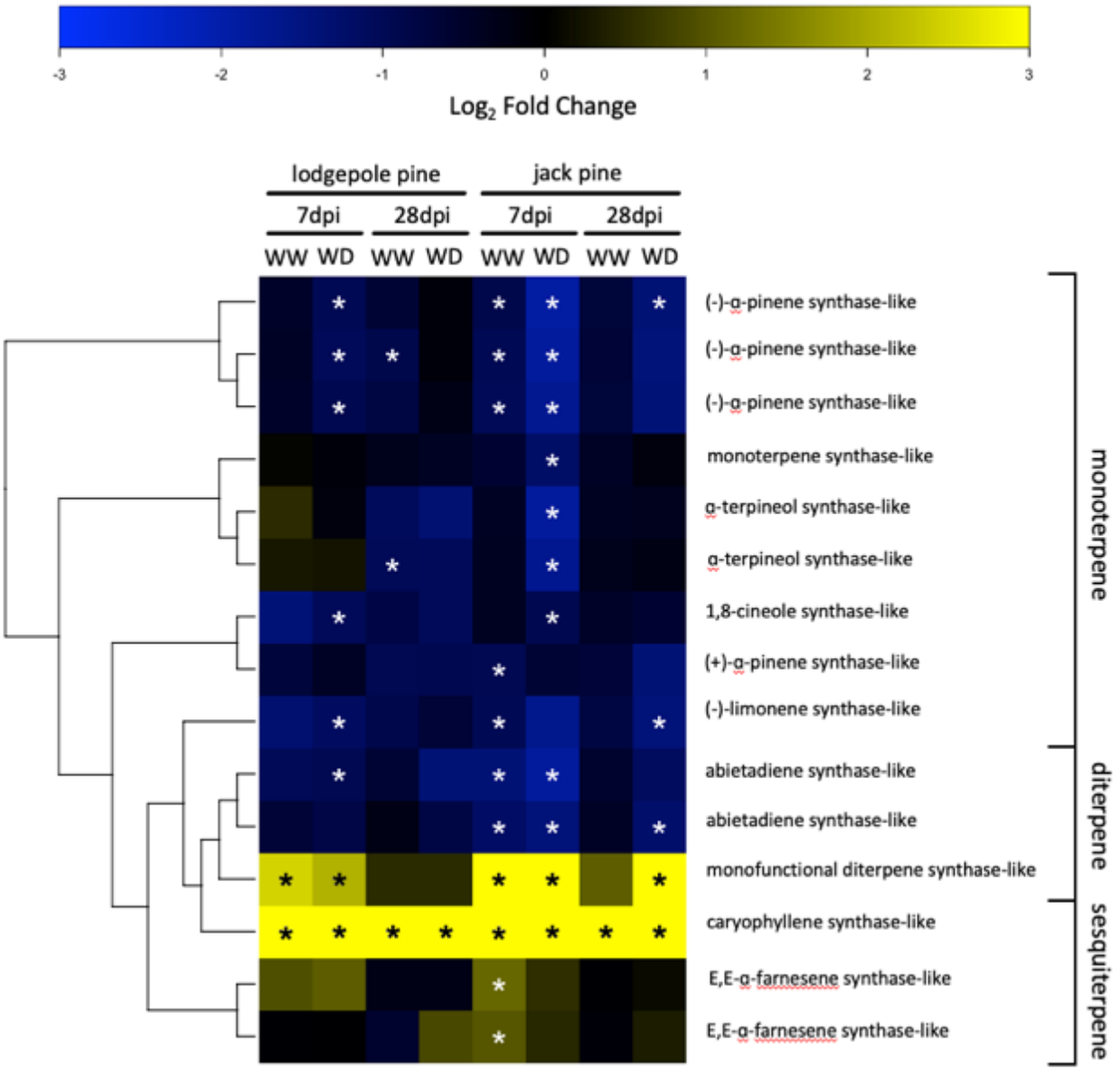

Figure 3.4. Many terpene synthase-like sequences are consistently downregulated early in *G. clavigera*-inoculated jack pine seedlings under well-watered (WW) and water deficit (WD) conditions, yet are only downregulated in inoculated lodgepole pine seedlings under water deficit. PtGen2 sequences with terpene synthase-like annotations differentially expressed under at least one treatment are ordered along the y-axis according to the phylogenetic relationship determined by maximum likelihood analysis. Yellow or blue represent higher or lower transcript abundance, respectively, of sequences in *G. clavigera*-inoculated trees relative to controls at 7 and 28 dpi. Fold change values are depicted on a $\log_2$ scale. Asterisks (*) indicate transcripts significantly DE between control and inoculated samples (adjusted $p < 0.05$, n = 4).

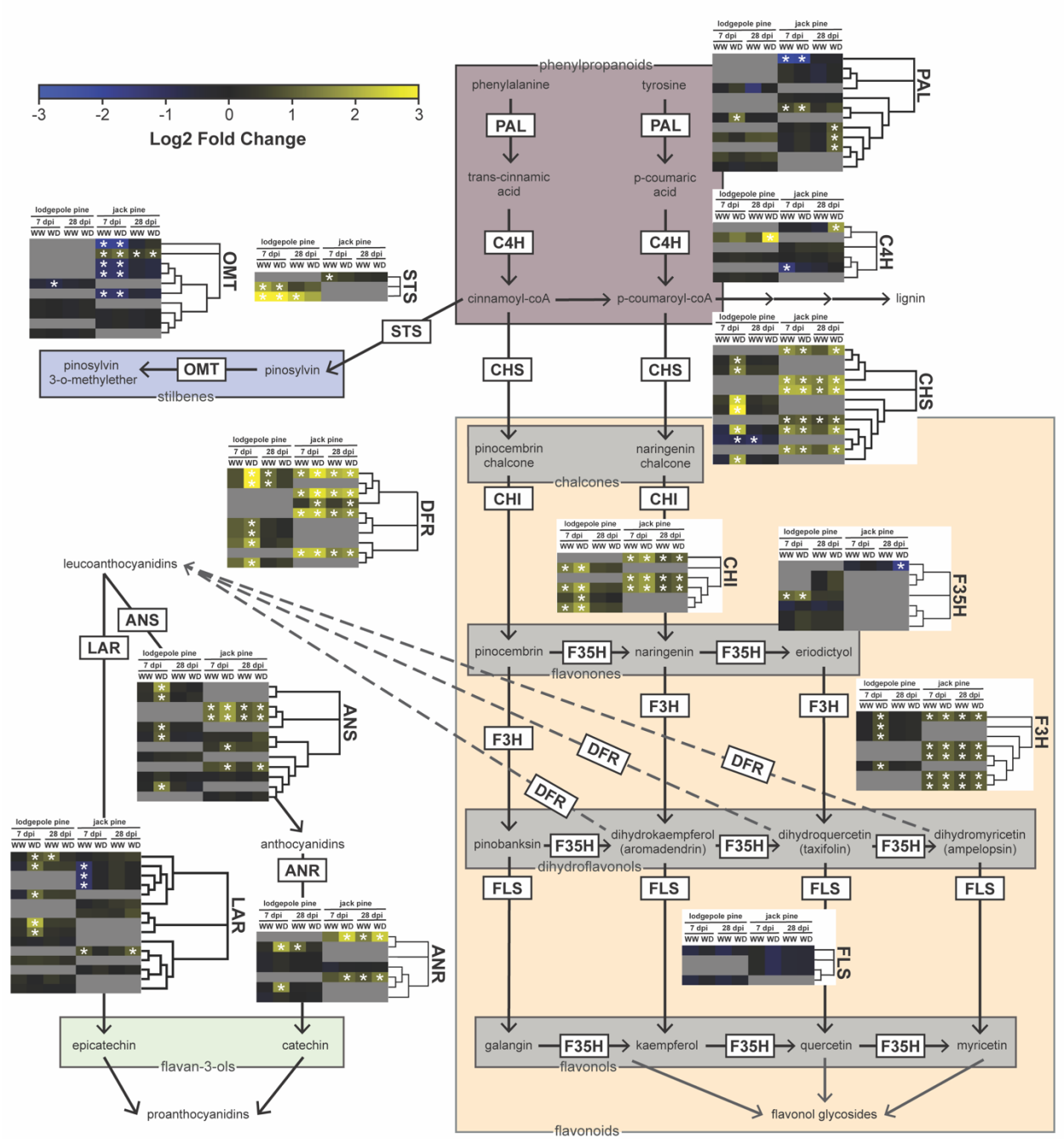

Figure 3.5. Expression profiles of phenolic biosynthesis genes following inoculation with *G. clavigera* reveals that different branches of the pathway show a greater number of DE sequences in lodgepole (*Pc*) versus jack pine (*Pb*) relative to controls. Phenolic biosynthesis genes are ordered along the Y-axis of the heatmap according to phylogenetic relationships determined by maximum likelihood analysis. Yellow/blue indicate higher/lower transcript abundance, respectively, in seedlings inoculated with *G. clavigera* relative to controls, respectively, depicted on a $\log_2$ scale. Asterisks (*) mark sequences significantly DE between

control and inoculated samples under well-watered (WW) or water deficit (WD) conditions (adjusted $p < 0.05$, n = 4). Grey spaces were used where microarray comparisons did not match the species of a given phenolic biosynthesis gene. Enzymes include *phenylalanine ammonia lyase* (*PAL*), *cinnamate 4-hydroxylase* (*C4H*), *stilbene synthase* (*STS*), *stilbene o-methyltransferase* (*OMT*), *chalcone synthase* (*CHS*), *chalcone isomerase* (*CHI*), *flavanone 3-hydroxylase* (*F3H*), *flavonoid 3,5-hydroxylase* (*F35H*), *flavanol synthase* (*FLS*), *anthocyanidin synthase* (*ANS*), *anthocyanidin reductase* (*ANR*), *leucoanthocyanidin reductase* (*LAR*), *dihydroflavonol reductase* (*DFR*). WW = well-watered.

upregulation in jack pine across treatments, while upregulation of these same genes in lodgepole pine was often limited to water deficit conditions at 7 dpi. In contrast, *stilbene synthase* (*STS*) sequences were upregulated primarily in lodgepole pine only, while *stilbene o-methyltransferase* (*OMT*) sequences were primarily downregulated in jack pine only (Figure 3.5).

To conduct more extensive profiling of phenolic biosynthesis gene expression across additional time points, we measured transcript abundance of genes at key branch points of phenolic biosynthesis using qRT-PCR (Figure 3.6). Mock-inoculation treatments were also included in qRT-PCR transcript abundance profiling, in addition to the uninoculated controls that were used in the microarray analyses. Relative changes in transcript abundance for selected sequences were compared between microarray and qRT-PCR data and found to show strong agreement between datasets (Appendix 2 Figure 5). *STS* and both *dihydroflavonol reductase* (*DFR*) genes exhibited greater transcript abundance in response to inoculation with *G. clavigera* in both lodgepole and jack pine, however this induction persisted longer in lodgepole pine than jack pine (Figure 3.6). Water deficit appeared to lower constitutive *OMT1* expression in both species, but this occurred later in jack pine. Finally, we observed that induced expression of *PcDFR1*, *PcDFR2*, and *PcOMT1* was enhanced under water deficit conditions relative to their

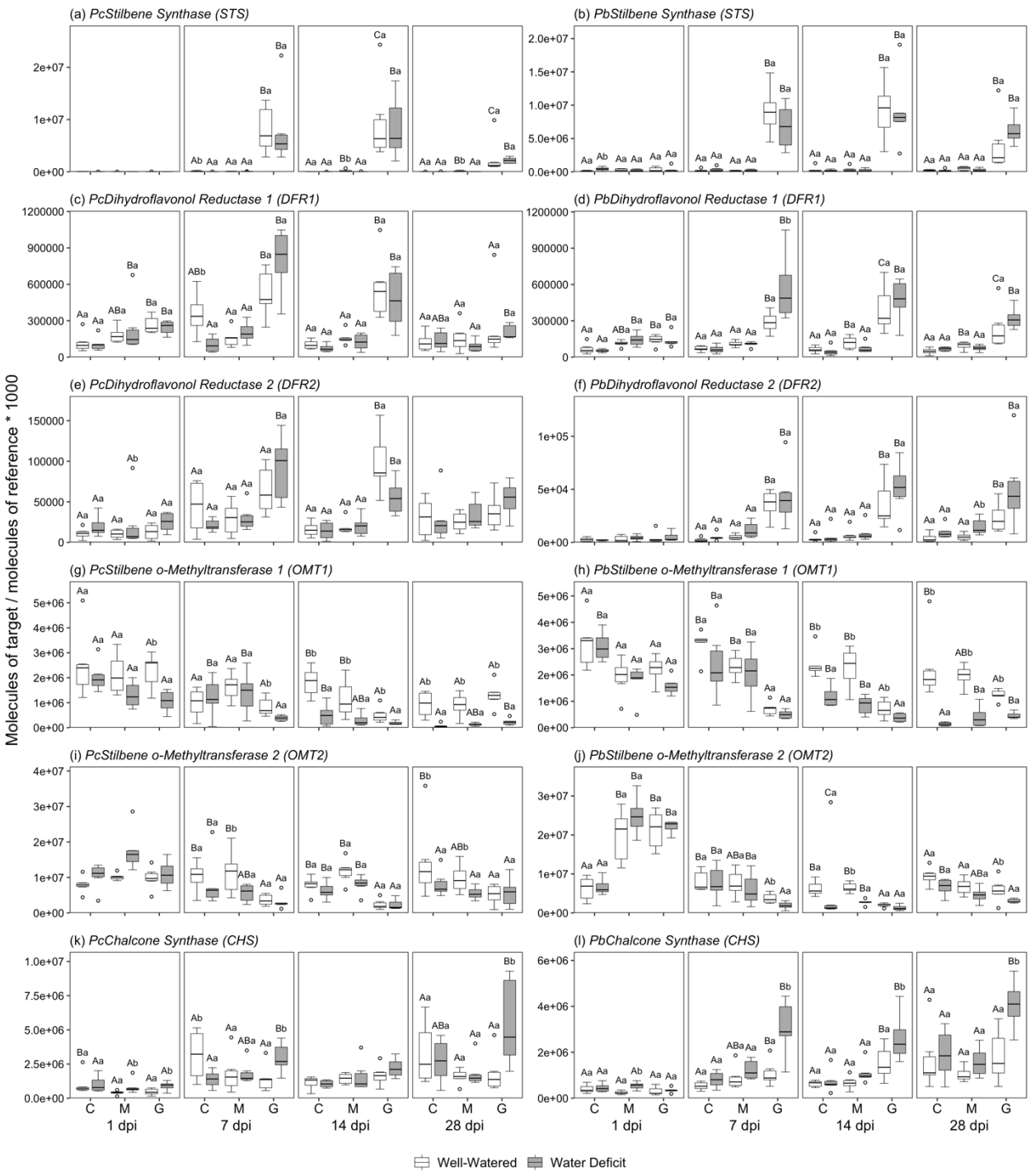

Figure 3.6. qRT-PCR profiling reveals that genes involved in stilbene and flavonoid biosynthesis are similarly upregulated across species in response to *G. clavigera*-challenge but show some differences in responses under water deficit between species. Expression of lodgepole (*Pc*) and jack pine (*Pb)* phenolic biosynthesis genes under well-watered (white boxes) and water deficit (grey boxes) conditions are grouped by control (C), mock- (M), or *G.*

clavigera-inoculation (G). Within a timepoint, capital letters indicate differences between inoculation treatments; lower-case letters denote differences between water treatments ($p < 0.05$, n = 5-6).

controls, but only at 7dpi, while *PcCHS* and *PbCHS* expression following *G. clavigera*-inoculation were significantly higher under water deficit conditions (Figure 3. 6).

3.3.4 Effect of G. clavigera *and water availability on phenolic metabolite profiles*

Phenolic metabolites were quantified using HPLC-DAD to determine total phenolic profiles and to identify a subset of phenolic compounds using authenticated standards. NMDS analysis was used to obtain ordination models based on this metabolite data, including known and unidentified compounds, at both 7 and 14 dpi (Figure 3.7). NMDS stress values for both models were less than 0.1, indicating a good fit. ANOSIM was used to determine the extent to which phenolic profiles differed between treatments; profiles significantly differed between inoculation treatments at both 7 ($p < 0.001$, R = 0.52) and 14 dpi ($p < 0.001$, R = 0.58), while profiles were not different between species (7 dpi $p = 0.10$, R = 0.04; 14 dpi $p = 0.07$, R = 0.04) or water treatments (7 dpi $p = 0.95$, R = -0.03; 14 dpi $p = 0.91$, R = -0.03; Figure 3.7). NMDS analysis additionally identified several compounds as significant predictors of differences in phenolic profiles across treatments (Figure 3.7), including stilbenes pinosylvin and PMME, lignin precursors coniferyl alcohol and *p*-coumaryl alcohol, lignan compounds pinoresinol and matairesinol, and the flavonoid pinostrobin. Closer inspection of predictor compounds which could be identified using authenticated standards revealed that almost all were detectable only in response to *G. clavigera* (Figure 3.8). Additionally, *trans*-cinnamic acid and matairesinol were initially only detectable in lodgepole pine under water deficit (Figure 3.8).

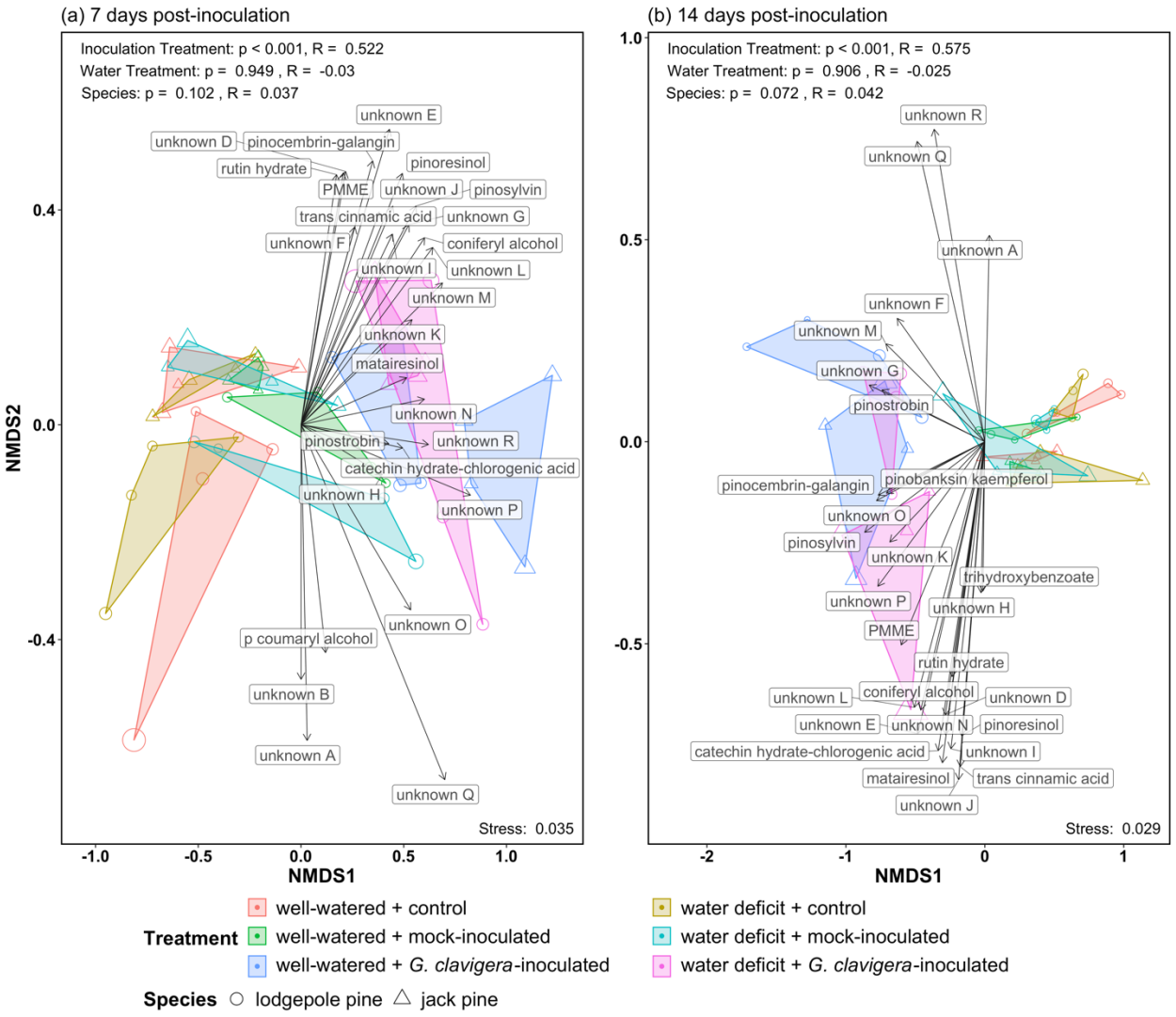

Figure 3.7. NMDS of phenolic metabolite profiles reveals that inoculation with *G. clavigera* significantly alters phenolic composition in lodgepole and jack pine secondary xylem under both well-watered (WW) and water deficit (WD) conditions. Point shape indicates species, point color indicates treatment, and point size is proportional to sample goodness of fit. Phenolic compounds identified as significantly contributing to differences in phenolic profiles between groups are included ($P < 0.05$); arrows represent the strength and direction of each predictor. Stress values indicate the fit of the ordination model; values less than 0.2 are considered a good fit. ANOSIM values indicate the influence of treatment or species on the phenolic profiles; *p*-values represent the significance of each factor while R values represent the similarity of phenolic profiles within a factor (R values of 1 indicate that samples are identical).

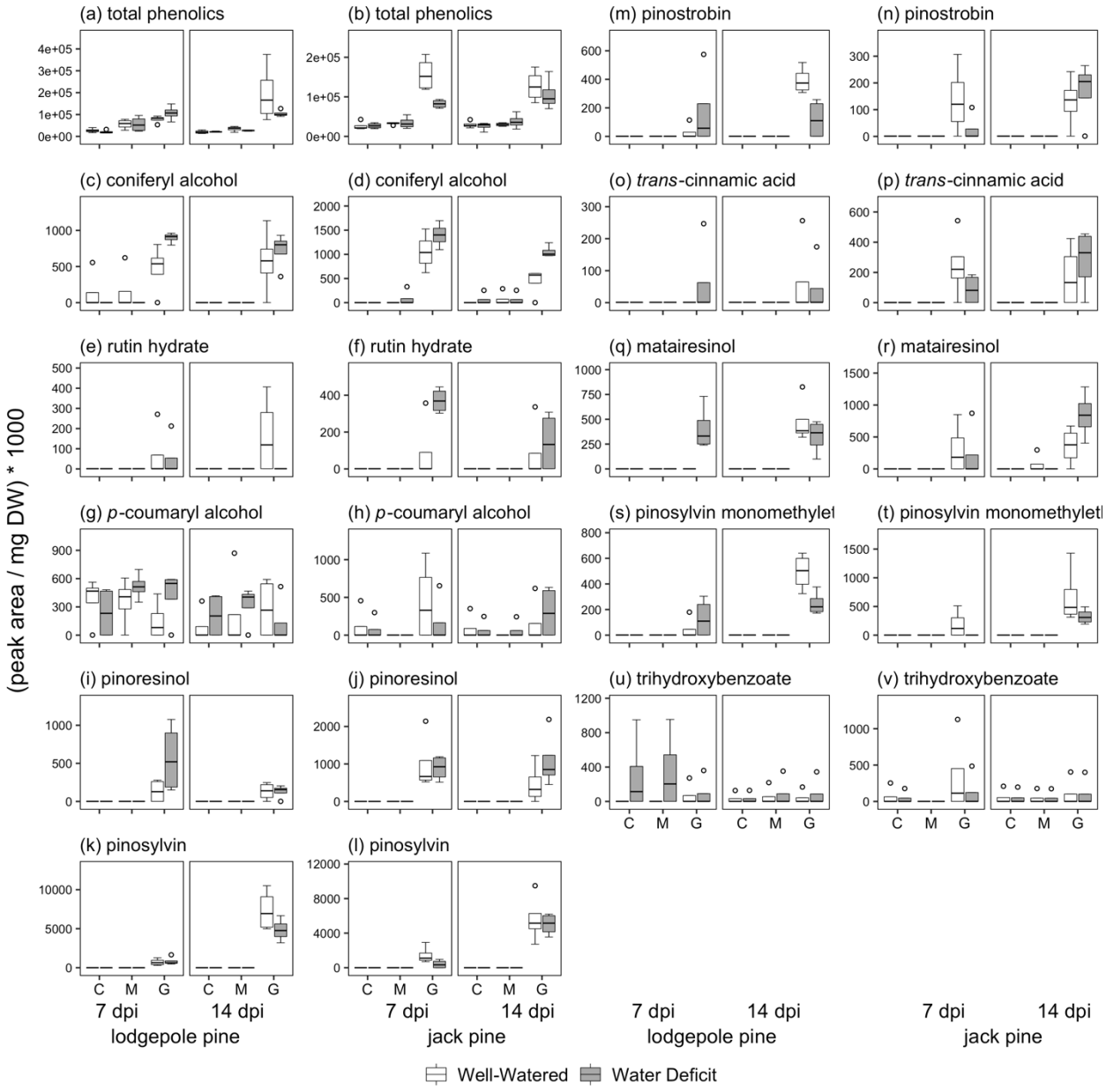

Figure 3.8. Many stilbenes, phenylpropanoids, and lignans exhibit *G. clavigera*-induced synthesis. Compounds identified as significant by NMDS and matching retention time of phenolic standards were compared across inoculated, unwounded control (C), mock-inoculated, and *G. clavigera*-inoculated trees at 7 and 14 dpi under well-watered (white bars) or water deficit (grey bars) conditions (n = 4).

3.4 Discussion

3.4.1 Lodgepole and jack pine share a core set of defenses including chitinase expression

Our first objective was to compare xylem defense responses to *G. clavigera* between lodgepole and jack pine. Both species exhibit a strong response to *G. clavigera* at 7 dpi, including several genes involved in ethylene biosynthesis and signal transduction that may activate necrotrophic-specific defenses. Within this core set of responses was the upregulation of several classes of chitinases, which are protein defenses that can break down chitin, a major component of fungal cell walls (Islam et al. 2011, Grover 2012). Chitinases are commonly expressed in response to pathogens, and the up-regulation of class IV and VII chitinases in xylem is consistent with chitinase expression in lodgepole and jack pine phloem in response to *G. clavigera* (Peery et al. 2021 and Chapter 2).

3.4.2 Secondary metabolism is a primary component of the jack pine defense response, but to a lesser extent in lodgepole pine

We observed many secondary metabolite sequences that were DE in both species under well-watered conditions. However, a much larger proportion of secondary metabolism sequences were found to be DE in jack pine at both timepoints compared to lodgepole pine. In a previously published study, we demonstrated that jack pine seedlings sustained less loss of hydraulic conductivity following *G. clavigera* inoculation than lodgepole pine seedlings (Arango-Velez et al. 2016). Based on this finding, we proposed that this may reflect reduced colonization of *G. clavigera* into the sapwood of jack pine than lodgepole pine, or alternatively, that a greater degree of embolism was triggered by fungal growth in lodgepole pine than jack pine (Arango-Velez et al. 2016). If this is true, then greater induction of secondary metabolites in jack pine may contribute to containing or slowing fungal growth. Furthermore, this may also contribute to

the delayed DE of sequences with stress-related annotations we observed in jack pine relative to lodgepole pine.

Work comparing xylem resin duct formation in lodgepole and jack pine seedlings has suggested that jack pine invests more resources in xylem terpene defenses than lodgepole pine (Arango-Velez et al. 2016). While we did not measure xylem monoterpene levels, our results indicate that expression of xylem TPS genes were more significantly downregulated in jack pine under well-watered conditions relative to lodgepole pine. This suggests that xylem resin duct formation does not require newly synthesized terpenes. It also indicates that the xylem does not contribute to induction of monoterpenes observed in phloem following inoculation (Arango-Velez et al. 2016).

Phenolic compounds constitute part of the lesion formed in response to *G. clavigera* inoculation, accounting for the rich discoloration of the cells within the lesion (Arango-Velez et al. 2016). Despite this, phenolics are relatively unstudied, particularly in the xylem. Our results indicated that biosynthesis of several phenolic compounds is strongly induced by *G. clavigera* infection in both lodgepole and jack pine, including several flavonoids and stilbenes measured. Some of these compounds, including pinosylvin, have been shown to accumulate in other host species such as *Pinus sylvestris* L. following infection with *Ophiostoma brunneo-cilatum* Math. (Croisé and Lieutier 1993) and *Ophiostoma ips* (Rumb.) Nannf (Croisé and Lieutier 1998) as well as in *Pinus strobus* L. infected with pine wood nematodes (*Bursaphelenchus xylophilus* Nematoda: Aphelenchoididae; Hwang et al. 2021). Although some differences in constitutive phenolic profiles were observed between lodgepole and jack pine, profiles following inoculation with *G. clavigera* were similar between species, particularly across the common phenolics that

were identified through use of standards. These results indicate that lodgepole and jack pine respond similarly to *G. clavigera* and utilize conserved mechanisms for fungal containment.

3.4.3 Water deficit did not alter phenolics at the metabolite level in either species

We next tested the effect of water deficit on constitutive and induced xylem defenses in lodgepole and jack pine seedlings. We did not observe an effect of water deficit on constitutive or induced phenolic metabolite profiles. These results are consistent with observations made in *P. sylvestris* inoculated with *O. ips* where it was observed that lesion-associated monophenols did not change under water deficit conditions (Croisé and Lieutier 1998). This lack of effect of water deficit on defense metabolites could be related to the carbon source utilized for synthesis of these compounds. A study by Guérard et al. (2007) found that most of the carbon utilized in induced defense responses of *P. sylvestris* to *Ips sexdentatus* Boern (Coleoptera:Curculionidae) and associated fungus *O. ips* were derived from stored carbon supplies, particularly in the sapwood. They also found that water-stressed trees relied more on stored carbon than new carbon. It is possible that either the water deficit treatment was not long enough to cause sufficient depletion of carbon stores to impact induced defenses, but also that the effects of water deficit would not likely be seen until these defense stores are depleted.

3.4.4 Water deficit had a greater effect on induced defenses in lodgepole pine than jack pine

We also tested whether water deficit had a greater effect on lodgepole pine defenses than jack pine, as we hypothesized that differences in water use strategies would influence host sensitivity to drought stress. Water deficit enhanced induction of secondary metabolite gene expression –including expression of genes involved in phenolic biosynthesis – in lodgepole pine relative to well-watered conditions. Conversely, water deficit had little effect on the proportion of secondary metabolism sequences that were DE in jack pine. This difference in effect of water

deficit between species may be reflective of differences in drought tolerance, as jack pine has been demonstrated to be more tolerant of drier conditions (Rweyongeza et al. 2007, Arango-Velez et al. 2016). Patterns of non-structural carbon (NSC) and starch allocation under water deficit have been found to differ between species as well as based on drought length and severity (Moran et al. 2017 and references within). Galiano et al. (2017) found that *P. sylvestris* exhibited increased NSC under drought conditions, indicating active formation and storage of NSC and contradicting previous predictions that carbon is rapidly depleted under drought. It is possible that under water deficit conditions, lodgepole pine quickly shifts resource allocation to carbon storage, which are then available upon induction of defenses and allow for a greater response than under well-watered conditions. In contrast, jack pine likely does not shift resource allocation as quickly or to as great an extent as lodgepole pine under water deficit conditions, which may account for why we did not see many differences in gene expression in water deficit jack pine.

Although we did not observe significant differences in phenolic metabolite levels of lodgepole pine under water deficit, it is possible that is the result of a delay between gene expression and metabolite synthesis. Previous work observed decreased lesion lengths in lodgepole and jack pine early under water deficit, but that lesion length increased under water deficit at later timepoints (Arango-Velez et al. 2016), possibly reflective of increased phenolic levels. However, when comparing between lodgepole and jack pine seedlings, increased lesion length under water deficit was observed earlier in jack pine (Arango-Velez et al. 2016), which is not explained by our phenolic gene expression data. Larger lesions were also observed in Norway spruce following drought (Öhrn et al. 2021). However, this was interpreted to indicate lower defence capacity as it was assumed that lesion length correlated with fungal growth, a

relationship we have found to be inconsistent in our host-pathogen system (McAllister et al. 2018). Furthermore, a constraint identified with using lesion length is that it does not measure radial deposition of defenses (McAllister et al. 2018). As we know that phenolics are accumulated across multiple rows of tracheids (Arango-Velez et al. 2016), measuring lesion length may under-represent the extent of phenolic deposition within the xylem.

3.5 Conclusion

Xylem responses to MPB and its Ophiostomatoid fungal associates, including *G. clavigera*, are relatively unstudied, and not well understood. We compared xylem molecular and biochemical defense responses of lodgepole and jack pine seedlings to MPB Ophiostomatoid fungal associate *G. clavigera* under well-watered and water deficit conditions. Both species exhibited a similarly strong upregulation of chitinases, likely downstream of jasmonic acid and ethylene biosynthesis genes DE at 7 dpi. Phenolics were also a core component of this shared response, indicative of their postulated role in containment of fungal growth.

We next tested the hypothesis that water deficit would alter xylem defense responses. Phenolic metabolite profiles of either species were not affected by water deficit, including newly synthesized phenolics induced by *G. clavigera* inoculation. These results support previous studies in *Pinus sylvestris* which determined that water deficit trees rely on stored carbon for induced defenses (Guérard et al. 2007). It also suggests that more prolonged water deficit, sufficient long enough to deplete stored resources, would have a more detrimental impact on induced defenses.

Lastly, we compared the effect of water deficit between lodgepole and jack pine. We hypothesized that water deficit would be more limiting to defense induction as previous results have suggested that lodgepole is more sensitive to water deficit than jack pine (Arango-Velez et

al. 2016 and Chapter 2). We did observe a larger transcriptomic response from lodgepole pine in response to water deficit conditions, while jack pine responses were relatively the same under well-watered and water deficit conditions. This shift in lodgepole pine gene expression was not reflected in phenolic metabolite levels and does not suggest differences in host susceptibility of lodgepole or jack pine to *G. clavigera* under water deficit conditions, at least at the level of stress that was imposed in this study.

Chapter 4: Determining the role of Ophiostomatoid fungal pathogens in overwhelming lodgepole pine defenses during mountain pine beetle mass attack

4.1 Introduction

Mountain pine beetle (MPB, *Dendroctonus ponderosae* Hopkins; Coleoptera: Curculionidae, Scolytinae) is an aggressive bark beetle in western North America that historically attacks and kills lodgepole pine (*Pinus contorta* Dougl. ex Loud. var. *latifolia* Engelm.). MPB utilizes a mass-attack strategy to overwhelm host defenses prior beetle establishment (Six and Klepzig 2021). MPB mass attack occurs over a relatively short period. Aggregation pheromone initiating mass attack is produced soon after a pioneer female lands and determines a host is suitable (Safranyik and Carroll 2006). Ensuing attacks generally peak 1-2 days following initial attack, and typically do not persist for more than 7 days (Raffa and Berryman 1983, Safranyik and Carroll 2006). During this short time frame, host constitutive defenses are exhausted by attacking MPB, and induced defense synthesis may not be sufficient to prevent successful MPB colonization (Krokene 2015).

Trees form distinct lesions containing host defense compounds following MPB attack, including terpene-rich oleoresin (Shrimpton 1973, Safranyik and Carroll 2006, Kolosova and Bohlmann 2012). Terpenes fulfill an important role in Pinaceae defense against pests and pathogens, including in *Pinus* spp. responses to MPB. As such, terpenoids have been studied extensively in lodgepole pine in response to MPB attack. MPB exploit host (-)-α-pinene as a precursor to the aggregation pheromone (-)-*trans*-verbenol (Chiu et al. 2019, Chiu and Bohlmann 2022), while other monoterpenes such as limonene have toxic effects on MPB (Reid et al. 2017). In addition to resinous compounds, lesions formed in MPB-attacked trees contain phenolics

(Raffa et al. 2008), which can be synthesized and accumulated in an attempt to slow or contain pathogen growth (Witzell and Martín 2008, Wallis and Galarneau 2020). The effect of phenolics on MPB are not as well understood as those of terpenoids, although polar extracts of lodgepole pine, presumably containing some phenolic compounds, were found to encourage MPB feeding (Raffa and Berryman 1982). Oxidation of phenolics can trigger the production of toxic reactive oxygen species (Barbehenn and Constabel 2011) and foliar phenolics are believed to play a role in resistance to several insects (Moctezuma et al. 2014, Qazi et al. 2018).

MPB vector several Ascomycota fungi in specialized structures called mycangia (Bleiker et al. 2009). Fungal assemblages can vary by geography (Roe, James, et al. 2011), and often consist of multiple fungal partners (Six and Bentz 2007, Roe, James, et al. 2011), including the Ophiostomatoid fungal species *Grosmannia clavigera* [Robinson-Jeffrey and Davidson] Zipfel, de Beer and Wingfield, *Ophiostoma montium* (Rumbold) von Arx., and *Leptographium longiclavatum* Lee, Kim and Breuil (Bleiker et al. 2009, Roe et al. 2010, Roe, Rice, et al. 2011, Six 2020a). Upon introduction to the host by MPB (Ballard et al. 1982, Safranyik and Carroll 2006, Six 2020a), fungi can then spread into xylem via ray parenchyma cells and permeate tracheids via pits (Ballard et al. 1984, Six 2020a). Early on, perception of the fungal pathogen triggers host formation of tyloses, blocking movement of materials through tracheids in an effort to restrict fungal access (Parmeter et al. 1987, Solheim 1995, Arango-Velez et al. 2016). This results in cavitation and reduced water transport capacity (Arango-Velez et al. 2016). Further fungal growth will cause occlusion and the complete blockage of water transport (Arango-Velez et al. 2016), and it is this water deficit that is the ultimate cause of tree mortality following MPB attack (Hubbard et al. 2013).

Ophiostomatoid fungal associates are an important nutritional resource for MPB. Fungi colonize ray cells and xylem, enabling them to translocate nutrients to the galleries and pupal chambers (Six 2020a). This concentration of resources can help support fungal sporulation (Six and Klepzig 2021) in addition to providing increased nitrogen (Bleiker and Six 2007, Cook et al. 2010, Goodsman et al. 2012), sterols (Bentz and Six 2006), and other nutrients to developing MPB (Ayres et al. 2000, Klepzig and Six 2004). MPB larvae and teneral adults show preferential feeding of phloem containing fungal spores over uncolonized phloem (Bleiker and Six 2007), and beetles reared on inoculated phloem exhibited faster development and reduced gallery construction (Myrholm and Langor 2016). MPB fitness is also dependent on these fungi, as MPB lacking fungal associates produced no brood (Six and Paine 1998).

While there is extensive research indicating that Ophiostomatoid fungi are important to MPB fitness (Klepzig and Six 2004, Six and Elser 2019, Six 2020b), the role that these fungi play in MPB's ability to successfully attack host trees is far from clear. One prevailing paradigm states that Ophiostomatoid fungal associates are critical for MPB successful attack as they help overwhelm and exhaust host defenses, in addition to facilitating beetle excavation and colonization (Lieutier et al. 2009, Six and Wingfield 2011). This paradigm is based in large part on the observation that *G. clavigera* and other MPB fungal associates are pathogens (Parker and Gilbert 2004) i.e., these Ophiostomatoid species colonize pine tissues, causing harm to the host and eliciting canonical defense responses (Arango-Velez et al. 2016). Additionally, trees inoculated with *G. clavigera* exhibit defense responses similar to those invoked by MPB attack, including lesion development (Arango-Velez et al. 2014, 2016), suggesting that *G. clavigera* and other Ophiostomatoid associates trigger these responses during MPB attack.

In their thought-provoking review, Six and Wingfield (2011) challenge the long-held view that the Ophiostomatoid fungal associates of bark beetles such as MPB contribute to the beetle's capacity to overcome defenses of healthy trees during mass attack. They outline several studies that provide indirect evidence that these fungi do not significantly contribute to the ability of mass-attacking bark beetles to overwhelm the tree's constitutive and induced defenses. Rather, the authors propose an alternative model in which the pathogenicity of Ophiostomatoid fungal associates provides an advantage in competing with other species of the MPB microbiome, enabling these fungi to colonize the host more efficiently for resource capture (Six and Wingfield 2011). However, to date no rigorous test of the hypothesis has been carried out.

In this study, we have used the distinctive hormone signatures of plant defense against herbivorous insect pests and fungal pathogens to assess the contribution of MPB-vectored Ophiostomatoid fungal symbionts to the ability of MPB to overcome lodgepole pine defenses during mass attack. In conifers, as in angiosperms, jasmonic acid (JA) plays a central role in activating defense responses against both insect herbivores and necrotrophic fungal pathogens (Miller et al. 2005, Lombardero et al. 2013, Pieterse et al. 2012, Arango-Velez et al. 2016). In contrast, extensive studies with angiosperms show that salicylic acid is synthesized in response to biotrophic fungal pathogens (Glazebrook 2005, Ullah et al. 2019). We have previously demonstrated that lodgepole pine synthesizes JA and its active form, JA-isoleucine (JA-Ile), in response to *G. clavigera* challenge (Arango-Velez et al. 2016), providing evidence that pines perceive *G. clavigera* as a necrotrophic pathogen. JA has also been implicated in conifer responses to other necrotrophs, including Norway spruce (*Picea abies* (L.) Karst) defense signalling against *Heterobasidion annosum* (Arnerup et al. 2013, Lundén et al. 2015). In angiosperms, ethylene (ET) acts synergistically with JA to regulate plant defense responses

against necrotrophic pathogens (Broekgaarden et al. 2015), but is not involved in defense signalling triggered by herbivorous insects (Garcia et al. 2021). The role of ET in conifer defense against fungal necrotrophic pathogens has received considerably less attention than JA, although there is indirect evidence implicating ET in conifer defense against necrotrophs from transcriptomic studies of the Norway spruce - *H. annosum* pathosystem (Arnerup et al. 2011).

We hypothesized that if *G. clavigera* contributes to MPB's capacity to overwhelm host defenses during the critical mass attack phase, then the host tree should perceive attack by both MPB and its vectored necrotrophic fungal pathogen symbionts, triggering synthesis of both JA and ET. In the null hypothesis, if *G. clavigera* does not contribute meaningfully to MPB's capacity to overwhelm host defenses during the attack phase, then the tree should perceive MPB but not its necrotrophic fungal symbionts, and we should detect increased JA but not ET. To test this hypothesis, we needed to establish whether ET is invoked by lodgepole pine in response to MPB Ophiostomatoid fungal associates. Accordingly, we used liquid chromatography-tandem mass spectrometry (LC-MS/MS) to the ET precursor 1-aminocyclopropane-1-carboxylate (ACC) together with JA, JA-Ile, and SA in lodgepole pines undergoing MPB mass attack and in *G. clavigera*-inoculated lodgepole pines. We focused on the attack phase when host defenses are being challenged and overcome, rather than the subsequent colonization phase that follows successful attack. Finally, we compared chemical defense responses of MPB-attacked and *G. clavigera*-inoculated lodgepole pines to determine whether lodgepole pine's perception of an herbivorous insect versus a necrotrophic fungal pathogen triggers markedly different suites of chemical defenses. Given that lesion development is a hallmark of pine responses to both MPB attack and inoculation with Ophiostomatoid MPB fungal associates, but that lesion development takes an extended period of time, we profiled phenolic compounds that are characteristic of these

lesions. This experimental approach allowed for the most rigorous test of the role that phytopathogenicity plays in MPB's ability to overcome host defenses during mass attack.

4.2 Materials and Methods

4.2.1 Field Experiment

The field study was carried out in a natural stand comprising predominantly even-aged mature lodgepole pine located south of Grande Prairie AB Canada (54º27′N, 118º37′W), as outlined in McAllister et al. (2018). Healthy lodgepole pine trees aged approximately 45 to 75 years old with no signs of recent damage or disease were randomly assigned to two different groups: 1) trees inoculated with *G. clavigera* and controls, and 2) trees mass attacked by MPB and controls (see Appendix 3 Figure 1). Diameter at breast height (1.3 m) for all trees (n = 57) averaged 31 cm (*sd* = 4 cm). We elected to carry out the *G. clavigera* inoculation portion of the study prior to the emergence window of MPB to avoid the possibility that *G. clavigera*-inoculated or control trees would be attacked by MPB during the course of the experiment. Accordingly, the *G. clavigera* inoculation portion of the study was conducted in June 2016, while the MPB attack portion of the study coincided with MPB emergence in July and August 2016. Thus, we refer to these two components of the study as the *G. clavigera* inoculation experiment and the MPB attack experiment.

4.2.2 G. clavigera *Inoculation Experiment*

Twenty-nine trees were randomly assigned to one of three treatments: 1) *G. clavigera*-inoculated (n = 10) 2) mock-inoculated (n = 9), and 3) uninoculated control (n = 10). For each of the *G. clavigera*- or mock-inoculated trees, a 1/2-inch round drive punch (Tandy Leather, Edmonton, AB) was used to penetrate the bark through to the cambium. The bark plug was then removed to expose the cambial zone. Two horizontal rows of 6-8 inoculation holes were created

on each tree: one row positioned at 1.9 m above ground level and a second row at 1.3 m. The inoculation holes within a row were positioned approximately 6 cm apart and covered half the tree's circumference. The two rows of inoculation holes were offset, such that the horizontal row of inoculation holes at 1.9 m was on the opposite side of the tree from the row of holes at 1.3 m. Inoculation holes were not created in the uninoculated control trees. For *G. clavigera*-inoculated trees, each hole was filled with a malt extract agar-mycellium plug of *G. clavigera* isolate M002-12-03-03-UC10G11 SS496 (described by Roe et al. 2010). This isolate was derived from single spore culture initiated from *G. clavigera* isolated from a single MPB larva collected from a naturally MPB-attacked tree near Sparwood, BC Canada (49º53′N, 114º54′W). For mock-inoculated trees, each hole was filled with a sterile MEA plug. Bark was replaced on top of the agar and the stem was wrapped with stretch wrap (Uline Canada, Milton, ON) to cover the inoculation sites. Uninoculated control trees were left untouched until sampling.

Secondary xylem and secondary phloem tissues were sampled from each of the 57 trees at 1.9 m at 7 days post inoculation (dpi) and resampled at 1.3 m at 14 dpi (Appendix 3 Figure 2). A rubber mallet chisel, and linoleum knife were used to remove bark strips of approximately 10 cm x 20 cm, each containing 1-2 inoculation sites (Appendix 3 Figure 3). The bark strips separated from the wood at the cambial zone. Secondary phloem was then peeled from this bark strip. A low angle spokeshave (Veritas; Lee Valley Tools Ltd., Ottawa, ON) was used to shave xylem from the wood exposed by removal of the bark strip (Appendix 3 Figure 3c). Xylem shavings were approximately 1-2 mm thick. Immediately after collecting, tissues were flash frozen using liquid nitrogen and stored on dry ice for transport. Samples were transferred to -80ºC for long term storage.

Following sampling at 7 dpi, exposed wood at the 1.9 m sampled inoculation sites was covered with aluminum foil secured with duct tape wrapped around the trunk to minimize infection by other agents prior to the 14 dpi sampling.

4.2.3 MPB Attack Experiment

Twenty-eight trees were assigned to one of three treatments: 1) MPB-attacked (n = 9), 2) mock-attacked (n = 9), and 3) control (untreated; n = 10). Bark beetle tree baits designed for *D. ponderosae* (Product #3122, Synergy Semiochemicals Corporation, Delta, BC) were attached to trees designated for the MPB-attack treatment to attract MPB. Baited trees were then monitored twice daily for evidence of MPB attack. To prevent MPB attack of mock-attacked and control trees, the trunk of each tree was wrapped in standard aluminum 18 x 16 mesh (openings per linear inch) screen from the base of the tree to 3 m high (Appendix 3 Figure 4). Styrofoam was used to fill in gaps at both ends of the wrapped sections between the mesh and trunk, and mesh was secured along the sides with zip ties and staples. These trees were also monitored to ensure that no MPB attacks occurred prior to sampling.

When all trees designated for the MPB-attacked group had received more than one MPB attack, MPB attacks were simulated on each of the trees in the mock-attacked group using a similar procedure to that described for the mock-inoculation group. A 1/2-inch round drive punch was used to create 7 wound sites approximately 6 cm apart in the bark, covering half of the tree's circumference in two horizontal rows on opposite sides of the tree at 1.9 m and 1.3 m. Each bark plug was replaced into the hole created by its removal, and the ring of wound sites wrapped until sampling.

The day that treatments were applied to the mock-attacked group of trees was designated Day 0, i.e., 0 days post wound (dpw). The first set of secondary phloem and secondary xylem

samples were collected at 1.9 m the following day from MPB-attacked, mock-attacked, and control untreated trees (Appendix 3 Figure 2). This first sampling time point is collectively referred to as 1 dpw for all treatments and corresponded to 1-7 days following initial detection of MPB attack for all trees in the MPB-attacked treatment group. The second set of samples for the MPB-attack experiment were collected at 1.3 m from all three treatment groups at 7 dpw, which corresponded to 7-13 days following initial detection of MPB attack. Each sampling of MPB-attacked trees was conducted on an area of the tree encompassing 0-2 pitch tubes. Baits were removed from MPB-attacked trees following the first sampling. Also as described above, areas where bark was removed during sampling at 1 dpw were covered with aluminum foil held in place with duct tape.

4.2.4 Hormone Analysis

Hormones were quantified at the Aquatic and Crop Resource Development Research Centre, part of the National Research Council Canada (Saskatoon, SK). The ET precursor 1-aminocylcopropane-1-carboxylic acid (ACC) was extracted using a procedure modified from Lulsdorf et al. (2013). Hydrolysis of conjugated salicylic acid (conj. SA) was based on procedure modified from Malamy et al. (1992). All quantification was performed by UPLC-ESI-MS/MS (ACQUITY UPLC, Waters Canada, Mississauga, ON) and quantified using JA, SA, ACC standards purchased from Sigma-Aldrich and JA-Ile purchased from OlChemim Ltd. (Olomouc, Czech Republic). JA and SA were quantified using a modified procedure from Murmu et al. (2014). ACC was quantified using a modified procedure from Chauvaux et al. (1997). Deuterated forms of the hormones synthesized according to Galka et al. (2005) were used as internal standards, in addition to 1-amino-[2,2,3,3-d_4]cylopropane-1-carboxylic acid (d_4-ACC) and 3,4,5,6-d_4-2-hydroxybenzoic acid standards purchased from CDN Isotopes (Point-Claire, QC).

4.2.5 Phenolic Metabolite Analysis

Twenty-five microlitres of 4 mg mL^{-1} gallic acid monohydrate (Sigma-Aldrich Cat. 398225) was added to approximately 100 mg of fresh frozen tissue prior to extraction of metabolites in 1mL HPLC-grade methanol by vortexing, then shaking, covered, for 1 h at 4ºC. The samples were centrifuged for 15 min at 14,000 rpm and the supernatant collected. The extraction was repeated three times, and supernatants were pooled. Eight hundred microlitres of the pooled supernatant was transferred to a glass vial and evaporated to dryness under a stream of nitrogen gas. Residues were stored at -20ºC for no more than 1 month prior to analysis. Six biological replicates were prepared for each of the 12 treatments, and three technical replicates were extracted separately from each sample.

Sample residues that had been resuspended in 200 µL HPLC-grade methanol no more than 16 hours prior to injection were filtered through an Ultrafree-MC 0.2 µm PTFE centrifugal filter (EMD Millipore Cat. UFC30LG25) and kept at 4ºC. Ten microlitres of filtered extract was injected on to a Luna 5 µm C18(2) 100Å 250 x 4.6 mm column (Phenomenex Cat. 00G-4252-E0) maintained at 25ºC (± 8ºC). Extracts were separated using a gradient modified from Lin and Harnly (2012) on an Agilent 1200 series HPLC. Formic acid (0.2%, v/v, in HPLC-grade water, ThermoFisher Scientific) and acetonitrile (ThermoFisher Scientific) represent mobile phases A and B, respectively; mobile phase flow rate was 1 mL min^{-1}; gradient profile: 0 to 35 min, 5% to 20% B in A; 35 to 65 min, 20% to 65% B; 65 to 80 min, 79% B; 80 to 90 min, 100% B; 95 to 100 min, 0% B to recover column. A diode array detector (DAD, Agilent G1315C) was used to measure the absorbance of eluting compounds at 270 nm.

The following standards purchased from Sigma-Aldrich were used for identification of compounds in methanol extracts based on similarities in retention time: coniferyl alcohol (Cat.

223735), dihydromyrcetin (Cat. SML0295), taxifolin (Cat. 78666), pinoresinol (Cat. 40674), p-coumaroyl alcohol (Cat. PHL82506), pinosylvin (Cat. 56297), (±)-dihydrokaemperol (Cat. 91216), kaempferol 3-glucoside (Cat. 04500585), trans-cinnamic acid (Cat. C80857), p-coumaric acid (Cat. C9008), dihydromyricetin (Cat. SML0295), coniferyl alcohol (Cat. 223735), matairesinol (Cat. 40043), quercetin 3-glucoside (Cat. 16654); and (+)-catechin hydrate (Fisher Scientific Cat C07051G). Compounds not matching retention times of standards were labeled alphabetically with the prefix "Unknown P-" or "Unknown X-" to indicate they were identified in phloem or xylem tissues, respectively, and that each letter may not represent the same compound between tissues.

4.2.6 Gene Expression Analysis

Frozen tissue was ground to a fine powder using a Retsch Mixer Mill (Verder Scientific, Newtown, PA). Approximately 150-200 mg of ground tissue was used for extraction of total RNA according to Pavy et al. (2008). RNA was quantified with a NanoQuant 200 (Tecan Infinite®, Morrisville, NC) and treated with DNase 1 (New England Biolabs, Whitby, ON). cDNA was synthesized using Invitrogen™ Superscript™ III Reverse Transcriptase (ThermoFisher Scientific, Mississauga, ON). Primers used for qRT-PCR (Appendix 3 Table 1) were designed manually or with Geneious Prime 2020.0 (https://www.geneious.com). qRT-PCR reaction conditions and quantification by standard curve are outlined in El Kayal et al. (2011). Six to nine biological replicates and two technical replicates were used for each of the 12 treatments. Target gene data from secondary phloem was normalized to the arithmetic mean of *Eukaryotic translation initiation factor 5A-1* (*PcTIF5A*; accession KF322083.1), *Vacuolar ATP synthase subunit A* (*PcVHA-A;* accession GT257942.1) and *Ubiquitin-activating enzyme 1* (*PcUBA1;* accession GT229647.1) was used for normalization of gene expression in secondary

phloem samples. Target gene data from secondary xylem was normalized to the arithmetic mean of *PcTIF5A*, *PcUBA1*, and *Ubiquitin-conjugating enzyme 11* (*PcUBC11*; accession GT239443.1).

4.2.7 Statistical Analysis

All statistical analyses were conducted with R v4.0.3 (R Core Team 2020) and RStudio v1.4.1106 (RStudio Team 2020) and all plots were generated using ggplot2 v3.3.3 (Wickham 2016) and cowplot v1.1.1 (Wilke 2020) packages for R. Hormone data was fit using the lmer package (Bates et al. 2015) to a generalized linear mixed model (GLMM) with the following formula: ng hormone g^{-1} sample ~ treatment * timepoint + (1 | tree), family = Gamma (link = log). Hormone GLMM outputs are summarized in Appendix 3.

Distinct peaks (not overlapping with other compounds) identified as consistently present across technical replicates and present in most (n = 4) biological replicates within at least one treatment (annotated in Appendix 3 Figure 5-6) were fit to a non-metric multidimensional scaling (NMDS) model with Bray-Curtis distances in the vegan package v2.5-7 (Oksanen et al. 2020). Covariance ellipses for each treatment were calculated using the vegan package. Statistical differences between treatments and timepoints based on compounds used for ordination were determined using the analysis of similarities (ANOSIM) test (Clarke 1993) within the vegan package. Total phenolics were calculated as the sum of compounds included in ordination, based on peak area normalized to the sample dry weight (mg^{-1}). GLMMs were fit using the lmer package (Bates et al. 2015) to individual compounds identified as significant predictors in the NMDS models, as well as total phenolics. GLMM formulas are outlined in Appendix 3 Table 4. Phenolic metabolite GLMM outputs are summarized in Appendix 3.

Suitability of reference gene combinations for qRT-PCR was analyzed using Normfinder (Andersen et al. 2004), BestKeeper (Pfaffl et al. 2004), GeNorm2 (Vandesompele et al. 2002), and by GLMM (Appendix 3). Reference-normalized gene expression data was fit to a GLMM with the following formula: normalized transcript abundance ~ treatment * timepoint + (1 | tree), family = Gamma (link = log). Normalized transcript abundance GLMM outputs are summarized in Appendix 3.

Generalized linear mixed models were assessed to ensure they met assumptions of normality and homoscedascity using Shapiro-Wilk test (Shapiro and Wilk 1965) and Bartlett's test (Snedecor and Cochran 1989) results. Post hoc comparisons were made using the emmeans package v1.5.3 (Lenth 2020) to determine significant differences between groups and letters were assigned using the multcomp package v1.4-15 (Hothorn et al. 2008). R files are available at https://github.com/c4tier/.

4.3 Results

In this study, we relied on natural MPB mass attack of mature lodgepole pine trees baited with a semiochemical mixture designed for *D. ponderosae* containing exo-brevicomin and transverbenol (https://semiochemical.com/bark-beetles/, Borden et al. 2008). Unlike conventional infestation experiments in which herbivorous insect pests are introduced to the host on a single day at the outset of the experiment, natural MPB mass-attack of the baited trees assigned to the MPB-attacked treatment resulted from multiple MPB attacks that occurred over several days. Samples collected at 1 dpw corresponded to 1-7 days after initial MPB attack, representing the midst of MPB mass attack. Based on the observation that MPB mass attack is typically completed within 7 days of the initial attack (Safranyik and Carroll 2006), we expected to see evidence of mass attack by 7 dpw, which corresponded to 7-13 days after initial MPB

attack for all trees. Indeed, by 7 dpw we observed that all trees in the MPB-attacked group had reached the threshold of greater than 40 attacks that is generally used as a benchmark for considering a host to be mass-attacked by MPB (Raffa and Berryman 1983, Safranyik and Carroll 2006).

JA signalling represents an early step in herbivorous insect pest perception and activation of specialized defenses by host plants (Aerts et al. 2021), while the hallmark of a plant's response to necrotrophic fungal pathogen attack is synthesis of both JA and ET. To determine whether the JA and ET signature triggered by necrotrophic fungal pathogen attack could be detected in MPB-attacked lodgepole pine, we first needed to establish whether *G. clavigera* challenge induced both JA and ET biosynthesis in lodgepole pine. In addition to measuring JA, we also measured levels of the active form of JA, JA-Ile. Given that ET is a gas and as such must be collected from the tree headspace, we used the common procedure of measuring the stable precursor of ET, ACC, as an indirect measure of ET (Chauvaux et al. 1997, Bulens et al. 2011). As predicted, levels of JA, JA-Ile and ACC all increased relative to mock-inoculated controls at 7 dpi and 14 dpi in secondary phloem (JA 14 dpi $z = -3.33$, $p = 0.005$; JA-Ile 7 dpi $z = -3.73$, $p = 0.001$; JA-Ile 14 dpi $z = -3.35$, $p = 0.004$; ACC 7 dpi $z = 3.46$, $p = 0.003$; ACC 14 dpi $z = -3.52$, $p = 0.002$; Figure 4.1). JA-Ile levels also increased significantly in xylem by 14 dpi ($z = -2.75$, $p = 0.03$), while measured increases in xylem ACC at 14 dpi were not statistically significant ($z = -0.51$, $p = 0.96$; Figure 4.2). In contrast, and consistent with expectations, SA and conjugated forms of SA did not increase significantly in response to *G. clavigera* inoculation in either xylem (SA 7 dpi $z = 0.76$, $p = 0.87$; SA 14 dpi $z = -0.42$, $p = 0.98$; conj. SA 7 dpi $z = 0.53$, $p = 0.95$; conj. SA 14 dpi $z = -0.01$, $p = 1.00$; Figure 4.2) or phloem (SA 7 dpi $z = 1.04$, $p = 0.73$; SA 14

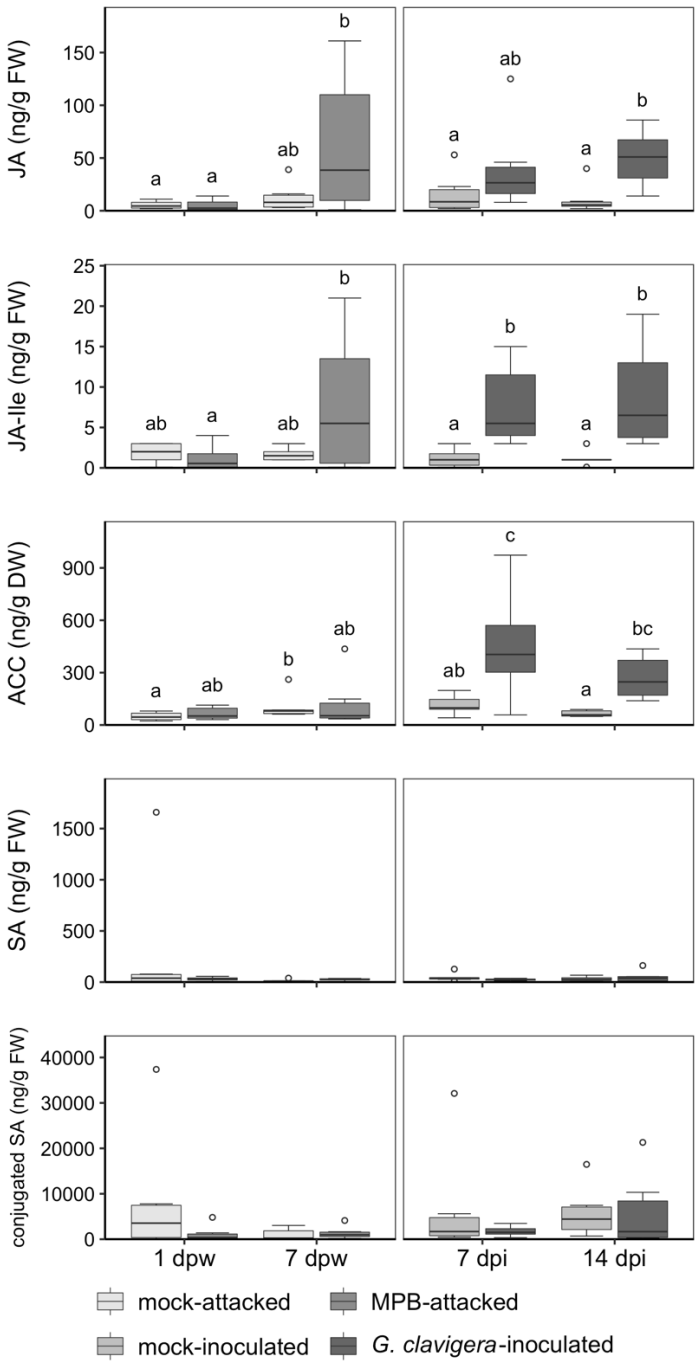

Figure 4.1. Differences in defense-associated hormone profiles between secondary phloem of MPB-attacked and *G. clavigera*-inoculated lodgepole pine. Boxplot shading represents mock-attacked, MPB-attacked, mock-inoculated, or *G. clavigera*-inoculated trees. Boxes indicate the median value bounded by the 75Th (upper) and 25th (lower) quantiles. Boxplot whiskers represent boundaries of 1.5 times the interquartile range added to each quantile. Letters indicate significant differences between treatments (Tukey-adjusted $p < 0.05$, n = 6).

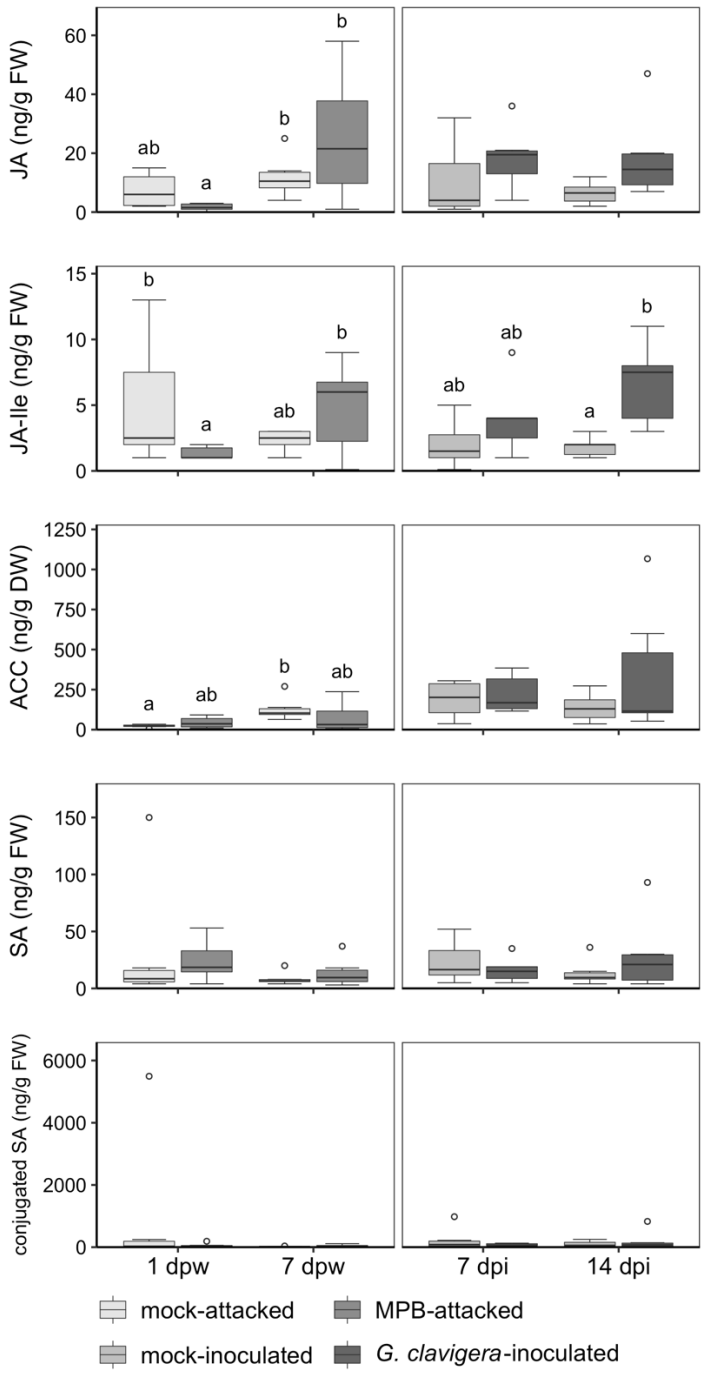

Figure 4.2. Secondary xylem hormone concentrations in lodgepole pine trees attacked by MPB or inoculated with *G. clavigera*. Shading of boxplots represents mock-attacked, MPB-attacked, mock-inoculated, or *G. clavigera*-inoculated trees. Boxes indicate the median value bounded by the 75Th (upper) and 25th (lower) quantiles. Boxplot whiskers represent boundaries of 1.5 times the interquartile range added to each quantile. Letters indicate significant differences between treatments (Tukey-adjusted $p < 0.05$, n = 6).

dpi z = -0.31, p = 0.99; conj. SA 7 dpi z = 1.03, p = 0.73; conj. SA 14 dpi z = 0.55, p = 0.95; Figure 4.1)

Having determined that lodgepole pine synthesize both JA and ET in response to *G. clavigera*, we next looked at defense hormone levels in MPB-attacked versus mock-attacked lodgepole pine. Consistent with a response to attack by an herbivorous insect pest, JA and JA-Ile levels were noticeably higher in phloem and xylem of MPB-attacked trees relative to mock-attacked trees by 7 dpw, although these differences were not significant (phloem JA z = -1.99, p = 0.19; phloem JA-Ile z = -2.31, p = 0.10; xylem JA z = -0.85, p = 0.83; xylem JA-Ile z = -1.71, p = 0.32; Fig. 4.1 and Figure 4.2). There were no significant differences in phloem or xylem ACC levels between MPB-attacked and mock-attacked trees at either 1 dpw (phloem ACC z = -1.23, p = 0.61; xylem ACC z = -0.97, p = 0.76) or 7 dpw (phloem ACC z = 0.44, p = 0.97; xylem ACC z = 2.04, p = 0.18). No significant differences were observed for SA or conjugated SA in either phloem (SA 1 dpw df = 14.06, p = 0.76; SA 7 dpw df = 14.06, p = 0.75; conj. SA 1 dpw z = 0.94, p = 0.78; conj. SA 7 dpw z = 0.48, p = 0.96; Figure 4.1) or xylem (SA 1 dpw df = 16.16, p = 1.00; SA 7 dpw df = 16.16, p = 0.86; conj. SA 1 dpw df = 14.07, p = 0.74; conj. SA 7 dpw df = 14.07, p = 0.79; Figure 4.2) of MPB-attacked trees.

To determine whether the differences in defense hormone profiles of defense hormones synthesized in response to MPB attack vs. *G. clavigera* challenge related to differences in defense responses, we examined phenolic metabolite profiles. Phenolics are a distinctive component of lesions and, because of the relatively short time course that we used in this study, we elected to measure phenolic compounds rather than the lesions themselves. Metabolite data used for NMDS is included in Appendix 3. Stress values reflect how well the ordination model summarizes differences among samples; models were found to fit our phloem data (stress =

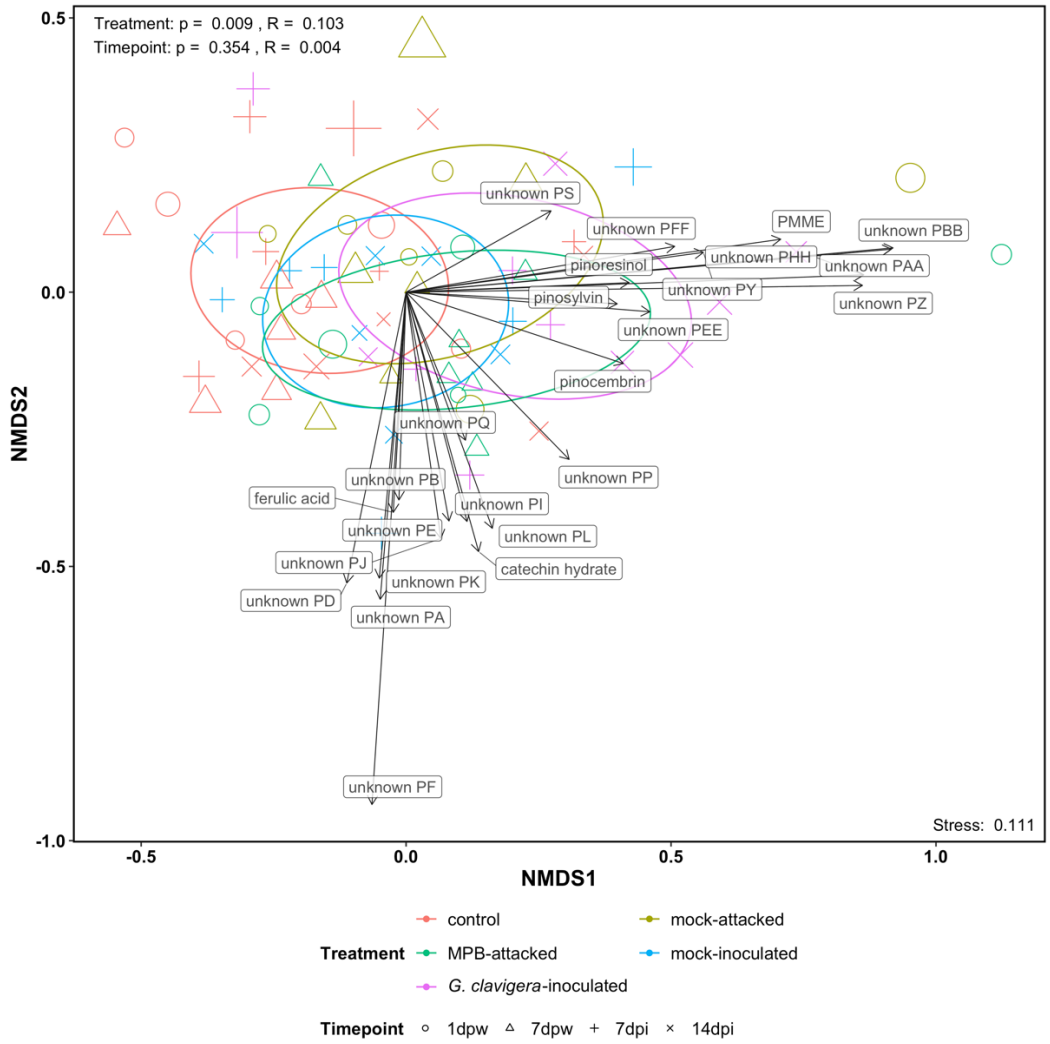

Figure 4.3. Two-dimensional NMDS reveals known and unknown compounds contributing to variance in secondary phloem phenolic profiles between MPB-attacked or *G. clavigera*-inoculated lodgepole pine. Point color indicates attack or inoculation status: control (unwounded), mock-attacked, MPB-attacked, mock-inoculated, or *G. clavigera*-inoculated. Point shape indicates time point, while point size is proportional to the goodness of fit of the ordination model for each sample. Ellipses represent covariance across each treatment. Arrows represent the strength and direction of significant ($p < 0.05$) phenolic predictors. Compounds that did not match the retention time of standards were alphabetically labeled with the prefix "Unknown P-" to indicate they were found in phloem. The stress value is representative of the fit of the ordination model to the sample data, with values less than 0.2 considered a good fit. ANOSIM *p*-values represent the significance of each factor, while R values represent the similarity of profiles within a treatment (R values of 1 indicate that samples are most similar).

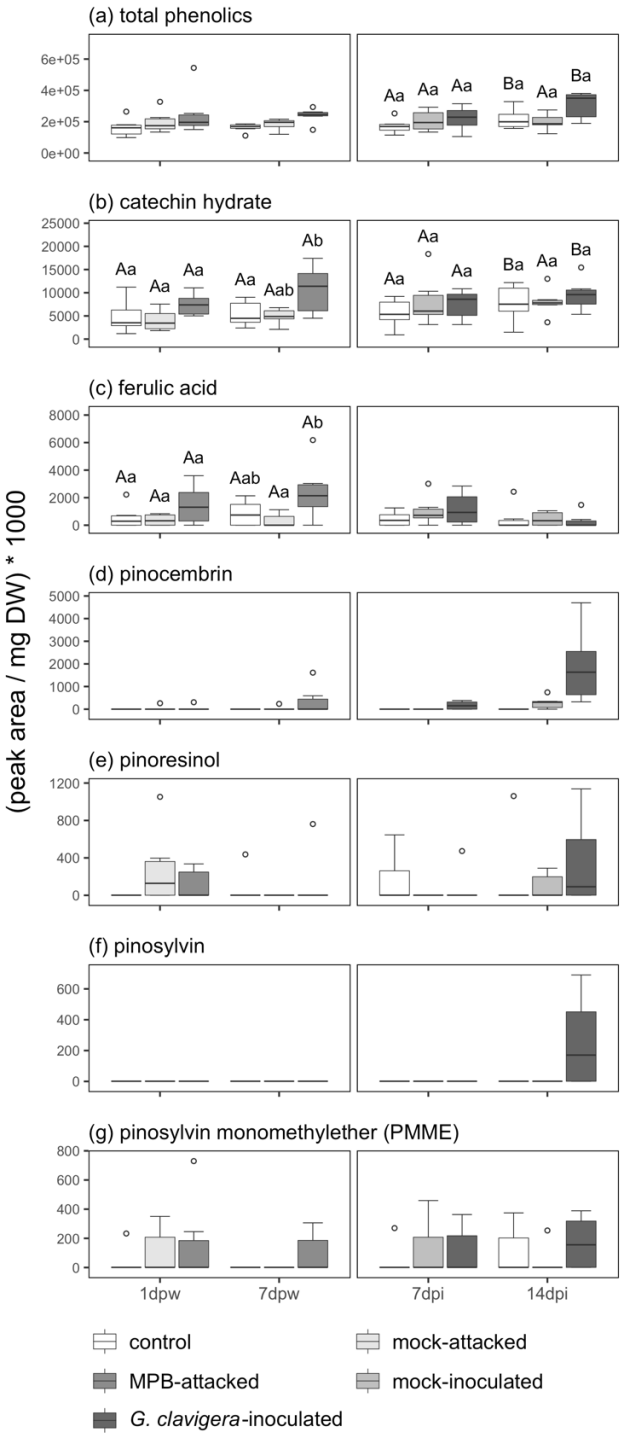

Figure 4.4. Profiles for select phenolic metabolites in secondary phloem of MPB-attacked and *G. clavigera*-inoculated lodgepole pine relative to controls. Each metabolite was identified as significantly contributing to differences across phenolic profiles in phloem by NMDS. Shaded boxplots represent control (unwounded), mock-attacked, MPB-attacked, mock-inoculated, or *G. clavigera*-inoculated trees (n = 6). Boxes indicate the median value bounded by

the 75Th (upper) and 25th (lower) quantiles. Boxplot whiskers represent boundaries of 1.5 times the interquartile range added to each quantile. Uppercase letters indicate significant differences between estimated marginal means of a treatment between time points; lowercase letters indicate significant differences between treatments within a time point (Tukey-adjusted $p < 0.05$, n = 6).

0.111) and xylem data (stress = 0.075), which are both generally considered to be of good fit. Ordination plots of NMDS values, paired with ANOSIM results, revealed that secondary phloem phenolic profiles varied significantly across treatments ($p = 0.008$, R = 0.103) but not across time points ($p = 0.366$, R = 0.004; Figure 4.3). The greatest resolution between treatments was between the three control treatments and the two challenge treatments. However, there was little resolution in the NMDS multivariate analysis between the phloem phenolic profiles of MPB-attacked and *G. clavigera*-inoculated trees. Closer inspection of total phenolic levels and of individual phenolic compounds identified as significant ($p < 0.05$) contributors to variation between samples supported this (Figure 4.4). For example, pinocembrin and pinosylvin increased dramatically in *G. clavigera*-inoculated phloem at 14 dpi only, and were low or undetected in all other treatments. Increased pinoresinol levels were also observed in both MPB-attacked and mock-attacked trees at 1 dpw, as well as *G. clavigera*-inoculated trees at 14 dpi. Pinosylvin 3-o-monomethyl ether (PMME), catechin hydrate, and ferulic acid did not show any treatment-specific responses in phloem (Figure 4.4).

In contrast to phloem, xylem phenolic metabolite profiles showed greater resolution across treatments (Figure 4.5). ANOSIM results indicated that both treatment ($p < 0.001$, R = 0.26) and time point ($p = 0.018$, R = 0.059) significantly differed among xylem metabolite profiles. Visualization using NMDS plots illustrated clear separation of MPB-attacked phenolic profiles from *G. clavigera*-inoculated phenolic profiles along NMDS1. *G. clavigera*-inoculated samples were further differentiated from the mock controls along NMDS2. Total phenolic levels

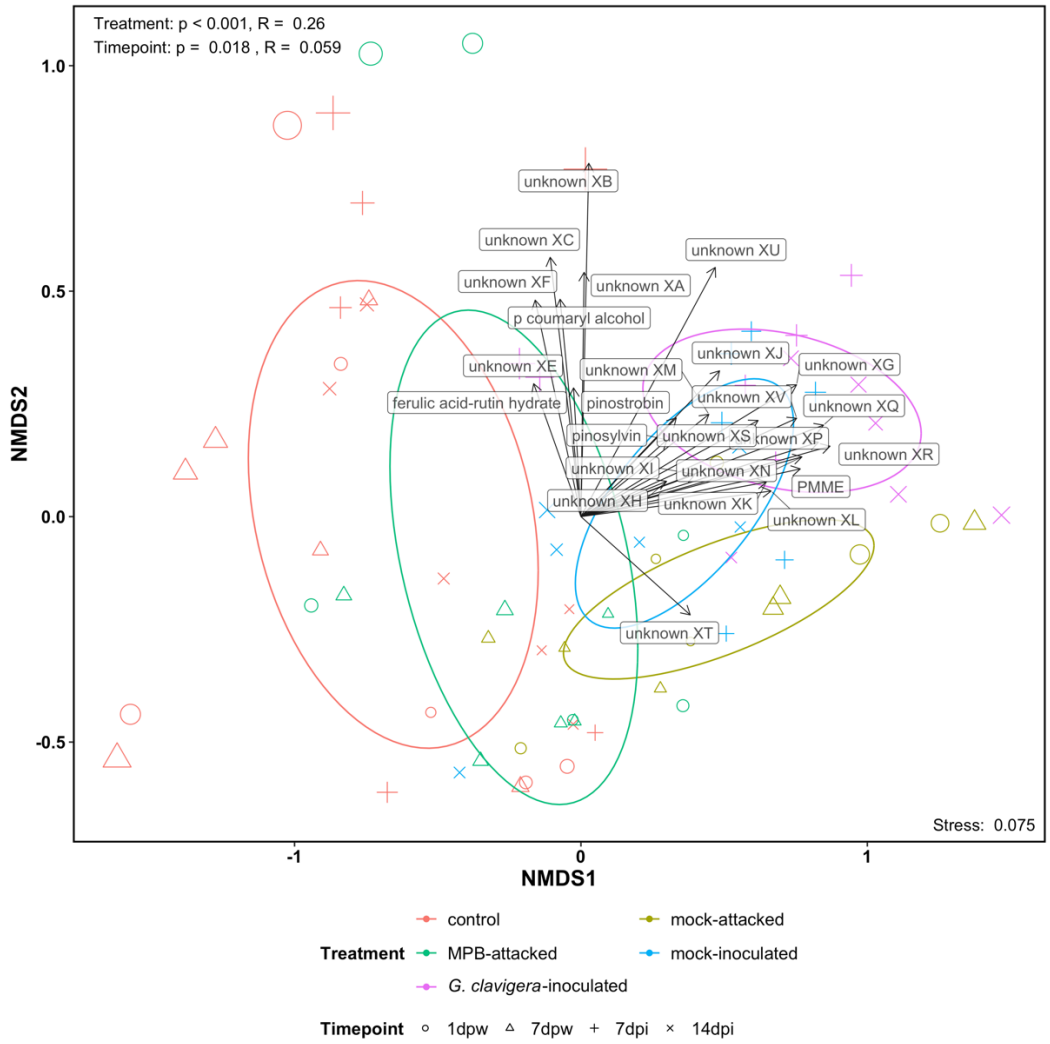

Figure 4.5. Two-dimension NMDS of phenolic compounds in secondary xylem shows patterns specific to MPB-attack or *G. clavigera*-inoculation that are consistent across time points in lodgepole pine and highlights several known and unknown phenolics contributing to these patterns. Point shape indicates time point and point size is proportional to the goodness of fit of the ordination model for each sample. Point color indicates treatment, including control (unwounded), mock-attacked, MPB-attacked, mock-inoculated, and *G. clavigera*-inoculated trees. Ellipses indicate the covariance across each treatment. Phenolic compounds identified as significant contributors to sample differences within the ordination model are included ($p < 0.05$); arrows represent the strength and direction of each predictor. Compounds that did not match the retention time of standards were alphabetically labeled with the prefix "Unknown X-" to indicate they were found in xylem. The stress value is representative of the fit of the ordination model to the sample data; values less than 0.2 are considered a good fit.

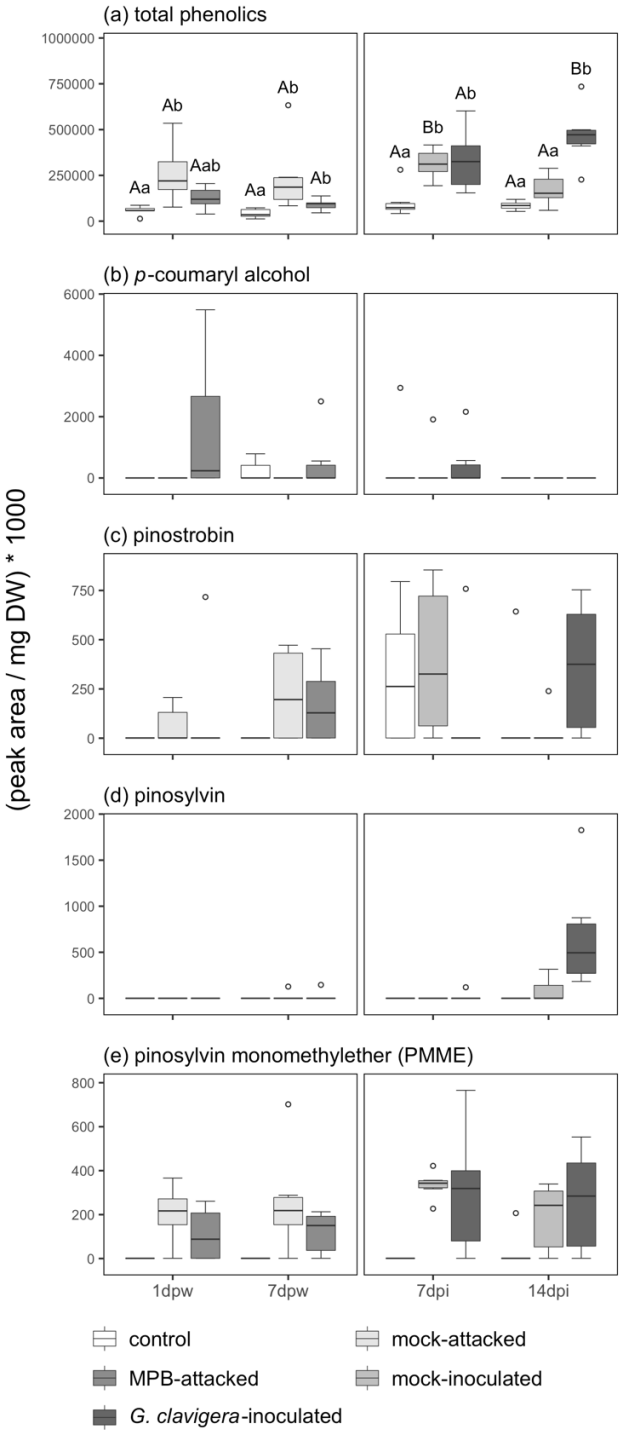

Figure 4.6. Xylem phenolic compounds in lodgepole pine trees attacked by MPB or inoculated with *G. clavigera*. Compounds included were identified as significantly contributing to differences across phenolic profiles in xylem by NMDS and were compounds with similar retention times to known standards. Shaded boxplots represent control (unwounded), mock-attacked, MPB-attacked, mock-inoculated, or *G. clavigera*-inoculated trees (n = 6). Boxes

indicate the median value bounded by the 75Th (upper) and 25th (lower) quantiles. Boxplot whiskers represent boundaries of 1.5 times the interquartile range added to each quantile. Uppercase letters indicate significant differences between estimated marginal means of a treatment between time points; lowercase letters indicate significant differences between treatments within a time point (Tukey-adjusted $p < 0.05$, n = 6).

were considerably higher in xylem (Figure 4.6) relative to phloem (Figure 4.4), and significant increases in total phenolic content were observed in mock-attacked (1dpw z = -4.20, $p < 0.001$; 7 dpw z = -4.61, $p < 0.001$), mock-inoculated (7 dpi z = -4.97, $p < 0.001$) xylem samples (relative to unwounded controls) that were not observed in phloem. Most notably, xylem total phenolics increased significantly in *G. clavigera*-inoculated trees at 14 dpi (z = -2.80, $p = 0.01$) relative to mock-inoculated trees. Increases in pinostrobin, pinosylvin, and PMME were observed in *G. clavigera*-inoculated xylem, principally at 14 dpi (Figure 4.6). Interestingly, while pinosylvin levels remained negligible in MPB-attacked and mock-attacked trees, PMME and pinostrobin levels increased in response to mock treatments and MPB attack. *p*-coumaryl alcohol was detectable at high levels early after MPB attack, but at low or undetectable levels otherwise (Figure 4.6).

To complement these biochemical metabolite analyses, we also looked at changes in the expression of genes encoding enzymes at key branch points of phenolic biosynthesis: *stilbene synthase (STS), stilbene o-methyltransferase 1 and 2 (OMT1 and OMT2), dihydroflavanol reductase 1 and 2 (DFR1 and DFR2),* and *chalcone synthase (CHS)*. These genes were previously found to be upregulated in lodgepole pine seedlings in response to *G. clavigera* inoculation (Chapter 2). In this study of mature lodgepole pine, *PcSTS, PcOMT1,* and *PcDFR1* showed significant increases in phloem transcript abundance in response to *G. clavigera* challenge (*PcSTS* 7 dpi z = -4.10, $p < 0.001$; *PcSTS* 14 dpi z = -3.10, $p = 0.006$; *PcOMT1* 7 dpi

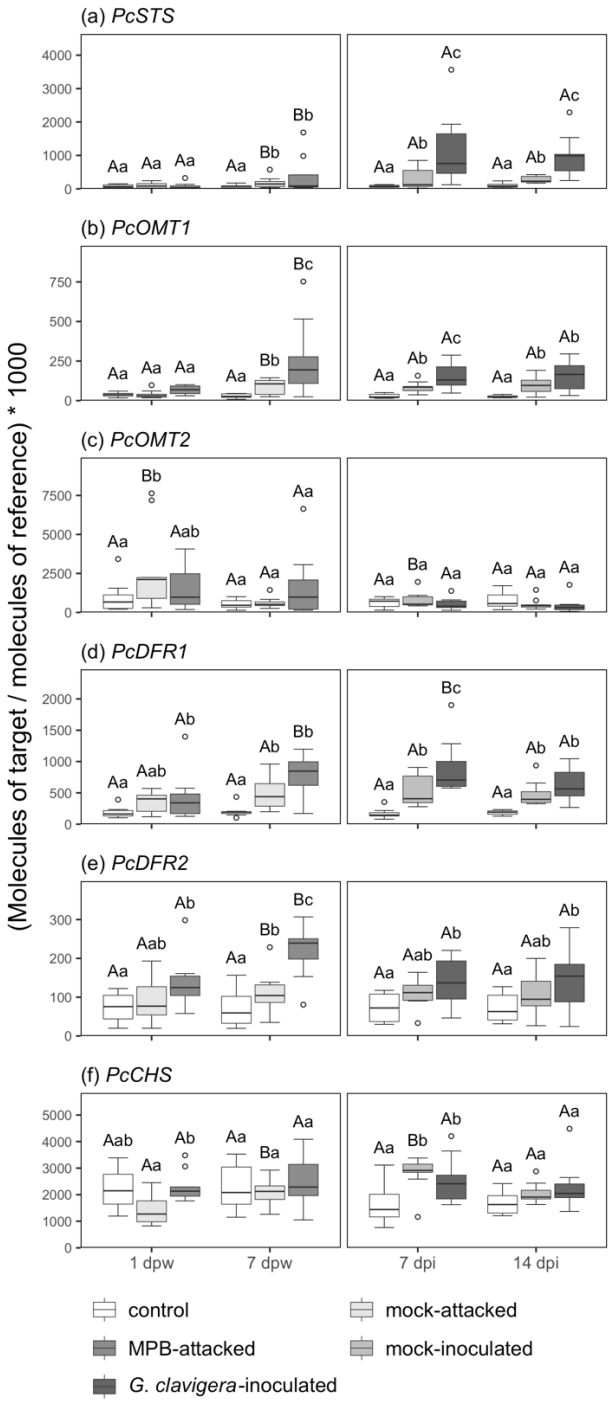

Figure 4.7. Expression profiling for genes encoding key enzymes of stilbene and flavonoid biosynthesis reveals differences in transcript abundance corresponding to these genes in secondary phloem of MPB-attacked and *G. clavigera*-inoculated lodgepole pine. Shading represents control (unwounded), mock-attacked, MPB-attacked, mock-inoculated, or *G. clavigera*-inoculated trees. Boxes indicate the median bounded by the 75Th (upper) and 25th

(lower) quantiles. Boxplot whiskers represent boundaries of 1.5 times the interquartile range added to each quantile. Uppercase letters indicate significant differences between estimated marginal means of a treatment between time points; lowercase letters indicate significant differences within a time point (Tukey-adjusted $p < 0.05$, n = 8-10).

z = -2.42, $p = 0.04$; *PcDFR1* 7 dpi z = -2.74, $p = 0.02$; Figure 4.7), while only *PcSTS* showed significant increases in xylem transcript abundance in response to *G. clavigera* challenge at 7 dpi (z = -2.58, $p = 0.03$; Figure 4.8), relative to mock-inoculated controls. In nearly all cases, expression of most of the remaining phenolic biosynthesis genes was also increased in phloem and xylem of mock-inoculated trees, suggesting that their induction was non-specific. Similar non-specific increases were observed in the phloem and xylem of MPB-attacked and mock-attacked trees, apart from *PcOMT1* and *PcDFR2*, which both exhibited significant increases in transcript abundance in phloem following MPB attack at 7 dpw (*PcOMT1* z = -3.55, $p = 0.001$; *PcDFR2* z = -2.97, $p = 0.008$; Figure 4.7 and Figure 4.8).

4.4 Discussion

In this study, we have used the tree's molecular responses to ascertain whether Ophiostomatoid fungal symbionts of mountain pine beetle are important contributors to MPB's capacity to overcome lodgepole pine defenses under mass attack scenarios. To test this hypothesis, we first established that lodgepole pine synthesizes both JA and ET – but not SA – in response to *G. clavigera* challenge. We chose to use *G. clavigera* because this species is (a) one of the most common MPB fungal associates (Lee et al. 2006, Roe, James, et al. 2011), (b) sufficiently virulent to kill pines in the absence of MPB (Owen et al. 1987, Yamaoka et al.1995), and (c) the earliest and fastest colonizer of the common Ophiostomatoid fungal associates (Solheim 1995, Solheim and Krokene 1998). That JA rather than SA is invoked in lodgepole

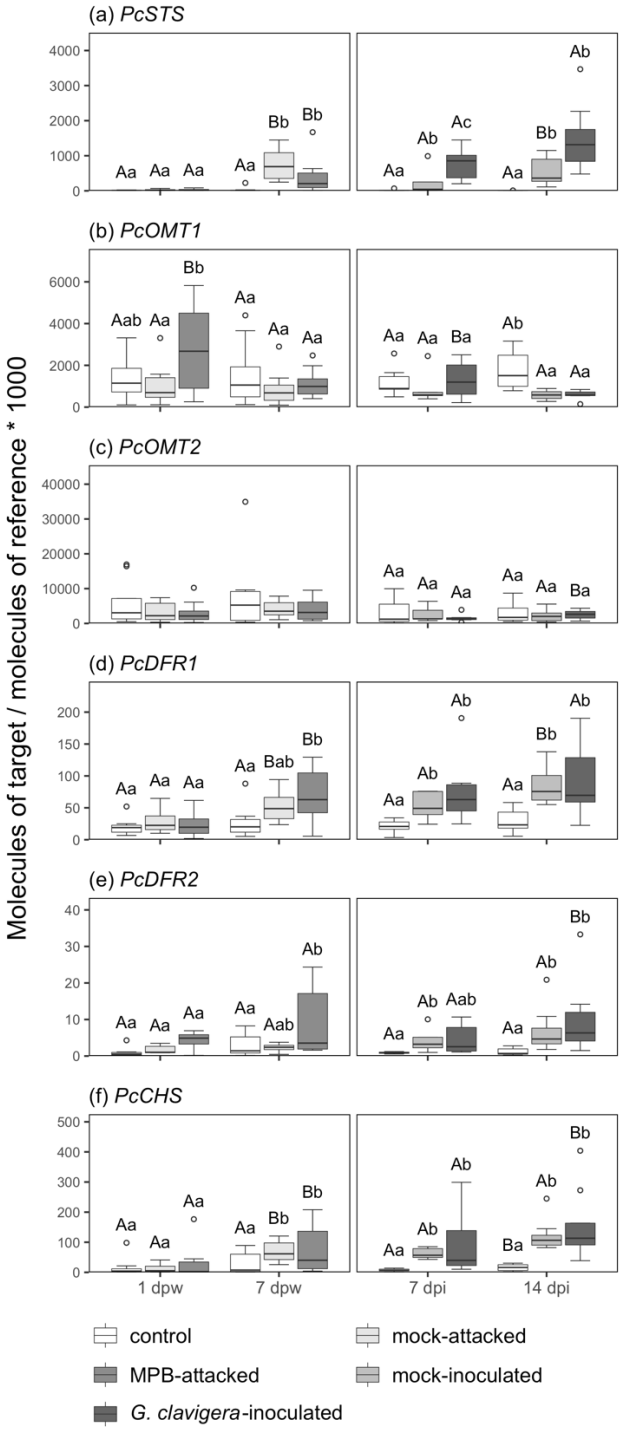

Figure 4.8. Secondary xylem qRT-PCR transcript profiles of phenolic biosynthesis genes in lodgepole pine trees attacked by MPB or inoculated with *G. clavigera*. Shaded boxplots represent control (unwounded), mock-attacked, MPB-attacked trees, mock-inoculated, and *G. clavigera*-inoculated trees. Boxes indicate the median value bounded by the 75Th (upper) and 25th (lower) quantiles. Boxplot whiskers represent boundaries of 1.5 times the interquartile range

added to each quantile. Uppercase letters indicate significant differences between estimated marginal means of a treatment between time points; lowercase letters indicate significant differences between treatments within a time point (Tukey-adjusted $p < 0.05$, n = 5-8).

pine's response to *G. clavigera* challenge confirms our earlier findings that *G. clavigera* is perceived by lodgepole and jack pine seedlings as a necrotrophic fungal pathogen (Arango-Velez et al. 2016) and demonstrates that this is also true in mature trees. We also confirmed our earlier finding that lodgepole pine synthesizes JA-Ile (Arango-Velez et al. 2016), the active form of JA in angiosperms (Ruan et al. 2019). We presume that JA-Ile is also an active form of JA in conifers, although this remains to be tested rigorously. Compared to JA, the role of ET in conifer defense against necrotrophic pathogens has received little attention. This study provides the first direct evidence that, like angiosperms (van Loon, Geraats, et al. 2006, Pieterse et al. 2012), lodgepole pine responds to necrotrophic fungal invasion by synthesizing both ET and JA. These *in planta* measures support the few studies in other conifer pathosystems carried out to date that have examined ET biosynthesis and signalling gene expression (Hudgins and Franceschi 2004, Hudgins et al. 2006, Barnes et al. 2008, Arnerup et al. 2011, 2013).

In this study, we used a pheromone bait strategy to ensure that MPB-attacked trees were subject to at least 40 MPB attacks during the time frame of the experiment, a threshold commonly considered to be sufficient for MPB to successfully attack and colonize the host (Raffa and Berryman 1983, Safranyik and Carroll 2006). The lack of ACC accumulation in MPB mass-attacked pines during the attack phase provides convincing evidence that lodgepole pine does not perceive challenge by MPB-vectored *G. clavigera* in either the phloem or xylem during this critical window when the mass-attack strategy used by MPB overcomes host defenses. Consequently, our findings do not support the oft-cited but contested theory that MPB-vectored Ophiostomatoid fungi are critical for MPB success by acting in concert to overwhelm host tree

defenses during the period of mass attack and initial beetle establishment (Lieutier et al. 2009, Six and Wingfield 2011).

If these MPB-vectored Ophiostomatoid fungi do not play a role in overwhelming host defenses during the attack phase of MPB-host tree interactions, then it is likely that these fungi play alternative roles that provide some benefit to MPB following establishment in the host, and that the pathogenic nature of these fungi facilitates at least some of these roles. There is compelling evidence, for example, that MPB-vectored Ophiostomatoid fungi contribute to nutrient provisioning for MPB at both larval and adult stages (Adams and Six 2007, Six 2020b). Relative to the nutritional needs of developing bark beetles such as MPB, phloem is considered to be limiting, particularly for nitrogen and phosphorous (Six and Elser 2019, Six 2020a). There are many examples of herbivores such as bark beetles that survive on nutrient-limiting tissues having evolved mutualisms to improve nutrient acquisition (Six and Elser 2019, Six 2020a, 2020a). Numerous studies of the MPB-Ophiostomatoid fungi nutrient-based mutualistic relationship have demonstrated that Ophiostomatoid fungal associates aid MPB development by providing supplemental sterols and nitrogen (Paine et al. 1997, Bentz and Six 2006, Bleiker and Six 2007, Goodsman et al. 2012), improving MPB fitness. For example, association with *G. clavigera* resulted in MPB producing more adult progeny who emerged earlier, while *G. clavigera* -free MPB were unable to produce brood (Six and Paine 1998). Lastly, the ability of Ophiostomatoid fungi to extract and supplement nutrition for bark beetles helps reduce the constraints of intra-specific competition resulting from mass attack, and likely has contributed to the close relationship many aggressive bark beetles have with Ophiostomatoids (Six 2020b).

To acquire and assimilate these host essential nutrients, MPB Ophiostomatoid fungal associates must colonize the host's phloem and sapwood (Six and Klepzig 2021). Thus,

Ophiostomatoid fungi must either evade detection by the host or they must withstand and overcome host defenses to effectively colonize these tissues. For example, *G. clavigera* has the capacity to detoxify terpene defenses (DiGuistini et al. 2011). The strong induction of JA, JA-Ile and ET synthesis in both xylem and phloem of lodgepole pine within a few days of *G. clavigera* challenge, together with increases in phenolic defenses, suggests that its pathogenic lifestyle enables *G. clavigera* to overcome host defenses to colonize the host without the aid of the MBP mutualism. MPB's primary fungal symbionts (*G. clavigera, L. longiclavatum,* and *O. montium*) exhibit differential pathogenicity (Rice et al. 2007a, Rice and Langor 2008) and growth rates (Addison et al. 2015, Moore and Six 2015), with *G. clavigera* being the most successful at host colonization. It is possible that these traits have evolved as result of competition between symbionts (Six and Wingfield 2011), allowing for denser growth in galleries early on when host defenses are stronger, ultimately aiding fungal transmission while also being advantageous to MPB.

Polyphenolic parenchyma cells are found in secondary phloem within the bark, and swell in response to fungal inoculation, filling with phenolic compounds (Franceschi et al. 2005, Arango-Velez et al. 2016). Within the time frames of this study, changes to lodgepole pine phloem phenolic profiles in response to MPB attack or *G. clavigera* inoculation were similar to those induced by mock-attack and mock-inoculation treatments. This pattern of non-specific induction was generally reflected in the transcript abundance profiling of *STS, OMT1* and *OMT2* representing the stilbene branch of phenolic biosynthesis and *CHS, DFR1* and *DFR2* representing the flavonoid branch of phenolic biosynthesis. Collectively, these results suggest that the phenolic defense strategy is a more generalized, reactive response rather than a defense mechanism that is customized in response to the biotic threat.

We observed stronger induction of phenolic biosynthesis gene expression and greater contrasts between phenolic profiles of *G. clavigera*-inoculated trees relative to mock treatments in xylem than was observed for phloem. These findings indicate that *G. clavigera* colonization of the xylem is perceived by these host tissues, leading to augmented phenolic biosynthesis. In contrast, MPB attack had a negligible effect on xylem phenolic profiles relative to mock-attacked trees during the time frame of these experiments, which likely reflects the limited physical damage that MPB incurred on xylem during this mass-attack phase.

That lesion development is a key part of the host response to fungal establishment is further supported by the compounds identified in this study. The stilbenes pinosylvin and PMME exhibited substantive increases in response to *G. clavigera* inoculation in both phloem and xylem, similar to increases observed in Scots pine (*Pinus sylvestris* L.) infected with *Heterobasidion annosum* (Fr.) Bref. s.l. (Kovalchuk et al. 2017) and in Eastern white pine (*Pinus strobus* L.) following pine wood nematode (*Bursaphelenchus xylophilus* Nematoda: Aphelenchoididae) infection (Hwang et al. 2021). Stilbenes have long been identified as important phytochemicals involved in containment of decay in trees (Hart and Shrimpton 1979, Hart 1981), with many such as pinosylvin exhibiting fungitoxicity (Lee et al. 2005). Another stilbene, resveratrol, has been linked with Norway spruce resistance to *E. polonica* (Hammerbacher et al. 2011, 2013). Consistent with the notion of an evolutionary arms race, strains of fungi that have developed detoxification mechanisms and are even able to use resveratrol as a carbon source have also been identified (Hammerbacher et al. 2013, Wadke et al. 2016, Zhao et al. 2019). Phenolics located within the lesion may also oxidize, creating oxygen radicals that can trigger host cell death and necrosis (Appel 1993). This plant-triggered cell death is potentially beneficial to necrotrophic pathogens that rely on release of nutrients from dead host

cells (Balint-Kurti 2019). Oxidation of foliar phenolic compounds has been linked with oxidative stress in some herbivores (Barbehenn et al. 2008, Barbehenn and Constabel 2011). Additionally, phenolic oxidation can change the tissue environment, triggering accumulation of reactive oxygen species, peroxidases and other host repair mechanisms that alter tissue quality (Almagro et al. 2009). Although it does not appear that phenolics are a significant part of host responses to MPB, changes in phenolic profiles triggered by wounding and fungal colonization may still influence MPB feeding and behaviour.

4.5 Conclusion

The goal of our research was to determine the relative contribution of symbiotic fungi to overwhelming host defenses during MPB mass attack. We observed that lodgepole pine produce JA and ET in response to *G. clavigera*, but not SA, consistent with previous reports that *G. clavigera* is a necrotrophic fungus. Additionally, our results indicate that conifers use similar defense signalling pathways as angiosperms to distinguish between pathogen types and mount more effective defense responses. We found that MPB-mass attacked lodgepole pines do exhibit hormonal signatures of necrotrophic pathogen challenge, specifically increased levels of ET, indicating that Ophiostomatoid fungi do not contribute to overwhelming host defenses within the time frame of MPB mass attack.

Instead, our findings support research suggesting that the reason MPB have evolved mechanisms for vectoring these fungi and maintaining these relationships is because of the important role Ophiostomatoids play in supporting MPB colonization, reproduction, and development. The strong response of lodgepole pine to *G. clavigera* is reflective of the fungus' pathogenicity, which has likely evolved because of competition with other MPB Ophiostomatoid associates and may help with resource capture that is also advantageous to MPB. Our results

indicate that phenolics play a larger role in defense against *G. clavigera* than to MPB, however, the spatial overlap of these responses in lodgepole tissues warrants further research into how phenolics may influence MPB feeding and behavior.

Chapter 5: Contributions of epicuticular wax and lignin deposition to white spruce (*Picea glauca)* needle toughness during bud burst

5.1 Introduction

Eastern spruce budworm (SBW, *Choristoneura fumiferana* [Clemens]) is considered one of the most important pests affecting conifers in Canada. White spruce (*Picea glauca* [Moench] Voss) and balsam fir (*Abies balsamea* [L.] Mill) are preferred hosts for this forest pest (Hennigar et al. 2008), which feeds on foliage. SBW herbivory causes decreased host growth and can lead to tree mortality (Delvas et al. 2011), with large-scale epidemics resulting in considerable losses of economically important timber products (Nealis 2016, Navarro et al. 2018). Warming temperatures associated with climate change are hypothesized to make SBW outbreaks more frequent and intense (Navarro et al. 2018).

SBW overwinter as first instar larvae and emerge when air temperatures exceed a certain threshold, which Pureswaran et al. (2019) recently determined to be 10ºC for the population that they studied. SBW larvae preferentially feed on expanding foliage of white spruce and balsam fir during host bud burst, although early emerging larvae will mine previous year foliage and pollen cones until buds begin to swell and developing needles are visible through the bud scales (Fuentealba et al. 2018). However, age of foliage is negatively correlated with SBW survival and weight (Thomas 1987), which in turn can be related to decreased fecundity (Honěk 1993). This relationship is particularly evident at later instars, when feeding volume increases (Thomas 1987). Thus, phenological synchrony between SBW development and host bud burst is a major determinant of insect fitness (Lawrence et al. 1997, Fuentealba et al. 2017). This period of synchrony is described as the window of phenological opportunity (Lawrence et al. 1997). Some

studies suggest that phenology is a greater predictor of host resistance than secondary metabolites (Carmona et al. 2011).

Identifying specific host foliar traits that define the window of phenological opportunity is not straightforward. Developmentally-associated changes in host quality of needles are strongly correlated with lower nutrient content, particularly percent nitrogen, decreased water content, and increased toughness (Thomas 1987, Lawrence et al. 1997). In black spruce, SBW feeding on older foliage is limited by mechanical toughness (Fuentealba et al. 2017), and foliar toughness of mature needles was shown to be a better predictor of SBW mining success than foliar nitrogen content (Fuentealba et al. 2020). However, changes in toughness during bud burst and foliage expansion, prior to the end of the feeding window, are not well understood. Importantly, the cellular and anatomical attributes that contribute to needle toughness are still largely unknown.

Conifer needles possess several features that enable these long-lived organisms to withstand abiotic and biotic threats. Some of these adaptive traits potentially contribute to foliar toughness, acting to deter spruce SBW herbivory and thus serving as biomarkers defining the phenological window of opportunity. For example, conifer needles typically display a thick cuticular layer, deposited early in needle development (Percy & Baker 1990), that protects against water loss (DeLucia and Berlyn 1984), pathogens (Serrano et al. 2014), and herbivory (Gorb and Gorb 2017). This highly hydrophobic material contains lipids, wax esters, hydrocarbons, long chain fatty acids and alcohols, and numerous lipid-soluble secondary metabolites (Jetter et al. 2006). As the outermost layer of the needles, cuticular wax also provides an interface for insect interaction and offers information about host suitability (Daoust et al. 2010). Wax chemical composition can impact the morphology, thickness, and reflectance of the

cuticle layers (Hanover and Reicosky 1971, Reicosky and Hanover 1978), in addition to perception and emission of soluble volatiles within the wax (Despland et al. 2016).

Another cellular component that influences needle toughness and digestibility is lignin (Lawrence et al. 1997, Hatcher 1990). A phenylpropanoid polymer found in secondary cell walls that imparts both mechanical strength and a degree of hydrophobicity to the cell wall, lignin is a hallmark of water-conducting tracheids and non-conducting fibres found in the needle vasculature (Polle et al. 1994). Lignin is also associated with Casparian strips of the endodermis and hypodermis (Naseer et al. 2012). Deposition of lignin is often presumed to occur after needle elongation is complete (Lirette and Despland 2021), and as such has received less attention as a contributor to foliar quality during bud burst. The rate at which these developmentally associated changes occur may influence feeding and digestion by a folivore and represent important host qualities marking the end of the phenological window of opportunity.

The phenological window of opportunity is also influenced by environmental and genetic factors (Campbell and Sugano 1979, Volney and Fleming 2007, Lirette and Despland 2021). Phenology of both trees and insects rely on seasonal cues such as photoperiod and temperature (Bellemin-Noël et al. 2021). Spring temperatures are the primary driver of both white spruce bud burst phenology and SBW emergence, which are expected to advance under current climate change projections and likely to lead to greater synchrony between insects and hosts (Bellemin-Noël et al. 2021). Bud burst phenology exhibits natural genetic variation in white spruce, with the timing of bud burst initiation as well as the duration of bud burst differing between genetically distinct provenances (Pelgas et al. 2011, Rossi and Bousquet 2014, Perrin et al. 2017).

While considerable research has been conducted on the role of secondary metabolites in conifer defense against insect herbivores – including folivores – much less attention has been paid to the role of defensive structural traits in mediating these interactions between forest insect pests and their conifer hosts. Accordingly, in this study we tested the hypothesis that increased foliar toughness that occurs during needle development over the course of bud burst for white spruce is influenced by deposition of cuticle and lignin. To address this hypothesis, we correlated needle toughness measured using a custom-designed penetrometer with cuticle quantity and spatial deposition of lignin during bud burst and subsequent shoot elongation of apical buds for seedlings and branch terminal buds of mature trees. We further examined potential roles of the cuticular layer in the phenological window of opportunity by quantifying cuticle composition of seedling apical buds and mature tree branch terminal buds using gas chromatography-mass spectrometry (GC-MS). Finally, we examined the effect of elevated temperature on family-level differences in the progression of bud burst to determine how this key environmental cue might affect the phenological window of opportunity.

5.2 Materials and Methods

5.2.1 Plant Material

Mature Trees. Mature white spruce trees planted as four-year-old seedlings in 2006 at the Alberta Innotech research facility near Vegreville, Alberta (53º30'9.0036" N, 112º*f*05'34.9764" W) were used for these experiments. These trees represented progeny from full-sib family C94-1-2516 with parents representing Quebec provenances (♀77111 × ♂2388) created by Natural Resources Canada, Canadian Forest Service (Pelgas et al. 2011). The same full-sib family was used by Pelgas et al. (2011) for a QTL study of adaptive traits, including time to bud burst. In 2017 and 2020, trees were phenotyped for bud burst stage essentially according to Dhont et al.

(2010). Phenotyping began at stage 2, given that all trees had met the chilling requirements required for release of endodormancy. Representative branches were cut from phenotyped trees, and the cut ends submerged immediately in water for transport to the University of Alberta, where terminal branch buds were sampled the same day for analyses.

Natural condition seedling experiments. White spruce seedlings in their second season of growth representing full five sib families (C9412494, C9412495, C9412539, C9412540, and C9412578) were used for these experiments. These families are hereafter referred to as families 494, 495, 539, 540 and 578, respectively. The crosses are part of the Québec breeding program, with parents of the five crosses covering a geographic range from eastern Ontario to south-western Québec (Beaulieu et al. 1996). Dormant one year old seedlings produced at the Alberta Tree Improvement and Seed Centre (ATISC, Smoky Lake, Alberta) in their second year of growth were potted in 1.18L pots (TP46, Stuewe & Sons, Inc., Tangent, Oregon) filled with Sunshine Mix 4 potting soil (Sun Gro Horticultural, Agawam, Massachusetts) and placed in 44.45 cm trays (TRAY5, Stuewe & Sons, Inc., Tangent, Oregon) in natural conditions on the roof of the University of Alberta Biotron Facility (53º31'44.3856" N, 113º31'33.8376" W). A complete randomized block design was used for these experiments. In 2019, the experiment commenced on May 7, while in 2020, the experiment commenced on June 2-3 due to COVID-19 public health restrictions of on-campus research activity. Trees were fertilized weekly, beginning with a 1g L^{-1} solution of 15-30-15 (NPK) fertilizer (Plant Products Company Ltd., Brampton Ont.) for the first 2 weeks, followed by 1g L^{-1} 20-20-20 (NPK) for the remainder of the experiment. Trees were watered to field capacity when precipitation was not sufficient to maintain adequate moisture levels. Temperature for seedling experiments was recorded at the site using an Inkbird IBS-TH1 Plus thermometer (Inkbird.com). Precipitation data for the

Edmonton Blatchford Station (53º34'23.008" N, 113º31'00.010" W) was retrieved from the Government of Canada historical climate database (climate.weather.gc.ca). Thirty six seedlings from each family were phenotyped every 1-3 days for stage of bud burst using essentially the same index as Dhont et al. (2010).

Controlled growth environment seedling experiment. Controlled environment experiments were conducted using the same seedling families as described above. Dormant one year old seedlings were planted as described above and placed in growth rooms under the following conditions: 60-70% relative humidity and 16-hour photoperiod (580 µmol photosynthetically active radiation). A split plot experimental design was used. Half of the seedlings were grown in 18ºC day/ 8ºC night conditions, representing historical spring temperatures in southern Quebec where families originated (climate.weather.gc.ca). In a separate room, the remaining trees were grown in 24ºC day/ 14ºC night conditions, representing historical + 6ºC temperatures. The use of +6ºC as the elevated growth temperature for both daytime and nighttime conditions is consistent with the range of elevated temperatures commonly used in other studies (e.g., Kroner and Way 2016, Ward et al. 2019, Dusenge et al. 2020). Within each room, trees were organized in a complete randomized block design. Trees were fertilized with a 1g L^{-1} solution of 15-30-15 (NPK) fertilizer (Plant Products Company Ltd., Brampton Ont.) after planting and then once a week with a 1g L^{-1} 20-20-20 (N-P-K) solution for the remainder of the experiment. Trees were additionally watered to field capacity twice per week. Trees were phenotyped three times per week (16 individuals per family per temperature regime) to determine bud burst stage based on the guide outlined in Dhont et al. (2010).

5.2.2 Foliar Toughness

A custom-designed penetrometer based on the instrument described in Fuentealba et al. (2020) was used to measure foliar toughness. Toughness was defined as the weight required to penetrate foliar tissue using a 20 gauge 2.5 cm bevel-pointed PrecisionGlide® needle (BD, Franklin Lakes, New Jersey). Bud scales were removed prior to foliar toughness measurements. For a subset of samples, foliar toughness was also measured for individual needles removed from elongating shoots beginning at stage 6.

5.2.3 Cuticular Wax Analysis

Cuticular wax extraction. Cuticular wax and chloroform-soluble compounds were extracted by submerging pre-weighed foliar material with bud scales removed in a volume of chloroform sufficient to cover the tissue in a pre-rinsed glass test tube. The submerged tissue was then immediately vortexed in the chloroform for 2 seconds before decanting the liquid through filter paper (Whatman No. 1) into a pre-weighed glass vial. The original test tube was rinsed two times with chloroform, and the volumes pooled. The pooled chloroform extract was then dried under a stream of nitrogen gas at room temperature. Vials containing residues were re-weighed and purged with nitrogen before storing at -80ºC. For analysis of expanding buds harvested from seedlings, apical buds from four different individuals of the same family were pooled to create one biological replicate. For analysis of expanding buds harvested from mature trees, four terminal branch buds removed from the same individual were pooled to create one biological replicate. For sampling following stage 8, when needles were no longer contained within a bud structure, 50 fully expanded needles were pooled from 3-4 individual seedlings of the same family. Following extraction, foliar material was oven-dried at 60ºC to obtain dry weight values.

Methanolysis. Wax residues from mature trees sampled in 2017 and seedlings sampled in 2019 were analyzed by GC-MS for wax composition. Prior to derivatization, wax-containing chloroform residues were thawed and resuspended in chloroform. Ten micrograms of tetracosane was added as an internal standard to an aliquot of 250 µg wax residue for each sample, then evaporated to dryness under a stream of nitrogen gas. Samples were derivatized using a procedure modified from Molina et al. (2006). Two microlitres of freshly prepared reaction buffer comprising 15% (v/v) methyl acetate and 6% (w/v) sodium methoxide in 12 mL methanol was added to each residue and heated at 60ºC for 2 hours. After cooling, 4 mL dichloromethane and 0.5 mL glacial acetic acid were added to neutralize to pH 4-5, followed by the addition of 1 mL wash buffer (0.9% (w/v) sodium chloride in 100 mM Tris, pH 8). Samples were gently vortexed then centrifuged for 2 min at 1500 g prior to collection of the lower organic phase. The organic phase was washed with another 2 mL of wash buffer, then water was removed by addition of sodium sulfate. The remaining solvent was collected and evaporated to dryness under a stream of nitrogen gas prior to sylilation.

Sylilation. Dried methanolysis products were resuspended in 150 µL chloroform and transferred to a 200 µL glass vial insert in a GC vial, and solvent evaporated under nitrogen gas. 10 µL pyridine and 10 µL N,O-Bis(trimethylsilyl)trifluoracetamide (BSTFA) were added before the glass vial was sealed tightly and incubated at 80ºC for 1 hour. Samples were cooled and solvent was evaporated under nitrogen gas before resuspension in 40 µL chloroform. Derivatized samples were then analyzed by GC-MS within 24 hours of preparation.

GC-MS. GC-MS analysis was performed on an Agilent 7890B gas chromatograph with an Agilent 5977A mass spectrometer with triple axis detector. One microlitre of derivatized wax extract was injected into HP-5MS column (30 m length, 0.25 mm inner diameter; Agilent

Technologies) using a 5:1 split ratio, then separated with the following program: 50ºC for 2 min; ramp 40ºC/min to 200ºC and hold for 2 min; ramp 3ºC/min to 320ºC and hold for 30 min. Peak areas were normalized to the peak area of the internal standard tetracosane and represent the proportions for 250 μg of wax for each sample.

5.2.4 Data Analysis

All analyses were conducted using R v4.0.3 (R Core Team 2020) and RStudio v1.4.1106 (RStudio Team 2020). All plots were generated using the ggplot2 v3.3.3 (Wickham 2016) and cowplot v1.1.1 (Wilke 2020) packages for R.

Toughness and Wax Correlations. Toughness and wax quantification data for elongating buds and foliage were fit to generalized linear models and formulas used for each dataset are outlined in Appendix 4. Models were assessed to ensure they met assumptions of normality and homoscedascity using Shapiro-Wilk test (Shapiro and Wilk 1965) and Bartlett's test (Snedecor and Cochran 1989) results. Post hoc comparisons were made using the emmeans package v1.5.3 (Lenth 2020) to determine significant differences between groups; letters were assigned to different groups using the multcomp package v1.4-15 (Hothorn et al. 2008). The car package v3.0-11 (Fox and Weisberg 2019) was used to calculate analysis of deviance, including Wald's chi square test statistics and Pearson's error estimate, for each GLM (Appendix 4). Pearson's correlation coefficient was calculated for the relationship between wax quantity and toughness using the cor.test() function in the stats package v4.1.1. Correlation equations and coefficients of determination were determined using the stat_poly_eq() function in the ggpmisc package v0.4.3 (Aphalo 2021).

Wax Metabolite Data. Metabolite peaks with sufficient resolution and consistency between technical replicates and that were detectable in most biological replicates in at least one

bud burst stage were selected for further analysis (Appendix 1 Figures 1-2). Filtered compound data was fit using the vegan package v2.5-7 (Oksanen et al. 2020) to a non-metric multidimensional scaling (NMDS) model with Bray-Curtis distances, and covariance ellipses were calculated for each stage. The analysis of similarities (ANOSIM) test (Clarke 1993) within the vegan package was used to determine statistical differences across stages. R files are available at https://github.com/c4tier/.

5.2.5 Microscopy

Whole mount and fresh sectioned images were collected from mature trees in 2017 and 2019, and from seedlings in 2019. Whole mount images were obtained from intact expanding buds with or without bud scales using a WILD TYP 376788 Stereo Microscope equipped with a Nikon DXM1200 digital camera. Phloroglucinol (4:1 saturated phloroglucinol in 95% ethanol:concentrated hydrochloric acid) stain to detect lignin and aldehyde groups or Sudan IV (1:1 saturated Sudan IV in 95% ethanol:glycerol) stain to detect wax and lipids were applied directly to transverse hand-sections mounted in water and imaged promptly using a Zeiss Axio Scope.A1 brightfield light microscope equipped with a SeBaCam 5.1 MP digital camera (Laxco™).

Samples for fixation and embedding were collected from mature trees in 2017 and 2020, and from seedlings in 2019 and 2020. Bud scales were removed from expanding buds, and the buds were halved medially to allow for better penetration of fixative. Later stage expanding shoots and individual needles were also cut transversely on both ends prior to fixation. Cut samples were immersed in glutaraldehyde fixative (2% v/v glutaraldehyde, 1% caffeine buffered in 0.1M sodium phosphate buffer; pH 7.2) for 5-7 days under vacuum (-12mmHg) until the tissue sank; fixative was replaced once. Fixed samples were dehydrated in 90% ethanol, 100%

ethanol, 100% ethanol, toluene, and toluene for 1 hour each prior to embedding in paraffin wax and cut into 8µm sections using a LEICA RM2235 microtome.

Sections were de-paraffinized by washing sections twice in toluene for 5 minutes, twice in separate solutions of 100% ethanol for 2 min, then in 90% ethanol, 70% ethanol, 50% ethanol, and distilled water each for 2 minutes. Sections were then stained 1 min in Richardson's stain (Richardson et al. 1960), rinsed in water for 2 min, dehydrated by dipping 10 times in 95% ethanol, 100% ethanol, and 100% ethanol each, Slides were rinsed twice in toluene prior to applying a cover slip with dibutylphthalate polystyrene xylene (DPX) mounting medium (Fisher Scientific). Images were taken on a Zeiss Axio Scope.A1 brightfield light microscope equipped with a SeBaCam 5.1 MP digital camera (Laxco™). To visualize lignin, excitation at 450-490 nm and autofluorescence at 510 nm of unstained sections was imaged using a LEICA DMRXA compound light microscope and QIClick™ digital camera (QImaging, Surrey, Canada) in epifluorescence mode (Leica I3 filter cube, 315 milliseconds exposure).

5.3 Results

During the course of bud burst in white spruce, stem units (primordia plus subtending stem) of the bud undergo elongation, causing bud scales to separate from each other to accommodate the expanding shoot. Adapting the schema developed by Dhont et al. (2010), we identified seven visually distinguishable phenological stages of bud burst, starting from a fully closed bud and concluding with an elongating shoot with clearly visible stem units (Fig. 5.1A). We have used the same stage notations as Dhont et al. (2010). For simplicity, the term "bud" is used throughout to refer to the continuum of structures from bud through expanding shoots that fall within the development window of bud burst staged by Dhont et al. (2010).

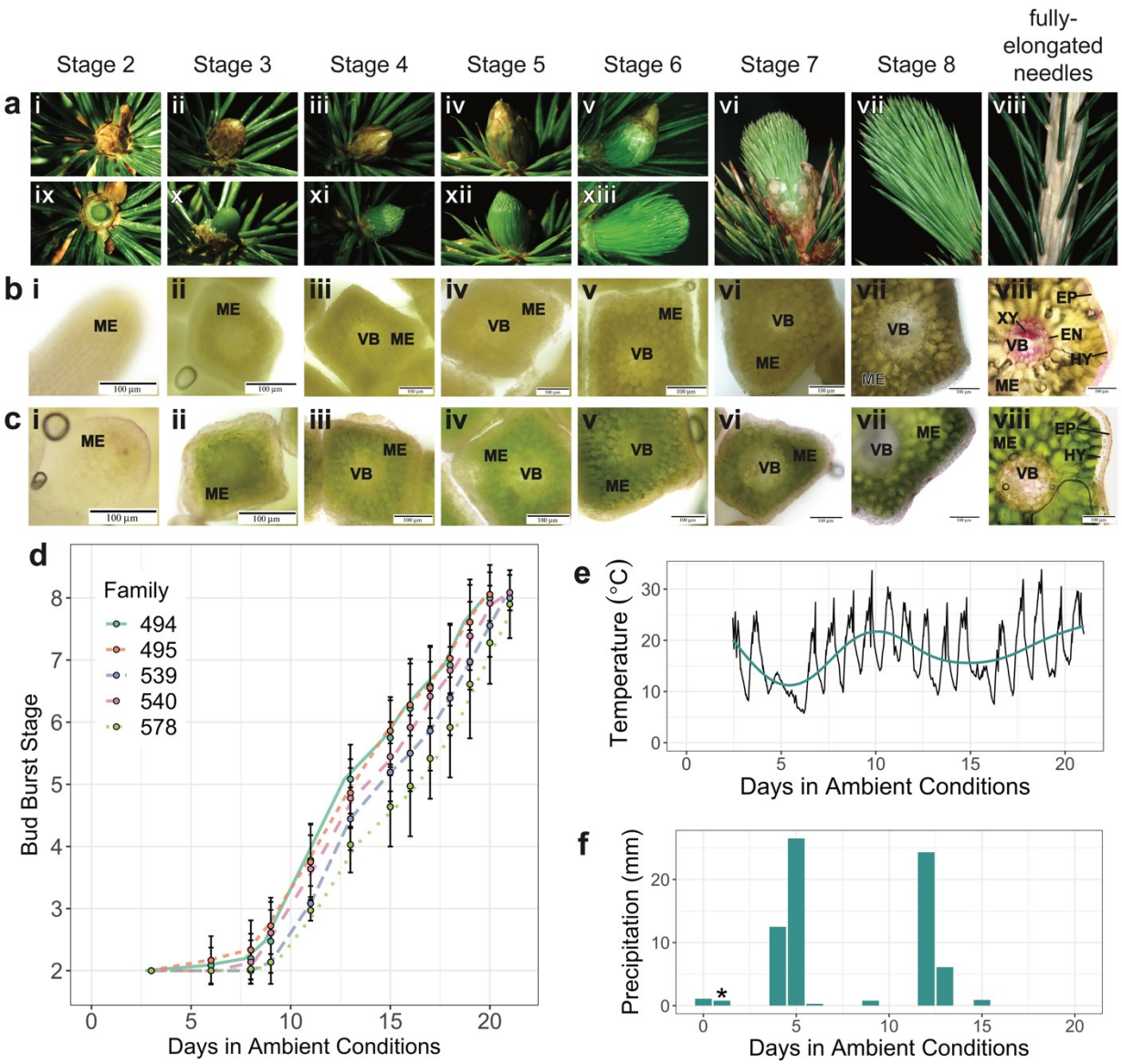

Figure 5.1. Bud burst phenology of white spruce seedlings. a Elongation of needles in apical buds during bud burst relative to fully–elongated needles. Stages with bud scales present (stages 2-6) were imaged with **(ai-av)** and without scales **(aix-axiii)**. **b** Deposition of lignin following bud burst in transverse sections of elongating needles stained red with phloroglucinol. **c** Accumulation of lipids and waxes stained red with Sudan IV. **d** Phenological differences between families grown under ambient (natural) conditions in June 2020. Points represent mean bud burst stage ± standard deviation (n = 36). **e** Temperature profile during bud burst; blue line represents the average daily temperature. **f** Precipitation during bud burst (bar graph); asterisk

represents the date when seedlings were watered manually. VB = vascular bundle, EP = epidermis, EN = endodermis, HY = hypodermis, ME = mesophyll, XY = xylem.

In the 2019 outdoor ambient conditions experiment, progression from fully closed buds (stage 2) to actively elongating branches (stage 8) took approximately 26 days (Fig. 5.1D), whereas the progression from stage 2 to stage 8 took only 21 days in the 2020 outdoor ambient conditions seedling experiment (Appendix 4 Figure 3A). Warmer temperatures were recorded during the 2020 experiment than during the 2019 experiment. The greatest variation in bud burst phenology between the five full-sib families occurred during stages 4 through 7, which corresponded to the phase of intense changes in needle development, including elongation (Fig. 5.1D). Under controlled environment conditions, bud burst was accelerated under elevated temperatures (24ºC days, 14ºC nights) relative to historic spring temperatures (18ºC days, 8ºC nights), leading to reduced differences in bud burst phenology observed between families (Appendix 4 Figure 4).

Hand sectioning of fresh foliage through the course of bud burst revealed tissue differentiation early in needle development, with the vascular tissues, mesophyll and epidermis all being distinguishable by stage 3, and all cell types, including the hypodermis, evident by stage 6. We used phloroglucinol and Sudan IV staining of fresh sections to reveal the presence of cinnamaldehydes and lipophilic substances, respectively, in hand-sectioned fresh seedling needles. Phloroglucinol was inferred to have stained lignin where coinciding Sudan VI staining was absent. We further inferred that cellular constituent staining with both phloroglucinol and Sudan IV represented suberin, a complex polymer containing both polyphenolic and lipid domains (Graça 2015). Phloroglucinol staining revealed the presence of lignin in the vascular tissues, endodermal and hypodermal cell layers in fully elongated needles, whereas

phloroglucinol staining was not detectable in needles at stage 8 (Figure 5.1B). Phloroglucinol staining did not overlap with Sudan IV staining in seedling needles. As expected, Sudan IV staining of the cuticle at the epidermis was evident in mature fully elongated seedling needles, with the first signs of cell-specific staining at stage 6 (Figure 5.1C).

The developmental progression observed during seedling bud burst was similar but not the same as the bud burst trajectory of mature trees (Figure 5.2A). COVID interruptions to research activities precluded sampling of materials prior to stage 4. Vascular tissue, endodermis, hypodermis and epidermis tissues could be distinguished even in stage 4 foliage, with maturation of these tissues continuing through to the fully elongated needle stage (Figure 5.2B).

Autofluorescence of phenolic cell wall components – presumed to be lignin and/or suberin – was detected as early as stage 7, and was most evident in the hypodermis, endodermis, and xylem in fully expanded needles (stage 9) of stained sections (Figure 5.2C). Strong phloroglucinol staining of the entire hypodermis accompanied by relatively faint Sudan IV staining of a subset of hypodermal cells indicated that the majority of the hypodermis autofluorescence was due to lignin. Similarly, there was much stronger staining of the endodermis and vascular bundle by phloroglucinol than by Sudan IV, again leading to the inference that lignin was the major cell wall constituent contributing to the staining of these tissues. As expected, Sudan IV staining of the cuticle at the epidermis was evident as early as stage 3 and was substantially thickened in mature fully elongated needles (Figure 5.2E).

Toughness of 2020 seedling intact apical buds with bud scales removed, as measured using a custom-fabricated penetrometer, significantly increased for all but one family by stage 5, corresponding to the phase of initial elongation when developing needles are still covered by bud scales (Figure 5.3A). Toughness further increased significantly in all families between stages 4

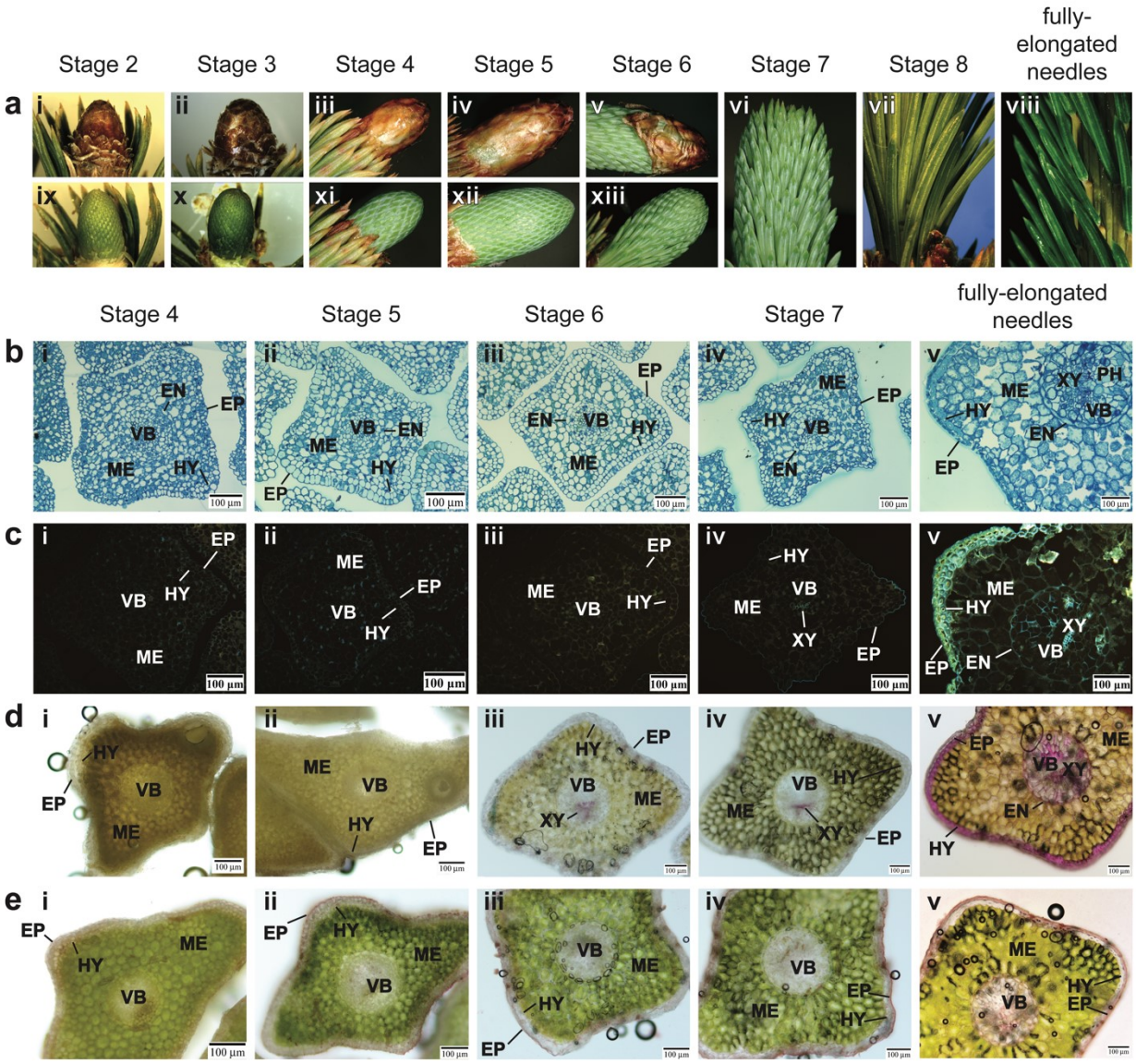

Figure 5.2. Bud burst phenology of mature white spruce. a Morphological changes of intact buds relative to fully elongated needles from lateral branches during stages of bud burst; stages where scales were present (stages 2-6) were imaged with **(ai-av)** and without scales **(aix-axiii)**. **b** Anatomical changes of elongating needles within buds were visible in transverse sections stained with Richardson's blue. **c** Autofluorescence (excitation = 450-490 nm, emission = 510 nm) of phenolic compounds, including lignin and suberin. **d** Phloroglucinol staining revealed lignin deposition in the hypodermis and vascular bundle of elongating needles. **e** Sudan IV staining coincided with deposition of lipophilic materials in the needle epidermis and vascular bundle. Sudan IV-positive cellular constituents at the epidermis were inferred to be cuticular waxes,

while staining that coincided with phloroglucinol was inferred to represent suberin. XY = xylem, VB = vascular bundle, EP = epidermis, EN = endodermis, HY = hypodermis, ME = mesophyll.

and 6 (family 494 z = -3.12, $p = 0.03$; family 495 z = -3.34, $p = 0.02$; family 539 z = -4.05, $p < 0.001$; family 540 z = -3.41, $p = 0.01$), when bud scales were shed and differentiation and maturation of specific cell types occurred in the needles, including the vasculature, hypodermis and epidermis. Most families also showed a significant increase in bud toughness between stages 7 and 8. An independently replicated experiment conducted in 2019 also showed that bud toughness increased significantly for all families except one starting at stage 6 (family 494 z = -3.68, $p = 0.002$; family 495 z = -3.25, $p = 0.01$; family 539 z = -4.93, $p < 0.001$; family 578 z = -3.24, $p = 0.01$; Appendix 4 Figure 3A). With a small number of exceptions, bud toughness was not significantly different between families at any given phenological stage for either year. However, we observed that family 578 typically had the highest toughness values at most stages of bud burst, consistent with phenology rankings where family 578 was generally slowest to each bud burst stage.

Foliar toughness of detached needles from 2020 seedling expanding shoots was the below detectable limits of our instrument until stage 6. Most families showed a slight but statistically significant increase in foliar toughness at stages 7 (family 494 z = -5.01, $p < 0.001$; family 495 z = -3.28, $p = 0.009$; family 539 z = -4.00, $p < 0.001$; family 540 z = -4.96, $p < 0.001$) and 8 (family 495 z = -3.12, $p = 0.02$), but a marked and significant increase in foliar toughness was only obtained once needles had fully elongated (family 494 z = -36.2, $p < 0.001$; family 495 z = -29.7, $p < 0.001$; family 539 z = -29.8, $p < 0.001$; family 540 z = -35.0, $p < 0.001$; family 578 z = -32.0, $p < 0.001$; Figure 5.3b). This corresponded with the substantial increase in phenolic-associated autofluorescence detected in fully elongated needles. With one exception, there was

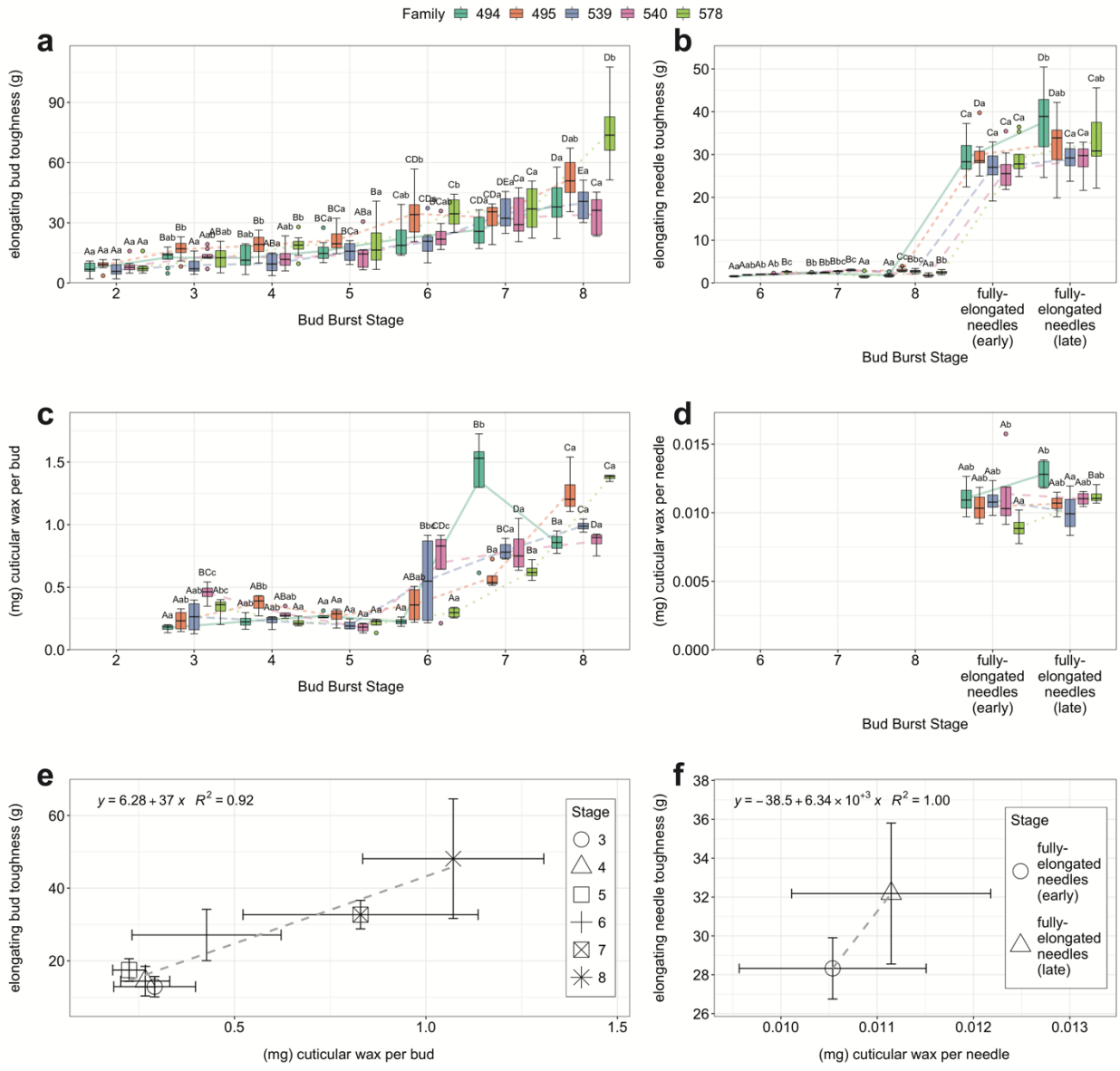

Figure 5.3. Toughness of elongating apical buds in seedlings is positively correlated with cuticular wax deposition during bud burst. Measurements were taken in 2020. **a,b** Toughness of **(a)** intact buds (n = 8) and **(b)** elongating needles (n = 8). **c,d** Cuticular wax extracted from **(c)** intact buds (n = 4) or **(d)** elongated needles (n = 4). For **(a-d)**, capitalized letters represent significant differences between stages with a family (adjusted $p < 0.05$), lower case letters represent differences within a stage between families. **e,f** Correlation of toughness and cuticular wax weights of **(e)** intact buds or **(f)** elongated needles across shared bud burst stages. For **(e,f)**, points represent the mean value across families ± standard deviation (n = 20-40).

no significant difference in foliar toughness between fully expanded needles sampled after 49 days in ambient conditions (fully elongated needles, early) and those sampled 80 days in ambient conditions (fully elongated needles, late; Figure 5.3b). For needles sampled from the 2019 seedling experiment, toughness increased significantly across families between early and late fully elongated needles, however these sampling points were further apart, representing 43 and 98 days in ambient conditions, respectively (Appendix 4 Figure 3b).

We next examined whether foliar toughness was correlated with deposition of cuticular wax for expanding foliage of seedlings. In 2020 seedlings, quantity of cuticular wax increased following the loss of bud scales at stages 6 or 7, depending on the family (Figure 5.3c). These results corroborate the increased lipophilic staining observed at stage 6 (Figure 5.1c). With few exceptions, seedling cuticular wax did not differ between families within a given stage, including in fully elongated needles (Figure 5.3c-d). Except for family 578, which had significantly more cuticular wax in fully elongated needles at the late time point ($z = -2.57$, $p = 0.01$), cuticular wax quantities did not significantly differ between early and late fully elongated needles (family 494 $z = -1.66$, $p = 0.10$; family 495 $z = -0.24$, $p = 0.81$; family 539 $z = 0.95$, $p = 0.34$; family 540 $z = 0.36$, $p = 0.72$). Results from the independently replicated experiment conducted in 2019 agreed with the findings of the 2020 experiment (Appendix 4 Figure 3). When measured on a per mg tissue dry weight basis, cuticular wax quantity declined for seedling apical buds over the course of bud burst in both years (Appendix 4 Figure 5).

Seedling apical bud toughness and cuticular wax quantity for corresponding bud burst stages were strongly and positively correlated for both the 2019 and 2020 experiments (2020 Pearson correlation coefficient = 0.96, d.f. = 4, $p = 0.003$; 2019 Pearson correlation coefficient = 0.89, d.f. = 2, $p = 0.11$; Figure 5.3E and Appendix 4 Figure 3E). However, we exhibited greater

differences between stages 4 and 5 in 2019. A positive relationship was also found between needle toughness and cuticular was quantity for detached early and late fully elongated needles in 2020 (Figure 5.3f).

Cuticular wax quantity increased significantly in mature tree buds at stage 6 and again between stages 6 and 7 (stages 4-6 $z = -2.59$, $p = 0.05$; stages 6-7 $z = -11.4$, $p < 0.001$; Figure 5.4c), similar to the trend observed in seedlings. In contrast, cuticular wax decreased significantly in late fully expanded needles relative to early fully expanded needles ($z = 2.76$, $p = 0.006$; Figure 5.4d). When expressed on a per mg tissue dry weight basis, cuticular wax generally increased in later stages of bud burst, unlike the trends observed for seedling apical buds (Appendix 4 Figure 5). Toughness of mature tree terminal branch buds with scales removed was substantially greater through stages 4 to 6 than that of stages 4 to 6 for seedling apical buds, while toughness of buds from mature trees and seedlings at stage 7 was comparable. Consequently, there were no significant differences in mature tree terminal branch bud toughness measures between bud burst stages 4 through 7, as had been observed for seedling apical buds (Figure 5.4a). However, there was a substantial and significant increase in needle toughness between stage 7 needles and stage 9 needles ($z = -34.0$, $p < 0.001$; Figure 5.4b). Because of these differences in foliar toughness profiles from seedling apical buds, mature tree terminal branch bud toughness and cuticular wax quantity were not strongly correlated across bud burst stages (Pearson correlation coefficient = -0.56, d.f. = 2, $p = 0.44$; Figure 5.4e), while needle toughness and cuticular waxes were negatively related (Figure 5.4f).

Given that very little has been published on the composition of cuticular waxes of actively expanding foliage in conifers, we examined cuticular wax profiles for both seedling and

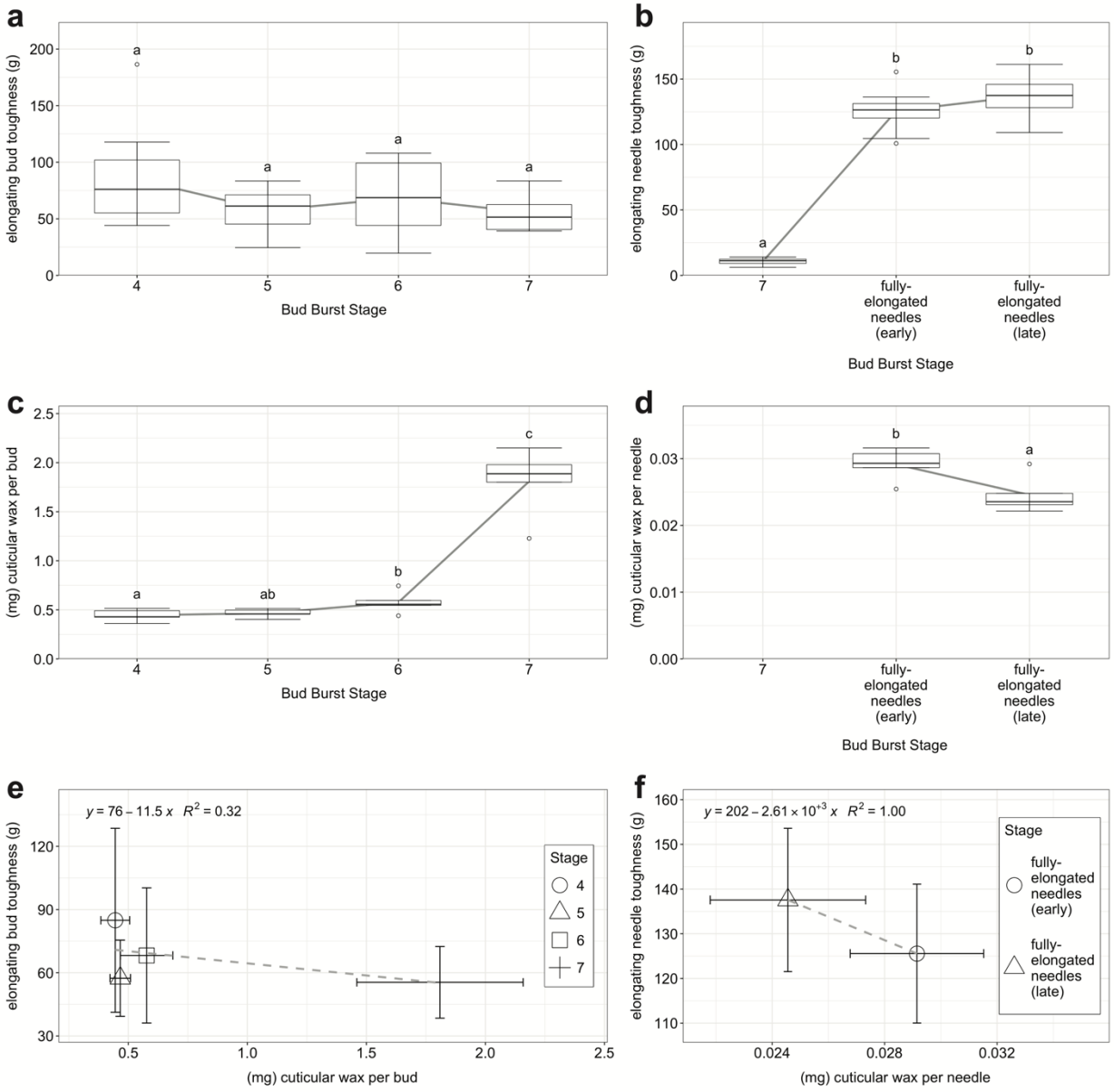

Figure 5.4. Toughness and cuticular wax deposition are not strongly correlated during bud burst of mature white spruce lateral branch buds. Measurements were taken in 2020. **a,b** Toughness of **(a)** intact buds (n = 10) or **(b)** elongating needles during bud burst (n = 10). **c,d** Cuticular wax extracted from **(c)** intact buds (n = 5) or **(d)** elongated needles (n = 5). For **(a-d)**, letters represent significant differences between bud burst stages (adjusted $p < 0.05$). **e,f** Correlation between toughness and cuticular wax weights of **(e)** intact buds or **(f)** elongated needles across shared bud burst stages. For **(e,f)**, points represent the average value across all individuals ± standard deviation (n = 5-10).

mature tree foliar tissues using GC-MS. For seedlings, chloroform-soluble components of the cuticular layer were analyzed from intact stage 3 buds with bud scales removed and stage 9 needles, as end points to foliar development. Wax extract compositions were found to dramatically differ in proportion of alkane/alkene, fatty acid, and both primary and secondary alcohol compounds between stage 3 buds and stage 9 needles (Figure 5.5a). Wax extract differences between stages as well as among families were examined further using non-metric multidimensional scaling (NMDS) to visually compare samples across an ordination plot (Figure 5.5b). As expected, samples grouped by bud burst stage rather than family. Of the compounds identified as significantly contributing to differences between samples ($p < 0.05$), differences between stages were related to changes in diols and many of the fatty acids (Figure 5.5b).

We also examined the epicuticular wax deposition of expanding needles in mature trees at stages 6, 7, 8, and 9. Defense-related terpenoids constituted a large proportion of cuticular wax composition in stage 6 when cuticle is thinner, decreasing dramatically between stages 6 and 7 and comprising only a small proportion of wax compounds in fully expanded needles (stage 9, Figure 5.6a). Inversely, primary alcohol proportion more than doubled between stages 6 and 7, after which they remained a prominent wax component. Many terpenoid and primary alcohol compounds were also found to significantly contribute to differences in wax extracts among samples based on NMDS ordination ($p < 0.05$; Figure 5.6b). Proximity of groups in NMDS indicated that composition of stage 6 wax was most distinct from stages 7 and 8, which were similar. Composition of fully expanded needles at stage 9 were very different than stages 6 through 8, with these differences driven by changes in a primary alcohol, a diol, and 2 fatty acid methyl esters (Figure 5.6b). Therefore, fully expanded needles at stage nine contained the most cuticle, and this epicuticular wax was distinct from that of earlier stages.

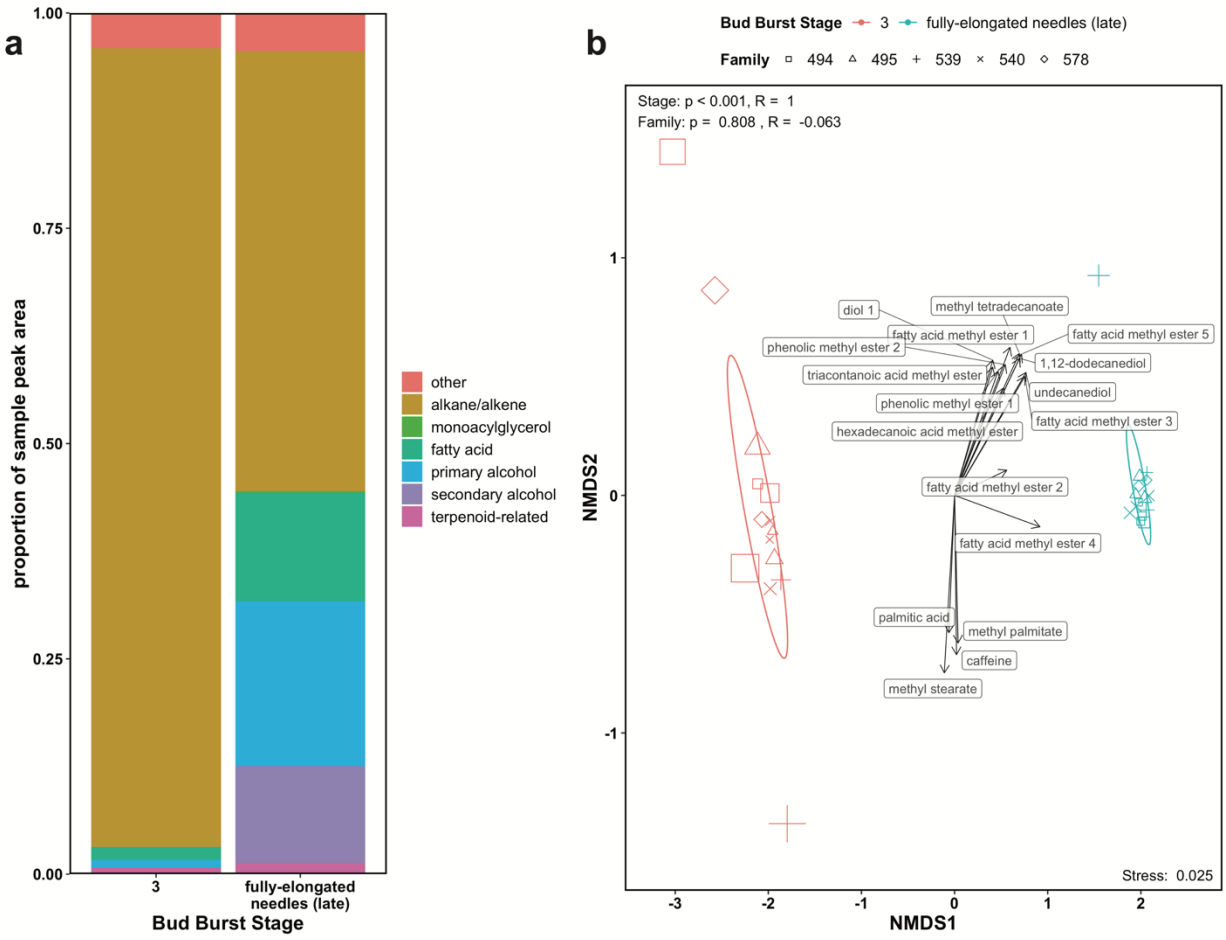

Figure 5.5. Cuticular wax composition of elongating needles in seedling apical buds is similar across families at early and late stages of bud burst. a Proportions of wax-soluble compounds in bud and needle cuticular wax extracts at early (stage 3) and late (fully-elongated needles) stages of bud burst (n = 4). **b** NMDS of cuticular wax extracts. Points represent individual trees and point size is proportional to sample goodness of fit within the ordination model. Compounds found to be significant predictors ($p < 0.05$) of differences between groups are labeled with arrows representing the strength and direction of each predictor. Stress values indicate the fit of the model; values less than 0.2 are considered a good fit.

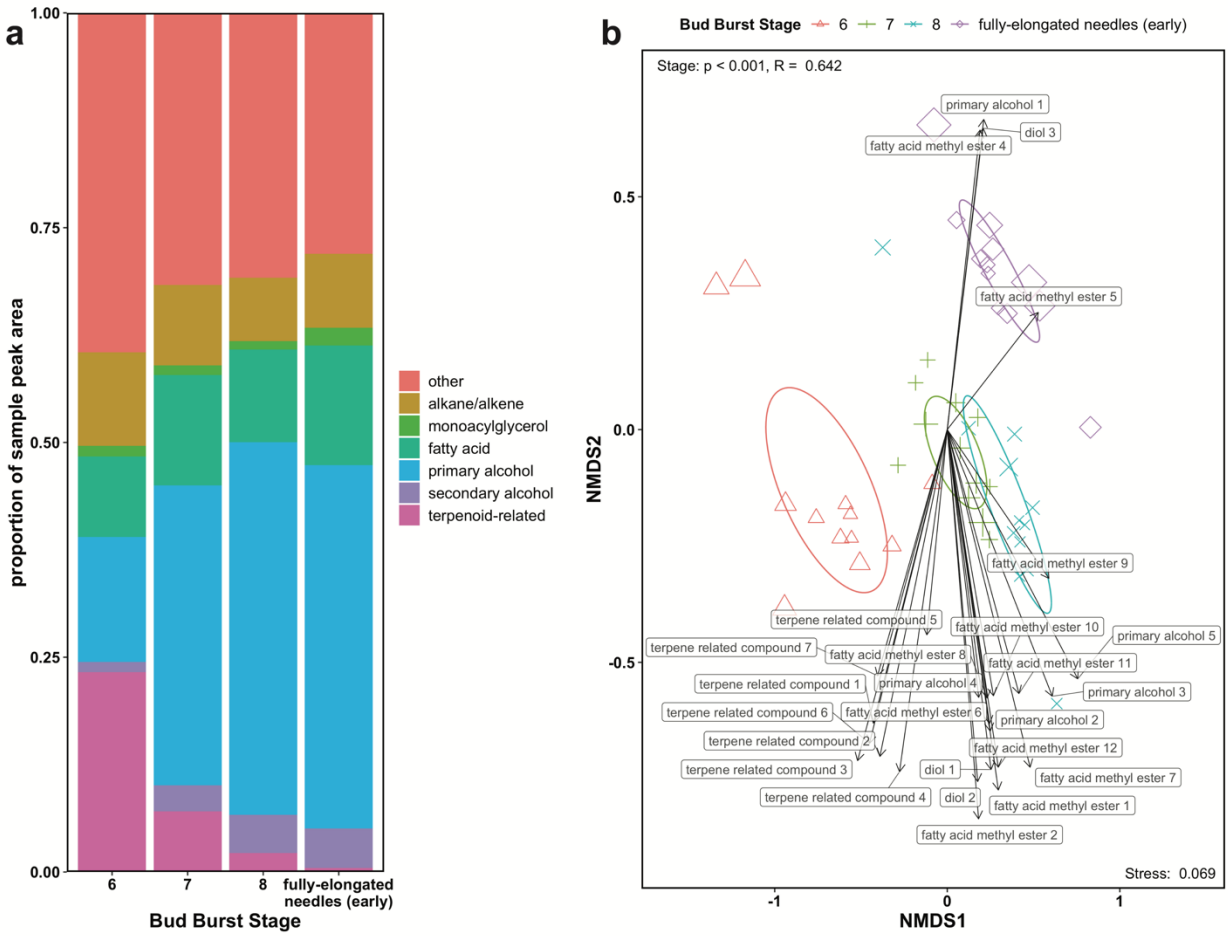

Figure 5.6. Cuticular wax composition of elongating buds and needles from mature white spruce lateral branches across bud burst stages. a Proportions of wax-soluble compounds in cuticular wax extracts of intact buds (stages 6-8) and needles (n = 10-12). **b** Ordination of cuticular wax extracts based on NMDS across bud burst stages. Points represent individual trees and point size is proportional to sample goodness-of-fit within the model. Compounds found to be significant predictors ($p < 0.05$) of differences between groups are labeled with arrows denoting the strength and direction of each predictor. Stress values indicate the fit of the model; values less than 0.2 are considered a good fit.

5.4 Discussion

SBW overwinters as second-instar larvae (Nealis 2016). Upon emerging from diapause in the spring, these second-instar larvae must quickly locate appropriate host foliage. Because of the barrier posed by the bud scales, second-instar larvae can only enter expanding buds after bud scale separation, when roughly 10-35% of the needles are exposed (Fuentealba et al. 2018). This developmental stage corresponds to approximately stage 5 in the phenological scale of Dhont et al. (2010) used in this study. Larvae that emerge earlier than this survive by mining previous year foliage (Volney and Fleming 2007, Fuentealba et al. 2018). This ability of SBW to exploit the overwintering foliage of its evergreen conifer hosts provides a distinct advantage relative to folivores that target deciduous tree species in north-temperate forests for which no foliage is available until bud burst has commenced. However, prolonged feeding on older, tougher, less nutritious foliage can prove detrimental to SBW development (Fuentealba et al. 2017, 2018), limiting the extent of phenological mismatch that the second-instar larvae are able to survive. Additionally, decreases in SBW survival have been observed in slow-developing larvae forced to continue feeding on current year foliage later in the season (Lawrence et al. 1997, Fuentealba and Bauce 2012). Numerous studies have suggested that foliar mechanical toughness is the primary trait contributing to host and needle suitability (Fuentealba et al. 2018, 2020, Lirette and Despland 2021) and is a determinant in defining the phenological window of opportunity in which host foliage is suitable for SBW feeding (Lawrence et al. 1997). Our results indicate that toughness of intact buds increases non-linearly during bud burst, reaching maximums shortly after the bud scales are shed and needles are fully exposed. While bud toughness plateaus, the needles themselves only gain significant toughness once they have fully elongated. Therefore, our data suggest that there are two points at which physical toughness of buds and needles have

the potential to impact nutritional quality of host tissues: when the expanding shoot has elongated sufficiently to cast its bud scales, and when needles have fully expanded. It is likely that the stage 6-8 transition is the most important for defining the close of the window because these coincide with later instars, when SBW feeding increases and SBW is most dependent on nutritious tissues (Thomas 1987). Late-emerging larvae which feed primarily on fully expanded foliage during their 6th instar experience delayed development and limited growth (Thomas 1987).

To ascertain the physical traits that are determinant(s) of this phenological window of opportunity, we conducted fine scale analyses of changes to foliar anatomy and histochemistry through bud burst and related these to changing foliar toughness through bud burst and needle development. These analyses revealed that development of the hypodermis, lignification and cuticle deposition all contribute to foliar toughness to varying degrees, and that the relative importance of these cellular features to foliar toughness differs between developing needles of seedlings and mature trees. We also identified suberin as potentially contributing to foliar toughness, although to a lesser degree than hypodermis development, lignification, and cuticle deposition. In expanding buds of seedlings, foliar toughness was associated in the mid and late stages with hypodermis development and cuticle deposition, and at late stages with hypodermis maturation, lignification, and further cuticle deposition. In expanding buds of mature trees, cuticular wax deposition was not a major contributor to needle toughness. Instead, hypodermis development, maturation and lignification were more closely associated with foliar toughness.

Not unexpectedly, toughness of elongating shoots increased much earlier in bud burst for mature trees than for seedlings, likely reflecting an ontogenetic shift in shoot characteristics that occurs between juvenile and mature trees (Steppe et al. 2011, Kuusk et al. 2018). COVID

restrictions to research activities precluded a full sampling of bud burst stages for mature trees for this thesis. Similarly, toughness of fully developed needles from mature trees was substantially greater than that of fully developed needles from seedlings, despite having very similar anatomical structure. We identified the degree of lignification of the hypodermis to be the major difference in foliar features associated with this difference in toughness between juvenile and mature foliage. A subset of these hypodermis cells in fully elongated needles of mature trees may have also been suberinized to some degree, based on colocalization of phloroglucinol and Sudan IV staining. Suberin is a biopolymer consisting of both aliphatic (lipid) and aromatic (phenolic) domains (Bernards 2002, Philippe et al. 2020), which can add structural and hydrophobic properties to cell walls (Graça 2015). In addition to the increased mechanical strength imparted by lignin and suberin, both are also large macromolecules that are not easily digested, decreasing a tissue's nutritional quality. Lower host nutritive quality has been shown to lengthen SBW development time and decrease pupal mass (Fuentealba and Bauce 2012). For a SBW trying to access more tender mesophyll tissue, mining an expanding hypodermal layer that is increasingly fortified with indigestible compounds would likely have detrimental impacts.

In this study, we determined that cuticular wax deposition not only increases over the course of needle development, but that wax profiles also change during needle development. Wax composition also differed between foliage of seedlings and mature trees, another indicator of the ontogenetic shifts that we captured for foliage of juvenile and mature trees. Early seedling wax profiles more predominantly consisted of simple alkane/alkene compounds, resembling proportions found in Cactaceae and Brassicaceae (Jetter et al. 2006), while later seedling wax contains much larger proportions of alcohols characteristic to conifers (Prügel and Lognay 1996, Gordon et al. 1998), which may play a role in overwintering and maintain wax fluidity under

colder conditions. However, our proportion of primary alcohols was much larger than expected, as spruce are known for having a high proportion of secondary alcohols (Günthardt-Goerg 1987, Gordon et al. 1998). As we did not measure wax profiles for older needles, it is possible this is a characteristic of newer foliage and would be worth investigating. Our wax profiles for mature trees were more complex than in seedlings, containing a much higher proportion of "other" compounds, like tocopherol (vitamin E). While the role of many of these compounds is unclear, antioxidants like tocopherol may contribute to maintaining foliar health (Falk and Munné-Bosch 2010, Hasanuzzaman et al. 2014) in evergreen white spruce trees.

We found that the proportion of terpene compounds in the cuticular wax profiles declines rapidly during bud burst during the phenological window of opportunity, as needles become more accessible to SBW, contradictory to expectations for defensive metabolites based on the apparency hypothesis (Feeny 1976). However, our findings are consistent with seasonal changes in foliar monoterpenes observed by Despland et al. (2016), who observed that changes in these compounds were specific to current year foliage. These variations in cuticular wax profiles are notable because SBW larvae probe foliage cuticular wax to discriminate between hosts (Daoust et al. 2010), based on the composition of secondary metabolites contained within (Despland et al. 2016). For example, at lower concentrations, monoterpenes act synergistically with wax to stimulate SBW feeding (Ennis et al. 2017), while higher concentrations may have a negative effect (Daoust et al. 2010) or no effect (Mattson et al. 1991). However, early instar larvae may be more sensitive to these toxic monoterpenes than later stages (Despland 2018), rendering host accumulation of these compounds to be the most effective when buds are first accessible, but less helpful later in development.

Our results also showed that for all families, timing of bud burst was faster and more consistent across families under warmer temperatures, shortening the phenological window of opportunity. Bud burst phenology/degree of mismatch to SBW development is a strong predictor of SBW outbreaks (Bouchard et al. 2018). Increased temperatures can also speed up SBW development (Han et al. 2000, Bellemin-Noël et al. 2021) and reduce phenological mismatch between bud burst and SBW development (Pureswaran et al. 2019). However, if bud burst is early enough that needles may gain sufficient toughness to impact SBW feeding at later instars, when consumption is higher and low foliar nutrition may have a greater impact on SBW growth (Pureswaran et al. 2019). In fact, advanced phenology was found to have a greater effect on budworm performance than delayed phenology, provided trees avoided late frost damage and the budworm's phenology also did not shift (Lawrence et al. 1997).

Across experiments monitoring seedling budburst phenology we found that the general order in which each family reached a particular stage to be consistent, even under different temperature conditions, with family order shifting at most one position between years. In contrast, we did not see consistency in the order in which families increased in foliar toughness between years or consistent with the phenological order. The exception to this was family 578, which was always the slowest but often had the highest toughness measurements at a given bud burst stage. These results indicate that the acquisition of traits defining the phenological window of opportunity are not necessarily reflected in bud burst phenology. This also means that while the time to a particular bud burst stage can be used as a measure to predict the span of the phenological window of opportunity for a given family, the physical leaf traits cannot be used as a predictor. It also suggests that factors other than genetics are contributing to differences observed in acquisition of these traits between families.

5.5 Conclusion

In this study, we tested the hypothesis that increases in foliar toughness are determined by deposition of cuticular wax and lignification during needle development. We identified key changes in foliar toughness during the course of bud burst that are important for defining the phenological window of opportunity for SBW feeding. Additionally, we found that development of the hypodermis, as well as lignification and cuticle deposition, contribute to these changes in foliar toughness. However, the relative importance of these contributors differed between seedling and mature trees, and cuticular wax quantity was not a major contributor to toughness in mature trees. Despite this, we found that compositions of wax extracts changed dramatically across bud burst stages. In mature trees, we propose that cuticular wax plays an important role in host-insect interaction, as terpenes present in cuticular wax at early bud burst stages may help discourage SBW feeding, until lignification and hypodermis development of expanding needles is sufficient to provide an alternative deterrent.

We also compared timing of bud burst and needle development between families under different temperature regimes, as spring temperature is the primary driver of both bud burst phenology and SBW emergence. We found that variation in phenology observed between families was tighter, and bud burst occurred faster under increased temperatures. These results suggest that any variation in asynchrony between white spruce and SBW observed across a landscape will be reduced under predicted climate change scenarios, but that the phenological window of opportunity will be smaller.

Chapter 6: Conclusions

In this thesis research, I explored the roles that several chemical and structural defenses play in the interactions that occur between multiple antagonists and their conifer hosts. Under predicted climate change scenarios, the frequency of insect outbreaks is anticipated to increase, as is the overlap between outbreaks (Navarro et al. 2018). Drought is becoming a more common occurrence, as are heat waves. Temperature increases are triggering shifts in host and insect phenology, and in many cases reducing asynchrony (Pureswaran et al. 2015, 2019, Bellemin-Noël et al. 2021). Understanding the degree to which host defenses change under these circumstances, and how those changes influence host susceptibility, is more important than ever.

In chapters two and three, I compared molecular and biochemical defense responses of lodgepole and jack pine seedlings to inoculation with the MPB fungal associate *G. clavigera*. I examined these responses in phloem, the site of entry for MPB and *G. clavigera*, and xylem, the final battleground against fungal growth. I observed different biochemical pathways favored in the defense responses between tissues – namely terpene biosynthesis and resin production in phloem and phenolic biosynthesis in xylem. These studies revealed that jack pine exhibits a greater response to *G. clavigera* earlier than lodgepole pine, with greater involvement of secondary metabolites. Additionally, lodgepole and jack pine showed similar patterns of regulation of hormonal signalling, including JA and ET, early in response to *G. clavigera*. These results suggested that both lodgepole and jack pine perceive challenge by the necrotrophic pathogen *G. clavigera* at similar times, and that both species activate similar signalling pathways, but that there exists a difference in which downstream defenses are induced and to what magnitude. My original hypothesis was that the shared evolutionary history between lodgepole pine and MPB/*G. clavigera* has resulted in a more effective defense response from

lodgepole pine to *G. clavigera* relative to the evolutionarily naïve host, jack pine. I propose that this difference in defense strategies is indeed reflective of lodgepole and jack pine co-evolution with different antagonists, respective of their different life histories and geographical distributions. Furthermore, I propose that the delayed induction of defenses in historic host lodgepole pine is indicative of a more strategic defense response, while naïve host jack pine exhibits a larger, but more non-specific defense response to *G. clavigera*.

The studies in chapters two and three also investigated the effects of abiotic stress, specifically water deficit, on lodgepole and jack pine defenses to *G. clavigera*. I observed that rather than a global change in defense gene expression, water deficit altered specific defenses but had no effect on others. This was true for both phloem and xylem and suggests that water deficit alters the composition of defenses rather than the magnitude, supporting my hypothesis that water deficit will impact host defenses and suitability. I propose that water deficit, which was sufficient to reduce photosynthetic output in both species, shifted allocation of carbon-based resources to production and storage of NSCs. This is supported by studies that were carried out with *Pinus sylvestris* L., which exhibits increased NSC formation under water deficit conditions (Galiano et al. 2017). We observed a decrease in constitutive expression of some defense genes, which I propose to be related to decreases in newly assimilated carbon resources. In contrast, induced defenses were less affected and sometimes even increased, as they rely more heavily on stored carbon (Guérard et al. 2007). In another study on *P. sylvestris*, it was found that water deficit trees relied more on stored carbon for induced defenses than trees under well-watered conditions (Guérard et al. 2007).

Additionally, I observed a greater effect of water deficit on the defense responses of lodgepole pine relative to jack pine. Lodgepole and jack pine generally occupy regions with

contrasting moisture conditions (Cullingham et al. 2011), as lodgepole is found to more commonly occupy wetter sites while jack pine is common to sandy, well-draining soils (Yeatman 1967, Rweyongeza et al. 2007). My results, together with previous work from our lab, indicate that jack pine is more tolerant of water limiting conditions, exhibiting relatively normal function under more negative water potentials. In contrast, lodgepole pine is more affected by water deficit, shutting photosynthesis down earlier and limiting carbon resources available. I propose that these differences directly influence the rate at which stored carbon is depleted, and degree to which we would expect to see host susceptibility increase under water deficit. I have illustrated this proposed conceptual model (Figure 6.1).

In chapters two and four, I identified that in conifers, like angiosperms, JA and ET are induced following challenge by necrotrophic pathogens, but not SA. To our knowledge, my research provides the first *in planta* measurements of ET via the precursor ACC and supports other work demonstrating involvement of ethylene gene expression in conifer pathogen response (Hudgins et al. 2006, Ralph et al. 2007). Understanding the role of these hormones was critical for investigating lodgepole pine mature tree responses to MPB mass attack to ascertain the contribution of *G. clavigera* in mass attack (Chapter 4). I hypothesized that fungi (*G. clavigera*) and insects (MPB) activate different signalling pathways in their conifer hosts, eliciting different hormonal signatures following attack. The contribution of MPB Ophiostomatoid fungal associates in initial MPB mass attack success is often assumed to be meaningful, although this viewpoint is controversial (Six and Wingfield 2011). To my knowledge, my research presents the first rigorous testing of this paradigm to date. I observed that while ET is involved in lodgepole pine phloem and xylem responses to *G. clavigera* inoculation, *G. clavigera* signatures of ET were not a part of host responses to MPB during the

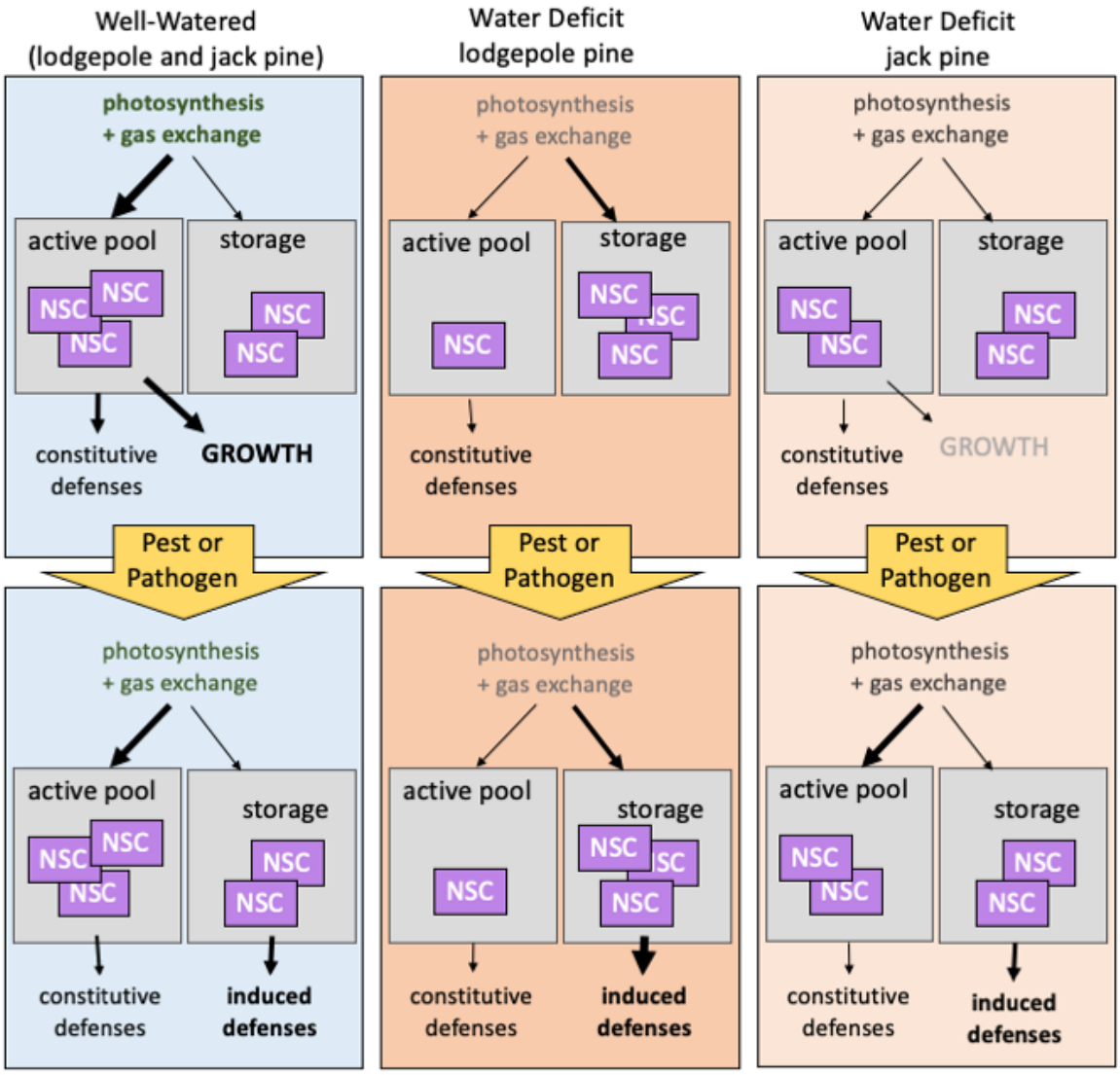

Figure 6.1. Conceptual model illustrating the allocation of non-structural carbohydrate (NSC) resources to growth and defense processes in lodgepole and jack pine inoculated with *G. clavigera* under well-watered and water deficit conditions. Bolded text and arrows indicate a greater emphasis on different metabolic processes, grey text indicates a reduction or cessation of a specific process.

period of mass attack. These results support my original hypothesis that necrotrophic pathogens and chewing insects elicit different host hormonal responses and reveal that *G. clavigera* does not contribute to overwhelming host defenses during MPB mass attack. I propose instead that *G.*

clavigera and other Ophiostomatoid fungal associates contribute to nutrient capture from host tissues to MPB larval galleries, and that *G. clavigera's* pathogencity is related to this role.

Shifting gears to focus on structural defenses, in Chapter 5 I examined the relationship between mechanical strength of white spruce foliage and anatomical changes during needle expansion and development. Foliar toughness has been identified as a primary predictor of host suitability for SBW (Lawrence et al. 1997, Fuentealba et al. 2020). I observed that deposition of cuticle, lignin, and suberin in expanding foliage of white spruce seedlings is correlated with mechanical toughness. In contrast, wax was not well correlated with increasing toughness in expanding foliage of mature trees. This difference is explained by changes in needle anatomy with age. Similar to a study in Douglas-fir (*Pseudotsuga mensiesii* Mirb.), we observed that expanding needles of seedlings had less-defined hypodermal cells than mature trees (Apple et al. 2002). The hypodermal layer, and to some extent the endodermal layer, was a prominent feature of mature needle anatomy during development, even before lignification was apparent. These findings support my original hypothesis that lignin is a reliable marker of toughness during needle development in both seedlings and mature white spruce. Additionally, I propose that suberin and lignin – specifically deposition in the hypodermis and endodermis – are the primary contributors to foliar toughness in developing white spruce needles and play a role in defining the phenological window of opportunity and host suitability to SBW. My research did not support my original hypothesis that cuticle deposition is also a reliable marker of toughness. Although it does appear to contribute to some extent to toughness of developing needles in seedlings, the contribution of cuticular wax decreases with age (Figure 6.2). In mature trees, I propose that cuticular wax plays an important role as an interface for host-insect interactions, with minor contributions to toughness (Figure 6.2). I observed that monoterpene levels decreased

as needle toughness increased, and I propose that these monoterpenes contribute to host defense early in bud burst before toughness is sufficient to deter feeding.

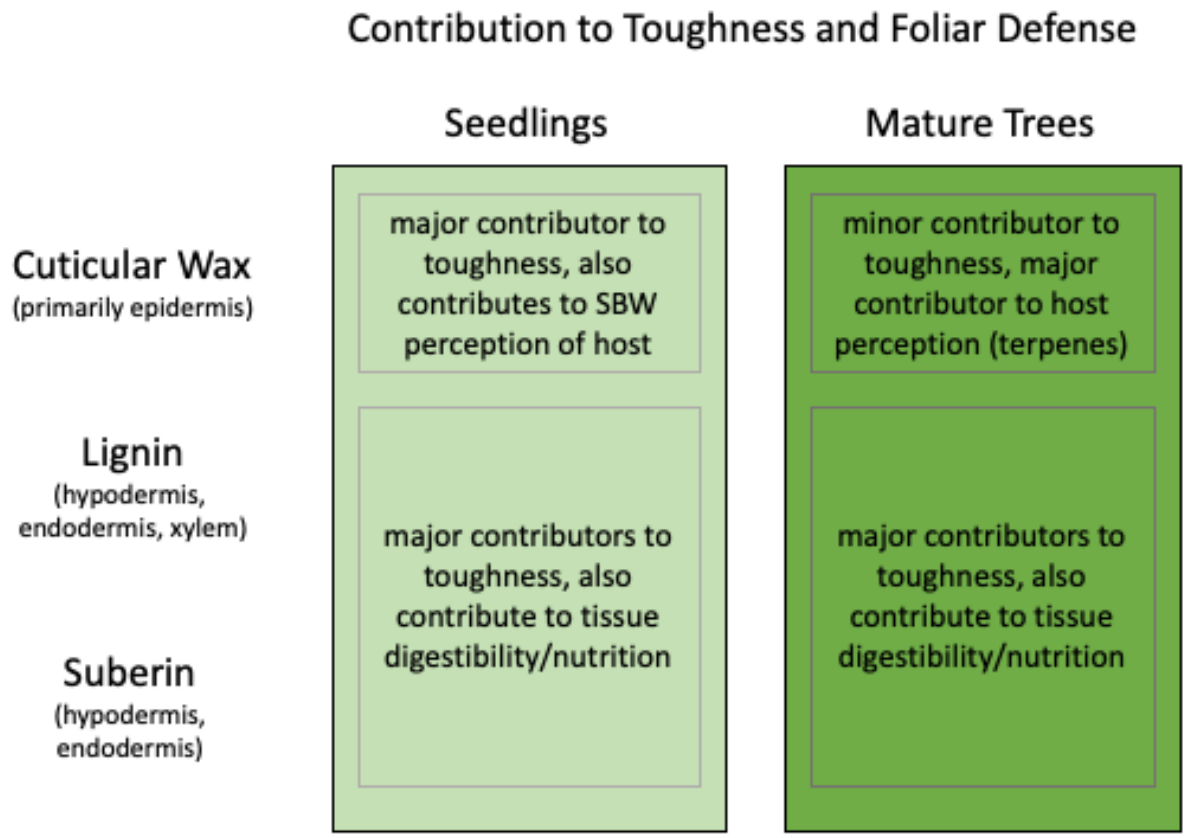

Figure 6.2. The relative contributions of traits to foliar toughness and defense during needle development in white spruce during bud burst.

6.1 Future Directions

My research has revealed that phenolics play a prominent role in pine defenses against *G. clavigera*, and to some extent MPB, yet are relatively understudied in this system compared to terpenoids. The stilbenes pinosylvin and pinosylvin monomethyl ether (PMME) are a component of Scots pine (*Pinus sylvestris* L.) induced defenses to the fungal pathogens *Heterobasidion annosum* (Fr.) Bref. s.l. (Kovalchuk et al. 2017) and *Ophiostoma ips* (Rumb.) Nannf (Croisé and Lieutier 1998). Similarly, in Norway spruce (*Picea abies* (L.) Karst), stilbene and flavanol biosynthesis are activated by the fungus *Endoconidiophora polonica* (formerly known as

Ceratocystis polonica (Siem.) C. Moreau, Hammerbacher et al. 2011, 2014, 2019), however, some strains of *E. polonica*, as well as the fungi *Grosmannia pencillata* (Grosmann) Goid. and *Grosmannai europhioides* have evolved mechanisms for metabolism of several spruce stilbenes (Hammerbacher et al. 2013, Wadke et al. 2016, Zhao et al. 2019). Additionally, while phenolics were less obviously involved in host defenses against MPB, their induction in phloem overlaps with MPB feeding. Some phenolics have been shown to influence feeding behavior in the bark beetle *Ips typographus* L. (Coleoptera: Curculionidae, Faccoli and Schlyter 2007, Zhao et al. 2019). More work needs to conducted examining the effects of phenolic compounds on *G. clavigera* and MPB so that we can make more informed conclusions regarding how these compounds influence host susceptibility. I also discovered several unknown phenolic compounds as being significant predictors of metabolite profiles of *G. clavigera*-inoculated or MPB-attacked trees. More work is needed to fully identify these compounds so that we can better understand their role in defense.

Research restrictions due to COVID had a significant impact on my research objectives, particularly my research looking at foliar traits during white spruce bud burst (Chapter 5). As a result, I was unable to finish work more accurately quantifying the deposition of lignin and suberin in developing needles. Additionally, our sampling period of mature white spruce was shortened, and did not include critical early stages of bud burst. To complete this research, re-sampling of mature white spruce during the entire period of bud burst is warranted to capture traits contributing to the early limit to the phenological window of opportunity. Semi-quantitative staining of lignin and suberin deposition in fixed sections of developing needles would also provide measures to better assess the relative contributions of each compound to foliar toughness.

6.2 Concluding Remarks

Under predicted climate change scenarios, forests are set to face an increase in insect outbreaks, while increased temperatures are also expected to trigger changes to host phenology and water availability (Pureswaran et al. 2015, Anderegg et al. 2015). My research has contributed meaningful knowledge to our collective understanding about how conifers, and forest trees in general, respond to biotic threats. Additionally, my work has shed light on the important influence of abiotic stress and host phenology on the presentation of host defense strategies. Altogether, my thesis research has furthered our understanding of the dynamics of host defenses and is an important piece of the puzzle for predicting host suitability and promoting long term forest health in a changing climate.

References

Adams AS, Six DL (2007) Temporal variation in mycophagy and prevalence of fungi associated with developmental stages of *Dendroctonus ponderosae* (Coleoptera: Curculionidae). Environmental Entomology 36:64–72.

Addison A, Powell JA, Bentz BJ, Six DL (2015) Integrating models to investigate critical phenological overlaps in complex ecological interactions: the mountain pine beetle-fungus symbiosis. Journal of Theoretical Biology 368:55–66.

Aerts N, Pereira Mendes M, Van Wees SCM (2021) Multiple levels of crosstalk in hormone networks regulating plant defense. The Plant Journal 105:489–504.

Almagro L, Gómez Ros LV, Belchi-Navarro S, Bru R, Ros Barceló A, Pedreño MA (2009) Class III peroxidases in plant defence reactions. Journal of Experimental Botany 60:377–390.

Anderegg WRL, Hicke JA, Fisher RA, Allen CD, Aukema J, Bentz B, Hood S, Lichstein JW, Macalady AK, McDowell N, Pan Y, Raffa K, Sala A, Shaw JD, Stephenson NL, Tague C, Zeppel M (2015) Tree mortality from drought, insects, and their interactions in a changing climate. New Phytologist 208:674–683.

Andersen CL, Jensen JL, Ørntoft TF (2004) Normalization of real-time quantitative reverse transcription-PCR data: a model-based variance estimation approach to identify genes suited for normalization, applied to bladder and colon cancer data sets. Cancer Research 64:5245–5250.

Aphalo PJ (2021) ggpmisc: miscellaneous extensions to 'ggplot2'. R package version 0.4.3.

Appel HM (1993) Phenolics in ecological interactions: The importance of oxidation. Journal of Chemical Ecology 19:1521–1552.

Apple M, Tiekotter K, Snow M, Young J, Soeldner A, Phillips D, Tingey D, Bond BJ (2002) Needle anatomy changes with increasing tree age in Douglas-fir. Tree Physiology 22:129–136.

Arango-Velez A, El Kayal W, Copeland CCJ, Zaharia LI, Lusebrink I, Cooke JEK (2016) Differences in defence responses of *Pinus contorta* and *Pinus banksiana* to the mountain pine beetle fungal associate *Grosmannia clavigera* are affected by water deficit. Plant, Cell and Environment 39:726–744.

Arango-Velez A, Gonzalez LMG, Meents MJ, El Kayal W, Cooke BJ, Linsky J, Lusebrink I, Cooke JEK (2014) Influence of water deficit on the molecular responses of *Pinus*

contorta x *Pinus banksiana* mature trees to infection by the mountain pine beetle fungal associate, *Grosmannia clavigera*. Tree Physiology 34:1220–1239.

Arango-Velez A, Zwiazek JJ, Thomas BR, Tyree MT (2011) Stomatal factors and vulnerability of stem xylem to cavitation in poplars. Physiologia Plantarum 143:154–165.

Arnerup J, Lind M, Olson A, Stenlid J, Elfstrand M (2011) The pathogenic white-rot fungus *Heterobasidion parviporum* triggers non-specific defence responses in the bark of Norway spruce. Tree Physiology 31:1262–1272.

Arnerup J, Nemesio-Gorriz M, Lundén K, Asiegbu FO, Stenlid J, Elfstrand M (2013) The primary module in Norway spruce defence signalling against *H. annosum* s.l. seems to be jasmonate-mediated signalling without antagonism of salicylate-mediated signalling. Planta 237:1037–1045.

Ayres MP, Wilkens RT, Ruel JJ, Lombardero MJ, Vallery E (2000) Nitrogen budgets of phloem-feeding bark beetles with and without symbiotic fungi. Ecology 81:2198–2210.

Bailey JD, Harrington CA (2006) Temperature regulation of bud-burst phenology within and among years in a young Douglas-fir (*Pseudotsuga menziesii*) plantation in western Washington, USA. Tree Physiology 26:421–430.

Balint-Kurti P (2019) The plant hypersensitive response: concepts, control and consequences. Molecular Plant Pathology:mpp.12821.

Ballard RG (1982) The pathogenicity of blue-stain fungi on lodgepole pines attacked by mountain pine beetle

Ballard RG, Walsh MA, Cole WE (1982) Blue-stain fungi in xylem of lodgepole pine: a light-microscope study on extent of hyphal distribution. Canadian Journal of Botany 60:2334–2341.

Ballard RG, Walsh MA, Cole WE (1984) The penetration and growth of blue-stain fungi in the sapwood of lodgepole pine attacked by mountain pine beetle. Canadian Journal of Botany 62:1724–1729.

Barbehenn RV, Constabel CP (2011) Tannins in plant–herbivore interactions. Phytochemistry 72:1551–1565.

Barbehenn RV, Maben RE, Knoester JJ (2008) Linking phenolic oxidation in the midgut lumen with oxidative stress in the midgut tissues of a tree-feeding caterpillar *Malacosoma disstria* (Lepidoptera: Lasiocampidae). Environmental Entomology 37:7.

Barnes JR, Lorenz WW, Dean JFD (2008) Characterization of a 1-aminocyclopropane-1-carboxylate synthase gene from loblolly pine (*Pinus taeda* L.). Gene 413:18–31.

Bates D, Mächler M, Bolker B, Walker S (2015) Fitting linear mixed-effects models using **lme4**. Journal of Statistical Software 67

Beaulieu J, Laurentian Forestry Centre, Canadian Forest Service - Quebec (1996) Breeding program and strategy for white spruce in Quebec. Canadian Forest Service, Quebec Region, Sainte Foy, Quebec.

Beck MW (2020) ggord: ordination plots with ggplot2. R package version 1.1.5.

Bellemin-Noël B, Bourassa S, Despland E, De Grandpré L, Pureswaran DS (2021) Improved performance of the eastern spruce budworm on black spruce as warming temperatures disrupt phenological defences. Global Change Biology 27:3358–3366.

Benjamini Y, Hochberg Y (1995) Controlling the false discovery rate: a practical and powerful approach to multiple testing. Journal of the Royal Statistical Society: Series B (Methodological) 57:289–300.

Bentz BJ, Six DL (2006) Ergosterol content of fungi associated with *Dendroctonus ponderosae* and *Dendroctonus rufipennis* (Coleoptera: Curculionidae, Scolytinae). Annals of the Entomological Society of America 99:189–194.

Berardini TZ, Reiser L, Li D, Mezheritsky Y, Muller R, Strait E, Huala E (2015) The Arabidopsis Information Resource: making and mining the "gold standard" annotated reference plant genome. genesis 53:474–485.

Berguet C, Martin M, Arseneault D, Morin H (2021) Spatiotemporal dynamics of 20th-century spruce budworm outbreaks in eastern Canada: three distinct patterns of outbreak severity. Frontiers in Ecology and Evolution 8:544088.

Bernards M (2002) Demystifying suberin. Canadian Journal of Botany 80:227–240.

Berryman AA (1982) Mountain pine beetle outbreaks in rocky mountain lodgepole pine forests. Journal of Forestry 80:5.

Bhuiyan NH, Selvaraj G, Wei Y, King J (2009) Gene expression profiling and silencing reveal that monolignol biosynthesis plays a critical role in penetration defence in wheat against powdery mildew invasion. Journal of Experimental Botany 60:509–521.

Biedermann PHW, Müller J, Grégoire J-C, Gruppe A, Hagge J, Hammerbacher A, Hofstetter RW, Kandasamy D, Kolarik M, Kostovcik M, Krokene P, Sallé A, Six DL, Turrini T,

Vanderpool D, Wingfield MJ, Bässler C (2019) Bark beetle population dynamics in the anthropocene: challenges and solutions. Trends in Ecology & Evolution 34:914–924.

Bleiker KP, Potter SE, Lauzon CR, Six DL (2009) Transport of fungal symbionts by mountain pine beetles. The Canadian Entomologist 141:503–514.

Bleiker KP, Six DL (2007) Dietary benefits of fungal associates to an eruptive herbivore: potential implications of multiple associates on host population dynamics. Environmental Entomology:1384–1396.

Bonello P, Gordon TR, Herms DA, Wood DL, Erbilgin N (2006) Nature and ecological implications of pathogen-induced systemic resistance in conifers: A novel hypothesis. Physiological and Molecular Plant Pathology 68:95–104.

Boone CK, Aukema BH, Bohlmann J, Carroll AL, Raffa KF (2011) Efficacy of tree defense physiology varies with bark beetle population density: a basis for positive feedback in eruptive species. Canadian Journal of Forest Research 41:1174–1188.

Borden JH, Pureswaran DS, Lafontaine JP (2008) Synergistic blends of monoterpenes for aggregation pheromones of the mountain pine beetle (Coleoptera: Curculionidae). Journal of Economic Entomology 101:10.

Bouchard M, Kneeshaw D, Bergeron Y (2006) Forest dynamics after sucessive spruce budworm outbreaks in mixed wood forests. Ecology 87:2319–2329.

Bouchard M, Régnière J, Therrien P (2018) Bottom-up factors contribute to large-scale synchrony in spruce budworm populations. Canadian Journal of Forest Research 48:277–284.

Boulanger Y, Arseneault D (2004) Spruce budworm outbreaks in eastern Quebec over the last 450 years. Canadian Journal of Forest Research 34:9.

Breshears DD, Myers OB, Meyer CW, Barnes FJ, Zou CB, Allen CD, McDowell NG, Pockman WT (2009) Tree die-off in response to global change-type drought: mortality insights from a decade of plant water potential measurements. Frontiers in Ecology and the Environment 7:185–189.

Broekgaarden C, Caarls L, Vos IA, Pieterse CMJ, Van Wees SCM (2015) Ethylene: traffic controller on hormonal crossroads to defense. Plant Physiology:pp.01020.2015.

Bulens I, de Poel BV, Hertog ML, Proft MPD, Geeraerd AH, Nicolaï BM (2011) Protocol: an updated integrated methodology for analysis of metabolites and enzyme activities of ethylene biosynthesis. :10.

Burke JL, Carroll AL (2016) The influence of variation in host tree monoterpene composition on secondary attraction by an invasive bark beetle: Implications for range expansion and potential host shift by the mountain pine beetle. Forest Ecology and Management 359:59–64.

Burns I, James PMA, Coltman DW, Cullingham CI (2019) Spatial and genetic structure of the lodgepole × jack pine hybrid zone. Canadian Journal of Forest Research 49:844–853.

Burow M, Halkier BA (2017) How does a plant orchestrate defense in time and space? Using glucosinolates in Arabidopsis as case study. Current Opinion in Plant Biology 38:142–147.

Cale JA, Muskens M, Najar A, Ishangulyyeva G, Hussain A, Kanekar SS, Klutsch JG, Taft S, Erbilgin N (2017) Rapid monoterpene induction promotes the susceptibility of a novel host pine to mountain pine beetle colonization but not to beetle-vectored fungi. Tree Physiology 37:1597–1610.

Camacho C, Coulouris G, Avagyan V, Ma N, Papadopoulos J, Bealer K, Madden TL (2009) BLAST+: architecture and applications. BMC Bioinformatics 10:421.

Campbell RK, Sugano AI (1979) Genecology of bud-burst phenology in Douglas-fir: response to flushing temperature and chilling. Botanical Gazette 140:223–231.

Cardinal E, Shepherd B, Krakowski J, Schwarz CJ, Stirrett-Wood J (2022) Verbenone and green-leaf volatiles reduce whitebark pine mortality in a northern range-expanding mountain pine beetle outbreak. Canadian Journal of Forest Research 52:158–168.

Carmona D, Lajeunesse MJ, Johnson MTJ (2011) Plant traits that predict resistance to herbivores: traits that predict resistance to herbivores. Functional Ecology 25:358–367.

Celedon JM, Bohlmann J (2019) Oleoresin defenses in conifers: chemical diversity, terpene synthases and limitations of oleoresin defense under climate change. New Phytologist 224:1444–1463.

Cerezke HF, Dhir NK, Barnhardt LK, Alberta, Alberta Environment and Sustainable Resource Development (2014) Review of insect and disease challenges to Alberta coniferous forests in relation to resistance breeding and climate change.

Chauvaux N, Van Dongen W, Esmans EL, Van Onckelen HA (1997) Quantitative analysis of 1-aminocyclopropane-1-carboxylic acid by liquid chromatography coupled to electrospray tandem mass spectrometry. Journal of Chromatography A 775:143–150.

Chezem WR, Memon A, Li F-S, Weng J-K, Clay NK (2017) SG2-type R2R3-MYB transcription factor MYB15 controls defense-induced lignification and basal immunity in Arabidopsis. The Plant Cell 29:1907–1926.

Chiu CC, Bohlmann J (2022) Mountain pine beetle epidemic: an interplay of terpenoids in host defense and insect pheromones. Annual Review of Plant Biology 73. https://www.annualreviews.org/doi/10.1146/annurev-arplant-070921-103617 (21 March 2022, date last accessed).

Chiu CC, Keeling CI, Bohlmann J (2017) Toxicity of pine monoterpenes to mountain pine beetle. Scientific Reports 7:8858.

Chiu CC, Keeling CI, Bohlmann J (2019) The cytochrome P450 CYP6DE1 catalyzes the conversion of α-pinene into the mountain pine beetle aggregation pheromone *trans*-verbenol. Scientific Reports 9:1477.

Choi HW, Klessig DF (2016) DAMPs, MAMPs, and NAMPs in plant innate immunity. BMC Plant Biology 16:232.

Clark EL, Pitt C, Carroll AL, Lindgren BS, Huber DPW (2014) Comparison of lodgepole and jack pine resin chemistry: implications for range expansion by the mountain pine beetle, *Dendroctonus ponderosae* (Coleoptera: Curculionidae). PeerJ 2:e240.

Clarke KR (1993) Non-parametric multivariate analyses of changes in community structure. Austral Ecology 18:117–143.

Clemens B (1865) North American micro-Lepidoptera. Proceedings of the Entomological Society of Philadelphia 5

Cook SP, Shirley BM, Zambino PJ (2010) Nitrogen concentration in mountain pine beetle larvae reflects nitrogen status of the tree host and two fungal associates. Environmental Entomology 39:821–826.

Critchfield WB (1985) The late Quaternary history of lodgepole and jack pines. Canadian Journal of Forest Research 15:749–772.

Croisé L, Lieutier F (1993) Effects of drought on the induced defence reaction of Scots pine to bark beetle-associated fungi. Annales des Sciences Forestières 50:91–97.

Croisé L, Lieutier F (1998) Effects of drought stress and severe pruning on the reaction zone induced by single inoculations with a bark beetle associated fungus (*Ophiostoma ips*) in the phloem of young Scots pines. Canadian Journal of Forest Research 28:11.

Cullingham CI, Cooke JEK, Dang S, Davis CS, Cooke BJ, Coltman DW (2011) Mountain pine beetle host-range expansion threatens the boreal forest. Molecular Ecology 20:2157–2171.

Cullingham CI, James PMA, Cooke JEK, Coltman DW (2012) Characterizing the physical and genetic structure of the lodgepole pine × jack pine hybrid zone: mosaic structure and differential introgression. Evolutionary Applications 5:879–891.

Dalio RJD, Magalhães DM, Rodrigues CM, Arena GD, Oliveira TS, Souza-Neto RR, Picchi SC, Martins PMM, Santos PJC, Maximo HJ, Pacheco IS, De Souza AA, Machado MA (2017) PAMPs, PRRs, effectors and R-genes associated with citrus–pathogen interactions. Annals of Botany:mcw238.

Daoust SP, Mader BJ, Bauce E, Despland E, Dussutour A, Albert PJ (2010) Influence of epicuticular-wax composition on the feeding pattern of a phytophagous insect: implications for host resistance. The Canadian Entomologist 142:261–270.

Davis TS (2020) Toxicity of two Engelmann spruce (Pinaceae) monoterpene chemotypes from the southern Rocky Mountains to North American spruce beetle (Coleoptera: Scolytidae). The Canadian Entomologist 152:790–796.

Davis JM, Wu H, Cooke JEK, Reed JM, Luce KS, Michler CH (2002) Pathogen challenge, salicylic acid, and jasmonic acid regulate expression of chitinase gene homologs in pine. Molecular Plant-Microbe Interactions 15:380–387.

De Micco V, Balzano A, Wheeler EA, Baas P (2016) Tyloses and gums: a review of structure, function and occurrence of vessel occlusions. IAWA Journal 37:186–205.

DeLucia EH, Berlyn GP (1984) The effect of increasing elevation on leaf cuticle thickness and cuticular transpiration in balsam fir. Canadian Journal of Botany 62:2423–2431.

Delvas N, Bauce É, Labbé C, Ollevier T, Bélanger R (2011) Phenolic compounds that confer resistance to spruce budworm: White spruce phenolics affect spruce budworm. Entomologia Experimentalis et Applicata 141:35–44.

DeRose RJ, Bekker MF, Long JN (2017) Traumatic resin ducts as indicators of bark beetle outbreaks. Canadian Journal of Forest Research 47:1168–1174.

Despland E (2018) Effects of phenological synchronization on caterpillar early-instar survival under a changing climate. Canadian Journal of Forest Research 48:247–254.

Despland E, Bourdier T, Dion E, Bauce E (2016) Do white spruce epicuticular wax monoterpenes follow foliar patterns? Canadian Journal of Forest Research 46:1051–1058.

Desprez-Loustau M-L, Marçais B, Nageleisen L-M, Piou D, Vannini A (2006) Interactive effects of drought and pathogens in forest trees. Annals of Forest Science 63:597–612.

Dhont C, Canada, Natural Resources Canada (2010) Field guide for identifying apical bud break and bud formation stages in white spruce. Natural Resources Canada, Canadian Forest Service, Laurentian Forestry Centre, Sainte-Foy, Quebec.

DiGuistini S, Wang Y, Liao NY, Taylor G, Tanguay P, Feau N, Henrissat B, Chan SK, Hesse-Orce U, Alamouti SM, Tsui CKM, Docking RT, Levasseur A, Haridas S, Robertson G, Birol I, Holt RA, Marra MA, Hamelin RC, Hirst M, Jones SJM, Bohlmann J, Breuil C (2011) Genome and transcriptome analyses of the mountain pine beetle-fungal symbiont *Grosmannia clavigera*, a lodgepole pine pathogen. Proceedings of the National Academy of Sciences 108:2504–2509.

Dolgikh VA, Pukhovaya EM, Zemlyanskaya EV (2019) Shaping ethylene response: the role of EIN3/EIL1 transcription factors. Frontiers in Plant Science 10:1030.

Domınguez E, Heredia-Guerrero JA (2010) The biophysical design of plant cuticles: an overview. New Phytologist:12.

Duchesne I, Zhang SY (2004) Variation in tree growth, wood density, and pulp fiber properties of 35 white spruce (*Picea glauca* (Moench) Voss) families grown in Quebec. Wood and Fiber Science 36:9.

Dusenge ME, Madhavji S, Way DA (2020) Contrasting acclimation responses to elevated CO_2 and warming between an evergreen and a deciduous boreal conifer. Global Change Biology 26:3639–3657.

Eckert AJ, Hall BD (2006) Phylogeny, historical biogeography, and patterns of diversification for *Pinus* (Pinaceae): Phylogenetic tests of fossil-based hypotheses. Molecular Phylogenetics and Evolution 40:166–182.

El Kayal W, Allen CCG, Ju CJ-T, Adams E, King-Jones S, Zaharia LI, Abrams SR, Cooke JEK (2011) Molecular events of apical bud formation in white spruce, *Picea glauca*: Bud formation in white spruce. Plant, Cell & Environment 34:480–500.

Ennis D, Despland E, Chen F, Forgione P, Bauce E (2017) Spruce budworm feeding and oviposition are stimulated by monoterpenes in white spruce epicuticular waxes: Monoterpenes in wax stimulate budworm. Insect Science 24:73–80.

Evensen PC, Solheim H, Høiland K, Stenersen J (2000) Induced resistance of Norway spruce, variation of phenolic compounds and their effects on fungal pathogens. Forest Pathology 30:97–108.

Faccoli M, Schlyter F (2007) Conifer phenolic resistance markers are bark beetle antifeedant semiochemicals. Agricultural and Forest Entomology 9:237–245.

Faiola CL, Buchholz A, Kari E, Yli-Pirilä P, Holopainen JK, Kivimäenpää M, Miettinen P, Worsnop DR, Lehtinen KEJ, Guenther AB, Virtanen A (2018) Terpene composition complexity controls secondary organic aerosol yields from Scots pine volatile emissions. Scientific Reports 8:3053.

Falk J, Munné-Bosch S (2010) Tocochromanol functions in plants: antioxidation and beyond. Journal of Experimental Botany 61:1549–1566.

Feeny P (1976) Plant apparency and chemical defense. In: Wallace JW, Mansell RL (eds) Biochemical Interaction Between Plants and Insects. Springer US, Boston, MA, pp 1–40.

Fossdal CG, Nagy NE, Hietala AM, Kvaalen H, Slimestad R, Woodward S, Solheim H (2012) Indications of heightened constitutive or primed host response affecting the lignin pathway transcripts and phenolics in mature Norway spruce clones. Tree Physiology 32:1137–1147.

Fox J, Weisberg S (2019) An R companion to applied regression, 3rd edn. Sage, Thousand Oaks, CA.

Franceschi VR, Krekling T, Berryman AA, Christiansen E (1998) Specialized phloem parenchyma cells in Norway spruce (Pinaceae) bark are an important site of defense reactions. Am J Bot 85:601–615.

Franceschi VR, Krekling T, Christiansen E (2002) Application of methyl jasmonate on *Picea abies* (Pinaceae) stems induces defense-related responses in phloem and xylem. American Journal of Botany 89:578–586.

Franceschi VR, Krokene P, Christiansen E, Krekling T (2005) Anatomical and chemical defenses of conifer bark against bark beetles and other pests: Tansley review. New Phytologist 167:353–376.

Franceschi VR, Krokene P, Krekling T, Christiansen E (2000) Phloem parenchyma cells are involved in local and distant defense responses to fungal inoculation or bark-beetle attack in Norway spruce (Pinaceae). Am J Bot 87:314–326.

Fuentealba A, Bauce É (2012) Carry-over effect of host nutritional quality on performance of spruce budworm progeny. Bulletin of Entomological Research 102:275–284.

Fuentealba A, Bauce É (2016) Interspecific variation in resistance of two host tree species to spruce budworm. Acta Oecologica 70:10–20.

Fuentealba A, Pureswaran D, Bauce É, Despland E (2017) How does synchrony with host plant affect the performance of an outbreaking insect defoliator? Oecologia 184:847–857.

Fuentealba A, Sagne S, Legendre G, Pureswaran D, Bauce É, Despland E (2020) Leaf toughness as a mechanism of defence against spruce budworm. Arthropod-Plant Interactions 14:481–489.

Fuentealba A, Sagne S, Pureswaran D, Bauce É, Despland E (2018) Defining the window of opportunity for feeding initiation by second-instar spruce budworm larvae. Canadian Journal of Forest Research 48:285–291.

Furniss M, Schenk J (1969) Sustained natural infestation by the mountain pine beetle in seven new *Pinus* and *Picea* hosts. Journal of Economic Entomology 62:518–519.

Galiano L, Timofeeva G, Saurer M, Siegwolf R, Martínez-Vilalta J, Hommel R, Gessler A (2017) The fate of recently fixed carbon after drought release: towards unravelling C storage regulation in *Tilia platyphyllos* and *Pinus sylvestris*. Plant, Cell & Environment 40:1711–1724.

Galindo González LM, El Kayal W, Ju CJ-T, Allen CCG, King-Jones S, Cooke JEK (2012) Integrated transcriptomic and proteomic profiling of white spruce stems during the transition from active growth to dormancy. Plant, Cell & Environment 35:682–701.

Galka PW, Ambrose SJ, Ross ARS, Abrams SR (2005) Syntheses of deuterated jasmonates for mass spectrometry and metabolism studies. J Label Compd Radiopharm 48:797–809.

Garcia A, Santamaria ME, Diaz I, Martinez M (2021) Disentangling transcriptional responses in plant defense against arthropod herbivores. Scientific Reports 11:12996.

Gentleman R, Carey V, Huber W, Irizarry R, Dudoit S (eds) (2005) Bioinformatics and computational biology solutions using R and Bioconductor. Springer Science+Business Media, New York.

Ghimire RP, Kasurinen A, Häikiö E, Holopainen JK, Julkunen-Tiitto R, Holopainen T, Kivimäenpää M (2019) Combined effects of elevated ozone, temperature, and nitrogen on stem phenolic concentrations of Scots pine (*Pinus sylvestris*) seedlings. Canadian Journal of Forest Research 49:246–255.

Glazebrook J (2005) Contrasting mechanisms of defense against biotrophic and necrotrophic pathogens. Annual Review of Phytopathology 43:205–227.

Gong B-Q, Wang F-Z, Li J-F (2020) Hide-and-seek: chitin-triggered plant immunity and fungal counterstrategies. Trends in Plant Science 25:805–816.

González LMG, El Kayal W, Morris JS, Cooke JEK (2015) Diverse chitinases are invoked during the activity-dormancy transition in spruce. Tree Genetics & Genomes 11:41.

Goodsman DW, Erbilgin N, Lieffers VJ (2012) The impact of phloem nutrients on overwintering mountain pine beetles and their fungal symbionts. Environmental Entomology 41:478–486.

Gorb EV, Gorb SN (2017) Anti-adhesive effects of plant wax coverage on insect attachment. Journal of Experimental Botany 68:5323–5337.

Gordon DC, Percy KE, Riding RT (1998) Effects of u.v.-B radiation on epicuticular wax production and chemical composition of four *Picea* species. New Phytologist 138:441–449.

Graça J (2015) Suberin: the biopolyester at the frontier of plants. Frontiers in Chemistry 3

Gray DR (2008) The relationship between climate and outbreak characteristics of the spruce budworm in eastern Canada. Climatic Change 87:361–383.

Grover A (2012) Plant chitinases: genetic diversity and physiological roles. Critical Reviews in Plant Sciences 31:57–73.

Gruber A, Strobl S, Veit B, Oberhuber W (2010) Impact of drought on the temporal dynamics of wood formation in *Pinus sylvestris*. Tree Physiology 30:490–501.

Guérard N, Maillard P, Bréchet C, Lieutier F, Dreyer E (2007) Do trees use reserve or newly assimilated carbon for their defense reactions? A 13C labeling approach with young Scots pines inoculated with a bark-beetle-associated fungus (*Ophiostoma brunneo ciliatum*). Annals of Forest Science 64:601–608.

Günthardt-Goerg MS (1987) Epicuticular wax formation on needles of *Picea Abies* and *Pinus Cembra*. In: The Metabolism, Structure, and Function of Plant Lipids. Springer, Boston, MA, p 3.

Hakim, Ullah A, Hussain A, Shaban M, Khan AH, Alariqi M, Gul S, Jun Z, Lin S, Li J, Jin S, Munis MFH (2018) Osmotin: a plant defense tool against biotic and abiotic stresses. Plant Physiology and Biochemistry 123:149–159.

Hall DE, Yuen MMS, Jancsik S, Quesada A, Dullat HK, Li M, Henderson H, Arango-Velez A, Liao NY, Docking RT, Chan SK, Cooke JE, Breuil C, Jones SJ, Keeling CI, Bohlmann J (2013) Transcriptome resources and functional characterization of monoterpene synthases for two host species of the mountain pine beetle, lodgepole pine (*Pinus contorta*) and jack pine (*Pinus banksiana*). BMC Plant Biology 13:80.

Hamilton JA, De la Torre AR, Aitken SN (2015) Fine-scale environmental variation contributes to introgression in a three-species spruce hybrid complex. Tree Genetics & Genomes 11:817.

Hammerbacher A, Kandasamy D, Ullah C, Schmidt A, Wright LP, Gershenzon J (2019) Flavanone-3-hydroxylase plays an important role in the biosynthesis of spruce phenolic defenses against bark beetles and their fungal associates. Frontiers in Plant Science 10:208.

Hammerbacher A, Paetz C, Wright LP, Fischer TC, Bohlmann J, Davis AJ, Fenning TM, Gershenzon J, Schmidt A (2014) Flavan-3-ols in Norway spruce: biosynthesis, accumulation, and function in response to attack by the bark beetle-associated fungus *Ceratocystis polonica*. Plant Physiology 164:2107–2122.

Hammerbacher A, Ralph SG, Bohlmann J, Fenning TM, Gershenzon J, Schmidt A (2011) Biosynthesis of the major tetrahydroxystilbenes in spruce, astringin and isorhapontin, proceeds via resveratrol and Is enhanced by fungal infection. Plant Physiology 157:876–890.

Hammerbacher A, Schmidt A, Wadke N, Wright LP, Schneider B, Bohlmann J, Brand WA, Fenning TM, Gershenzon J, Paetz C (2013) A common fungal associate of the spruce bark beetle metabolizes the stilbene defenses of norway spruce. Plant Physiology 162:1324–1336.

Han E-N, Bauce E, Trempe-Bertrand F (2000) Development of the first-instar spruce budworm (Lepidoptera: Tortricidae). Annals of the Entomological Society of America 93:536–540.

Hanover JW, Reicosky DA (1971) Surface wax deposits on foliage of *Picea pungens* and other conifers. American Journal of Botany 58:681–687.

Harmatha J, Dinan L (2003) Biological activities of lignans and stilbenoids associated with plant-insect chemical interactions. Phytochemistry Reviews 2:321–330.

Hart JH (1981) Role of phytostilbenes in decay and disease resistance. Annual Review of Phytopathology 19:437–458.

Hart SJ, Schoennagel T, Veblen TT, Chapman TB (2015) Area burned in the western United States is unaffected by recent mountain pine beetle outbreaks. Proceedings of the National Academy of Sciences 112:4375–4380.

Hart JH, Shrimpton DM (1979) Role of stilbenes in resistance of wood to decay. Phytopathology 69:1138–1143.

Hasanuzzaman M, Nahar K, Fujita M (2014) Role of tocopherol (vitamin E) in plants. In: Emerging Technologies and Management of Crop Stress Tolerance. Elsevier, pp 267–289.

Hassegawa M, Savard M, Lenz PRN, Duchateau E, Gélinas N, Bousquet J, Achim A (2019) White spruce wood quality for lumber products: priority traits and their enhancement through tree improvement. Forestry: An International Journal of Forest Research:cpz050.

Heil M (2014) Herbivore-induced plant volatiles: targets, perception and unanswered questions. New Phytologist 204:297–306.

Hennigar CR, MacLean DA, Quiring DT, Kershaw JA (2008) Differences in spruce budworm defoliation among balsam fir and white, red, and black spruce. Forest Science 54:158–166.

Herms DA, Mattson WJ (1992) The dilemma of plants: to grow or defend. The Quarterly Review of Biology 67:283–335.

Hietala AM, Kvaalen H, Schmidt A, Jøhnk N, Solheim H, Fossdal CG (2004) Temporal and spatial profiles of chitinase expression by Norway spruce in response to rark colonization by *Heterobasidion annosum*. Applied and Environmental Microbiology 70:3948–3953.

Hodge J, Cooke B, McIntosh R (2017) A strategic approach to slow the spread of mountain pine beetle across Canada. Canadian Council of Forest Ministers:44.

Hogg EH, Michaelian M (2015) Factors affecting fall down rates of dead aspen (*Populus tremuloides*) biomass following severe drought in west-central Canada. Global Change Biology 21:1968–1979.

Honěk A (1993) Intraspecific variation in body size and fecundity in insects: a general relationship. Oikos 66:483.

Hopkins AD (1902) Insect enemies of the pine in the Black Hills forest reserve. U.S. Dept. of Agriculture, Division of Entomology, Washington, D.C. :

Hopkins RJ, van Dam NM, van Loon JJA (2009) Role of glucosinolates in insect-plant relationships and multitrophic interactions. Annual Review of Entomology 54:57–83.

Hothorn T, Bretz F, Westfall P (2008) Simultaneous inference in general parametric models. Biometrical Journal 50:346–363.

Hubbard RM, Rhoades CC, Elder K, Negron J (2013) Changes in transpiration and foliage growth in lodgepole pine trees following mountain pine beetle attack and mechanical girdling. Forest Ecology and Management 289:312–317.

Huber DPW, Aukema BH, Hodgkinson RS, Lindgren BS (2009) Successful colonization, reproduction, and new generation emergence in live interior hybrid spruce *Picea engelmannii* × *glauca* by mountain pine beetle *Dendroctonus ponderosae*. Agricultural and Forest Entomology 11:83–89.

Huber DPW, Ralph S, Bohlmann J (2004) Genomic hardwiring and phenotypic plasticity of terpenoid-based defenses in conifers. J Chem Ecol 30:2399–2418.

Hudgins JW, Franceschi VR (2004) Methyl jasmonate-induced ethylene production Is responsible for conifer phloem defense responses and reprogramming of stem cambial zone for traumatic resin duct formation. Plant Physiology 135:2134–2149.

Hudgins JW, Krekling T, Franceschi VR (2003) Distribution of calcium oxalate crystals in the secondary phloem of conifers: a constitutive defense mechanism? New Phytologist 159:677–690.

Hudgins JW, Ralph SG, Franceschi VR, Bohlmann J (2006) Ethylene in induced conifer defense: cDNA cloning, protein expression, and cellular and subcellular localization of 1-aminocyclopropane-1-carboxylate oxidase in resin duct and phenolic parenchyma cells. Planta 224:865–877.

Hwang H-S, Han JY, Choi YE (2021) Enhanced accumulation of pinosylvin stilbenes and related gene expression in *Pinus strobus* after infection of pine wood nematode Plomion C (ed). Tree Physiology 41:1972–1987.

Islam MA, Sturrock RN, Ekramoddoullah AKM (2011) Conifer Chitinases. The Americas Journal of Plant Science and Biotechnology

Jang JH, Seo HS, Lee OR (2022) Overexpression of pPLAIIIγ in Arabidopsis reduced xylem lignification of stem by regulating peroxidases. Plants 11:200.

Jetter R, Kunst L, Samuels AL (2006) Composition of plant cuticular waxes. In: Biology of the Plant Cuticle. Blackwell Publishing, p 37.

Kalyaanamoorthy S, Minh BQ, Wong TKF, von Haeseler A, Jermiin LS (2017) ModelFinder: fast model selection for accurate phylogenetic estimates. Nature Methods 14:587–589.

Kännaste A, Laanisto L, Pazouki L, Copolovici L, Suhorutšenko M, Azeem M, Toom L, Borg-Karlson A-K, Niinemets Ü (2018) Diterpenoid fingerprints in pine foliage across an environmental and chemotypic matrix: Isoabienol content is a key trait differentiating chemotypes. Phytochemistry 147:80–88.

Katoh K, Rozewicki J, Yamada KD (2019) MAFFT online service: multiple sequence alignment, interactive sequence choice and visualization. Briefings in Bioinformatics 20:1160–1166.

Keeling CI, Bohlmann J (2006a) Genes, enzymes and chemicals of terpenoid diversity in the constitutive and induced defence of conifers against insects and pathogens. New Phytologist 170:657–675.

Keeling CI, Bohlmann J (2006b) Diterpene resin acids in conifers. Phytochemistry 67:2415–2423.

Kichas NE, Trowbridge AM, Raffa KF, Malone SC, Hood SM, Everett RG, McWethy DB, Pederson GT (2021) Growth and defense characteristics of whitebark pine (*Pinus albicaulis*) and lodgepole pine (*Pinus contorta* var *latifolia*) in a high-elevation, disturbance-prone mixed-conifer forest in northwestern Montana, USA. Forest Ecology and Management 493:119286.

Klepzig KD, Six DL (2004) Bark beetle-fungal symbiosis: context dependency in complex associations. Symbiosis 37:189–205.

Klutsch JG, Shamoun SF, Erbilgin N (2017) Drought stress leads to systemic induced susceptibility to a nectrotrophic fungus associated with mountain pine beetle in *Pinus banksiana* seedlings Reinhart KO (ed). PLoS ONE 12:e0189203.

Kolb TE, Fettig CJ, Ayres MP, Bentz BJ, Hicke JA, Mathiasen R, Stewart JE, Weed AS (2016) Observed and anticipated impacts of drought on forest insects and diseases in the United States. Forest Ecology and Management 380:321–334.

Kolosova N, Bohlmann J (2012) Conifer defense against insects and fungal pathogens. In: Matyssek R, Schnyder H, Oßwald W, Ernst D, Munch JC, Pretzsch H (eds) Growth and Defence in Plants. Springer Berlin Heidelberg, Berlin, Heidelberg, pp 85–109.

Kolosova N, Breuil C, Bohlmann J (2014) Cloning and characterization of chitinases from interior spruce and lodgepole pine. Phytochemistry 101:32–39.

Kopaczyk JM, Warguła J, Jelonek T (2020) The variability of terpenes in conifers under developmental and environmental stimuli. Environmental and Experimental Botany 180:104197.

Koricheva J, Larsson S, Haukioja E (1998) Insect performance on experimentally stressed woody plants: a meta-analysis. Annual Review of Entomology 43:195–216.

Kovalchuk A, Raffaello T, Jaber E, Keriö S, Ghimire R, Lorenz WW, Dean JF, Holopainen JK, Asiegbu FO (2015) Activation of defence pathways in Scots pine bark after feeding by pine weevil (*Hylobius abietis*). BMC Genomics 16:352.

Kovalchuk A, Zhu L, Keriö S, Asiegbu FO (2017) Differential responses of Scots pine stilbene synthase and chalcone synthase genes to *Heterobasidion annosum* infection Klopfenstein NB (ed). Forest Pathology 47:e12348.

Krokene P (2015) Conifer defense and resistance to bark beetles. In: Bark Beetles. Elsevier, pp 177–207.

Krokene P, Lahr E, Dalen LS, Skrøppa T, Solheim H (2012) Effect of phenology on susceptibility of Norway spruce (*Picea abies*) to fungal pathogens: Effect of tree phenology on susceptibility to pathogens. Plant Pathology 61:57–62.

Krokene P, Nagy NE, Krekling T (2008) Traumatic resin ducts and polyphenolic parenchyma cells in conifers. In: Schaller A (ed) Induced Plant Resistance to Herbivory. Springer Netherlands, Dordrecht, pp 147–169.

Krokene P, Nagy NE, Solheim H (2008) Methyl jasmonate and oxalic acid treatment of Norway spruce: anatomically based defense responses and increased resistance against fungal infection. Tree Physiology 28:29–35.

Kroner Y, Way DA (2016) Carbon fluxes acclimate more strongly to elevated growth temperatures than to elevated CO_2 concentrations in a northern conifer. Global Change Biology 22:2913–2928.

Kundu P, Vadassery J (2021) Role of WRKY transcription factors in plant defense against lepidopteran insect herbivores: an overview. Journal of Plant Biochemistry and Biotechnology 30:698–707.

Kuusk V, Niinemets Ü, Valladares F (2018) A major trade-off between structural and photosynthetic investments operative across plant and needle ages in three Mediterranean pines. Tree Physiology 38:543–557.

Lacerda AF, Vasconcelos ÃAR, Pelegrini PB, Grossi de Sa MF (2014) Antifungal defensins and their role in plant defense. Frontiers in Microbiology 5. http://journal.frontiersin.org/article/10.3389/fmicb.2014.00116/abstract (21 March 2022, date last accessed).

Lawrence RK, Mattson WJ, Haack RA (1997) White spruce and the spruce budworm: defining the phenological window of susceptibility. The Canadian Entomologist 129:291–318.

Lee S, Kim J-J, Breuil C (2006) Diversity of fungi associated with mountain pine beetle, *Dendroctonus ponderosae*, and infested lodgepole pines in British Columbia. Natural Resources Canada, Canadian Forest Service:22.

Lee SK, Lee HJ, Min HY, Park EJ, Lee KM, Ahn YH, Cho YJ, Pyee JH (2005) Antibacterial and antifungal activity of pinosylvin, a constituent of pine. Fitoterapia 76:258–260.

Lenth R (2020) emmeans: estimated marginal means, aka least-squares means. R package version 1.5.3. https://CRAN.R-project.org/package=emmeans

Li H, Greene LH (2010) Sequence and structural analysis of the chitinase insertion domain reveals two conserved motifs involved in chitin-binding Yang H (ed). PLoS ONE 5:e8654.

Li S-H, Nagy NE, Hammerbacher A, Krokene P, Niu X-M, Gershenzon J, Schneider B (2012) Localization of phenolics in phloem parenchyma cells of norway spruce (*Picea abies*). ChemBioChem 13:2707–2713.

Lieutier F, Yart A, Salle A (2009) Stimulation of tree defenses by Ophiostomatoid fungi can explain attack success of bark beetles on conifers. Annals of Forest Science 66:801–801.

Lin L-Z, Harnly JM (2012) LC-PDA-ESI/MS identification of the phenolic components of three compositae spices: chamomile, tarragon, and mexican arnica. Natural Product Communications 7:1934578X1200700.

Lippert D, Chowrira S, Ralph SG, Zhuang J, Aeschliman D, Ritland C, Ritland K, Bohlmann J (2007) Conifer defense against insects: proteome analysis of Sitka spruce (*Picea sitchensis*) bark induced by mechanical wounding or feeding by white pine weevils (*Pissodes strobi*). Proteomics 7:248–270.

Lirette A-O, Despland E (2021) Defensive traits during white spruce (*Picea glauca*) leaf ontogeny. Insects 12:644.

Liu M, Jaber E, Zeng Z, Kovalchuk A, Asiegbu FO (2021) Physiochemical and molecular features of the necrotic lesion in the *Heterobasidion* –Norway spruce pathosystem Mock H-P (ed). Tree Physiology 41:791–800.

Liu J-J, Sturrock R, Ekramoddoullah AKM (2010) The superfamily of thaumatin-like proteins: its origin, evolution, and expression towards biological function. Plant Cell Reports 29:419–436.

Lohse M, Nagel A, Herter T, May P, Schroda M, Zrenner R, Tohge T, Fernie AR, Stitt M, Usadel B (2014) Mercator: a fast and simple web server for genome scale functional annotation of plant sequence data. Plant, Cell & Environment 37:1250–1258.

Lombardero MJ, Ayres MP, Lorio Jr PL, Ruel JJ (2000) Environmental effects on constitutive and inducible resin defences of *Pinus taeda*. Ecology Letters 3:329–339.

Lombardero MJ, Pereira-Espinel J, Ayres MP (2013) Foliar terpene chemistry of *Pinus pinaster* and *P. radiata* responds differently to Methyl Jasmonate and feeding by larvae of the pine processionary moth. Forest Ecology and Management 310:935–943.

van Loon LC, Geraats BPJ, Linthorst HJM (2006) Ethylene as a modulator of disease resistance in plants. Trends in Plant Science 11:184–191.

van Loon LC, Rep M, Pieterse CMJ (2006) Significance of inducible defense-related proteins in infected plants. Annual Review of Phytopathology 44:135–162.

Lorenz WW, Alba R, Yu Y-S, Bordeaux JM, Simões M, Dean JF (2011) Microarray analysis and scale-free gene networks identify candidate regulators in drought-stressed roots of loblolly pine (*P. taeda* L.). BMC Genomics 12:264.

Lorenz WW, Yu Y-S, Simões M, Dean JFD (2009) Processing the loblolly pine PtGen2 cDNA microarray. Journal of Visualized Experiments:1182.

Lorio PL, Stephen FM, Paine TD (1995) Environment and ontogeny modify loblolly pine response to induced acute water deficits and bark beetle attack. Forest Ecology and Management 73:97–110.

Lotan JE, Critchfield WB (1990) *Pinus contorta* Dougl ex Loud. In: Silvics of North America. USDA Forest Service, Washinton, D.C., pp 302–315.

Lundborg L, Nordlander G, Björklund N, Nordenhem H, Borg-Karlson A-K (2016) Methyl jasmonate-induced monoterpenes in Scots pine and Norway spruce tissues affect pine weevil orientation. Journal of Chemical Ecology 42:1237–1246.

Lundborg L, Sampedro L, Borg-Karlson A-K, Zas R (2019) Effects of methyl jasmonate on the concentration of volatile terpenes in tissues of Maritime pine and Monterey pine and its relation to pine weevil feeding. Trees 33:53–62.

Lundén K, Danielsson M, Durling MB, Ihrmark K, Gorriz MN, Stenlid J, Asiegbu FO, Elfstrand M (2015) Transcriptional responses associated with virulence and defence in the interaction between *Heterobasidion annosum* s.s. and Norway spruce Papa R (ed). PLoS ONE 10:e0131182.

Lusebrink I, Erbilgin N, Evenden ML The effect of water limitation on volatile emission, tree defense response, and brood success of *Dendroctonus ponderosae* in two pine hosts, lodgepole, and jack pine. Frontiers in Ecology and Evolution 4. http://journal.frontiersin.org/article/10.3389/fevo.2016.00002 (21 March 2022, date last accessed).

Lusebrink I, Evenden ML, Blanchet FG, Cooke JEK, Erbilgin N (2011) Effect of water stress and fungal inoculation on monoterpene emission from an historical and a new pine host of the mountain pine beetle. Journal of Chemical Ecology:14.

Lütz C, Heinzmann U, Gülz P-G (1990) Surface structures and epicuticular wax composition of spruce needles after long-term treatment with ozone and acid mist. Environmental Pollution 64:313–322.

MacAllister S, Mencuccini M, Sommer U, Engel J, Hudson A, Salmon Y, Dexter KG (2019) Drought-induced mortality in Scots pine: opening the metabolic black box Plomion C (ed). Tree Physiology 39:1358–1370.

Mageroy MH, Jancsik S, Man Saint Yuen M, Fischer M, Withers SG, Paetz C, Schneider B, Mackay J, Bohlmann J (2017) A conifer UDP-sugar dependent glycosyltransferase contributes to acetophenone metabolism and defense against insects. Plant Physiology 175:641–651.

Malamy J, Hennig J, Klessig D (1992) Temperature-dependent induction of salicylic acid and its conjugates during the resistance response to tobacco mosaic virus infection. The Plant Cell 4:359–366.

Manninen AM, Utriainen J, Holopainen T, Kainulainen P (2002) Terpenoids in the wood of Scots pine and Norway spruce seedlings exposed to ozone at different nitrogen availability. Canadian Journal of Forest Research 32:2140–2145.

Marshall KE, Roe AD (2021) Surviving in a frozen forest: the physiology of eastern spruce budworm overwintering. Physiology 36:174–182.

Massad TJ, Dyer LA, Vega C. G (2012) Costs of defense and a test of the carbon-nutrient balance and growth-differentiation balance hypotheses for two co-occurring classes of plant defense Heil M (ed). PLoS ONE 7:e47554.

Mattson WJ, Haack RA, Lawrence RK, Slocum SS (1991) Considering the nutritional ecology of the spruce budworm in its management. Forest Ecology and Management 39:183–210.

Mattson W, Simmons G, Witter J (1988) Chapter 16: the spruce budworm in eastern North America. In: Dynamics of Forest Insect Populations. Springer

McAllister CH, Fortier CE, St Onge KR, Sacchi BM, Nawrot MJ, Locke T, Cooke JEK (2018) A novel application of RNase H2-dependent quantitative PCR for detection and quantification of *Grosmannia clavigera*, a mountain pine beetle fungal symbiont, in environmental samples. Tree Physiology 38:485–501.

McDowell N, Pockman WT, Allen CD, Breshears DD, Cobb N, Kolb T, Plaut J, Sperry J, West A, Williams DG, Yepez EA (2008) Mechanisms of plant survival and mortality during drought: why do some plants survive while others succumb to drought? New Phytologist 178:719–739.

Miller B, Madilao LL, Ralph S, Bohlmann J (2005) Insect-induced conifer defense. White pine weevil and methyl Jjasmonate induce traumatic resinosis, de novo formed volatile emissions, and accumulation of terpenoid synthase and putative octadecanoid pathway transcripts in Sitka spruce. Plant Physiology 137:369–382.

Miresmailli S, Isman MB (2014) Botanical insecticides inspired by plant–herbivore chemical interactions. Trends in Plant Science 19:29–35.

Mithöfer A, Boland W (2012) Plant defense against herbivores: chemical aspects. Annual Review of Plant Biology 63:431–450.

Moctezuma C, Hammerbacher A, Heil M, Gershenzon J, Méndez-Alonzo R, Oyama K (2014) Specific polyphenols and tannins are associated with defense against insect herbivores in the tropical oak *Quercus oleoides*. Journal of Chemical Ecology 40:458–467.

Moerschbacher BM, Noll U, Gorrichon L, Reisener H-J (1990) Specific inhibition of lignification breaks hypersensitive resistance of wheat to stem rust. Plant Physiology 93:465–470.

Molina I, Bonaventure G, Ohlrogge J, Pollard M (2006) The lipid polyester composition of *Arabidopsis thaliana* and *Brassica napus* seeds. Phytochemistry 67:2597–2610.

Moore ML, Six DL (2015) Effects of temperature on growth, sporulation, and competition of mountain pine beetle fungal symbionts. Microbial Ecology 70:336–347.

Moran E, Lauder J, Musser C, Stathos A, Shu M (2017) The genetics of drought tolerance in conifers. New Phytologist 216:1034–1048.

Müller C, Riederer M (2005) Plant surface properties in chemical ecology. Journal of Chemical Ecology 31:2621–2651.

Murmu J, Wilton M, Allard G, Pandeya R, Desveaux D, Singh J, Subramaniam R (2014) Arabidopsis GOLDEN2-LIKE (GLK) transcription factors activate jasmonic acid (JA)-dependent disease susceptibility to the biotrophic pathogen Hyaloperonospora arabidopsidis, as well as JA-independent plant immunity against the necrotrophic pathogen Botryti: GLK1 in plant defence. Molecular Plant Pathology 15:174–184.

Myrholm CL, Langor DW (2016) Assessment of the impact of symbiont Ophiostomatales (fungi) on mountain pine beetle (Coleoptera: Curculionidae) performance on a jack pine (Pinaceae) diet using a novel *in vitro* rearing method. The Canadian Entomologist 148:68–82.

Nagy NE, Kvaalen H, Fongen M, Fossdal CG, Clarke N, Solheim H, Hietala AM (2012) The pathogenic white-rot fungus *Heterobasidion parviporum* responds to spruce xylem defense by enhanced production of oxalic acid. MPMI 25:1450–1458.

Nagy NE, Norli HR, Fongen M, Østby RB, Heldal IM, Davik J, Hietala AM (2022) Patterns and roles of lignan and terpenoid accumulation in the reaction zone compartmentalizing pathogen-infected heartwood of Norway spruce. Planta 255:63.

Nagy NE, Sikora K, Krokene P, Hietala AM, Solheim H, Fossdal CG (2014) Using laser micro-dissection and qRT-PCR to analyze cell type-specific gene expression in Norway spruce phloem. PeerJ 2:e362.

Naseer S, Lee Y, Lapierre C, Franke R, Nawrath C, Geldner N (2012) Casparian strip diffusion barrier in *Arabidopsis* is made of a lignin polymer without suberin. Proceedings of the National Academy of Sciences 109:10101–10106.

Navarro L, Morin H, Bergeron Y, Girona MM (2018) Changes in spatiotemporal patterns of 20th century spruce budworm outbreaks in eastern Canadian Boreal forests. Frontiers in Plant Science 9:1905.

Nealis VG (2016) Comparative ecology of conifer-feeding spruce budworms (Lepidoptera: Tortricidae). The Canadian Entomologist 148:S33–S57.

Nealis VG, Nault JR (2005) Seasonal changes in foliar terpenes indicate suitability Of Douglas-fir buds for western spruce budworm. Journal of Chemical Ecology 31:683–696.

Netherer S, Matthews B, Katzensteiner K, Blackwell E, Henschke P, Hietz P, Pennerstorfer J, Rosner S, Kikuta S, Schume H, Schopf A (2015) Do water-limiting conditions predispose Norway spruce to bark beetle attack? New Phytologist 205:1128–1141.

Neuhaus J-M (1999) Plant chitinases (PR-3, PR-4, PR-8, PR-11). In: Datta SK, Muthukrishnan S (eds) Pathogenesis-Related Proteins in Plants, 1st edn.p 29.

Nienstaedt H, Zasada J (1990) *Picea glauca* (Moench) Voss. In: Silvics of North America. Volume 1. Conifers. Agriculture Handbook 654. U.S. Dept. of Agriculture, Forest Service, Washington, D.C., p 675.

Öhrn P, Berlin M, Elfstrand M, Krokene P, Jönsson AM (2021) Seasonal variation in Norway spruce response to inoculation with bark beetle-associated bluestain fungi one year after a severe drought. Forest Ecology and Management 496:119443.

Oksanen J, Blanchet FG, Friendly M, Kindt R, Legendre P, McGlinn D, Minchin PR, O'Hara RB, Simpson GL, Solymos P, Stevens MHH, Szoecs E, Wagner H (2020) vegan: community ecology package. R package version 2.5-7. https://CRAN.R-project.org/package=vegan

Owen DR, Lindahl, Jr. KQ, Wood DL, Parmeter, Jr. JR (1987) Pathogenicity of fungi isolated from *Dendroctonus valens, D. brevicomis,* and *D. ponderosae* to ponderosa pine seedlings. Phytopathology 77:631.

Paine TD, Raffa KF, Harrington TC (1997) Interactions among Scolytid bark beetles, their associated fungi, and live host conifers. Annual Review of Entomology 42:179–206.

Pan Y, Zhao T, Krokene P, Yu Z, Qiao M, Lu J, Chen P, Ye H (2018) Bark beetle-associated blue-stain fungi increase antioxidant enzyme activities and monoterpene concentrations in *Pinus yunnanensis*. Frontiers in Plant Science 9:1731.

Parker IM, Gilbert GS (2004) The evolutionary ecology of novel plant-pathogen interactions. Annual Review of Ecology, Evolution, and Systematics 35:675–700.

Parmeter JR, Slaughter GW, Chen M, Wood DL (1987) Rate and depth of sapwood occlusion following inoculation of pines with bluestain fungi. Forest Science 38:34–44.

Pavy N, Boyle B, Nelson C, Paule C, Giguère I, Caron S, Parsons LS, Dallaire N, Bedon F, Bérubé H, Cooke J, Mackay J (2008) Identification of conserved core xylem gene sets: conifer cDNA microarray development, transcript profiling and computational analyses. New Phytologist 180:766–786.

Peery RM, McAllister CH, Cullingham CI, Mahon EL, Arango-Velez A, Cooke JEK (2021) Comparative genomics of the chitinase gene family in lodgepole and jack pines: contrasting responses to biotic threats and landscape level investigation of genetic differentiation. Botany 99:355–378.

Pelgas B, Bousquet J, Meirmans PG, Ritland K, Isabel N (2011) QTL mapping in white spruce: gene maps and genomic regions underlying adaptive traits across pedigrees, years and environments. BMC Genomics 12:145.

Percy KE, Krause CR, Jensen KF (1990) Effects of ozone and acidic fog on red spruce needle epicuticular wax ultrastructure. Canadian Journal of Forest Research 20

Perrin M, Rossi S, Isabel N (2017) Synchronisms between bud and cambium phenology in black spruce: early-flushing provenances exhibit early xylem formation. Tree Physiology 37:593–603.

Pfaffl MW, Tichopad A, Prgomet C, Neuvians TP (2004) Determination of stable housekeeping genes, differentially regulated target genes and sample integrity: BestKeeper – Excel-based tool using pair-wise correlations. Biotechnology Letters 26:509–515.

Philippe G, Sørensen I, Jiao C, Sun X, Fei Z, Domozych DS, Rose JK (2020) Cutin and suberin: assembly and origins of specialized lipidic cell wall scaffolds. Current Opinion in Plant Biology 55:11–20.

Pieterse CMJ, Van der Does D, Zamioudis C, Leon-Reyes A, Van Wees SCM (2012) Hormonal Modulation of Plant Immunity. Annual Review of Cell and Developmental Biology 28:489–521.

Pimentel CS, Gonçalves EV, Firmino PN, Calvão T, Fonseca L, Abrantes I, Correia O, Máguas C (2017) Differences in constitutive and inducible defences in pine species determining susceptibility to pinewood nematode. Plant Pathology 66:131–139.

Pollastrini M, Luchi N, Michelozzi M, Gerosa G, Marzuoli R, Bussotti F, Capretti P (2015) Early physiological responses of *Pinus pinea* L. seedlings infected by *Heterobasidion* sp.pl. in an ozone-enriched atmospheric environment. Tree Physiology 35:331–340.

Polle A, Otter T, Seifert F (1994) Apoplastic peroxidases and lignification in needles of Norway spruce (*Picea abies* L.). Plant Physiology 106:8.

Prügel B, Lognay G (1996) Composition of the cuticular waxes of *Picea abies* and *P. sitchensis*. Phytochemical Analysis 7:29–36.

Pruitt RN, Gust AA, Nürnberger T (2021) Plant immunity unified. Nature Plants 7:382–383.

Pureswaran DS, De Grandpré L, Paré D, Taylor A, Barrette M, Morin H, Régnière J, Kneeshaw DD (2015) Climate-induced changes in host tree–insect phenology may drive ecological state-shift in boreal forests. Ecology 96:1480–1491.

Pureswaran DS, Gries R, Borden JH (2004) Quantitative variation in monoterpenes in four species of conifers. Biochemical Systematics and Ecology 32:1109–1136.

Pureswaran DS, Neau M, Marchand M, De Grandpré L, Kneeshaw D (2019) Phenological synchrony between eastern spruce budworm and its host trees increases with warmer temperatures in the boreal forest. Ecology and Evolution 9:576–586.

Qazi S, Lombardo D, Abou-Zaid M (2018) A metabolomic and HPLC-MS/MS analysis of the foliar phenolics, flavonoids and coumarins of the *Fraxinus* species resistant and susceptible to emerald ash borer. Molecules 23:2734.

R Core Team (2013) R: A language and environment for statistical computing. R Foundation for Statistical Computing, Vienna, Austria. https://www.R-project.org/.

R Core Team (2020) R: A language and environment for statistical computing. R Foundation for Statistical Computing, Vienna, Austria. https://www.R-project.org/.

Raffa KF, Andersson MN, Schlyter F (2016) Host selection by bark beetles. In: Advances in Insect Physiology. Elsevier, pp 1–74.

Raffa KF, Aukema BH, Bentz BJ, Carroll AL, Hicke JA, Turner MG, Romme WH (2008) Cross-scale drivers of natural disturbances prone to anthropogenic amplification: the dynamics of bark beetle eruptions. BioScience 58:501–517.

Raffa KF, Berryman AA (1982) Gustatory cues in the prientation of *Dendroctonus ponderosae* (Coleoptera: Scolytidae) to host trees. The Canadian Entomologist 114:97–104.

Raffa KF, Berryman AA (1983) The role of host plant resistance in the colonization behavior and ecology of bark beetles (Coleoptera: Scolytidae). Ecological Monographs 53:27–49.

Ralph SG, Hudgins JW, Jancsik S, Franceschi VR, Bohlmann J (2007) Aminocyclopropane carboxylic acid synthase is a regulated step in ethylene-dependent induced conifer defense. Full-length cDNA cloning of a multigene family, differential constitutive, and wound- and insect-induced expression, and cellular and subcellular localization in spruce and Douglas Fir. Plant Physiology 143:410–424.

Reicosky DA, Hanover JW (1978) Physiological effects of surface waxes: I. Light reflectance for glaucous and nonglaucous *Picea pungens*. Plant Physiology 62:101–104.

Reid ML, Sekhon JK, LaFramboise LM (2017) Toxicity of monoterpene structure, diversity and concentration to mountain pine beetles, *Dendroctonus ponderosae*: beetle traits matter more. Journal of Chemical Ecology 43:351–361.

Rice AV, Langor DW (2008) A comparison of heat pulse velocity and lesion lengths for assessing the relative virulence of mountain pine beetle-associated fungi on jack pine. Forest Pathology 38:257–262.

Rice AV, Thormann MN, Langor DW (2007a) Virulence of, and interactions among, mountain pine beetle associated blue-stain fungi on two pine species and their hybrids in Alberta. Canadian Journal of Botany 85:316–323.

Rice AV, Thormann MN, Langor DW (2007b) Mountain pine beetle associated blue-stain fungi cause lesions on jack pine, lodgepole pine, and lodgepole × jack pine hybrids in Alberta. Canadian Journal of Botany 85:307–315.

Riederer M, Muller C (eds) (2006) Biology of the plant cuticle. Blackwell Publishing, Oxford ; Ames, Iowa.

Roe AD, James PMA, Rice AV, Cooke JEK, Sperling FAH (2011) Spatial community structure of mountain pine beetle fungal symbionts across a latitudinal gradient. Microbial Ecology 62:347–360.

Roe AD, Rice AV, Bromilow SE, Cooke JEK, Sperling FAH (2010) Multilocus species identification and fungal DNA barcoding: insights from blue stain fungal symbionts of the mountain pine beetle. Molecular Ecology Resources 10:946–959.

Roe AD, Rice AV, Coltman DW, Cooke JEK, Sperling FAH (2011) Comparative phylogeography, genetic differentiation and contrasting reproductive modes in three fungal symbionts of a multipartite bark beetle symbiosis. Molecular Ecology 20:584–600.

Rossi S, Bousquet J (2014) The bud break process and its variation among local populations of boreal black spruce. Frontiers in Plant Science 5. http://journal.frontiersin.org/article/10.3389/fpls.2014.00574/abstract (30 June 2021, date last accessed).

Rouault G, Candau J-N, Lieutier F, Nageleisen L-M, Martin J-C, Warzée N (2006) Effects of drought and heat on forest insect populations in relation to the 2003 drought in Western Europe. Ann For Sci 63:613–624.

Rovenich H, Boshoven JC, Thomma BP (2014) Filamentous pathogen effector functions: of pathogens, hosts and microbiomes. Current Opinion in Plant Biology 20:96–103.

RStudio Team (2020) RStudio: integrated development for R. RStudio, PBC, Boston, MA. http://www.rstudio.com/.

Ruan J, Zhou Y, Zhou M, Yan J, Khurshid M, Weng W, Cheng J, Zhang K (2019) Jasmonic acid signaling pathway in plants. International Journal of Molecular Sciences 20:2479.

Rudolph TD, Laidly PR (1990) *Pinus banksiana* Lamb. jack pine. In: Silvics of North America. USDA Forest Service, Washinton, D.C., pp 280–293.

Rweyongeza DM, Barnhardt LK, Hansen C (2011) Patterns of optimal growth for white spruce provenances in Alberta. Alberta Sustainable Resource Development.

Rweyongeza DM, Dhir NK, Barnhardt LK, Hansen C, Yang R-C (2007) Population differentiation of the lodgepole pine (*Pinus contorta*) and jack pine (*Pinus banksiana*) complex in Alberta: growth, survival, and responses to climate. Canadian Journal of Botany 85:545–556.

Safranyik L, Carroll AL (2006) Chapter 1: The biology and epidemiology of the mountain pine beetle in lodgepole pine forests. In: The mountain pine beetle: a synthesis of biology, management, and impacts on lodgepole pine. Natural Resources Canada, Canadian Forest Service, Pacific Forestry Centre, Victoria, British Columbia, pp 3–66.

Safranyik L, Carroll AL, Régnière J, Langor DW, Riel WG, Shore TL, Peter B, Cooke BJ, Nealis VG, Taylor SW (2010) Potential for range expansion of mountain pine beetle into the boreal forest of North America. The Canadian Entomologist 142:415–442.

Schiebe C, Hammerbacher A, Birgersson G, Witzell J, Brodelius PE, Gershenzon J, Hansson BS, Krokene P, Schlyter F (2012) Inducibility of chemical defenses in Norway spruce bark is correlated with unsuccessful mass attacks by the spruce bark beetle. Oecologia 170:183–198.

Serrano M, Coluccia F, Torres M, Lâ€™Haridon F, MÃ©traux J-P (2014) The cuticle and plant defense to pathogens. Frontiers in Plant Science 5. http://journal.frontiersin.org/article/10.3389/fpls.2014.00274/abstract (20 January 2022, date last accessed).

Shain L, Hillis W (1971) Phenolic extractives in Norway Spruce and their effects on *Fomes annosus*. Phytopathology 61:841–845.

Shapiro SS, Wilk MB (1965) An analysis of variance test for normality (complete samples). Biometrika 52:591–611.

Shrimpton DM (1973) Extractives associated with wound response of lodgepole pine attacked by the mountain pine beetle and associated microorganisms. Canadian Journal of Botany 51:527–534.

Six DL (2020a) A major symbiont shift supports a major niche shift in a clade of tree-killing bark beetles. Ecological Entomology 45:190–201.

Six DL (2020b) Niche construction theory can link bark beetle-fungus symbiosis type and colonization behavior to large scale causal chain-effects. Current Opinion in Insect Science 39:27–34.

Six DL, Bentz BJ (2007) Temperature determines symbiont abundance in a multipartite bark beetle-fungus ectosymbiosis. Microbial Ecology 54:112–118.

Six DL, Bracewell R (2015) Dendroctonus. In: Bark Beetles. Elsevier, pp 305–350.

Six DL, Elser JJ (2019) Extreme ecological stoichiometry of a bark beetle–fungus mutualism. Ecological Entomology 44:543–551.

Six DL, Klepzig KD (2021) Context dependency in bark beetle-fungus mutualisms revisited: assessing potential shifts in interaction outcomes against varied genetic, ecological, and evolutionary backgrounds. Frontiers in Microbiology 12:682187.

Six DL, Paine TD (1998) Effects of mycangial fungi and host tree species on progeny survival and emergence of *Dendroctonus ponderosae* (Coleoptera: Scolytidae). Environmental Entomology 27:1393–1401.

Six DL, Trowbridge A, Howe M, Perkins D, Berglund E, Brown P, Hicke JA, Balasubramanian G (2021) Growth, chemistry, and genetic profiles of whitebark pine forests affected by climate-driven mountain pine beetle outbreaks. Frontiers in Forests and Global Change 4:671510.

Six DL, Wingfield MJ (2011) The role of phytopathogenicity in bark beetle–fungus symbioses: a challenge to the classic paradigm. Annual Review of Entomology 56:255–272.

Smyth GK (2005) limma: linear models for microarray data. In: Gentleman R, Carey VJ, Huber W, Irizarry RA, Dudoit S (eds) Bioinformatics and Computational Biology Solutions Using R and Bioconductor. Springer-Verlag, New York, pp 397–420.

Snedecor GM, Cochran W (1989) Statistical methods, 8th edn. Iowa State University Press.

Solheim H (1995) Early stages of blue-stain fungus invasion of lodgepole pine sapwood following mountain pine beetle attack. Canadian Journal of Botany 73:70–74.

Solheim H, Krokene P (1998) Growth and virulence of mountain pine beetle associated blue-stain fungi, *Ophiostoma clavigerum* and *Ophiostoma montium*. Canadian Journal of Botany 76:6.

Stamp N (2003) Out of the quagmire of plant defense hypotheses. The Quarterly Review of Biology 78:23–55.

Staudt M, Bertin N, Frenzel B, Seufert G (2000) Seasonal variation in amount and composition of monoterpenes emitted by young *Pinus pinea* trees – implications for emission modeling. Journal of Atmospheric Chemistry:23.

Steppe K, Niinemets Ü, Teskey RO (2011) Tree size- and age-related changes in leaf physiology and their influence on carbon gain. In: Meinzer FC, Lachenbruch B, Dawson TE (eds) Size- and Age-Related Changes in Tree Structure and Function. Springer Netherlands, Dordrecht, pp 235–253.

Thomas AW (1987) The effect of age of current-year shoots of *Picea glauca* on survival, development time, and feeding efficiency of 6th-instar larvae of *Choristoneura fumiferana*. Entomologia Experimentalis et Applicata 43:251–260.

Trifinopoulos J, Nguyen L-T, von Haeseler A, Minh BQ (2016) W-IQ-TREE: a fast online phylogenetic tool for maximum likelihood analysis. Nucleic Acids Research 44:W232–W235.

Trowbridge AM, Adams HD, Collins A, Dickman LT, Grossiord C, Hofland M, Malone S, Weaver DK, Sevanto S, Stoy PC, McDowell NG (2021) Hotter droughts alter resource allocation to chemical defenses in piñon pine. Oecologia 197:921–938.

Ullah C, Tsai C, Unsicker SB, Xue L, Reichelt M, Gershenzon J, Hammerbacher A (2019) Salicylic acid activates poplar defense against the biotrophic rust fungus *Melampsora larici-populina* via increased biosynthesis of catechin and proanthocyanidins. New Phytologist 221:960–975.

Usadel B, Poree F, Nagel A, Lohse M, Czedik-Eysenberg A, Stitt M (2009) A guide to using MapMan to visualize and compare omics data in plants: a case study in the crop species, maize. Plant, Cell & Environment 32:1211–1229.

Vandesompele J, Preter KD, Roy NV, Paepe AD (2002) Accurate normalization of real-time quantitative RT-PCR data by geometric averaging of multiple internal control genes. Genome Biology 3:12.

Vanholme R, Demedts B, Morreel K, Ralph J, Boerjan W (2010) Lignin biosynthesis and structure. Plant Physiology 153:895–905.

Vázquez-González C, Zas R, Erbilgin N, Ferrenberg S, Rozas V, Sampedro L (2020) Resin ducts as resistance traits in conifers: linking dendrochronology and resin-based defences. Tree Physiology 40:1313–1326.

Villari C, Battisti A, Chakraborty S, Michelozzi M, Bonello P, Faccoli M (2012) Nutritional and pathogenic fungi associated with the pine engraver beetle trigger comparable defenses in Scots pine. Tree Physiology 32:867–879.

Volney WJA, Fleming RA (2007) Spruce budworm (*Choristoneura* spp.) biotype reactions to forest and climate characteristics. Global Change Biology 13:1630–1643.

Vos IA, Pieterse CMJ, van Wees SCM (2013) Costs and benefits of hormone-regulated plant defences. Plant Pathology 62:43–55.

de Vries S, de Vries J, von Dahlen JK, Gould SB, Archibald JM, Rose LE, Slamovits CH (2018) On plant defense signaling networks and early land plant evolution. Communicative & Integrative Biology 11:1–14.

Wadke N, Kandasamy D, Vogel H, Lah L, Wingfield BD, Paetz C, Wright LP, Gershenzon J, Hammerbacher A (2016) Catechol dioxygenases catalyzing the first step in Norway spruce phenolic degradation are key virulence factors in the bark beetle-vectored fungus Endoconidiophora polonica. Plant Physiology:pp.01916.2015.

Wainhouse D, Cross DJ, Howell RS (1990) The role of lignin as a defence against the spruce bark beetle *Dendroctonus micans*: effect on larvae and adults. Oecologia 85:257–265.

Wallis CM, Galarneau ER-A (2020) Phenolic compound induction in plant-microbe and plant-insect interactions: a meta-analysis. Frontiers in Plant Science 11:580753.

Ward EJ, Warren JM, McLennan DA, Dusenge ME, Way DA, Wullschleger SD, Hanson PJ (2019) Photosynthetic and respiratory responses of two bog shrub species to whole ecosystem warming and elevated CO2 at the Boreal-temperate ecotone. Frontiers in Forests and Global Change 2:54.

Warnes GR, Bolker B, Bonebakker L, Gentleman R, Huber W, Liaw A, Lumley T, Maechler M, Magnusson A, Moeller S, Schwartz M, Venables B (2020) gplots: various R programming tools for plotting data. R package version 3.1.1. https://CRAN.R-project.org/package=gplots

Wasternack C, Song S (2016) Jasmonates: biosynthesis, metabolism, and signaling by proteins activating and repressing transciption. Journal of Experimental Botany:erw443.

Whitehill JGA, Henderson H, Schuetz M, Skyba O, Yuen MMS, King J, Samuels AL, Mansfield SD, Bohlmann J (2016) Histology and cell wall biochemistry of stone cells in the physical defence of conifers against insects: Stone cells and defence against insects. Plant, Cell & Environment 39:1646–1661.

Whitehill JGA, Yuen MMS, Henderson H, Madilao L, Kshatriya K, Bryan J, Jaquish B, Bohlmann J (2019) Functions of stone cells and oleoresin terpenes in the conifer defense syndrome. New Phytologist 221:1503–1517.

Wickham H (2016) ggplot2: elegant graphics for data analysis. Springer-Verlag, New York. https://ggplot2.tidyverse.org

Wilke CO (2020) cowplot: streamlined plot theme and plot annotations for 'ggplot2'. R package version 1.1.1. https://CRAN.R-project.org/package=cowplot

Wilkinson SW, Magerøy MH, López Sánchez A, Smith LM, Furci L, Cotton TEA, Krokene P, Ton J (2019) Surviving in a hostile world: plant strategies to resist pests and diseases. Annual Review of Phytopathology 57:505–529.

Witzell J, Martín JA (2008) Phenolic metabolites in the resistance of northern forest trees to pathogens — past experiences and future prospects. Canadian Journal of Forest Research 38:2711–2727.

Wood S (1963) A revision of the bark beetle genus *Dendroctonus* Erichson (Coleoptera: Scolytidae). The Great Basin naturalist 23:1–117.

Wood DL (1982) The role of pheromones, kairomones, and allomones in the host selection and colonization behavior of bark beetles. Annual Review of Entomology 27:411–446.

Yamada T (2001) Defense mechanisms in the dapwood of living trees against microbial infection. Journal of Forest Research 6:127–137.

Yamaoka Y, Hiratsuka Y, Maruyama PJ (1995) The ability of *Ophiostoma clavigerum* to kill mature lodgepole pine trees. Forest Pathology 25:401–404.

Yang YH, Paquet AC (2005) Preprocessing two-color spotted arrays. In: Gentleman R, Carey VJ, Huber W, Irizarry RA, Dudoit S (eds) Bioinformatics and Computational Biology Solutions Using R and Bioconductor. Springer-Verlag, New York, pp 49–69.

Yeatman CW (1967) Biogeography of jack pine. Canadian Journal of Botany:11.

Zhang W, Wang S, Yang J, Kang C, Huang L, Guo L (2022) Glycosylation of plant secondary metabolites: regulating from chaos to harmony. Environmental and Experimental Botany 194:104703.

Zhang Y, Xu S, Ding P, Wang D, Cheng YT, He J, Gao M, Xu F, Li Y, Zhu Z, Li X, Zhang Y (2010) Control of salicylic acid synthesis and systemic acquired resistance by two members of a plant-specific family of transcription factors. Proceedings of the National Academy of Sciences 107:18220–18225.

Zhao T, Kandasamy D, Krokene P, Chen J, Gershenzon J, Hammerbacher A (2019) Fungal associates of the tree-killing bark beetle, *Ips typographus*, vary in virulence, ability to degrade conifer phenolics and influence bark beetle tunneling behavior. Fungal Ecology 38:71–79.

Zipfel C (2014) Plant pattern-recognition receptors. Trends in Immunology 35:345–351.

Appendix 1

List of Figures and Tables

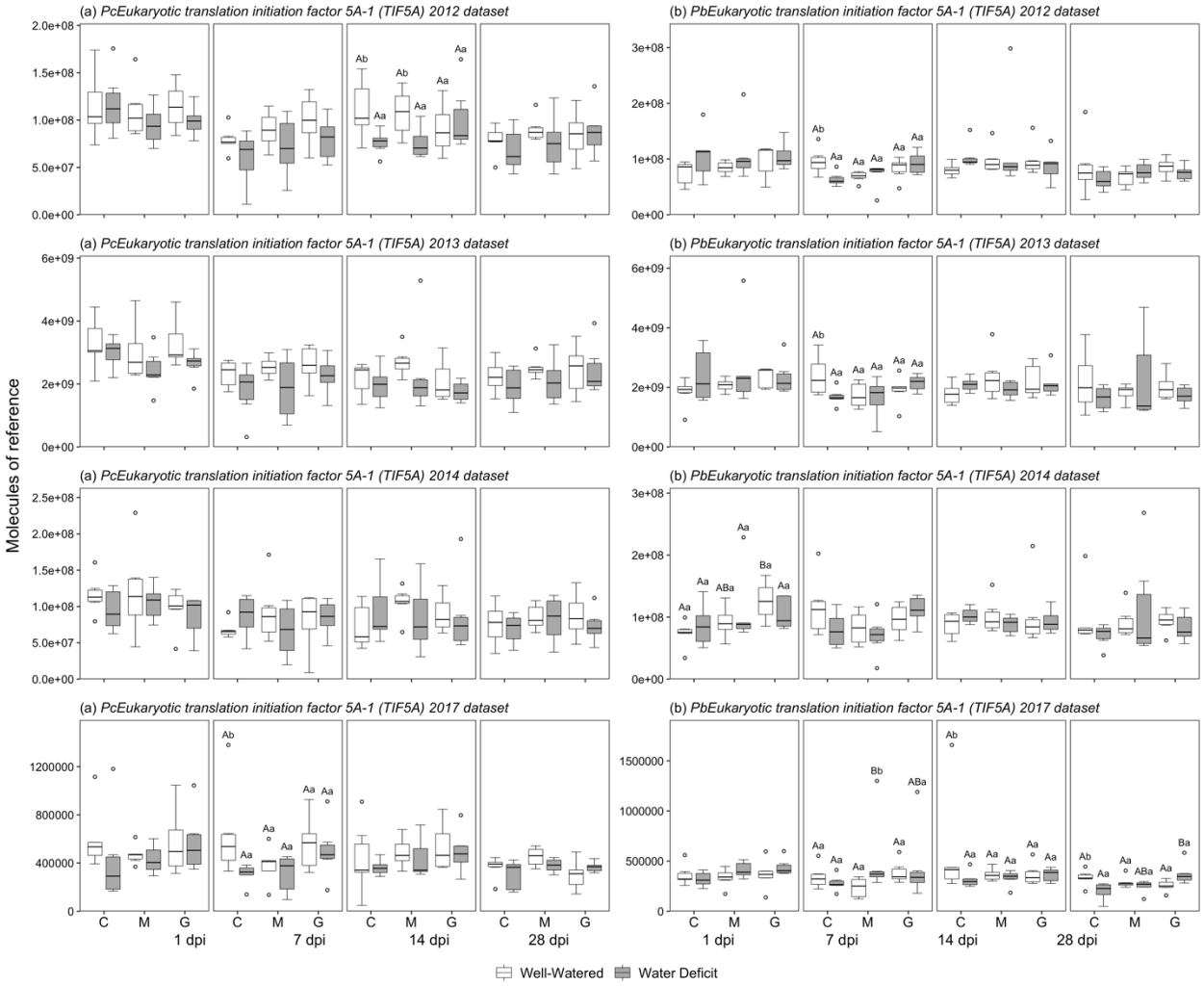

Appendix 1 Figure 1. qRT-PCR expression of the reference gene *Eukaryotic translation initiation factor 5A-1* (*TIF5A*) in lodgepole (*Pc*) and jack pine (*Pb*) seedlings inoculated with *G. clavigera*. *TIF5A* expression profiles of well-watered (white boxes) and water deficit (grey boxes) seedlings are grouped by control (C), mock-inoculation (M), or *G. clavigera*-inoculation (G) for each time point. Within each time point, capitalized letters indicate significant differences between estimated marginal means of inoculation treatments while lower-case letters indicate differences between water treatments (Tukey-adjusted $p < 0.05$, n = 5-6).

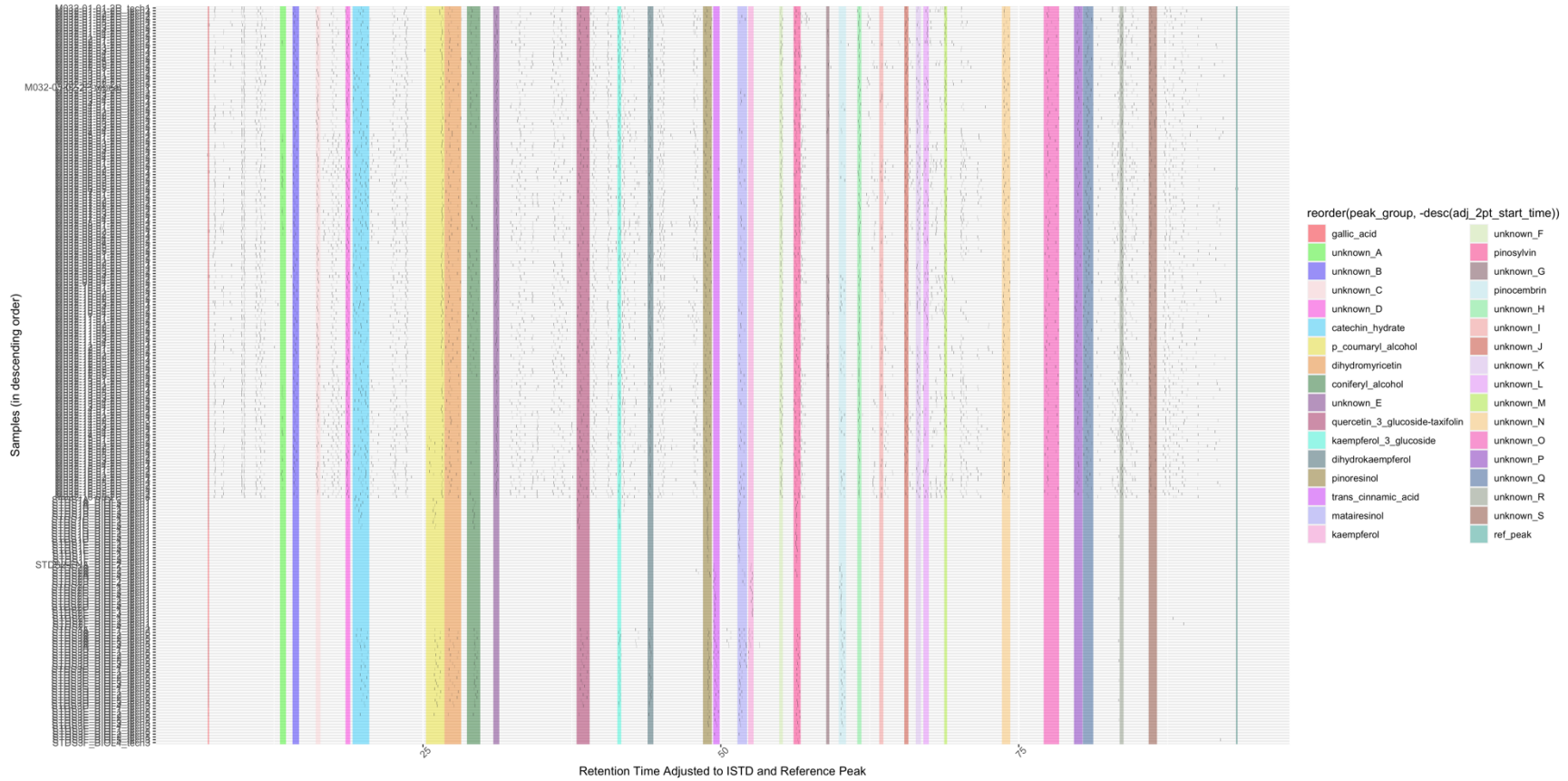

Appendix 1 Figure 2. Annotation of lodgepole and jack pine phloem phenolic metabolite peaks and selection for NMDS. Black vertical dashes represent peaks detected at specific retention times (x-axis) for each sample (y-axis). Colored lines indicate peak assignment to a compound group, based on a range of retention times (i.e. the width of the colored line). Peak retention times were adjusted to improve alignment across samples and to account for drift between runs. Retention time for peaks eluting before 55 min has been adjusted to the retention time of the internal standard (Rt_{sample}-Rt_{ISTD}); likewise, retention times for peaks eluting after 55 minutes has been adjusted to the retention time of a reference peak related to column loading (Rt_{sample}-Rt_{REF}). Peak groups were manually assigned based on the approximate alignment of a single peak across samples, without overlap with other groups, and based

on the detection of included peaks in the majority of samples in at least one treatment (n = 4). Groups encompassing peaks of verified standards were named accordingly, while remaining groups were labeled “Unknown_” and assigned a unique letter. All labeled groups were included in NMDS analysis; peaks not included within the colored lines for the shown groups were omitted from analysis.

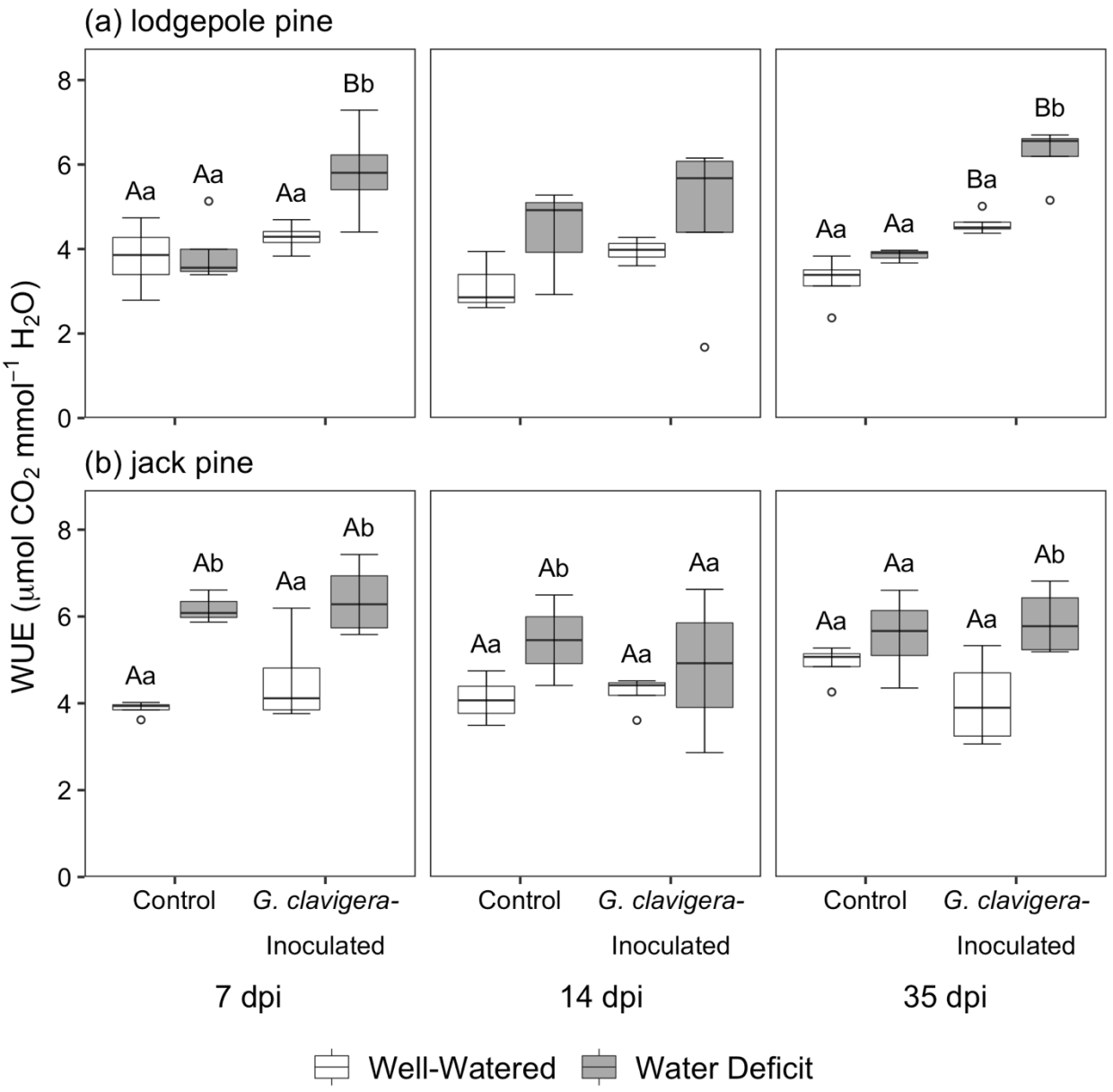

Appendix 1 Figure 3. Water use efficiency (WUE) of lodgepole (a) and jack pine (b) seedlings inoculated with *G. clavigera* under well-watered and water deficit conditions. Error bars represent the standard deviation; uppercase letters indicate significant differences between estimated marginal means of control and inoculated seedlings under the same water condition, lower case letters indicate significant differences between water treatments (adjusted $p < 0.05$, n = 3-4).

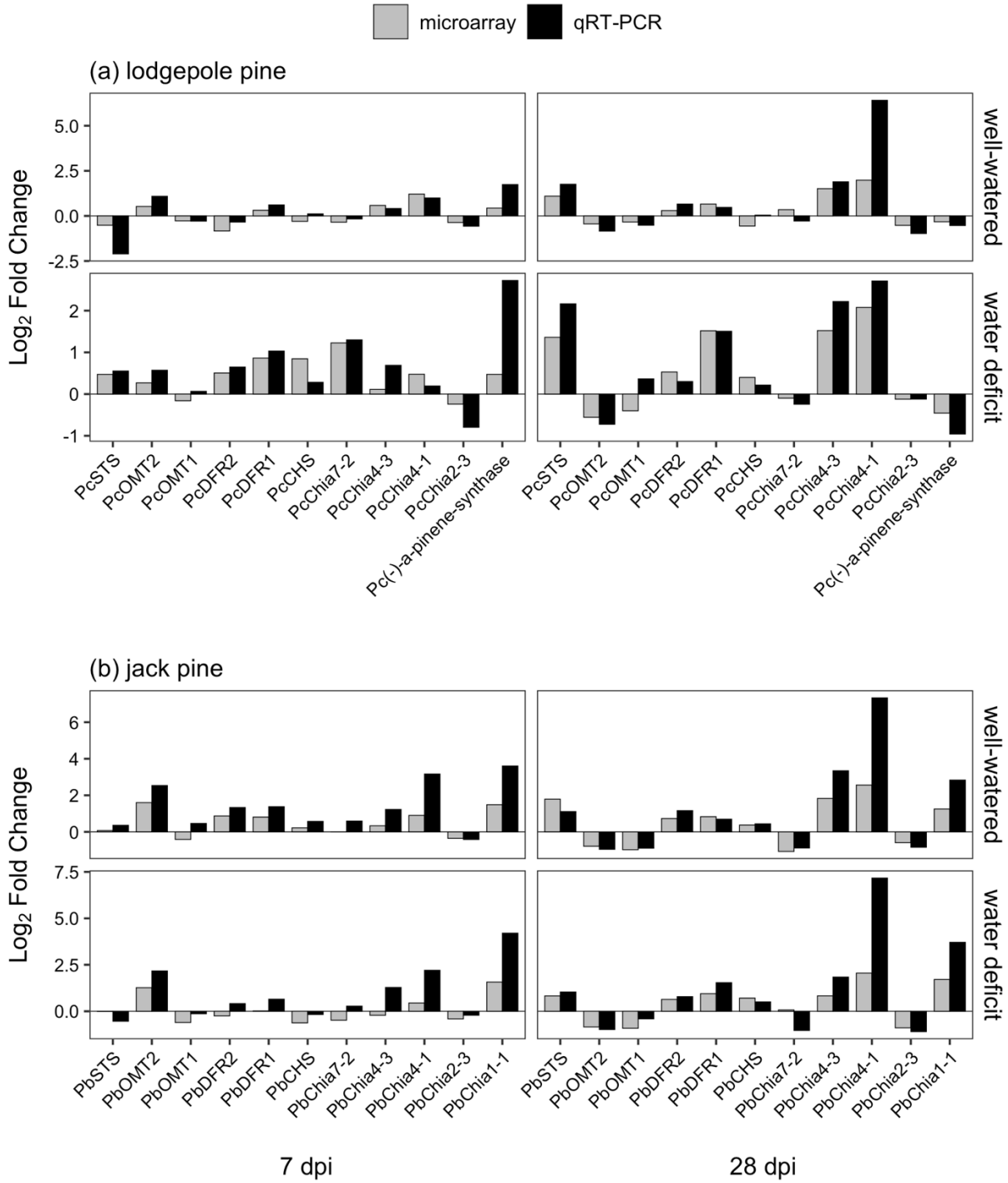

Appendix 1 Figure 4. Comparison of log2 fold change of transcript abundance in inoculated samples relative to the corresponding control for lodgepole (*Pc*) and jack (*Pb*) pine genes shows good agreement between microarray (grey bars) and qRT-PCR (black bars) measurements. qRT-PCR $\log_2$ fold change values were normalized to a reference gene. Microarray values represent the average expression of all microarray sequences theoretically amplified by the qRT-PCR primers for each gene.

Appendix 1 Table 1. Forward and reverse primer sequences used in qRT-PCR analyses.

Gene	Species	Forward Primer 5'-3'	Reverse Primer 5'-3'
Pb(-)-a-pinene synthase	*Pinus banksiana*	GTACTACACTTTGGCTTCTTGC	TACATCACTGATCATGGCGTT
Pc(-)-a-pinene synthase	*Pinus contorta*	GACAGGCTTGGGAGGAATATATTG	CACCACTGGCGATCCACTTT
Pb(+)-a-pinene synthase	*Pinus banksiana*	GTGGAGGTTGCCTACGGATGT	CAACTCCACCACCTCCTCCATA
Pc(+)-a-pinene synthase	*Pinus contorta*	GTGGAGGTTGCCTACGGATGT	TCCACCACCTCCTCCATATAATG
PcChia1-1	*Pinus contorta*	CGATCTCGCTACTCGGAAAAG	CCATCCTGTGGTTTCGT
PbChia1-1	*Pinus banksiana*	CGGCTTCTACCAGCGATAT	AGTCCAGGTTGGCTCCAT
PcChia2-3	*Pinus contorta*	AGTCCAGACATGGTGTCAAACAA	ATTCATCCACCTCCACATTGC
PbChia2-3	*Pinus banksiana*	AGTCCAGACATGGTGTCAAACAA	ATTCATCCACCTCCACATTGC
PcChia4-1	*Pinus contorta*	CTCCACCATTTCGTTCAA	GCAGTTGCTGTTGTCCAT
PbChia4-1	*Pinus banksiana*	ATCAACAGCCAGGAATGC	GTTCACTCTGCTATTCACTTCTC
PcChia4-10	*Pinus contorta*	GCCTGAACAACCCAGAGAAAGT	AACCACACAGCCGTCTTGAAC
PbChia4-10	*Pinus banksiana*	GCCTGAACAACCCAGAGAAAGT	AACCACACAGCCGTCTTGAAC
PcChia4-3	*Pinus contorta*	GTTCAAGACGGCTGTGTGGTT	CGGAGGTTATGGCAGAATGG
PbChia4-3	*Pinus banksiana*	GTTCAAGACGGCTGTGTGGTT	CGGAGGTTATGGCAGAATGG
PcChia7-2	*Pinus contorta*	GCTGGTGATTACCTGGGCTTT	GAGCCATTCTGGGCTACAATTT
PbChia7-2	*Pinus banksiana*	GCTGGTGATTACCTGGGCTTT	GAGCCATTCTGGGCTACAATTT
PcCHS	*Pinus contorta*	CGCAGGAATCAGAGTGAAATTAACCCG	CGGTCGTTTACATAATACCCCACCAAG
PbCHS	*Pinus banksiana*	CGCAGGAATCAGAGTGAAATTAACCCG	CGGTCGTTTACATAATACCCCACCAAG
PcDFR1	*Pinus contorta*	CCTCATTACATGATACTGAGACAGGTA	GCCACTTGGACAATGGTAGCATC
PbDFR1	*Pinus banksiana*	CCTCATTACATGATACTGAGACAGGTA	GCCACTTGGACAATGGTAGCATC
PcDFR2	*Pinus contorta*	CGAAGGGAAGATACATCTCTTCTTCAG	GGATTCATCCACATCCTTGAACTCG
PbDFR2	*Pinus banksiana*	CGAAGGGAAGATACATCTCTTCTTCAG	GGATTCATCCACATCCTTGAACTCG
PcOMT1	*Pinus contorta*	CACCATTCTCCCTGTTGCTGC	CCCACCTCCTTAGCCAAATCTC
PbOMT1	*Pinus banksiana*	CACCATTCTCCCTGTTGCTGC	CCCACCTCCTTAGCCAAATCTC
PcOMT2	*Pinus contorta*	TGTCCAAAGCCTAATAAGCTGTTGC	TACTGCATGATAACAACCCCAGC
PbOMT2	*Pinus banksiana*	TGTCCAAAGCCTAATAAGCTGTTGC	TACTGCATGATAACAACCCCAGC
PcSTS	*Pinus contorta*	TGGTGGGGCAAGCTCTGTTC	GCCTTCTCCACTTGAGGGATGG
PbSTS	*Pinus banksiana*	TGGTGGGGCAAGCTCTGTTC	GCCTTCTCCACTTGAGGGATGG
PcTIF5A	*Pinus contorta*	CTGTGTGTAGCATTTGCCATTTT	CCCGCACAGGTACATTAAAATAGA
PbTIF5A	*Pinus banksiana*	TCTGTCTCTAGCATTTGCCATTATC	CCGGCACAGGTACATTAAAATAGA

Appendix 1 Table 2. PtGen2 microarray sequences DE at 1 and 7 dpi in phloem of both lodgepole and jack pine inoculated with *G. clavigera* relative to uninoculated controls under both well-watered and water deficit conditions. TAIR annotations were assigned based on lodgepole and jack pine contigs representing the best match to each PtGen2 sequence; unique annotations between lodgepole and jack pine contigs are separated by a vertical bar (|). PtGen2 sequences were collapsed into non-redundant annotations based on identical TAIR and MapMan annotations.

Putative Identity	PtGen2 Spot ID	TAIR Accession	TAIR Annotation	MapMan Bin	MapMan Annotation
Defense-related sequences DE in lodgepole and jack pine at 1 and 7 dpi					
chitinase-like	64.10.1	AT3G12500.1	basic chitinase	20.1	stress; biotic
dirigent-like	16.18.12, 27.20.7	AT1G64160.1	Disease resistance-responsive (dirigent-like protein) family protein	20.1.7	stress; biotic; PR-proteins
dirigent-like	64.8.7	AT1G64160.1	Disease resistance-responsive (dirigent-like protein) family protein	35.2	not assigned; unknown
Defense-related sequences DE in lodgepole and jack pine at 7 dpi only					
salicylic acid biosynthesis	48.14.16, 6.18.16	AT4G36470.1	S-adenosyl-L-methionine-dependent methyltransferases superfamily protein	17.8.1	hormone metabolism; salicylic acid; synthesis-degradation
BSP-like	45.15.15	AT2G15220.1	Plant basic secretory protein (BSP) family protein	20.1	stress; biotic
NBS-LRR-like	8.6.16	AT3G51560.1 | AT3G44670.2	Disease resistance protein (TIR-NBS-LRR class) family	35.2	not assigned; unknown
NBS-LRR-like	64.1.5	N/A | AT5G43740.2	NA | Disease resistance protein (CC-NBS-LRR class) family	35.2	not assigned; unknown
chitinase-like	6.5.12, 66.24.14, 9.6.8	AT2G43590.1	Chitinase family protein	20.1	stress; biotic

Putative Identity	PtGen2 Spot ID	TAIR Accession	TAIR Annotation	MapMan Bin	MapMan Annotation
chitinase-like	30.2.12, 63.22.12	AT3G54420.1	homolog of carrot EP3-3 chitinase	20.1	stress; biotic
chitinase-like	2.22.8	AT3G54420.1 | AT2G43590.1	homolog of carrot EP3-3 chitinase | Chitinase family protein	20.1	stress; biotic
PR gene-like	2.9.5	AT4G25780.1 | AT4G33720.1	CAP (Cysteine-rich secretory proteins, Antigen 5, and Pathogenesis-related 1 protein) superfamily protein	20.1	stress; biotic
thaumatin-like	22.9.8	AT1G19320.1 | AT1G75040.1	Pathogenesis-related thaumatin superfamily protein | pathogenesis-related gene 5	20.1	stress; biotic
thaumatin-like	63.13.12	AT1G19320.1 | AT4G11650.1	Pathogenesis-related thaumatin superfamily protein | osmotin 34	35.2	not assigned; unknown
thaumatin-like	45.3.1	AT1G75800.1 | AT4G11650.1	Pathogenesis-related thaumatin superfamily protein | osmotin 34	20.1	stress; biotic
thaumatin-like	32.4.6, 41.22.12, 61.10.8, 64.15.7, 65.8.13, 9.1.12	AT4G11650.1	osmotin 34	20.2	stress; abiotic
thaumatin-like	67.22.9	AT4G11650.1	osmotin 34	35.2	not assigned; unknown
thaumatin-like	61.19.9	N/A | AT4G11650.1	NA | osmotin 34	35.2	not assigned; unknown
flavonoid biosynthesis	63.23.15	AT2G39980.1	HXXXD-type acyl-transferase family protein	16.8.1	secondary metabolism; flavonoids; anthocyanins
flavonoid biosynthesis	50.21.1	AT4G10500.1 | AT4G10490.1	2-oxoglutarate (2OG) and Fe(II)-dependent oxygenase superfamily protein	16.8.3	secondary metabolism; flavonoids; dihydroflavonols

Putative Identity	PtGen2 Spot ID	TAIR Accession	TAIR Annotation	MapMan Bin	MapMan Annotation
flavonoid biosynthesis	25.23.5	N/A | AT4G10490.1	NA | 2-oxoglutarate (2OG) and Fe(II)-dependent oxygenase superfamily protein	16.8.3	secondary metabolism; flavonoids; dihydroflavonols
flavonoid biosynthesis	9.3.7	N/A | AT4G39230.1	NA | NmrA-like negative transcriptional regulator family protein	16.8.5.1	secondary metabolism; flavonoids; isoflavones; isoflavone reductase
isoprenoid biosynthesis	47.20.6	AT1G76490.1	hydroxy methylglutaryl CoA reductase 1	16.1.2.3	secondary metabolism; isoprenoids; mevalonate pathway; HMG-CoA reductase
isoprenoid biosynthesis	36.22.5	AT4G16730.1 | AT1G61120.1	terpene synthase 02 | terpene synthase 04	16.1.5	secondary metabolism; isoprenoids; terpenoids
isoprenoid biosynthesis	40.5.7, 63.20.12	AT4G16730.1 | AT4G02780.1	terpene synthase 02 | Terpenoid cyclases/Protein prenyltransferases superfamily protein	16.1.5	secondary metabolism; isoprenoids; terpenoids
WRKY-like TF	49.3.2	AT1G69810.1 | AT5G45400.1	WRKY DNA-binding protein 36 | Replication factor-A protein 1-related	35.2	not assigned; unknown
WRKY-like TF	67.8.5	AT5G64810.1	WRKY DNA-binding protein 51	27.3.32	RNA; regulation of transcription; WRKY domain transcription factor family
WRKY-like TF	67.21.8	AT5G64810.1	WRKY DNA-binding protein 51	35.2	not assigned; unknown

Appendix 1 Table 3. Enrichment analysis of sequences differentially expressed in phloem of *G. clavigera*-inoculated lodgepole and jack pine seedlings relative to uninoculated controls. Only MapMan annotation categories significantly over-represented relative to proportions represented in all PtGen2 sequences are included, as determined using the hypergeometric distribution probability statistic (adjusted $p < 0.001$). Sequences annotated as "not assigned" were omitted, as were comparisons with no significant over-represented annotation categories.

Functional Category	Comparison Sequences in Category	Total PtGen2 Sequences in Category	Probability Density Function (Hypergeometric Distribution)	Adjusted *p*-Value (Benjamini & Hochberg Method)
Under well-watered conditions: sequences DE in lodgepole and jack pine on the same day				
stress	57	447	1.49×10^{-8}	4.33×10^{-7}
amino acid metabolism	23	158	4.23×10^{-5}	6.13×10^{-4}
misc	60	620	6.35×10^{-5}	6.14×10^{-4}
Under well-watered conditions: sequences DE exclusively in jack pine				
secondary metabolism	154	388	4.27×10^{-5}	7.70×10^{-4}
misc	233	620	4.53×10^{-5}	7.70×10^{-4}
Under water deficit conditions: sequences DE in lodgepole and jack pine on the same day				
secondary metabolism	93	388	2.56×10^{-20}	7.41×10^{-19}
misc	102	620	1.04×10^{-10}	1.51×10^{-9}
Under water deficit conditions: sequences DE exclusively in lodgepole pine				
PS	75	157	5.15×10^{-22}	1.70×10^{-20}
Under water deficit conditions: sequences DE exclusively in jack pine				
cell wall	54	178	2.86×10^{-7}	9.16×10^{-6}
In lodgepole pine: sequences DE on the same day in well-watered and water deficit conditions				
stress	56	447	7.17×10^{-13}	1.86×10^{-11}
misc	51	620	9.50×10^{-6}	1.24×10^{-4}
In lodgepole pine: sequences DE later under water deficit conditions				

Functional Category	Comparison Sequences in Category	Total PtGen2 Sequences in Category	Probability Density Function (Hypergeometric Distribution)	Adjusted *p*-Value (Benjamini & Hochberg Method)
misc	48	620	2.28×10^{-8}	5.92×10^{-7}
In jack pine: sequences DE on the same day in well-watered and water deficit conditions				
misc	130	620	1.13×10^{-10}	3.61×10^{-9}
cell wall	42	178	1.46×10^{-5}	2.33×10^{-4}
fermentation	16	43	2.23×10^{-5}	2.38×10^{-4}
stress	82	447	7.37×10^{-5}	5.90×10^{-4}
In jack pine: sequences DE later under water deficit conditions				
secondary metabolism	55	388	2.25×10^{-10}	6.09×10^{-9}
In lodgepole pine: sequences DE exclusively under well-watered conditions				
amino acid metabolism	23	158	1.53×10^{-5}	4.60×10^{-4}
In lodgepole pine: sequences DE exclusively under water deficit conditions				
PS	78	157	4.12×10^{-19}	1.36×10^{-17}
secondary metabolism	132	388	7.34×10^{-14}	1.21×10^{-12}
In jack pine: sequences DE exclusively under well-watered conditions				
PS	57	157	2.17×10^{-5}	7.36×10^{-4}
In jack pine: sequences DE exclusively under water deficit conditions				
secondary metabolism	49	388	2.37×10^{-5}	6.64×10^{-4}

Appendix 1 Table 4. Count of sequences with secondary metabolism annotations differentially expressed in seedlings inoculated with *G. clavigera* relative to controls. PtGen2 sequences were grouped into flavonoid, phenylpropanoid, and isoprenoid groups using MapMan annotations. PtGen2 sequences were further condensed into non-redundant annotations based on identical NCBI, TAIR, and MapMan annotations.

	DE in both lodgepole and jack pine		**DE exclusively in lodgepole pine**		**DE exclusively in jack pine**	
	PtGen2 sequences	Non-redundant annotations	PtGen2 sequences	Non-redundant annotations	PtGen2 sequences	Non-redundant annotations
flavonoids						
DE under well-watered conditions	12	11	3	3	63	30
DE under water deficit conditions	51	27	42	19	23	18
phenylpropanoids						
DE under well-watered conditions	14	10	3	3	42	19
DE under water deficit conditions	27	15	14	9	19	13
isoprenoids						
DE under well-watered conditions	18	13	0	0	39	27
DE under water deficit conditions	20	13	8	7	24	17

Appendix 1 Table 5. PtGen2 microarray sequences DE earlier between phloem of lodgepole or jack pine inoculated with G. clavigera relative to uninoculated controls under well-watered conditions. TAIR annotations were assigned based on lodgepole and jack pine contigs representing the best match to each PtGen2 sequence; unique annotations between lodgepole and jack pine contigs are separated by a vertical bar (|). PtGen2 sequences were collapsed into non-redundant annotations based on identical TAIR and MapMan annotations.

Putative Identity	PtGen2 Spot ID	TAIR Accession	TAIR Annotation	MapMan Bin	MapMan Annotation
Defense-related sequences DE earlier in lodgepole pine than jack pine under well-watered conditions					
auxin-regulated	2.15.4	AT1G60730.3	NAD(P)-linked oxidoreductase superfamily protein	17.2.3	hormone metabolism; auxin; induced-regulated-responsive-activated
auxin-regulated	6.4.4	AT2G42290.1 | AT4G34760.1	Leucine-rich repeat protein kinase family protein | SAUR-like auxin-responsive protein family	17.2.3	hormone metabolism; auxin; induced-regulated-responsive-activated
ethylene biosynthesis	28.2.5	AT1G77330.1	2-oxoglutarate (2OG) and Fe(II)-dependent oxygenase superfamily protein	17.5.1.2	hormone metabolism; ethylene; synthesis-degradation; 1-aminocyclopropane-1-carboxylate oxidase
NBS-LRR-like	4.8.1	AT4G19050.1 | AT3G44670.2	NB-ARC domain-containing disease resistance protein | Disease resistance protein (TIR-NBS-LRR class) family	35.2	not assigned; unknown
dirigent-like	3.17.8	AT5G42510.1	Disease resistance-responsive (dirigent-like protein) family protein	35.2	not assigned; unknown
PR gene-like	56.1.6	AT1G65010.1 | AT1G23120.1	Plant protein of unknown function (DUF827) | Polyketide cyclase/dehydrase and lipid transport superfamily protein	35.2	not assigned; unknown

Putative Identity	PtGen2 Spot ID	TAIR Accession	TAIR Annotation	MapMan Bin	MapMan Annotation
PR gene-like	36.16.1	N/A | AT1G23120.1	NA | Polyketide cyclase/dehydrase and lipid transport superfamily protein	35.2	not assigned; unknown
thaumatin-like	25.17.10	AT1G19320.1 | AT4G11650.1	Pathogenesis-related thaumatin superfamily protein | osmotin 34	20.1	stress; biotic
thaumatin-like	33.14.1, 17.19.1, 7.7.6, 31.8.10, 55.22.13, 63.16.13	AT4G11650.1	osmotin 34	20.2	stress; abiotic
flavonoid biosynthesis	67.13.10	AT5G42800.1	dihydroflavonol 4-reductase	16.8.3.1	secondary metabolism; flavonoids; dihydroflavonols; dihydroflavonol 4-reductase
phenylpropanoid biosynthesis	50.15.5	N/A | AT5G01210.1	NA | HXXXD-type acyl-transferase family protein	16.2	secondary metabolism; phenylpropanoids
ERF-like TF	7.13.5	AT5G18610.2 | AT3G20310.1	Protein kinase superfamily protein | ethylene response factor 7	17.5.2	hormone metabolism; ethylene; signal transduction
MYB-like TF	65.4.5	AT1G22640.1 | AT5G49620.2	myb domain protein 3 | myb domain protein 78	35.2	not assigned; unknown
WRKY-like TF	16.12.2	AT2G30590.1	WRKY DNA-binding protein 21	27.3.32	RNA; regulation of transcription; WRKY domain transcription factor family
Defense-related sequences DE earlier in jack pine than lodgepole pine under well-watered conditions					
auxin-regulated	27.20.15	AT2G34680.1	Outer arm dynein light chain 1 protein	17.2.3	hormone metabolism; auxin; induced-regulated-responsive-activated
salicylic acid biosynthesis	65.21.13, 47.8.2	AT4G36470.1	S-adenosyl-L-methionine-dependent methyltransferases superfamily protein	17.8.1	hormone metabolism; salicylic acid; synthesis-degradation

Putative Identity	PtGen2 Spot ID	TAIR Accession	TAIR Annotation	MapMan Bin	MapMan Annotation
BSP-like	67.23.8	AT2G15220.1	Plant basic secretory protein (BSP) family protein	20.1	stress; biotic
NBS-LRR-like	59.20.3	AT5G11250.1	Disease resistance protein (TIR-NBS-LRR class)	35.2	not assigned; unknown
chitinase-like	17.12.14, 22.23.9, 3.17.16	AT2G43590.1	Chitinase family protein	20.1	stress; biotic
chitinase-like	64.6.10, 66.23.7, 67.21.1, 61.6.6	AT3G12500.1	basic chitinase	20.1	stress; biotic
chitinase-like	4.20.9	AT3G12500.1 | AT3G09890.1	basic chitinase | Ankyrin repeat family protein	20.1	stress; biotic
chitinase-like	7.15.6	AT3G54420.1	homolog of carrot EP3-3 chitinase	20.1	stress; biotic
chitinase-like	25.22.16	N/A | AT3G54420.1	NA | homolog of carrot EP3-3 chitinase	20.1	stress; biotic
chitinase-like	63.12.9	N/A | AT3G54420.1	NA | homolog of carrot EP3-3 chitinase	35.2	not assigned; unknown
dirigent-like	3.17.2	AT5G42510.1	Disease resistance-responsive (dirigent-like protein) family protein	20.1.7	stress; biotic; PR-proteins
PR gene-like	11.9.14	AT3G04720.1	pathogenesis-related 4	20.1	stress; biotic
thaumatin-like	48.24.5	AT1G19320.1 | AT1G75040.1	Pathogenesis-related thaumatin superfamily protein | pathogenesis-related gene 5	20.1	stress; biotic
thaumatin-like	63.17.3	AT1G75800.1 | AT4G11650.1	Pathogenesis-related thaumatin superfamily protein | osmotin 34	20.2	stress; abiotic

Putative Identity	PtGen2 Spot ID	TAIR Accession	TAIR Annotation	MapMan Bin	MapMan Annotation
thaumatin-like	66.18.6	AT4G11650.1	osmotin 34	20.1	stress; biotic
thaumatin-like	4.8.10	AT4G11650.1	osmotin 34	20.2	stress; abiotic
isoprenoid biosynthesis	5.10.16	AT1G06570.1	phytoene desaturation 1	16.1.3.1	secondary metabolism; isoprenoids; tocopherol biosynthesis; hydroxyphenylpyruvate dioxygenase
isoprenoid biosynthesis	10.22.9, 69.22.9	AT1G76490.1	hydroxy methylglutaryl CoA reductase 1	16.1.2.3	secondary metabolism; isoprenoids; mevalonate pathway; HMG-CoA reductase
isoprenoid biosynthesis	64.5.12	AT2G17370.1 | AT1G76490.1	3-hydroxy-3-methylglutaryl-CoA reductase 2 | hydroxy methylglutaryl CoA reductase 1	16.1.2.3	secondary metabolism; isoprenoids; mevalonate pathway; HMG-CoA reductase
isoprenoid biosynthesis	64.21.8	AT4G11820.2	hydroxymethylglutaryl-CoA synthase / HMG-CoA synthase / 3-hydroxy-3-methylglutaryl coenzyme A synthase	16.1.2.2	secondary metabolism; isoprenoids; mevalonate pathway; HMG-CoA synthase
isoprenoid biosynthesis	61.19.10	AT4G16730.1	terpene synthase 02	16.1.5	secondary metabolism; isoprenoids; terpenoids
WRKY-like TF	61.4.15	AT1G62300.1	WRKY family transcription factor	35.2	not assigned; unknown

Appendix 1 Table 6. PtGen2 microarray sequences DE earlier between phloem of lodgepole or jack pine inoculated with G. clavigera relative to uninoculated controls under water deficit conditions. TAIR annotations were assigned based on lodgepole and jack pine contigs representing the best match to each PtGen2 sequence; unique annotations between lodgepole and jack pine contigs are separated by a vertical bar (|). PtGen2 sequences were collapsed into non-redundant annotations based on identical TAIR and MapMan annotations.

Putative Identity	PtGen2 Spot ID	TAIR Accession	TAIR Annotation	MapMan Bin	MapMan Annotation
Defense-related sequences DE earlier in lodgepole pine than jack pine under water deficit conditions					
jasmonate biosynthesis	58.4.1	AT1G72520.1	PLAT/LH2 domain-containing lipoxygenase family protein	17.7.1.2	hormone metabolism; jasmonate; synthesis-degradation; lipoxygenase
Defense-related sequences DE earlier in jack pine than lodgepole pine under water deficit conditions					
salicylic acid biosynthesis	47.8.2	AT4G36470.1	S-adenosyl-L-methionine-dependent methyltransferases superfamily protein	17.8.1	hormone metabolism; salicylic acid; synthesis-degradation
chitinase-like	38.14.8, 4.9.8, 40.21.10, 53.7.5, 6.13.15, 7.24.4, 61.6.6	AT3G12500.1	basic chitinase	20.1	stress; biotic
chitinase-like	32.3.15	AT3G12500.1 | AT2G25760.2	basic chitinase | Protein kinase family protein	20.1	stress; biotic
chitinase-like	4.20.9	AT3G12500.1 | AT3G09890.1	basic chitinase | Ankyrin repeat family protein	20.1	stress; biotic
dirigent-like	66.11.5, 39.23.11, 44.9.1	AT1G64160.1	Disease resistance-responsive (dirigent-like protein) family protein	20.1.7	stress; biotic; PR-proteins

Putative Identity	PtGen2 Spot ID	TAIR Accession	TAIR Annotation	MapMan Bin	MapMan Annotation
dirigent-like	3.17.2	AT5G42510.1	Disease resistance-responsive (dirigent-like protein) family protein	20.1.7	stress; biotic; PR-proteins
PR gene-like	7.24.12, 8.5.9	AT1G23120.1	Polyketide cyclase/dehydrase and lipid transport superfamily protein	35.2	not assigned; unknown
PR gene-like	38.1.4	AT3G04720.1	pathogenesis-related 4	20.1	stress; biotic
thaumatin-like	11.21.10	AT1G75030.1 | AT1G19320.1	thaumatin-like protein 3 | Pathogenesis-related thaumatin superfamily protein	20.1	stress; biotic
thaumatin-like	7.15.16	AT4G11650.1	osmotin 34	20.2	stress; abiotic
flavonoid biosynthesis	32.15.16	AT1G33720.1 | AT5G07990.1	cytochrome P450, family 76, subfamily C, polypeptide 6 | Cytochrome P450 superfamily protein	16.8.3.3	secondary metabolism; flavonoids; dihydroflavonols; flavonoid 3-monooxygenase
isoprenoid biosynthesis	10.22.9, 69.22.9	AT1G76490.1	hydroxy methylglutaryl CoA reductase 1	16.1.2.3	secondary metabolism; isoprenoids; mevalonate pathway; HMG-CoA reductase
isoprenoid biosynthesis	68.2.15, 65.9.8	AT4G16730.1 | AT2G41710.1	terpene synthase 02 | Integrase-type DNA-binding superfamily protein	16.1.5	secondary metabolism; isoprenoids; terpenoids
phenylpropanoid biosynthesis	65.21.3	AT1G15950.1	cinnamoyl coa reductase 1	16.2.1.7	secondary metabolism; phenylpropanoids; lignin biosynthesis; CCR1
phenylpropanoid biosynthesis	68.4.5	AT1G32100.1	pinoresinol reductase 1	16.2	secondary metabolism; phenylpropanoids
phenylpropanoid biosynthesis	11.20.2, 24.5.3, 69.22.8	AT4G34050.1	S-adenosyl-L-methionine-dependent methyltransferases superfamily protein	16.2.1.6	secondary metabolism; phenylpropanoids; lignin biosynthesis; CCoAOMT

Putative Identity	PtGen2 Spot ID	TAIR Accession	TAIR Annotation	MapMan Bin	MapMan Annotation
NAC-like TF	2.9.12	AT5G63790.1 | AT3G24715.1	NAC domain containing protein 102 | Protein kinase superfamily protein with octicosapeptide/Phox/Bem1p domain	35.2	not assigned; unknown
WRKY-like TF	63.6.13	AT4G22070.1	WRKY DNA-binding protein 31	35.2	not assigned; unknown

Appendix 1 Table 7. PtGen2 microarray sequences DE later under water deficit in phloem of lodgepole or jack pine inoculated with G. clavigera relative to uninoculated controls. TAIR annotations were assigned based on lodgepole and jack pine contigs representing the best match to each PtGen2 sequence; unique annotations between lodgepole and jack pine contigs are separated by a vertical bar (|). PtGen2 sequences were collapsed into non-redundant annotations based on identical TAIR and MapMan annotations.

Putative Identity	PtGen2 Spot ID	TAIR Accession	TAIR Annotation	MapMan Bin	MapMan Annotation
Defense-related sequences with DE delayed by water deficit exclusively in lodgepole pine					
auxin-regulated	6.4.4	AT2G42290.1 | AT4G34760.1	Leucine-rich repeat protein kinase family protein | SAUR-like auxin-responsive protein family	17.2.3	hormone metabolism; auxin; induced-regulated-responsive-activated
auxin-regulated	1.17.16, 4.5.6, 55.15.9	AT4G27450.1	Aluminium induced protein with YGL and LRDR motifs	17.2.3	hormone metabolism; auxin; induced-regulated-responsive-activated
ethylene biosynthesis	28.2.5	AT1G77330.1	2-oxoglutarate (2OG) and Fe(II)-dependent oxygenase superfamily protein	17.5.1.2	hormone metabolism; ethylene; synthesis-degradation; 1-aminocyclopropane-1-carboxylate oxidase
jasmonate biosynthesis	3.9.13	AT1G76690.1	12-oxophytodienoate reductase 2	17.7.1.5	hormone metabolism; jasmonate; synthesis-degradation; 12-Oxo-PDA-reductase
NBS-LRR-like	4.8.1	AT4G19050.1 | AT3G44670.2	NB-ARC domain-containing disease resistance protein | Disease resistance protein (TIR-NBS-LRR class) family	35.2	not assigned; unknown
chitinase-like	38.14.8, 4.9.8, 40.21.10, 53.7.5, 6.13.15, 7.24.4, 52.6.6	AT3G12500.1	basic chitinase	20.1	stress; biotic
chitinase-like	32.3.15	AT3G12500.1 | AT2G25760.2	basic chitinase | Protein kinase family protein	20.1	stress; biotic

Putative Identity	PtGen2 Spot ID	TAIR Accession	TAIR Annotation	MapMan Bin	MapMan Annotation
chitinase-like	61.14.7	AT3G54420.1	homolog of carrot EP3-3 chitinase	20.1	stress; biotic
dirigent-like	66.11.5, 39.23.11, 44.9.1	AT1G64160.1	Disease resistance-responsive (dirigent-like protein) family protein	20.1.7	stress; biotic; PR-proteins
dirigent-like	3.17.8, 8.10.8	AT5G42510.1	Disease resistance-responsive (dirigent-like protein) family protein	35.2	not assigned; unknown
PR gene-like	6.10.3, 7.24.12, 8.5.9	AT1G23120.1	Polyketide cyclase/dehydrase and lipid transport superfamily protein	35.2	not assigned; unknown
PR gene-like	56.1.6	AT1G65010.1 | AT1G23120.1	Plant protein of unknown function (DUF827) | Polyketide cyclase/dehydrase and lipid transport superfamily protein	35.2	not assigned; unknown
PR gene-like	3.24.8, 38.1.4	AT3G04720.1	pathogenesis-related 4	20.1	stress; biotic
PR gene-like	36.16.1	N/A | AT1G23120.1	NA | Polyketide cyclase/dehydrase and lipid transport superfamily protein	35.2	not assigned; unknown
thaumatin-like	25.17.10	AT1G19320.1 | AT4G11650.1	Pathogenesis-related thaumatin superfamily protein | osmotin 34	20.1	stress; biotic
thaumatin-like	44.13.3	AT1G20030.1	Pathogenesis-related thaumatin superfamily protein	35.2	not assigned; unknown
thaumatin-like	33.14.1, 31.8.10, 55.22.13, 63.16.13, 7.15.16	AT4G11650.1	osmotin 34	20.2	stress; abiotic
flavonoid biosynthesis	50.18.10	AT2G22590.1 | AT5G65550.1	UDP-Glycosyltransferase superfamily protein	16.8.1	secondary metabolism; flavonoids; anthocyanins

Putative Identity	PtGen2 Spot ID	TAIR Accession	TAIR Annotation	MapMan Bin	MapMan Annotation
flavonoid biosynthesis	6.4.5	AT5G13930.1	Chalcone and stilbene synthase family protein	16.8.2.1	secondary metabolism; flavonoids; chalcones; naringenin-chalcone synthase
isoprenoid biosynthesis	22.8.12	AT3G54250.1	GHMP kinase family protein	16.1.2.6	secondary metabolism; isoprenoids; mevalonate pathway; mevalonate diphosphate decarboxylase
isoprenoid biosynthesis	65.9.8	AT4G16730.1 | AT2G41710.1	terpene synthase 02 | Integrase-type DNA-binding superfamily protein	16.1.5	secondary metabolism; isoprenoids; terpenoids
isoprenoid biosynthesis	25.11.7, 6.8.6	AT5G47720.1	Thiolase family protein	16.1.2.1	secondary metabolism; isoprenoids; mevalonate pathway; acetyl-CoA C-acyltransferase
phenylpropanoid biosynthesis	65.21.3	AT1G15950.1	cinnamoyl coa reductase 1	16.2.1.7	secondary metabolism; phenylpropanoids; lignin biosynthesis; CCR1
phenylpropanoid biosynthesis	6.24.16, 26.21.1	AT2G30490.1	cinnamate-4-hydroxylase	16.2.1.2	secondary metabolism; phenylpropanoids; lignin biosynthesis; C4H
phenylpropanoid biosynthesis	63.17.16	AT2G37040.1 | AT3G53260.1	PHE ammonia lyase 1 | phenylalanine ammonia-lyase 2	16.2.1.1	secondary metabolism; phenylpropanoids; lignin biosynthesis; PAL
phenylpropanoid biosynthesis	21.2.11, 10.22.8, 11.20.14, 69.22.8, 7.22.13	AT4G34050.1	S-adenosyl-L-methionine-dependent methyltransferases superfamily protein	16.2.1.6	secondary metabolism; phenylpropanoids; lignin biosynthesis; CCoAOMT
phenylpropanoid biosynthesis	22.14.2	AT4G36220.1	ferulic acid 5-hydroxylase 1	16.2.1.8	secondary metabolism; phenylpropanoids; lignin biosynthesis; F5H
phenylpropanoid biosynthesis	50.15.5	N/A | AT5G01210.1	NA | HXXXD-type acyl-transferase family protein	16.2	secondary metabolism; phenylpropanoids

Putative Identity	PtGen2 Spot ID	TAIR Accession	TAIR Annotation	MapMan Bin	MapMan Annotation
ERF-like TF	7.13.5	AT5G18610.2 | AT3G20310.1	Protein kinase superfamily protein | ethylene response factor 7	17.5.2	hormone metabolism; ethylene; signal transduction
MYB-like TF	17.24.1	AT4G12540.1 | AT5G12280.2	unknown protein | SWAP (Suppressor-of-White-APricot)/surp RNA-binding domain-containing protein	35.2	not assigned; unknown
NAC-like TF	2.9.12	AT5G63790.1 | AT3G24715.1	NAC domain containing protein 102 | Protein kinase superfamily protein with octicosapeptide/Phox/Bem1p domain	35.2	not assigned; unknown
WRKY-like TF	63.6.13	AT4G22070.1	WRKY DNA-binding protein 31	35.2	not assigned; unknown
WRKY-like TF	3.11.8	AT4G22070.1 | AT3G28470.1	WRKY DNA-binding protein 31 | Duplicated homeodomain-like superfamily protein	27.3.32	RNA; regulation of transcription; WRKY domain transcription factor family
WRKY-like TF	23.4.2	AT5G49520.1 | AT1G75260.1	WRKY DNA-binding protein 48 | oxidoreductases, acting on NADH or NADPH	35.2	not assigned; unknown
Defense-related sequences with DE delayed by water deficit exclusively in jack pine					
auxin-regulated	45.1.1, 35.22.4, 59.9.5, 64.22.10	AT1G60710.1 | AT1G60730.3	NAD(P)-linked oxidoreductase superfamily protein	17.2.3	hormone metabolism; auxin; induced-regulated-responsive-activated
auxin-regulated	3.22.9, 40.9.1, 60.1.12	AT1G60730.3	NAD(P)-linked oxidoreductase superfamily protein	17.2.3	hormone metabolism; auxin; induced-regulated-responsive-activated
auxin-regulated	27.20.15, 15.7.10	AT2G34680.1	Outer arm dynein light chain 1 protein	17.2.3	hormone metabolism; auxin; induced-regulated-responsive-activated

Putative Identity	PtGen2 Spot ID	TAIR Accession	TAIR Annotation	MapMan Bin	MapMan Annotation
ethylene biosynthesis	9.8.15	AT1G12010.1 | AT1G05010.1	2-oxoglutarate (2OG) and Fe(II)-dependent oxygenase superfamily protein | ethylene-forming enzyme	17.5.1.2	hormone metabolism; ethylene; synthesis-degradation; 1-aminocyclopropane-1-carboxylate oxidase
ethylene-regulated	22.18.2	AT1G50640.1 | AT1G28370.1	ethylene responsive element binding factor 3 | ERF domain protein 11	17.5.2	hormone metabolism; ethylene; signal transduction
jasmonate biosynthesis	58.4.1	AT1G72520.1	PLAT/LH2 domain-containing lipoxygenase family protein	17.7.1.2	hormone metabolism; jasmonate; synthesis-degradation; lipoxygenase
jasmonate biosynthesis	69.6.13	AT3G22400.1	PLAT/LH2 domain-containing lipoxygenase family protein	17.7.1.2	hormone metabolism; jasmonate; synthesis-degradation; lipoxygenase
salicylic acid biosynthesis	65.21.13	AT4G36470.1	S-adenosyl-L-methionine-dependent methyltransferases superfamily protein	17.8.1	hormone metabolism; salicylic acid; synthesis-degradation
BSP-like	67.23.8	AT2G15220.1	Plant basic secretory protein (BSP) family protein	20.1	stress; biotic
NBS-LRR-like	67.17.11	AT1G69550.1	disease resistance protein (TIR-NBS-LRR class)	20.1.7	stress; biotic; PR-proteins
NBS-LRR-like	22.22.9	AT1G69550.1	disease resistance protein (TIR-NBS-LRR class)	35.2	not assigned; unknown
NBS-LRR-like	2.21.8	AT5G41740.2 | AT5G19340.1	Disease resistance protein (TIR-NBS-LRR class) family | unknown protein	35.2	not assigned; unknown
chitinase-like	17.12.14, 22.23.9, 3.17.16	AT2G43590.1	Chitinase family protein	20.1	stress; biotic

Putative Identity	PtGen2 Spot ID	TAIR Accession	TAIR Annotation	MapMan Bin	MapMan Annotation
chitinase-like	63.24.13, 64.6.10, 66.23.7, 67.21.1	AT3G12500.1	basic chitinase	20.1	stress; biotic
chitinase-like	7.15.6	AT3G54420.1	homolog of carrot EP3-3 chitinase	20.1	stress; biotic
chitinase-like	25.22.16	N/A | AT3G54420.1	NA | homolog of carrot EP3-3 chitinase	20.1	stress; biotic
chitinase-like	63.12.9	N/A | AT3G54420.1	NA | homolog of carrot EP3-3 chitinase	35.2	not assigned; unknown
dirigent-like	42.5.10, 60.23.11	AT5G42510.1 | AT5G42500.1	Disease resistance-responsive (dirigent-like protein) family protein	20.1	stress; biotic
PR gene-like	11.9.14	AT3G04720.1	pathogenesis-related 4	20.1	stress; biotic
thaumatin-like	6.21.13	AT1G19320.1	Pathogenesis-related thaumatin superfamily protein	20.1	stress; biotic
thaumatin-like	48.24.5, 14.19.10, 63.11.13	AT1G19320.1 | AT1G75040.1	Pathogenesis-related thaumatin superfamily protein | pathogenesis-related gene 5	20.1	stress; biotic
thaumatin-like	66.6.5	AT1G19320.1 | AT1G75040.1	Pathogenesis-related thaumatin superfamily protein | pathogenesis-related gene 5	20.1.7	stress; biotic; PR-proteins
thaumatin-like	63.17.3	AT1G75800.1 | AT4G11650.1	Pathogenesis-related thaumatin superfamily protein | osmotin 34	20.2	stress; abiotic
thaumatin-like	4.8.10	AT4G11650.1	osmotin 34	20.2	stress; abiotic

Putative Identity	PtGen2 Spot ID	TAIR Accession	TAIR Annotation	MapMan Bin	MapMan Annotation
flavonoid biosynthesis	17.10.16	AT1G01420.1 | AT5G65550.1	UDP-glucosyl transferase 72B3 | UDP-Glycosyltransferase superfamily protein	16.8.1	secondary metabolism; flavonoids; anthocyanins
flavonoid biosynthesis	61.6.3	AT1G75290.1	NAD(P)-binding Rossmann-fold superfamily protein	16.8.5.1	secondary metabolism; flavonoids; isoflavones; isoflavone reductase
flavonoid biosynthesis	21.3.8	AT4G10490.1	2-oxoglutarate (2OG) and Fe(II)-dependent oxygenase superfamily protein	16.8.3	secondary metabolism; flavonoids; dihydroflavonols
flavonoid biosynthesis	66.10.8	AT5G35732.1 | AT1G01390.1	unknown protein | UDP-Glycosyltransferase superfamily protein	16.8.3	secondary metabolism; flavonoids; dihydroflavonols
flavonoid biosynthesis	15.6.7, 55.3.14, 58.3.1	AT5G42800.1	dihydroflavonol 4-reductase	16.8.3.1	secondary metabolism; flavonoids; dihydroflavonols; dihydroflavonol 4-reductase
flavonoid biosynthesis	14.6.3	AT5G54060.1 | AT5G65550.1	UDP-glucose:flavonoid 3-o-glucosyltransferase | UDP-Glycosyltransferase superfamily protein	16.8.1.12	secondary metabolism; flavonoids; anthocyanins; anthocyanidin 3-O-glucosyltransferase
flavonoid biosynthesis	4.24.7	N/A | AT5G65550.1	NA | UDP-Glycosyltransferase superfamily protein	16.8.1.12	secondary metabolism; flavonoids; anthocyanins; anthocyanidin 3-O-glucosyltransferase
isoprenoid biosynthesis	5.10.16, 19.18.11	AT1G06570.1	phytoene desaturation 1	16.1.3.1	secondary metabolism; isoprenoids; tocopherol biosynthesis; hydroxyphenylpyruvate dioxygenase
isoprenoid biosynthesis	33.15.8	AT1G31910.1	GHMP kinase family protein	16.1.2.5	secondary metabolism; isoprenoids; mevalonate pathway; phosphomevalonate kinase
isoprenoid biosynthesis	29.5.2	AT1G64970.1	gamma-tocopherol methyltransferase	16.1.3.5	secondary metabolism; isoprenoids; tocopherol biosynthesis; tocopherol methyltransferase

Putative Identity	PtGen2 Spot ID	TAIR Accession	TAIR Annotation	MapMan Bin	MapMan Annotation
isoprenoid biosynthesis	42.2.5	AT1G76490.1	hydroxy methylglutaryl CoA reductase 1	16.1.2.3	secondary metabolism; isoprenoids; mevalonate pathway; HMG-CoA reductase
isoprenoid biosynthesis	64.5.12	AT2G17370.1 | AT1G76490.1	3-hydroxy-3-methylglutaryl-CoA reductase 2 | hydroxy methylglutaryl CoA reductase 1	16.1.2.3	secondary metabolism; isoprenoids; mevalonate pathway; HMG-CoA reductase
isoprenoid biosynthesis	10.1.16, 5.10.3, 69.1.16	AT3G02780.1 | AT5G16440.1	isopentenyl pyrophosphate:dimethylallyl pyrophosphate isomerase 2 | isopentenyl diphosphate isomerase 1	16.1.2.7	secondary metabolism; isoprenoids; mevalonate pathway; isopentenyl pyrophosphate:dimethyllallyl pyrophosphate isomerase
isoprenoid biosynthesis	64.4.2	AT3G25810.1	Terpenoid cyclases/Protein prenyltransferases superfamily protein	16.1.5	secondary metabolism; isoprenoids; terpenoids
isoprenoid biosynthesis	35.14.6, 36.20.11, 64.21.8	AT4G11820.2	hydroxymethylglutaryl-CoA synthase / HMG-CoA synthase / 3-hydroxy-3-methylglutaryl coenzyme A synthase	16.1.2.2	secondary metabolism; isoprenoids; mevalonate pathway; HMG-CoA synthase
isoprenoid biosynthesis	61.19.10	AT4G16730.1	terpene synthase 02	16.1.5	secondary metabolism; isoprenoids; terpenoids
isoprenoid biosynthesis	10.22.15, 69.22.15	AT4G16730.1 | AT2G41710.1	terpene synthase 02 | Integrase-type DNA-binding superfamily protein	16.1.5	secondary metabolism; isoprenoids; terpenoids
isoprenoid biosynthesis	38.10.3	AT5G27450.3	mevalonate kinase	16.1.2.4	secondary metabolism; isoprenoids; mevalonate pathway; mevalonate kinase
isoprenoid biosynthesis	42.15.9	AT5G47770.1	farnesyl diphosphate synthase 1	16.1.2.9	secondary metabolism; isoprenoids; mevalonate pathway; farnesyl pyrophosphate synthetase
phenylpropanoid biosynthesis	65.20.12	AT3G21240.1	4-coumarate:CoA ligase 2	16.2.1.3	secondary metabolism; phenylpropanoids; lignin biosynthesis; 4CL

Putative Identity	PtGen2 Spot ID	TAIR Accession	TAIR Annotation	MapMan Bin	MapMan Annotation
phenylpropanoid biosynthesis	3.21.4, 34.4.5, 63.19.7	AT3G53260.1	phenylalanine ammonia-lyase 2	16.2.1.1	secondary metabolism; phenylpropanoids; lignin biosynthesis; PAL
phenylpropanoid biosynthesis	67.22.1	AT4G30470.1	NAD(P)-binding Rossmann-fold superfamily protein	16.2.1.7	secondary metabolism; phenylpropanoids; lignin biosynthesis; CCR1
phenylpropanoid biosynthesis	63.9.14	AT4G34050.1	S-adenosyl-L-methionine-dependent methyltransferases superfamily protein	16.2.1.6	secondary metabolism; phenylpropanoids; lignin biosynthesis; CCoAOMT
phenylpropanoid biosynthesis	40.13.12	AT4G34050.2 | AT4G34050.1	S-adenosyl-L-methionine-dependent methyltransferases superfamily protein	16.2.1.6	secondary metabolism; phenylpropanoids; lignin biosynthesis; CCoAOMT
phenylpropanoid biosynthesis	6.23.11	AT4G36220.1 | AT5G04330.1	ferulic acid 5-hydroxylase 1 | Cytochrome P450 superfamily protein	16.2.1.8	secondary metabolism; phenylpropanoids; lignin biosynthesis; F5H
phenylpropanoid biosynthesis	50.5.11, 6.23.6	AT4G39330.1	cinnamyl alcohol dehydrogenase 9	16.2.1.10	secondary metabolism; phenylpropanoids; lignin biosynthesis; CAD
phenylpropanoid biosynthesis	10.4.4, 10.4.5, 69.4.4	AT5G54160.1	O-methyltransferase 1	16.2.1.9	secondary metabolism; phenylpropanoids; lignin biosynthesis; COMT
MYB-like TF	3.22.16	AT5G67300.1	myb domain protein r1	35.2	not assigned; unknown
NAC-like TF	25.3.6, 54.8.6	AT1G77450.1	NAC domain containing protein 32	35.2	not assigned; unknown
WRKY-like TF	61.4.15	AT1G62300.1	WRKY family transcription factor	35.2	not assigned; unknown

Appendix 1 Table 8. PtGen2 microarray sequences DE earlier under water deficit in phloem of lodgepole or jack pine inoculated with G. clavigera relative to uninoculated controls. TAIR annotations were assigned based on lodgepole and jack pine contigs representing the best match to each PtGen2 sequence; unique annotations between lodgepole and jack pine contigs are separated by a vertical bar (|). PtGen2 sequences were collapsed into non-redundant annotations based on identical TAIR and MapMan annotations.

Putative Identity	PtGen2 Spot ID	TAIR Accession	TAIR Annotation	MapMan Bin	MapMan Annotation
Defense-related sequences with DE earlier under water deficit exclusively in jack pine					
auxin biosynthesis	23.1.13	AT5G55250.2	IAA carboxylmethyltransferase 1	17.2.1	hormone metabolism; auxin; synthesis-degradation
NBS-LRR-like	54.5.11	AT1G69550.1 | AT2G14080.1	disease resistance protein (TIR-NBS-LRR class) | Disease resistance protein (TIR-NBS-LRR class) family	20.1.7	stress; biotic; PR-proteins

Appendix 1 Table 9. Summary of analysis of deviance of generalized linear models fit to phloem chitinase qRT-PCR expression data. Asterisks (*) indicate interactions between factors. All genes were fit to the following formula: normalized transcript abundance ~ time point * water treatment * inoculation treatment, family = Gamma (link = log).

	lodgepole pine			jack pine		
	df	χ^2	*p*	df	χ^2	*p*
chitinase 1-1 (Chia1-1)						
water treatment	1	25.01	$\mathbf{5.69 \times 10^{-7}}$	1	1.87	1.72×10^{-1}
inoculation treatment	2	37.30	$\mathbf{7.95 \times 10^{-9}}$	2	110.53	$\mathbf{9.96 \times 10^{-25}}$
time point	3	27.95	$\mathbf{3.72 \times 10^{-6}}$	3	59.18	$\mathbf{8.79 \times 10^{-13}}$
water * inoculation	2	0.30	8.61×10^{-1}	2	4.05	1.32×10^{-1}
water * time point	3	4.93	1.77×10^{-1}	3	11.47	$\mathbf{9.44 \times 10^{-3}}$
inoculation * time point	6	26.68	$\mathbf{1.66 \times 10^{-4}}$	6	55.33	$\mathbf{3.98 \times 10^{-10}}$
water * inoculation * time point	6	16.64	1.07×10^{-2}	6	2.59	8.59×10^{-1}
chitinase 2-3 (Chia2-3)						
water treatment	1	34.22	$\mathbf{4.91 \times 10^{-9}}$	1	46.46	$\mathbf{9.33 \times 10^{-12}}$
inoculation treatment	2	34.84	$\mathbf{2.72 \times 10^{-8}}$	2	28.38	$\mathbf{6.88 \times 10^{-7}}$
time point	3	22.87	$\mathbf{4.29 \times 10^{-5}}$	3	8.80	$\mathbf{3.21 \times 10^{-2}}$
water * inoculation	2	2.00	3.68×10^{-1}	2	0.37	8.33×10^{-1}
water * time point	3	10.81	$\mathbf{1.28 \times 10^{-2}}$	3	10.28	$\mathbf{1.64 \times 10^{-2}}$
inoculation * time point	6	4.34	6.30×10^{-1}	6	19.69	$\mathbf{3.15 \times 10^{-3}}$
water * inoculation * time point	6	11.00	8.85×10^{-2}	6	2.71	8.45×10^{-1}
chitinase 4-1 (Chia4-1)						
water treatment	1	4.08	$\mathbf{4.35 \times 10^{-2}}$	1	0.11	7.37×10^{-1}
inoculation treatment	2	43.53	$\mathbf{3.53 \times 10^{-10}}$	2	238.30	$\mathbf{1.79 \times 10^{-52}}$
time point	3	22.03	$\mathbf{6.43 \times 10^{-5}}$	3	38.98	$\mathbf{1.75 \times 10^{-8}}$
water * inoculation	2	9.18	$\mathbf{1.02 \times 10^{-2}}$	2	0.17	9.20×10^{-1}
water * time point	3	2.32	5.08×10^{-1}	3	1.24	7.43×10^{-1}

	lodgepole pine			jack pine		
	df	**χ^2**	***p***	**df**	**χ^2**	***p***
inoculation * time point	6	44.15	**6.91×10^{-8}**	6	68.08	**1.01×10^{-12}**
water * inoculation * time point	6	14.46	**2.49×10^{-2}**	6	7.24	2.99×10^{-1}
chitinase 4-3 (Chia4-3)						
water treatment	1	0.54	4.64×10^{-1}	1	4.68	**3.04×10^{-2}**
inoculation treatment	2	73.65	**1.01×10^{-16}**	2	90.36	**2.39×10^{-20}**
time point	3	16.61	**8.52×10^{-4}**	3	11.38	**9.83×10^{-3}**
water * inoculation	2	3.01	2.22×10^{-1}	2	1.38	5.02×10^{-1}
water * time point	3	2.42	4.90×10^{-1}	3	1.49	6.84×10^{-1}
inoculation * time point	6	36.84	**1.89×10^{-6}**	6	16.22	**1.26×10^{-2}**
water * inoculation * time point	6	5.01	5.43×10^{-1}	6	10.18	1.17×10^{-1}
chitinase 4-10 (Chia4-10)						
water treatment	1	6.75	**9.39×10^{-3}**	1	1.92	1.66×10^{-1}
inoculation treatment	2	5.99	5.00×10^{-2}	2	86.88	**1.37×10^{-19}**
time point	3	17.75	**4.96×10^{-4}**	3	15.12	**1.71×10^{-3}**
water * inoculation	2	5.68	5.84×10^{-2}	2	1.24	5.39×10^{-1}
water * time point	3	0.50	9.18×10^{-1}	3	0.10	9.92×10^{-1}
inoculation * time point	6	25.10	**3.27×10^{-4}**	6	27.39	**1.22×10^{-4}**
water * inoculation * time point	6	6.67	3.52×10^{-1}	6	9.87	1.30×10^{-1}
chitinase 7-2 (Chia7-2)						
water treatment	1	22.21	**2.45×10^{-6}**	1	30.07	**4.17×10^{-8}**
inoculation treatment	2	12.25	**2.19×10^{-3}**	2	6.51	**3.86×10^{-2}**
time point	3	71.35	**2.20×10^{-15}**	3	44.78	**1.03×10^{-9}**
water * inoculation	2	4.50	1.05×10^{-1}	2	0.67	7.14×10^{-1}
water * time point	3	34.52	**1.54×10^{-7}**	3	12.94	**4.76×10^{-3}**
inoculation * time point	6	36.79	**1.94×10^{-6}**	6	10.98	8.90×10^{-2}
water * inoculation * time point	6	7.79	2.54×10^{-1}	6	4.30	6.36×10^{-1}

Appendix 1 Table 10. Summary of analysis of deviance of generalized linear models fit to phloem terpene synthase qRT-PCR expression data. Asterisks (*) indicate interactions between factors. All genes were fit to the following formula: normalized transcript abundance ~ time point * water treatment * inoculation treatment, family = Gamma (link = log).

	lodgepole pine			jack pine		
	df	**χ^2**	***p***	**df**	**χ^2**	***p***
(+)-a-pinene synthase						
water treatment	1	4.13	$\mathbf{4.22 \times 10^{-2}}$	1	14.17	$\mathbf{1.67 \times 10^{-4}}$
inoculation treatment	2	5.10	7.80×10^{-2}	2	14.57	$\mathbf{6.87 \times 10^{-4}}$
time point	3	17.47	$\mathbf{5.67 \times 10^{-4}}$	3	12.29	$\mathbf{6.45 \times 10^{-3}}$
water * inoculation	2	2.60	2.72×10^{-1}	2	2.17	3.38×10^{-1}
water * time point	3	9.93	1.92×10^{-2}	3	7.63	5.43×10^{-2}
inoculation * time point	6	3.95	6.83×10^{-1}	6	25.77	$\mathbf{2.45 \times 10^{-4}}$
water * inoculation * time point	6	8.15	2.27×10^{-1}	6	5.34	5.02×10^{-1}
(-)-a-pinene synthase						
water treatment	1	1.07	3.01×10^{-1}	1	13.52	$\mathbf{2.36 \times 10^{-4}}$
inoculation treatment	2	3.15	2.07×10^{-1}	2	15.93	$\mathbf{3.47 \times 10^{-4}}$
time point	3	17.63	$\mathbf{5.24 \times 10^{-4}}$	3	37.81	$\mathbf{3.09 \times 10^{-8}}$
water * inoculation	2	1.44	4.88×10^{-1}	2	1.38	5.02×10^{-1}
water * time point	3	11.45	$\mathbf{9.51 \times 10^{-3}}$	3	2.45	4.84×10^{-1}
inoculation * time point	6	28.02	$\mathbf{9.32 \times 10^{-5}}$	6	46.83	$\mathbf{2.02 \times 10^{-8}}$
water * inoculation * time point	6	14.90	$\mathbf{2.10 \times 10^{-2}}$	6	2.72	8.43×10^{-1}

Appendix 1 Table 11. Summary of analysis of deviance of generalized linear models fit to phloem phenolic biosynthesis qRT-PCR expression data. Asterisks (*) indicate interactions between factors. All genes were fit to the following formula: normalized transcript abundance ~ time point * water treatment * inoculation treatment, family = Gamma (link = log).

	lodgepole pine			jack pine		
	df	**χ^2**	***p***	**df**	**χ^2**	***p***
stilbene synthase (STS)						
water treatment	1	13.96	$\mathbf{1.87 \times 10^{-4}}$	1	10.74	$\mathbf{1.05 \times 10^{-3}}$
inoculation treatment	2	40.03	$\mathbf{2.03 \times 10^{-9}}$	2	9.41	$\mathbf{9.05 \times 10^{-3}}$
time point	3	23.08	$\mathbf{3.89 \times 10^{-5}}$	3	7.17	6.66×10^{-2}
water * inoculation	2	0.39	8.23×10^{-1}	2	1.60	4.49×10^{-1}
water * time point	3	1.72	6.32×10^{-1}	3	1.60	6.60×10^{-1}
inoculation * time point	6	35.51	$\mathbf{3.43 \times 10^{-6}}$	6	10.89	9.18×10^{-2}
water * inoculation * time point	6	44.97	$\mathbf{4.75 \times 10^{-8}}$	6	8.54	2.01×10^{-1}
dihydroflavonol reductase 1 (DFR1)						
water treatment	1	31.07	$\mathbf{2.49 \times 10^{-8}}$	1	6.53	$\mathbf{1.06 \times 10^{-2}}$
inoculation treatment	2	18.91	$\mathbf{7.81 \times 10^{-5}}$	2	73.63	$\mathbf{1.03 \times 10^{-16}}$
time point	3	37.81	$\mathbf{3.10 \times 10^{-8}}$	3	28.45	$\mathbf{2.92 \times 10^{-6}}$
water * inoculation	2	3.74	1.54×10^{-1}	2	1.73	4.21×10^{-1}
water * time point	3	14.42	$\mathbf{2.39 \times 10^{-3}}$	3	11.79	$\mathbf{8.15 \times 10^{-3}}$
inoculation * time point	6	45.97	$\mathbf{3.00 \times 10^{-8}}$	6	13.18	$\mathbf{4.03 \times 10^{-2}}$
water * inoculation * time point	6	3.94	6.85×10^{-1}	6	13.74	$\mathbf{3.27 \times 10^{-2}}$
dihydroflavonol reductase 2 (DFR2)						
water treatment	1	8.87	$\mathbf{2.90 \times 10^{-3}}$	1	1.07	3.01×10^{-1}
inoculation treatment	2	2.67	2.63×10^{-1}	2	41.29	$\mathbf{1.08 \times 10^{-9}}$
time point	3	20.23	$\mathbf{1.52 \times 10^{-4}}$	3	10.84	$\mathbf{1.26 \times 10^{-2}}$
water * inoculation	2	2.30	3.16×10^{-1}	2	0.31	8.55×10^{-1}
water * time point	3	15.96	$\mathbf{1.16 \times 10^{-3}}$	3	13.43	$\mathbf{3.80 \times 10^{-3}}$

	lodgepole pine			jack pine		
	df	**χ^2**	***p***	**df**	**χ^2**	***p***
inoculation * time point	6	11.68	6.95×10^{-2}	6	6.82	3.37×10^{-1}
water * inoculation * time point	6	5.45	4.88×10^{-1}	6	13.48	$\mathbf{3.60 \times 10^{-2}}$
stilbene o-methyltransferase 1 (OMT1)						
water treatment	1	43.64	$\mathbf{3.95 \times 10^{-11}}$	1	64.28	$\mathbf{1.08 \times 10^{-15}}$
inoculation treatment	2	0.62	7.33×10^{-1}	2	8.00	$\mathbf{1.83 \times 10^{-2}}$
time point	3	14.88	$\mathbf{1.93 \times 10^{-3}}$	3	27.87	$\mathbf{3.86 \times 10^{-6}}$
water * inoculation	2	2.48	2.90×10^{-1}	2	4.01	1.34×10^{-1}
water * time point	3	33.22	$\mathbf{2.89 \times 10^{-7}}$	3	20.90	$\mathbf{1.10 \times 10^{-4}}$
inoculation * time point	6	6.33	3.87×10^{-1}	6	37.55	$\mathbf{1.37 \times 10^{-6}}$
water * inoculation * time point	6	4.55	6.03×10^{-1}	6	10.75	9.66×10^{-2}
stilbene o-methyltransferase 2 (OMT2)						
water treatment	1	5.43	$\mathbf{1.98 \times 10^{-2}}$	1	48.63	$\mathbf{3.09 \times 10^{-12}}$
inoculation treatment	2	12.46	$\mathbf{1.97 \times 10^{-3}}$	2	18.22	$\mathbf{1.10 \times 10^{-4}}$
time point	3	53.22	$\mathbf{1.65 \times 10^{-11}}$	3	314.64	$\mathbf{6.73 \times 10^{-68}}$
water * inoculation	2	1.39	4.98×10^{-1}	2	2.94	2.30×10^{-1}
water * time point	3	14.33	$\mathbf{2.49 \times 10^{-3}}$	3	30.22	$\mathbf{1.24 \times 10^{-6}}$
inoculation * time point	6	31.06	$\mathbf{2.47 \times 10^{-5}}$	6	133.60	$\mathbf{2.24 \times 10^{-26}}$
water * inoculation * time point	6	10.33	1.11×10^{-1}	6	2.53	8.65×10^{-1}
chalcone synthase (CHS)						
water treatment	1	0.02	8.98×10^{-1}	1	4.44	$\mathbf{3.51 \times 10^{-2}}$
inoculation treatment	2	0.20	9.03×10^{-1}	2	12.06	$\mathbf{2.41 \times 10^{-3}}$
time point	3	16.58	$\mathbf{8.61 \times 10^{-4}}$	3	31.74	$\mathbf{5.94 \times 10^{-7}}$
water * inoculation	2	1.31	5.21×10^{-1}	2	0.71	7.01×10^{-1}
water * time point	3	5.65	1.30×10^{-1}	3	1.28	7.34×10^{-1}
inoculation * time point	6	5.63	4.66×10^{-1}	6	3.46	7.49×10^{-1}
water * inoculation * time point	6	2.33	8.87×10^{-1}	6	5.34	5.00×10^{-1}

Appendix 2

List of Figures and Tables

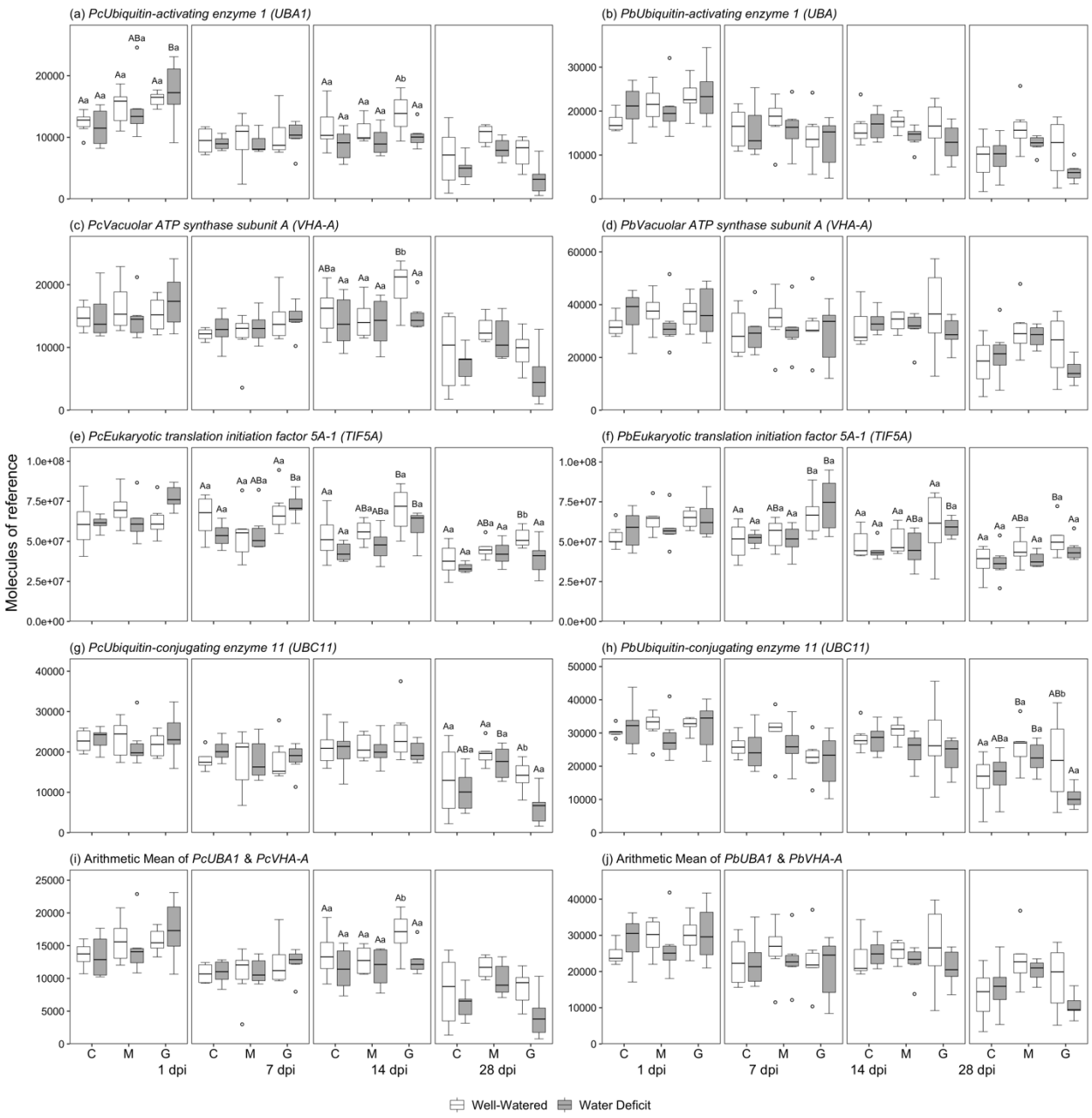

Appendix 2 Figure 1. qRT-PCR transcript profiles of reference genes in secondary xylem of lodgepole (*Pc*) and jack pine (*Pb*) seedlings inoculated with *G. clavigera*. Gene expression was measured in unwounded control (C), mock-inoculated (M) and *G. clavigera*-inoculated (G) trees under well-watered (white boxes) or water deficit (grey boxes) conditions (n = 5-6). Within each timepoint, capitalized letters indicate significant differences between estimated marginal means of inoculation treatments while lower-case letters indicate differences between water treatments (Tukey-adjusted $p < 0.05$, n = 5-6).

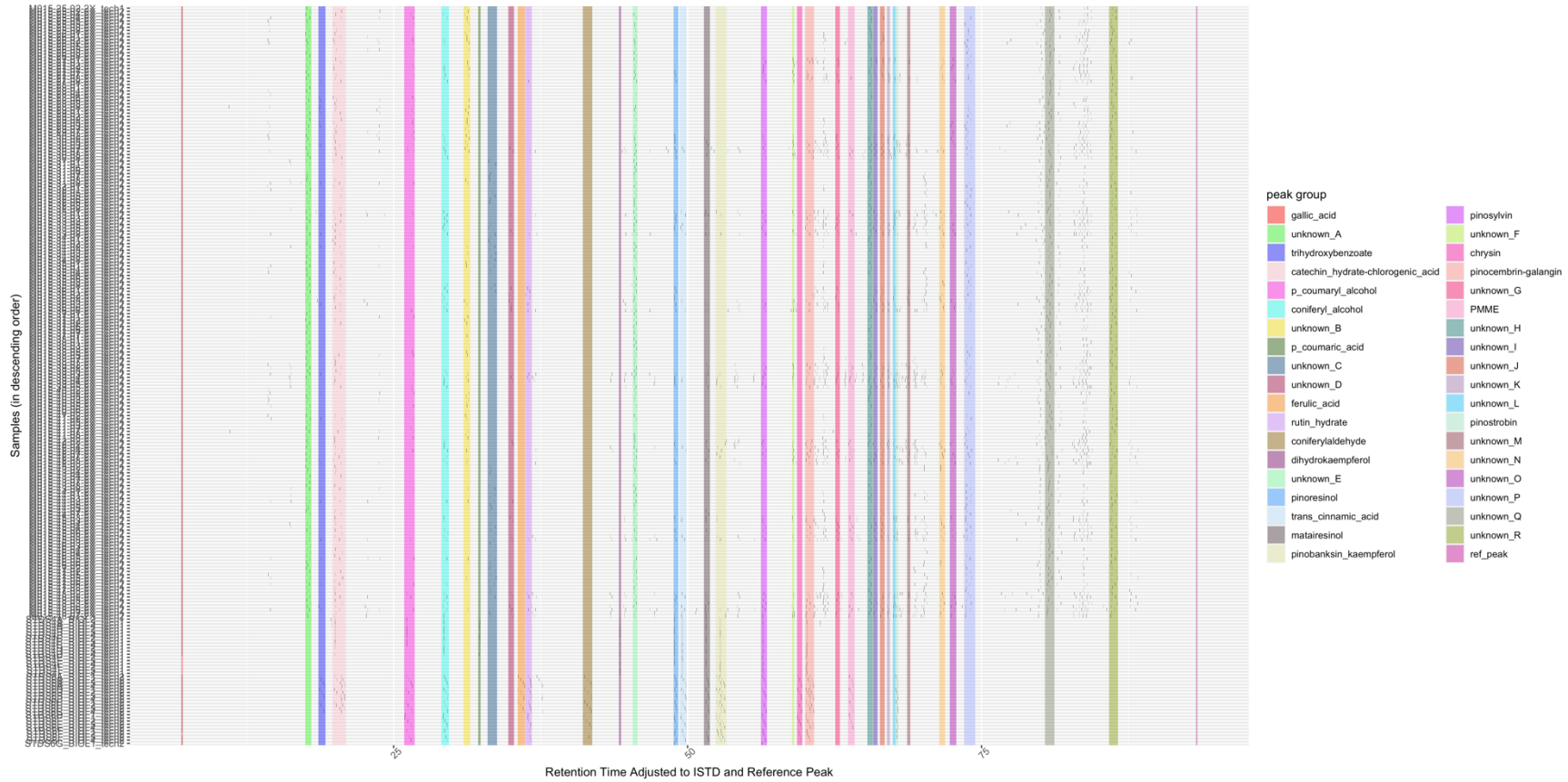

Appendix 2 Figure 2. Annotation of lodgepole and jack pine xylem phenolic metabolite peaks and selection for NMDS. Black vertical dashes represent peaks detected at specific retention times (x-axis) for each sample (y-axis). Colored lines indicate peak assignment to a compound group, based on a range of retention times (i.e. the width of the colored line). Peak retention times were adjusted to improve alignment across samples and to account for drift between runs. Retention time for peaks eluting before 55 min has been adjusted to the retention time of the internal standard (Rt_{sample}-Rt_{ISTD}); likewise, retention times for peaks eluting after 55 minutes has been adjusted to the retention time of a reference peak related to column loading (Rt_{sample}-Rt_{REF}). Peak groups were manually assigned based on the approximate alignment of a single peak across samples, without overlap with other groups, and based

on the detection of included peaks in the majority of samples in at least one treatment (n = 4). Groups encompassing peaks of verified standards were named accordingly, while remaining groups were labeled “Unknown_” and assigned a unique letter. All labeled groups were included in NMDS analysis; peaks not included within the colored lines for the shown groups were omitted from analysis.

Appendix 2 Table 1. Forward and reverse primer sequences of lodgepole pine genes used in qRT-PCR analyses. Asterisks (*) indicate genes tested as references. Target gene expression was normalized to the arithmetic mean of *UBA1* and *VHA-A*.

Gene	Forward Primer 5'-3'	Reverse Primer 5'-3'
PcCHS	CGCAGGAATCAGAGTGAAATTAACCCG	CGGTCGTTTACATAATACCCCACCAAG
PbCHS	CGCAGGAATCAGAGTGAAATTAACCCG	CGGTCGTTTACATAATACCCCACCAAG
PcDFR1	CCTCATTACATGATACTGAGACAGGTA	GCCACTTGGACAATGGTAGCATC
PbDFR1	CCTCATTACATGATACTGAGACAGGTA	GCCACTTGGACAATGGTAGCATC
PcDFR2	CGAAGGGAAGATACATCTCTTCTTCAG	GGATTCATCCACATCCTTGAACTCG
PbDFR2	CGAAGGGAAGATACATCTCTTCTTCAG	GGATTCATCCACATCCTTGAACTCG
PcOMT1	CACCATTCTCCCTGTTGCTGC	CCCACCTCCTTAGCCAAATCTC
PbOMT1	CACCATTCTCCCTGTTGCTGC	CCCACCTCCTTAGCCAAATCTC
PcOMT2	TGTCCAAAGCCTAATAAGCTGTTGC	TACTGCATGATAACAACCCCAGC
PbOMT2	TGTCCAAAGCCTAATAAGCTGTTGC	TACTGCATGATAACAACCCCAGC
PcSTS	TGGTGGGGCAAGCTCTGTTC	GCCTTCTCCACTTGAGGGATGG
PbSTS	TGGTGGGGCAAGCTCTGTTC	GCCTTCTCCACTTGAGGGATGG
PcTIF5A*	CTGTGTGTAGCATTTGCCATTTT	CCCGCACAGGTACATTAAAATAGA
PbTIF5A*	TCTGTCTCTAGCATTTGCCATTATC	CCGGCACAGGTACATTAAAATAGA
PcUBA1*	TGCAAACCTAGCCCTTCCTC	ACCCATCGATCCCAGACAGA
PbUBA1*	TGCAAACCTAGCCCTTCCTC	ACCCATCGATCCCAGACAGA
PcVHA-A*	TTGTACCAAGGCAGGCTCTC	GCTGTAGAAAGAGGAGCTGGT
PbVHA-A*	TTGTACCAAGGCAGGCTCTC	GCTGTAGAAAGAGGAGCTGGT
PcUBC11*	TCCATGCTCTTGCTGTCTCC	GTCCCGCACTGACAATCTCT
PbUBC11*	TCCATGCTCTTGCTGTCTCC	GTCCCGCACTGACAATCTCT

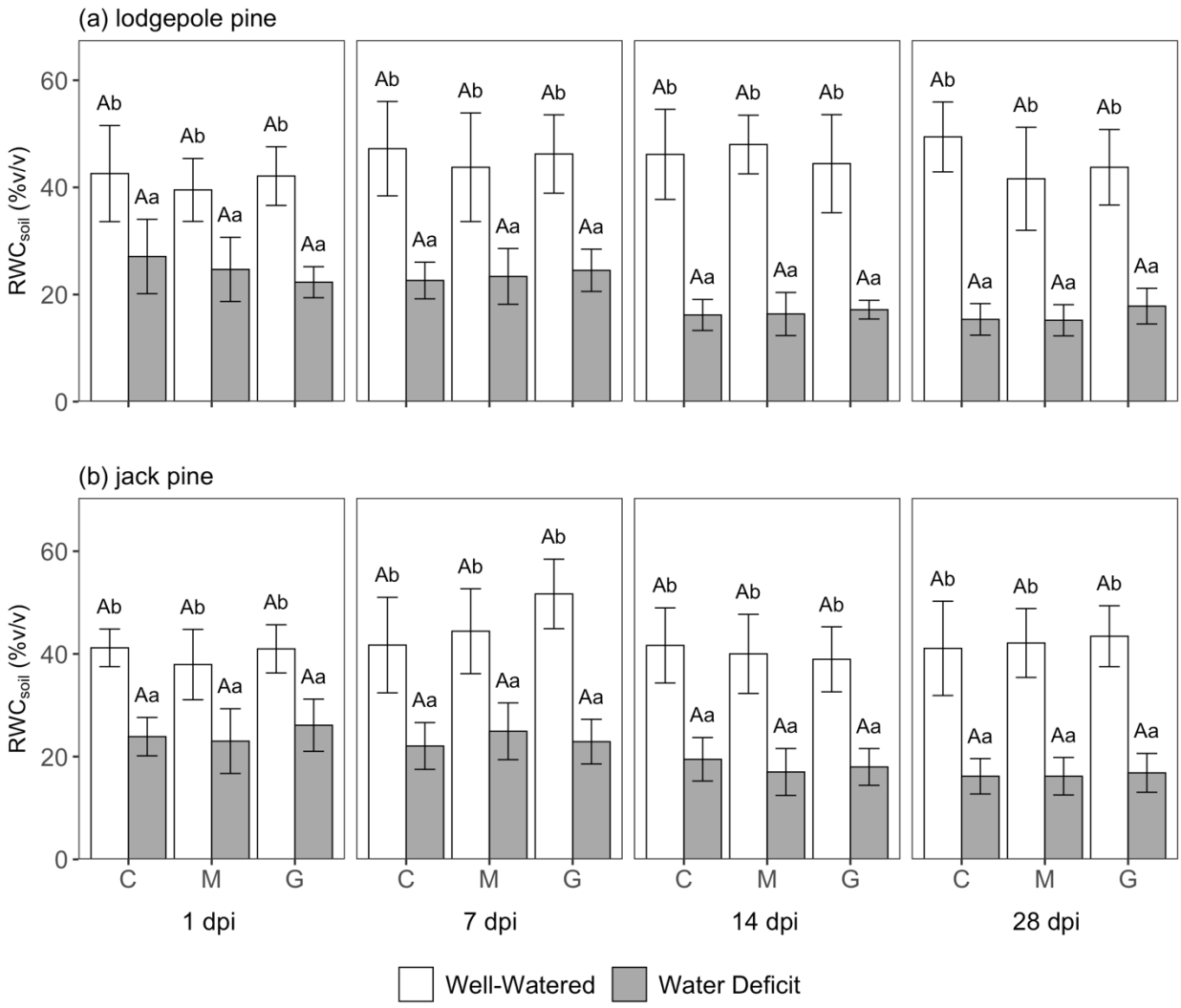

Appendix 2 Figure 3. Soil relative water content (RWC_{soil}) of lodgepole and jack pine seedlings under different water conditions. Average RWC_{soil} was measured for unwounded control (C), mock-inoculated (M), and *G. clavigera*-inoculated (G) seedlings (n = 7-9). Error bars represent the standard deviation. Letters indicate significant differences (Tukey-adjusted $p < 0.05$) between estimated marginal means of comparisons within a timepoint, using a generalized linear model. Uppercase letters represent comparisons between inoculation treatments within a water treatment; lowercase letters represent comparisons between well-watered (white bars) and water deficit (grey bars) trees within an inoculation treatment.

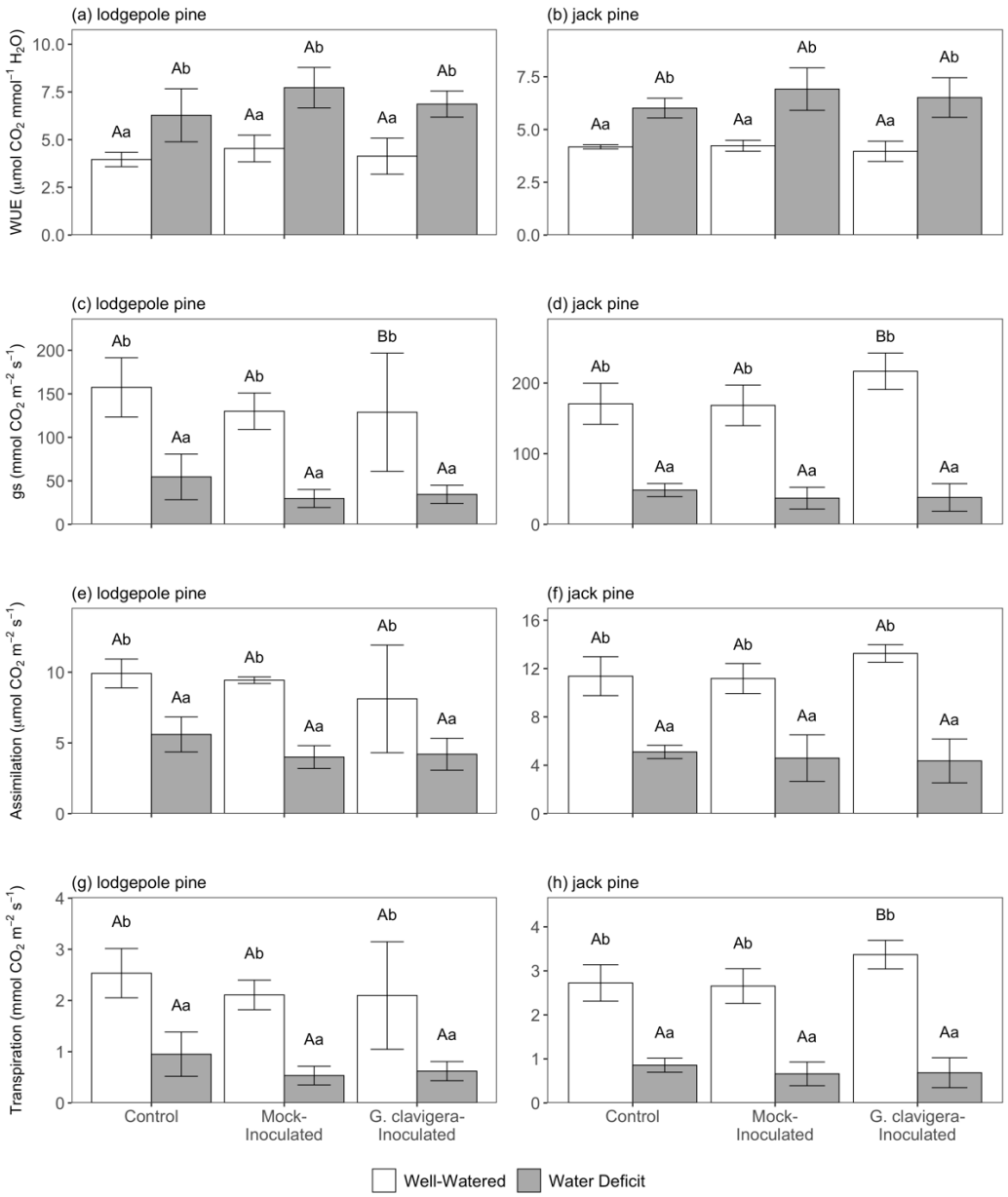

Appendix 2 Figure 4. Effect of water deficit on gas exchange of lodgepole and jack pine seedlings at 28 days post inoculation. Average water use efficiency (WUE, a-b), stomatal conductance (gs, c-d), assimilation (e-f), and transpiration (g-h) was measured for control (unwounded), mock-inoculated, and G. clavigera-inoculated trees under well-watered (white bars) or water deficit (grey bars) conditions (n = 3-4). Error bars represent the standard deviation. Letters represent significant differences (Tukey-adjusted $p < 0.05$) between estimated marginal means across comparisons using a generalized linear model. Uppercase letters represent comparisons between inoculation treatments within a water treatment; lowercase letters represent comparisons between water treatments within an inoculation treatment.

Appendix 2 Table 2. Enrichment analysis of DE sequences in lodgepole and jack pine inoculated with *G. clavigera* under well-watered or water deficit conditions. MapMan annotation categories included were significantly over-represented relative category proportions of all PtGen2 sequences, as determined using the hypergeometric distribution probability statistic (Benjamini & Hochberg adjusted *p*-value <0.001).

Functional Category	Comparison Sequences in Category	Total PtGen Sequences in Category	Probability Density Function (Hypergeometric Distribution)	Adjusted *p*-Value (Benjamini & Hochberg Method)
Under well-watered conditions: sequences DE in lodgepole and jack pine on the same day				
stress	114	447	3.01×10^{-14}	9.03×10^{-13}
hormone metabolism	46	190	7.42×10^{-6}	1.11×10^{-4}
glycolysis	20	58	1.45×10^{-5}	1.45×10^{-4}
Under well-watered conditions: sequences DE exclusively in jack pine				
secondary metabolism	135	388	5.58×10^{-7}	1.79×10^{-5}
In lodgepole pine: sequences DE on the same day in well-watered and water deficit conditions				
stress	71	447	2.77×10^{-6}	8.57×10^{-5}
hormone metabolism	35	190	4.87×10^{-5}	7.54×10^{-4}
In jack pine: sequences DE on the same day in well-watered and water deficit conditions				
secondary metabolism	136	388	3.13×10^{-8}	1.03×10^{-6}
stress	149	447	2.58×10^{-7}	4.26×10^{-6}
In lodgepole pine: sequences DE exclusively under water deficit conditions				
secondary metabolism	117	388	2.47×10^{-16}	7.67×10^{-15}

Appendix 2 Table 3. Comparison of sequences putatively involved in secondary metabolism DE in lodgepole and jack pine seedlings inoculated with *G. clavigera* under well-watered and water deficit conditions. PtGen2 sequences were grouped into flavonoid, phenylpropanoid, and isoprenoid groups using MapMan annotations. PtGen2 sequences were further condensed into non-redundant annotations based on identical NCBI, TAIR, and MapMan annotations.

	DE in both lodgepole and jack pine		DE exclusively in lodgepole pine		DE exclusively in jack pine	
	PtGen2 sequences	Non-redundant annotations	PtGen2 sequences	Non-redundant annotations	PtGen2 sequences	Non-redundant annotations
flavonoids						
DE under well-watered conditions	40	23	4	4	63	35
DE under water deficit conditions	88	40	14	9	21	14
phenylpropanoids						
DE under well-watered conditions	10	6	4	2	32	18
DE under water deficit conditions	31	17	4	4	20	9
isoprenoids						
DE under well-watered conditions	28	19	2	2	29	20
DE under water deficit conditions	46	27	4	3	15	11

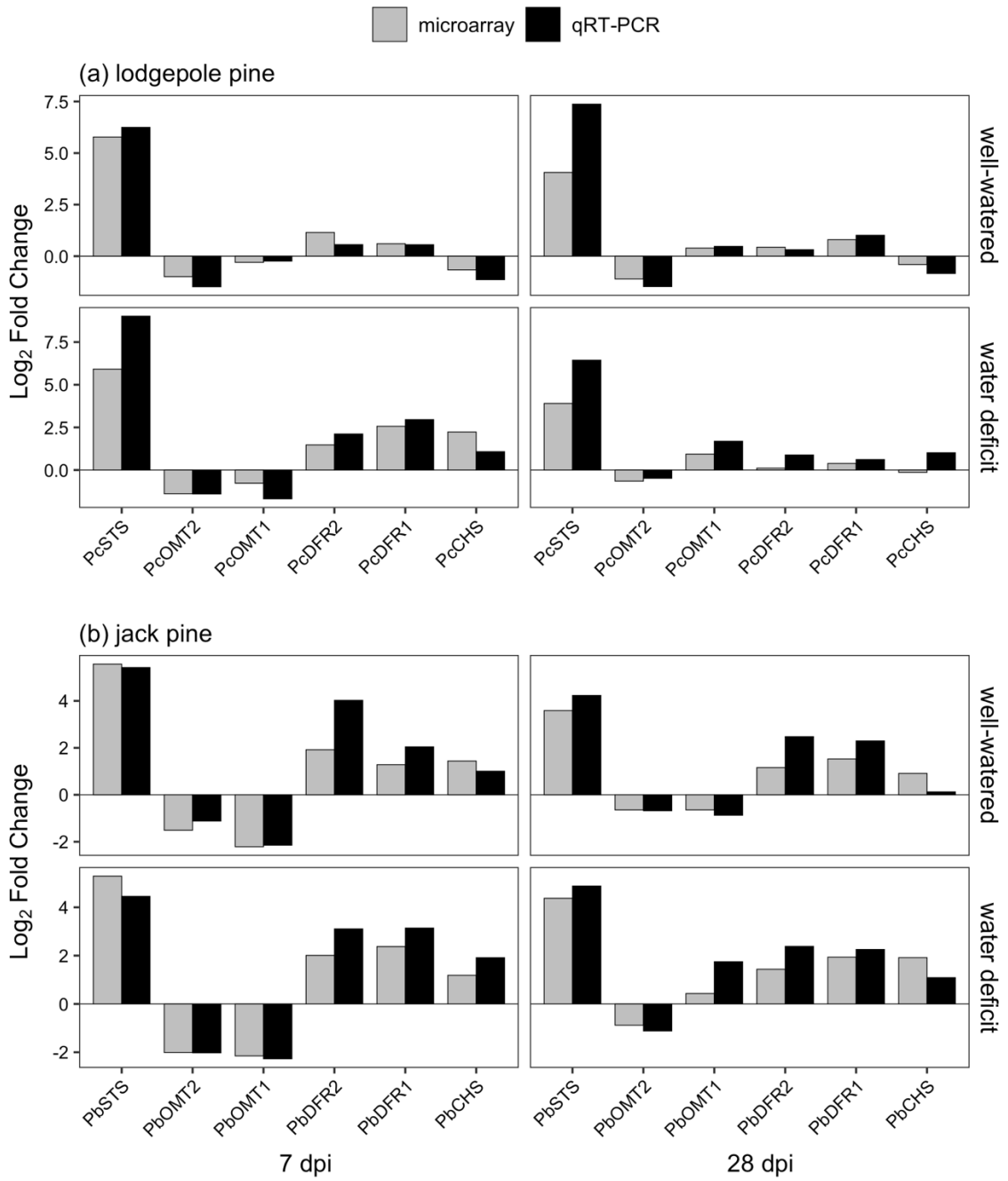

Appendix 2 Figure 5. Comparison of relative gene expression of lodgepole and jack pine seedlings measured using microarray and qRT-PCR methods. Bars represent the average $\log_2$ fold change between transcript abundance in seedlings inoculated with *G. clavigera* and unwounded controls under well-watered or water deficit conditions. Microarray values (grey bars) were averaged across all PtGen2 sequences that would theoretically be amplified by each qRT-PCR primer set (mismatches < 3). qRT-PCR transcript abundance (black bars) were normalized to reference gene expression prior to calculating fold change.

Appendix 2 Table 4. PtGen2 microarray sequences DE at 7 and 28 dpi in xylem of both lodgepole and jack pine inoculated with *G. clavigera* relative to uninoculated controls under both well-watered and water deficit conditions. TAIR annotations were assigned based on lodgepole and jack pine contigs representing the best match to each PtGen2 sequence; unique annotations between lodgepole and jack pine contigs are separated by a vertical bar (|). PtGen2 sequences were collapsed into non-redundant annotations based on identical TAIR and MapMan annotations.

Putative Identity	PtGen2 Spot ID	TAIR Accession	TAIR Annotation	MapMan Bin	MapMan Annotation
Defense-related sequences DE in lodgepole and jack pine at 7 and 28 dpi					
salicylic acid biosynthesis	47.8.2	AT4G36470.1	S-adenosyl-L-methionine-dependent methyltransferases superfamily protein	17.8.1	hormone metabolism; salicylic acid; synthesis-degradation
dirigent-like	3.17.2	AT5G42510.1	Disease resistance-responsive (dirigent-like protein) family protein	20.1.7	stress; biotic; PR-proteins
dirigent-like	8.10.8	AT5G42510.1	Disease resistance-responsive (dirigent-like protein) family protein	35.2	not assigned; unknown
PR gene-like	7.6.3	AT3G04720.1	pathogenesis-related 4	20.1	stress; biotic
PR gene-like	2.9.5, 20.20.2	AT4G25780.1 | AT4G33720.1	CAP (Cysteine-rich secretory proteins, Antigen 5, and Pathogenesis-related 1 protein) superfamily protein	20.1	stress; biotic
thaumatin-like	48.24.5	AT1G19320.1 | AT1G75040.1	Pathogenesis-related thaumatin superfamily protein | pathogenesis-related gene 5	20.1	stress; biotic

Putative Identity	PtGen2 Spot ID	TAIR Accession	TAIR Annotation	MapMan Bin	MapMan Annotation
thaumatin-like	52.14.10, 63.13.12	AT1G19320.1 | AT4G11650.1	Pathogenesis-related thaumatin superfamily protein | osmotin 34	35.2	not assigned; unknown
thaumatin-like	41.22.12, 42.10.2, 67.16.4, 7.15.16	AT4G11650.1	osmotin 34	20.2	stress; abiotic
isoprenoid biosynthesis	64.4.2	AT3G25810.1	Terpenoid cyclases/Protein prenyltransferases superfamily protein	16.1.5	secondary metabolism; isoprenoids; terpenoids
WRKY-like TF	63.6.13	AT4G22070.1	WRKY DNA-binding protein 31	35.2	not assigned; unknown
WRKY-like TF	67.21.8	AT5G64810.1	WRKY DNA-binding protein 51	35.2	not assigned; unknown
Defense-related sequences DE in lodgepole and jack pine at 7 dpi only					
auxin biosynthesis	23.1.13	AT5G55250.2	IAA carboxylmethyltransferase 1	17.2.1	hormone metabolism; auxin; synthesis-degradation
auxin-regulated	16.20.6, 22.14.15, 55.11.12	AT5G43830.1	Aluminium induced protein with YGL and LRDR motifs	17.2.3	hormone metabolism; auxin; induced-regulated-responsive-activated
ethylene biosynthesis	46.23.12	AT1G77330.1	2-oxoglutarate (2OG) and Fe(II)-dependent oxygenase superfamily protein	17.5.1.2	hormone metabolism; ethylene; synthesis-degradation; 1-aminocyclopropane-1-carboxylate oxidase

Putative Identity	PtGen2 Spot ID	TAIR Accession	TAIR Annotation	MapMan Bin	MapMan Annotation
ethylene-regulated	15.24.6, 22.18.2	AT1G50640.1 | AT1G28370.1	ethylene responsive element binding factor 3 | ERF domain protein 11	17.5.2	hormone metabolism; ethylene; signal transduction
ethylene-regulated	67.2.5	N/A | AT5G47220.1	NA | ethylene responsive element binding factor 2	17.5.2	hormone metabolism; ethylene; signal transduction
jasmonate biosynthesis	45.7.7	AT3G22400.1	PLAT/LH2 domain-containing lipoxygenase family protein	17.7.1.2	hormone metabolism; jasmonate; synthesis-degradation; lipoxygenase
NBS-LRR-like	22.22.9	AT1G69550.1	disease resistance protein (TIR-NBS-LRR class)	35.2	not assigned; unknown
NBS-LRR-like	2.21.8	AT5G41740.2 | AT5G19340.1	Disease resistance protein (TIR-NBS-LRR class) family | unknown protein	35.2	not assigned; unknown
NBS-LRR-like	64.1.5	N/A | AT5G43740.2	NA | Disease resistance protein (CC-NBS-LRR class) family	35.2	not assigned; unknown
chitinase-like	4.9.8, 6.13.15, 8.11.4	AT3G12500.1	basic chitinase	20.1	stress; biotic
chitinase-like	54.11.14, 67.14.8	AT4G19810.1	Glycosyl hydrolase family protein with chitinase insertion domain	20.1	stress; biotic
chitinase-like	37.4.16	N/A | AT4G19810.1	NA | Glycosyl hydrolase family protein with chitinase insertion domain	35.2	not assigned; unknown

Putative Identity	PtGen2 Spot ID	TAIR Accession	TAIR Annotation	MapMan Bin	MapMan Annotation
dirigent-like	20.5.11	AT2G21100.1	Disease resistance-responsive (dirigent-like protein) family protein	20.1.7	stress; biotic; PR-proteins
thaumatin-like	6.21.13	AT1G19320.1	Pathogenesis-related thaumatin superfamily protein	20.1	stress; biotic
thaumatin-like	58.7.8	AT4G11650.1	osmotin 34	20.2	stress; abiotic
flavonoid biosynthesis	69.23.15	AT4G10500.1	2-oxoglutarate (2OG) and Fe(II)-dependent oxygenase superfamily protein	16.8.1	secondary metabolism; flavonoids; anthocyanins
flavonoid biosynthesis	65.14.8	AT5G42800.1	dihydroflavonol 4-reductase	16.8.1.2	secondary metabolism; flavonoids; anthocyanins; anthocyanidin reductase
phenylpropanoid biosynthesis	7.20.7	AT5G54160.1 | AT1G77520.1	O-methyltransferase 1 | O-methyltransferase family protein	16.2.1.9	secondary metabolism; phenylpropanoids; lignin biosynthesis; COMT
ERF-like TF	66.9.8	AT3G20310.1 | AT1G27170.2	ethylene response factor 7 | transmembrane receptors	35.2	not assigned; unknown
WRKY-like TF	61.4.15	AT1G62300.1	WRKY family transcription factor	35.2	not assigned; unknown

Appendix 2 Table 5. PtGen2 microarray sequences DE earlier between xylem of lodgepole or jack pine inoculated with *G. clavigera* relative to uninoculated controls under well-watered conditions. TAIR annotations were assigned based on lodgepole and jack pine contigs representing the best match to each PtGen2 sequence; unique annotations between lodgepole and jack pine contigs are separated by a vertical bar (|). PtGen2 sequences were collapsed into non-redundant annotations based on identical TAIR and MapMan annotations.

Putative Identity	PtGen2 Spot ID	TAIR Accession	TAIR Annotation	MapMan Bin	MapMan Annotation
Defense-related sequences DE earlier in lodgepole pine than jack pine under well-watered conditions					
chitinase-like	10.22.14, 3.20.14, 46.12.5, 50.3.4, 69.22.14	AT3G12500.1	basic chitinase	20.1	stress; biotic
isoprenoid biosynthesis	63.20.12	AT4G16730.1 | AT4G02780.1	terpene synthase 02 | Terpenoid cyclases/Protein prenyltransferases superfamily protein	16.1.5	secondary metabolism; isoprenoids; terpenoids
phenylpropanoid biosynthesis	66.14.13	AT4G39330.1	cinnamyl alcohol dehydrogenase 9	16.2.1.10	secondary metabolism; phenylpropanoids; lignin biosynthesis; CAD
MYB-like TF	4.19.3	AT4G38620.1 | AT1G48490.3	myb domain protein 4 | Protein kinase superfamily protein	27.3.25	RNA; regulation of transcription; MYB domain transcription factor family
WRKY-like TF	43.20.9	AT5G26170.1 | N/A	WRKY DNA-binding protein 50 | NA	27.3.32	RNA; regulation of transcription; WRKY domain transcription factor family
Defense-related sequences DE earlier in jack pine than lodgepole pine under well-watered conditions					
auxin-regulated	22.2.5	AT1G60710.1 | N/A	NAD(P)-linked oxidoreductase superfamily protein | NA	17.2.3	hormone metabolism; auxin; induced-regulated-responsive-activated

Putative Identity	PtGen2 Spot ID	TAIR Accession	TAIR Annotation	MapMan Bin	MapMan Annotation
jasmonate biosynthesis	37.7.3	AT3G22400.1 | AT1G55020.1	PLAT/LH2 domain-containing lipoxygenase family protein | lipoxygenase 1	17.7.1.2	hormone metabolism; jasmonate; synthesis-degradation; lipoxygenase
jasmonate biosynthesis	50.4.9	N/A	NA	17.7.1.5	hormone metabolism; jasmonate; synthesis-degradation; 12-Oxo-PDA-reductase
NBS-LRR-like	5.6.4	AT5G46450.1 | N/A	Disease resistance protein (TIR-NBS-LRR class) family | NA	2.2.1.5	major CHO metabolism; degradation; sucrose; Susy
NBS-LRR-like	4.11.7	AT5G46510.1	Disease resistance protein (TIR-NBS-LRR class) family	35.2	not assigned; unknown
dirigent-like	15.18.7	AT5G42510.1	Disease resistance-responsive (dirigent-like protein) family protein	35.2	not assigned; unknown
PR gene-like	27.23.6, 56.2.12	AT4G25780.1 | N/A	CAP (Cysteine-rich secretory proteins, Antigen 5, and Pathogenesis-related 1 protein) superfamily protein | NA	20.1	stress; biotic
flavonoid biosynthesis	36.13.8	AT3G21480.1 | N/A	BRCT domain-containing DNA repair protein | NA	16.8.1.1	secondary metabolism; flavonoids; anthocyanins; leucocyanidin dioxygenase
flavonoid biosynthesis	8.6.3	AT3G51240.2 | AT3G51240.1	flavanone 3-hydroxylase	16.8.3.2	secondary metabolism; flavonoids; dihydroflavonols; flavanone 3-hydroxylase
flavonoid biosynthesis	21.3.8	AT4G10490.1	2-oxoglutarate (2OG) and Fe(II)-dependent oxygenase superfamily protein	16.8.3	secondary metabolism; flavonoids; dihydroflavonols

Putative Identity	PtGen2 Spot ID	TAIR Accession	TAIR Annotation	MapMan Bin	MapMan Annotation
flavonoid biosynthesis	61.10.1	AT4G22880.2	leucoanthocyanidin dioxygenase	16.8.1.1	secondary metabolism; flavonoids; anthocyanins; leucocyanidin dioxygenase
flavonoid biosynthesis	35.13.12	AT5G05270.2	Chalcone-flavanone isomerase family protein	16.8.2	secondary metabolism; flavonoids; chalcones
flavonoid biosynthesis	56.11.13	AT5G13930.1	Chalcone and stilbene synthase family protein	16.8.2.1	secondary metabolism; flavonoids; chalcones; naringenin-chalcone synthase
flavonoid biosynthesis	15.6.7	AT5G42800.1	dihydroflavonol 4-reductase	16.8.3.1	secondary metabolism; flavonoids; dihydroflavonols; dihydroflavonol 4-reductase
isoprenoid biosynthesis	64.4.5, 66.14.3	AT1G63970.1	isoprenoid F	16.1.1.5	secondary metabolism; isoprenoids; non-mevalonate pathway; MCS
isoprenoid biosynthesis	15.13.2	AT2G17370.1	3-hydroxy-3-methylglutaryl-CoA reductase 2	16.1.2.3	secondary metabolism; isoprenoids; mevalonate pathway; HMG-CoA reductase
isoprenoid biosynthesis	10.22.15	AT4G16730.1 | AT2G41710.1	terpene synthase 02 | Integrase-type DNA-binding superfamily protein	16.1.5	secondary metabolism; isoprenoids; terpenoids
isoprenoid biosynthesis	42.15.9	AT5G47770.1	farnesyl diphosphate synthase 1	16.1.2.9	secondary metabolism; isoprenoids; mevalonate pathway; farnesyl pyrophosphate synthetase
phenylpropanoid biosynthesis	10.10.7	AT4G34050.2 | AT4G34050.1	S-adenosyl-L-methionine-dependent methyltransferases superfamily protein	16.2.1.6	secondary metabolism; phenylpropanoids; lignin biosynthesis; CCoAOMT
WRKY-like TF	67.7.3	AT5G26170.1 | N/A	WRKY DNA-binding protein 50 | NA	27.3.32	RNA; regulation of transcription; WRKY domain transcription factor family

Appendix 2 Table 6. PtGen2 microarray sequences DE earlier between xylem of lodgepole or jack pine inoculated with *G. clavigera* relative to uninoculated controls under water deficit conditions. TAIR annotations were assigned based on lodgepole and jack pine contigs representing the best match to each PtGen2 sequence; unique annotations between lodgepole and jack pine contigs are separated by a vertical bar (|). PtGen2 sequences were collapsed into non-redundant annotations based on identical TAIR and MapMan annotations.

Putative Identity	PtGen2 Spot ID	TAIR Accession	TAIR Annotation	MapMan Bin	MapMan Annotation
Defense-related sequences DE earlier in lodgepole pine than jack pine under water deficit conditions					
auxin-regulated	38.21.2	AT1G60710.1	NAD(P)-linked oxidoreductase superfamily protein	17.2.3	hormone metabolism; auxin; induced-regulated-responsive-activated
auxin-regulated	59.9.5, 35.22.4	AT1G60710.1 | AT1G60730.3	NAD(P)-linked oxidoreductase superfamily protein	17.2.3	hormone metabolism; auxin; induced-regulated-responsive-activated
auxin-regulated	2.15.4	AT1G60730.3	NAD(P)-linked oxidoreductase superfamily protein	17.2.3	hormone metabolism; auxin; induced-regulated-responsive-activated
ethylene-regulated	2.13.13	AT5G47220.1	ethylene responsive element binding factor 2	17.5.2	hormone metabolism; ethylene; signal transduction
jasmonate biosynthesis	4.14.1	AT1G76690.1	12-oxophytodienoate reductase 2	17.7.1.5	hormone metabolism; jasmonate; synthesis-degradation; 12-Oxo-PDA-reductase
salicylic acid biosynthesis	10.5.13	AT5G55250.2	IAA carboxylmethyltransferase 1	17.8.1	hormone metabolism; salicylic acid; synthesis-degradation

Putative Identity	PtGen2 Spot ID	TAIR Accession	TAIR Annotation	MapMan Bin	MapMan Annotation
BSP-like	7.6.7	AT2G15220.1	Plant basic secretory protein (BSP) family protein	20.1	stress; biotic
chitinase-like	10.22.14, 3.20.14, 46.12.5, 50.3.4, 69.22.14	AT3G12500.1	basic chitinase	20.1	stress; biotic
dirigent-like	39.23.11	AT1G64160.1	Disease resistance-responsive (dirigent-like protein) family protein	20.1.7	stress; biotic; PR-proteins
thaumatin-like	8.24.16	AT1G19320.1	Pathogenesis-related thaumatin superfamily protein	20.1	stress; biotic
thaumatin-like	30.3.2, 62.4.7	AT4G11650.1	osmotin 34	20.2	stress; abiotic
flavonoid biosynthesis	13.22.9	AT4G01070.2 | AT5G26310.1	UDP-Glycosyltransferase superfamily protein	16.8.3	secondary metabolism; flavonoids; dihydroflavonols
flavonoid biosynthesis	27.9.6, 63.19.6	AT5G13930.1	Chalcone and stilbene synthase family protein	16.8.2.1	secondary metabolism; flavonoids; chalcones; naringenin-chalcone synthase
isoprenoid biosynthesis	63.7.6	AT1G48800.1 | AT4G16730.1	Terpenoid cyclases/Protein prenyltransferases superfamily protein | terpene synthase 02	16.1.5	secondary metabolism; isoprenoids; terpenoids
isoprenoid biosynthesis	64.4.5	AT1G63970.1	isoprenoid F	16.1.1.5	secondary metabolism; isoprenoids; non-mevalonate pathway; MCS
isoprenoid biosynthesis	29.5.2	AT1G64970.1	gamma-tocopherol methyltransferase	16.1.3.5	secondary metabolism; isoprenoids; tocopherol biosynthesis; tocopherol methyltransferase

Putative Identity	PtGen2 Spot ID	TAIR Accession	TAIR Annotation	MapMan Bin	MapMan Annotation
phenylpropanoid biosynthesis	64.7.9	AT5G58490.1	NAD(P)-binding Rossmann-fold superfamily protein	16.2.1.7	secondary metabolism; phenylpropanoids; lignin biosynthesis; CCR1
ARF-like TF	65.1.12	AT5G62000.3	auxin response factor 2	27.3.4	RNA; regulation of transcription; ARF, Auxin Response Factor family
MYB-like TF	4.19.3	AT4G38620.1 | AT1G48490.3	myb domain protein 4 | Protein kinase superfamily protein	27.3.25	RNA; regulation of transcription; MYB domain transcription factor family
NAC-like TF	1.20.14	N/A | AT1G65910.1	NA | NAC domain containing protein 28	35.2	not assigned; unknown
WRKY-like TF	43.20.9	AT5G26170.1 | N/A	WRKY DNA-binding protein 50 | NA	27.3.32	RNA; regulation of transcription; WRKY domain transcription factor family
Defense-related sequences DE earlier in jack pine than lodgepole pine under water deficit conditions					
chitinase-like	33.6.7, 40.20.6	AT3G16920.1	chitinase-like protein 2	20.1	stress; biotic

Appendix 2 Table 7. PtGen2 microarray sequences DE later under water deficit in xylem of lodgepole or jack pine inoculated with *G. clavigera* relative to uninoculated controls. TAIR annotations were assigned based on lodgepole and jack pine contigs representing the best match to each PtGen2 sequence; unique annotations between lodgepole and jack pine contigs are separated by a vertical bar (|). PtGen2 sequences were collapsed into non-redundant annotations based on identical TAIR and MapMan annotations.

Putative Identity	PtGen2 Spot ID	TAIR Accession	TAIR Annotation	MapMan Bin	MapMan Annotation
Defense-related sequences with DE delayed by water deficit exclusively in jack pine					
auxin-regulated	35.22.4	AT1G60710.1 | AT1G60730.3	NAD(P)-linked oxidoreductase superfamily protein	17.2.3	hormone metabolism; auxin; induced-regulated-responsive-activated
auxin-regulated	2.15.4	AT1G60730.3	NAD(P)-linked oxidoreductase superfamily protein	17.2.3	hormone metabolism; auxin; induced-regulated-responsive-activated
jasmonate biosynthesis	4.3.16	AT1G55020.1	lipoxygenase 1	17.7.1.2	hormone metabolism; jasmonate; synthesis-degradation; lipoxygenase
jasmonate biosynthesis	4.14.1	AT1G76690.1	12-oxophytodienoate reductase 2	17.7.1.5	hormone metabolism; jasmonate; synthesis-degradation; 12-Oxo-PDA-reductase
BSP-like	1.23.8	AT2G15220.1	Plant basic secretory protein (BSP) family protein	20.1	stress; biotic
NBS-LRR-like	62.9.5	AT1G27180.1 | AT5G44510.1	disease resistance protein (TIR-NBS-LRR class), putative | target of AVRB operation1	20.1.7	stress; biotic; PR-proteins
NBS-LRR-like	7.15.11	AT1G69550.1	disease resistance protein (TIR-NBS-LRR class)	35.2	not assigned; unknown

Putative Identity	PtGen2 Spot ID	TAIR Accession	TAIR Annotation	MapMan Bin	MapMan Annotation
NBS-LRR-like	62.18.16	AT5G35450.1 | AT4G12010.1	Disease resistance protein (CC-NBS-LRR class) family | Disease resistance protein (TIR-NBS-LRR class) family	35.2	not assigned; unknown
NBS-LRR-like	5.6.4	AT5G46450.1 | N/A	Disease resistance protein (TIR-NBS-LRR class) family | NA	2.2.1.5	major CHO metabolism; degradation; sucrose; Susy
dirigent-like	39.23.11	AT1G64160.1	Disease resistance-responsive (dirigent-like protein) family protein	20.1.7	stress; biotic; PR-proteins
thaumatin-like	30.3.2, 62.4.7	AT4G11650.1	osmotin 34	20.2	stress; abiotic
flavonoid biosynthesis	53.22.6	AT3G21420.1	2-oxoglutarate (2OG) and Fe(II)-dependent oxygenase superfamily protein	16.8.4	secondary metabolism; flavonoids; flavonols
flavonoid biosynthesis	26.19.4, 5.21.13	AT4G39230.1	NmrA-like negative transcriptional regulator family protein	16.8.5.1	secondary metabolism; flavonoids; isoflavones; isoflavone reductase
flavonoid biosynthesis	29.21.12	AT5G01210.1	HXXXD-type acyl-transferase family protein	16.8.1	secondary metabolism; flavonoids; anthocyanins
flavonoid biosynthesis	27.9.6	AT5G13930.1	Chalcone and stilbene synthase family protein	16.8.2.1	secondary metabolism; flavonoids; chalcones; naringenin-chalcone synthase
isoprenoid biosynthesis	63.7.6	AT1G48800.1 | AT4G16730.1	Terpenoid cyclases/Protein prenyltransferases superfamily protein | terpene synthase 02	16.1.5	secondary metabolism; isoprenoids; terpenoids
isoprenoid biosynthesis	64.4.5	AT1G63970.1	isoprenoid F	16.1.1.5	secondary metabolism; isoprenoids; non-mevalonate pathway; MCS

Putative Identity	PtGen2 Spot ID	TAIR Accession	TAIR Annotation	MapMan Bin	MapMan Annotation
phenylpropanoid biosynthesis	10.10.7	AT4G34050.2 | AT4G34050.1	S-adenosyl-L-methionine-dependent methyltransferases superfamily protein	16.2.1.6	secondary metabolism; phenylpropanoids; lignin biosynthesis; CCoAOMT
phenylpropanoid biosynthesis	64.7.9	AT5G58490.1	NAD(P)-binding Rossmann-fold superfamily protein	16.2.1.7	secondary metabolism; phenylpropanoids; lignin biosynthesis; CCR1

Appendix 2 Table 8. PtGen2 microarray sequences DE earlier under water deficit in xylem of lodgepole or jack pine inoculated with *G. clavigera* relative to uninoculated controls. TAIR annotations were assigned based on lodgepole and jack pine contigs representing the best match to each PtGen2 sequence; unique annotations between lodgepole and jack pine contigs are separated by a vertical bar (|). PtGen2 sequences were collapsed into non-redundant annotations based on identical TAIR and MapMan annotations.

Putative Identity	PtGen2 Spot ID	TAIR Accession	TAIR Annotation	MapMan Bin	MapMan Annotation
Defense-related sequences with DE earlier under water deficit exclusively in lodgepole pine					
auxin-regulated	2.5.4, 55.18.7	AT1G60710.1	NAD(P)-linked oxidoreductase superfamily protein	17.2.3	hormone metabolism; auxin; induced-regulated-responsive-activated
auxin-regulated	22.2.5	AT1G60710.1 | N/A	NAD(P)-linked oxidoreductase superfamily protein | NA	17.2.3	hormone metabolism; auxin; induced-regulated-responsive-activated
ethylene-regulated	5.8.7	AT1G09740.1	Adenine nucleotide alpha hydrolases-like superfamily protein	17.5.3	hormone metabolism; ethylene; induced-regulated-responsive-activated
jasmonate biosynthesis	37.7.3	AT3G22400.1 | AT1G55020.1	PLAT/LH2 domain-containing lipoxygenase family protein | lipoxygenase 1	17.7.1.2	hormone metabolism; jasmonate; synthesis-degradation; lipoxygenase
jasmonate biosynthesis	50.4.9	N/A	NA	17.7.1.5	hormone metabolism; jasmonate; synthesis-degradation; 12-Oxo-PDA-reductase
NBS-LRR-like	4.11.7	AT5G46510.1	Disease resistance protein (TIR-NBS-LRR class) family	35.2	not assigned; unknown
PR gene-like	27.23.6, 56.2.12	AT4G25780.1 | N/A	CAP (Cysteine-rich secretory proteins, Antigen 5, and Pathogenesis-related 1 protein) superfamily protein | NA	20.1	stress; biotic

Putative Identity	PtGen2 Spot ID	TAIR Accession	TAIR Annotation	MapMan Bin	MapMan Annotation
thaumatin-like	8.24.16	AT1G19320.1	Pathogenesis-related thaumatin superfamily protein	20.1	stress; biotic
flavonoid biosynthesis	36.10.15	AT1G61720.1	NAD(P)-binding Rossmann-fold superfamily protein	16.8.1.2	secondary metabolism; flavonoids; anthocyanins; anthocyanidin reductase
flavonoid biosynthesis	16.3.5	AT1G75290.1	NAD(P)-binding Rossmann-fold superfamily protein	16.8.5.1	secondary metabolism; flavonoids; isoflavones; isoflavone reductase
flavonoid biosynthesis	36.13.8	AT3G21480.1 | N/A	BRCT domain-containing DNA repair protein | NA	16.8.1.1	secondary metabolism; flavonoids; anthocyanins; leucocyanidin dioxygenase
flavonoid biosynthesis	8.6.3	AT3G51240.2 | AT3G51240.1	flavanone 3-hydroxylase	16.8.3.2	secondary metabolism; flavonoids; dihydroflavonols; flavanone 3-hydroxylase
flavonoid biosynthesis	33.3.14	AT4G01070.1 | AT3G46700.1	UDP-Glycosyltransferase superfamily protein	16.8.3	secondary metabolism; flavonoids; dihydroflavonols
flavonoid biosynthesis	21.3.8	AT4G10490.1	2-oxoglutarate (2OG) and Fe(II)-dependent oxygenase superfamily protein	16.8.3	secondary metabolism; flavonoids; dihydroflavonols
flavonoid biosynthesis	61.10.1	AT4G22880.2	leucoanthocyanidin dioxygenase	16.8.1.1	secondary metabolism; flavonoids; anthocyanins; leucocyanidin dioxygenase
flavonoid biosynthesis	35.13.12	AT5G05270.2	Chalcone-flavanone isomerase family protein	16.8.2	secondary metabolism; flavonoids; chalcones
flavonoid biosynthesis	56.11.13	AT5G13930.1	Chalcone and stilbene synthase family protein	16.8.2.1	secondary metabolism; flavonoids; chalcones; naringenin-chalcone synthase

Putative Identity	PtGen2 Spot ID	TAIR Accession	TAIR Annotation	MapMan Bin	MapMan Annotation
flavonoid biosynthesis	15.6.7	AT5G42800.1	dihydroflavonol 4-reductase	16.8.3.1	secondary metabolism; flavonoids; dihydroflavonols; dihydroflavonol 4-reductase
isoprenoid biosynthesis	64.4.5, 66.14.3	AT1G63970.1	isoprenoid F	16.1.1.5	secondary metabolism; isoprenoids; non-mevalonate pathway; MCS
isoprenoid biosynthesis	15.13.2	AT2G17370.1	3-hydroxy-3-methylglutaryl-CoA reductase 2	16.1.2.3	secondary metabolism; isoprenoids; mevalonate pathway; HMG-CoA reductase
isoprenoid biosynthesis	10.22.15	AT4G16730.1 | AT2G41710.1	terpene synthase 02 | Integrase-type DNA-binding superfamily protein	16.1.5	secondary metabolism; isoprenoids; terpenoids
Defense-related sequences with DE earlier under water deficit exclusively in jack pine					
jasmonate biosynthesis	10.6.13, 69.6.13	AT3G22400.1	PLAT/LH2 domain-containing lipoxygenase family protein	17.7.1.2	hormone metabolism; jasmonate; synthesis-degradation; lipoxygenase
flavonoid biosynthesis	17.9.15	AT1G61720.1	NAD(P)-binding Rossmann-fold superfamily protein	16.8.1.2	secondary metabolism; flavonoids; anthocyanins; anthocyanidin reductase
flavonoid biosynthesis	38.9.16	AT5G42800.1 | AT1G61720.1	dihydroflavonol 4-reductase | NAD(P)-binding Rossmann-fold superfamily protein	16.8.3.1	secondary metabolism; flavonoids; dihydroflavonols; dihydroflavonol 4-reductase
isoprenoid biosynthesis	63.20.12	AT4G16730.1 | AT4G02780.1	terpene synthase 02 | Terpenoid cyclases/Protein prenyltransferases superfamily protein	16.1.5	secondary metabolism; isoprenoids; terpenoids
phenylpropanoid biosynthesis	66.14.13	AT4G39330.1	cinnamyl alcohol dehydrogenase 9	16.2.1.10	secondary metabolism; phenylpropanoids; lignin biosynthesis; CAD

Appendix 2 Table 9. Summary of analysis of deviance of generalized linear models fit to xylem phenolic biosynthesis qRT-PCR expression data. Asterisks (*) indicate interactions between factors. All genes were fit to the following formula: normalized transcript abundance ~ time point * water treatment * inoculation treatment, family = Gamma (link = log).

	lodgepole pine			jack pine		
	df	χ^2	*p*	df	χ^2	*p*
stilbene synthase (STS)						
water treatment	1	9.28	$\mathbf{2.32 \times 10^{-3}}$	1	0.00	9.62×10^{-1}
inoculation treatment	2	375.43	$\mathbf{3.00 \times 10^{-82}}$	2	278.61	$\mathbf{3.16 \times 10^{-61}}$
time point	3	130.22	$\mathbf{4.84 \times 10^{-28}}$	3	43.53	$\mathbf{1.90 \times 10^{-9}}$
water * inoculation	2	3.36	1.87×10^{-1}	2	1.90	3.87×10^{-1}
water * time point	3	2.42	4.90×10^{-1}	3	1.92	5.89×10^{-1}
inoculation * time point	6	181.74	$\mathbf{1.45 \times 10^{-36}}$	6	76.84	$\mathbf{1.60 \times 10^{-14}}$
water * inoculation * time point	6	17.58	$\mathbf{7.37 \times 10^{-3}}$	6	6.37	3.83×10^{-1}
dihydroflavonol reductase 1 (DFR1)						
water treatment	1	2.11	1.47×10^{-1}	1	0.17	6.81×10^{-1}
inoculation treatment	2	104.09	$\mathbf{2.50 \times 10^{-23}}$	2	318.76	$\mathbf{6.05 \times 10^{-70}}$
time point	3	18.97	$\mathbf{2.78 \times 10^{-4}}$	3	13.60	$\mathbf{3.50 \times 10^{-3}}$
water * inoculation	2	2.51	2.85×10^{-1}	2	6.21	$\mathbf{4.49 \times 10^{-2}}$
water * time point	3	1.26	7.38×10^{-1}	3	4.11	2.49×10^{-1}
inoculation * time point	6	26.29	$\mathbf{1.97 \times 10^{-4}}$	6	44.43	$\mathbf{6.07 \times 10^{-8}}$
water * inoculation * time point	6	14.04	$\mathbf{2.92 \times 10^{-2}}$	6	8.32	2.15×10^{-1}
dihydroflavonol reductase 2 (DFR2)						
water treatment	1	1.85	1.74×10^{-1}	1	13.16	$\mathbf{2.87 \times 10^{-4}}$
inoculation treatment	2	40.54	$\mathbf{1.57 \times 10^{-9}}$	2	119.94	$\mathbf{9.00 \times 10^{-27}}$
time point	3	38.52	$\mathbf{2.19 \times 10^{-8}}$	3	59.41	$\mathbf{7.87 \times 10^{-13}}$
water * inoculation	2	1.73	4.21×10^{-1}	2	0.43	8.06×10^{-1}
water * time point	3	9.06	$\mathbf{2.85 \times 10^{-2}}$	3	4.50	2.12×10^{-1}

	lodgepole pine			jack pine		
	df	**χ^2**	***p***	**df**	**χ^2**	***p***
inoculation * time point	6	18.15	$\mathbf{5.88 \times 10^{-3}}$	6	21.17	$\mathbf{1.71 \times 10^{-3}}$
water * inoculation * time point	6	4.16	6.55×10^{-1}	6	1.98	9.21×10^{-1}
stilbene o-methyltransferase 1 (OMT1)						
water treatment	1	114.46	$\mathbf{1.04 \times 10^{-26}}$	1	123.02	$\mathbf{1.38 \times 10^{-28}}$
inoculation treatment	2	13.15	$\mathbf{1.39 \times 10^{-3}}$	2	91.14	$\mathbf{1.62 \times 10^{-20}}$
time point	3	164.11	$\mathbf{2.38 \times 10^{-35}}$	3	154.59	$\mathbf{2.70 \times 10^{-33}}$
water * inoculation	2	0.23	8.90×10^{-1}	2	5.68	5.85×10^{-2}
water * time point	3	54.09	$\mathbf{1.08 \times 10^{-11}}$	3	94.45	$\mathbf{2.42 \times 10^{-20}}$
inoculation * time point	6	44.26	$\mathbf{6.57 \times 10^{-8}}$	6	91.57	$\mathbf{1.43 \times 10^{-17}}$
water * inoculation * time point	6	9.76	1.35×10^{-1}	6	28.88	$\mathbf{6.41 \times 10^{-5}}$
stilbene o-methyltransferase 2 (OMT2)						
water treatment	1	3.24	$\mathbf{7.19 \times 10^{-2}}$	1	9.78	$\mathbf{1.76 \times 10^{-3}}$
inoculation treatment	2	62.26	$\mathbf{3.02 \times 10^{-14}}$	2	28.46	$\mathbf{6.60 \times 10^{-7}}$
time point	3	39.93	$\mathbf{1.10 \times 10^{-8}}$	3	139.53	$\mathbf{4.78 \times 10^{-30}}$
water * inoculation	2	2.13	3.45×10^{-1}	2	2.35	3.09×10^{-1}
water * time point	3	11.23	$\mathbf{1.06 \times 10^{-2}}$	3	6.76	7.98×10^{-2}
inoculation * time point	6	37.43	$\mathbf{1.45 \times 10^{-6}}$	6	88.44	$\mathbf{6.38 \times 10^{-17}}$
water * inoculation * time point	6	5.88	4.36×10^{-1}	6	3.95	6.83×10^{-1}
chalcone synthase (CHS)						
water treatment	1	6.36	$\mathbf{1.17 \times 10^{-2}}$	1	33.98	$\mathbf{5.56 \times 10^{-9}}$
inoculation treatment	2	6.09	$\mathbf{4.75 \times 10^{-2}}$	2	43.11	$\mathbf{4.36 \times 10^{-10}}$
time point	3	100.82	$\mathbf{1.03 \times 10^{-21}}$	3	227.05	$\mathbf{6.02 \times 10^{-49}}$
water * inoculation	2	16.32	$\mathbf{2.85 \times 10^{-4}}$	2	5.29	7.09×10^{-2}
water * time point	3	4.01	2.61×10^{-1}	3	1.54	6.73×10^{-1}
inoculation * time point	6	15.76	$\mathbf{1.51 \times 10^{-2}}$	6	39.71	$\mathbf{5.19 \times 10^{-7}}$
water * inoculation * time point	6	5.76	4.50×10^{-1}	6	7.79	2.54×10^{-1}

Appendix 3

List of Figures and Tables

Appendix 3 Figure 1. Distribution of trees selected for MPB attack (purple) and *G. clavigera* inoculation (green) experiments at field site (54º27′N, 118º37′W).

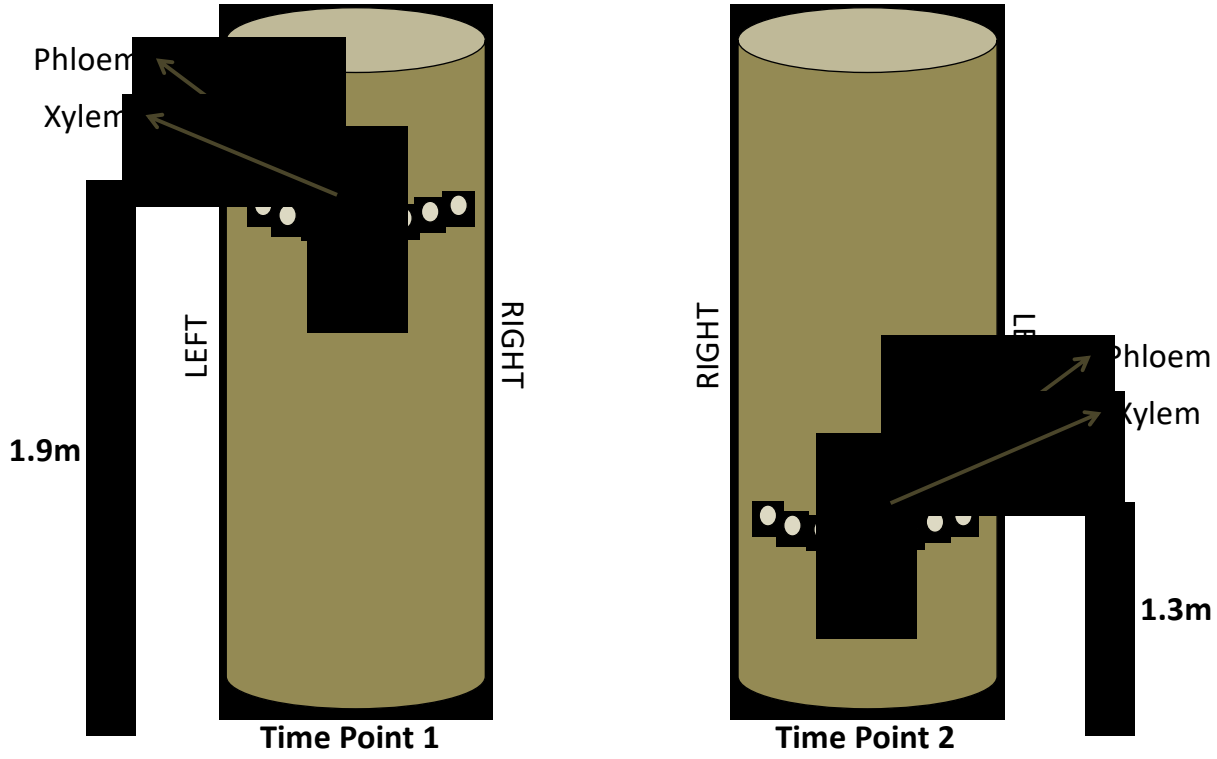

Appendix 3 Figure 2. Tissue collection from lodgepole pine trunks at each timepoint. Phloem and xylem were sampled at 1.9 m height for the first collection (1 dpw or 7 dpi), while tissue for second collection (7 dpw or 14 dpi) was sampled at 1.3 m on the opposite side of the trunk for the same trees. Circles represent locations of mock-inoculation, G. clavigera-inoculation, or mock-attack. Control samples were collected at the same locations on untreated trees.

Appendix 3 Figure 3. Collection of phloem and xylem tissue from *G. clavigera*-inoculated lodgepole pine trees. a Removal of bark and secondary phloem using a chisel at 1.9 m (1.6 m tall researcher for reference). **b** Secondary phloem removed from bark. **c** Collection of secondary xylem using a spokeshave.

Appendix 3 Figure 4. Control tree wrapped to 3m with aluminum mesh to prevent MPB attack prior to sampling. Mesh was wrapped with Styrofoam and secured with duct tape and staples to ensure a tight seal. Middle sections were overlapped and secured with zip ties.

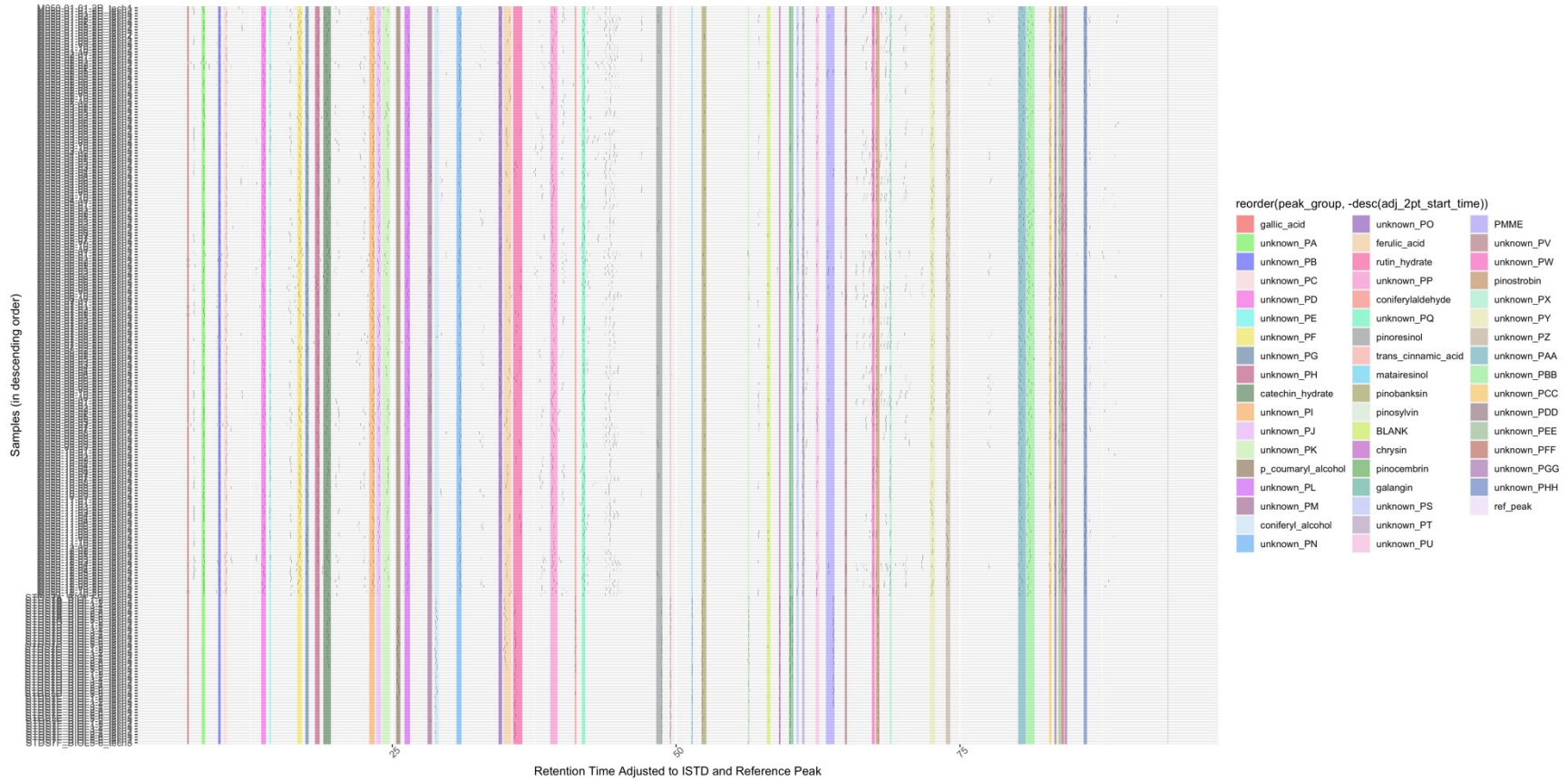

Appendix 3 Figure 5. Annotation of lodgepole pine phloem phenolic metabolite peaks and selection for NMDS. Black vertical dashes represent peaks detected at specific retention times (x-axis) for each sample (y-axis). Colored lines indicate peak assignment to a compound group, based on a range of retention times (i.e., the width of the colored line). Peak retention times were adjusted to imrove alignment across samples and to account for drift between runs. Retention time for peaks eluting before 55 min has been adjusted to the retention time of the internal standard (Rt_{sample}-Rt_{ISTD}); likewise, retention times for peaks eluting after 55 minutes has been adjusted to the retention time of a reference peak related to column loading (Rt_{sample}-Rt_{REF}). Peak groups were manually assigned based on the approximate alignment of a single peak across samples, without overlap with other groups, and based on the detection of

included peaks in most samples in at least one treatment (n = 6). Groups encompassing peaks of verified standards were named accordingly, while remaining groups were labeled “Unknown_P” denoting they came from phloem and assigned a unique letter. All labeled groups were included in NMDS analysis; peaks not included within the colored lines for the shown groups were omitted from analysis.

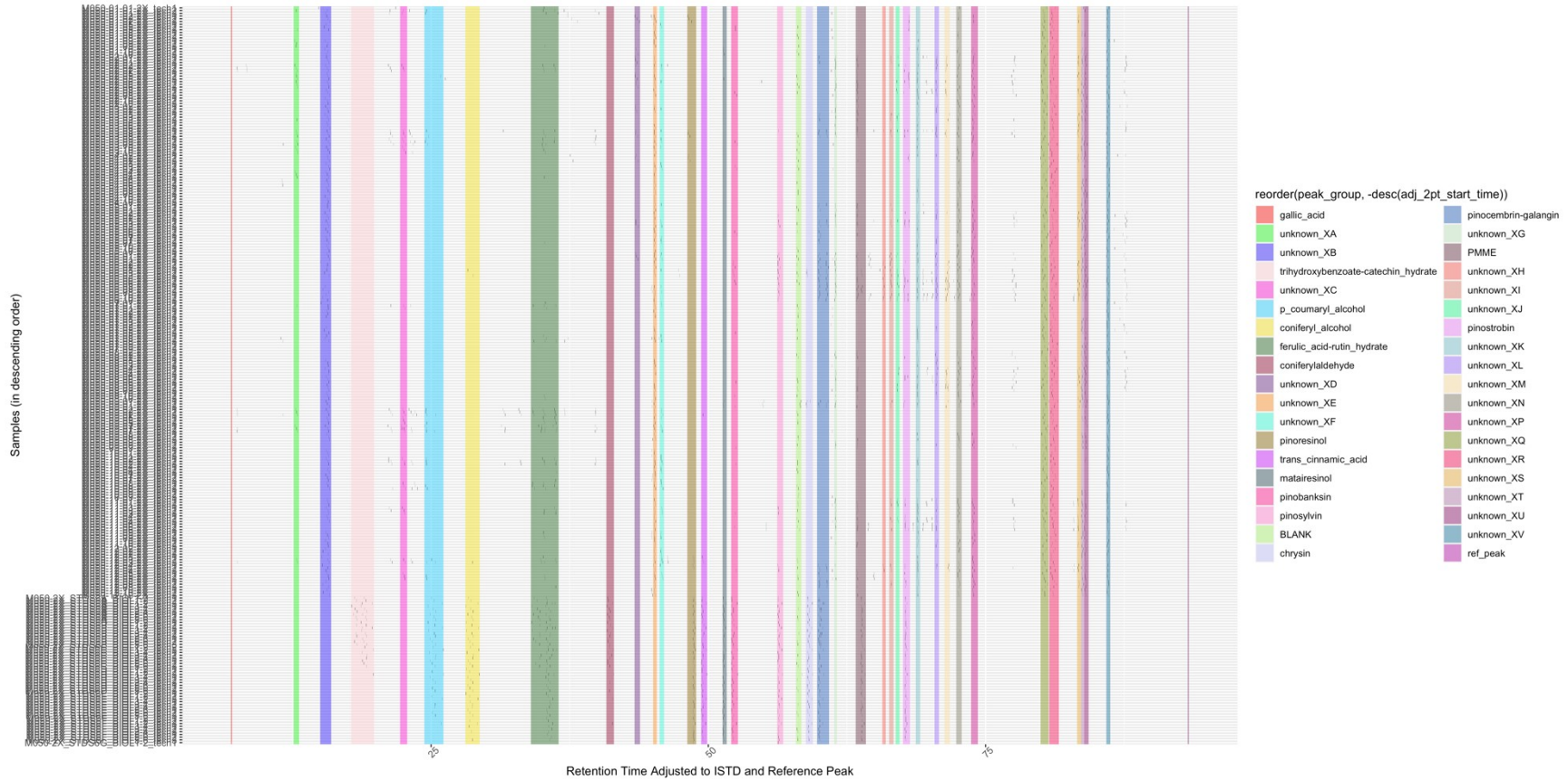

Appendix 3 Figure 6. Annotation of lodgepole pine xylem phenolic metabolite peaks and selection for NMDS. Black vertical dashes represent peaks detected at specific retention times (x-axis) for each sample (y-axis). Colored lines indicate peak assignment to a compound group, based on a range of retention times (i.e., the width of the colored line). Peak retention times were adjusted to imrove alignment across samples and to account for drift between runs. Retention time for peaks eluting before 55 min has been adjusted to the retention time of the internal standard (Rt_{sample}-Rt_{ISTD}); likewise, retention times for peaks eluting after 55 minutes has been adjusted to the retention time of a reference peak related to column loading (Rt_{sample}-Rt_{REF}). Peak groups were manually assigned based on the approximate alignment of a single peak across samples, without overlap with other groups, and based on the detection of

included peaks in most samples in at least one treatment (n = 6). Groups encompassing peaks of verified standards were named accordingly, while remaining groups were labeled “Unknown_X” denoting they came from xylem and assigned a unique letter. All labeled groups were included in NMDS analysis; peaks not included within the colored lines for the shown groups were omitted from analysis.

Appendix 3 Table 1. Forward and reverse primer sequences used in qRT-PCR analyses. Asterisks (*) indicate genes used for reference. Secondary phloem data was normalized to the arithmetic mean of *PcTIF5a*, *PcVHA-A*, and *PcUBA1* gene expression. Secondary xylem data was normalized to the arithmetic mean of *PcTIF5a*, *PcUBC11*, and *PcUBA1* gene expression.

Gene	Forward Primer 5'-3'	Reverse Primer 5'-3'
PcCHS	CGCAGGAATCAGAGTGAAATTAACCCG	CGGTCGTTTACATAATACCCCACCAAG
PcDFR1	CCTCATTACATGATACTGAGACAGGTA	GCCACTTGGACAATGGTAGCATC
PcDFR2	CGAAGGGAAGATACATCTCTTCTTCAG	GGATTCATCCACATCCTTGAACTCG
PcOMT1	CACCATTCTCCCTGTTGCTGC	CCCACCTCCTTAGCCAAATCTC
PcOMT2	TGTCCAAAGCCTAATAAGCTGTTGC	TACTGCATGATAACAACCCCAGC
PcSTS	TGGTGGGGCAAGCTCTGTTC	GCCTTCTCCACTTGAGGGATGG
*PcTIF5a**	CTGTGTGTAGCATTTGCCATTTT	CCCGCACAGGTACATTAAAATAGA
*PcUBA1**	TGCAAACCTAGCCCTTCCTC	ACCCATCGATCCCAGACAGA
*PcVHA-A**	TTGTACCAAGGCAGGCTCTC	GCTGTAGAAAGAGGAGCTGGT
*PcUBC11**	TCCATGCTCTTGCTGTCTCC	GTCCCGCACTGACAATCTCT

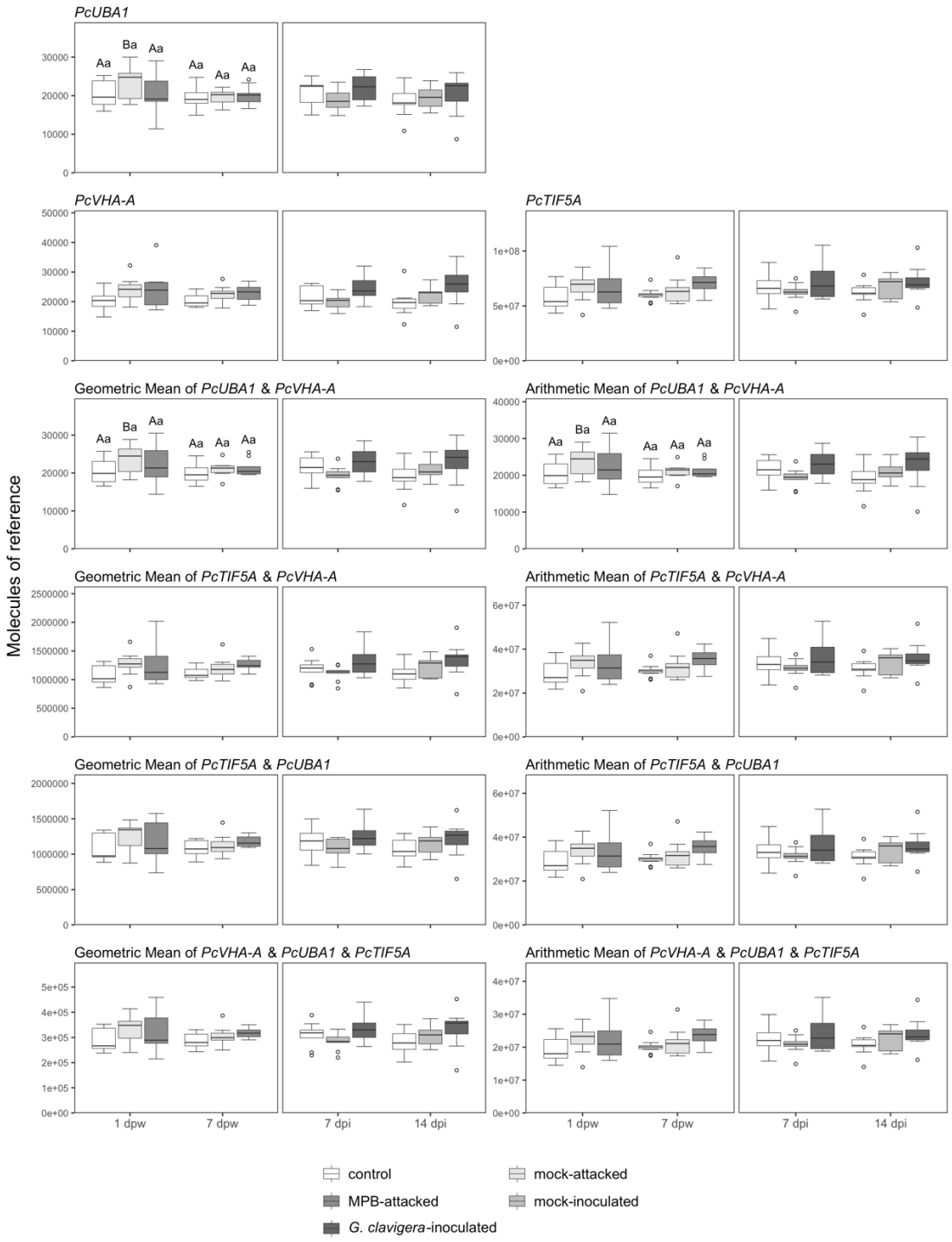

Appendix 3 Figure 7. qRT-PCR transcript profiles of reference genes in secondary phloem of lodgepole pine trees inoculated with *G. clavigera* or attacked by MPB. White, light grey, medium grey, and dark grey boxplots represent control, mock-wounded, *G. clavigera*-inoculated, and mountain pine beetle-attacked trees, respectively. Significant differences between estimated marginal means of treatment groups are indicated by letters (adjusted p-value < 0.05, n = 8-10).

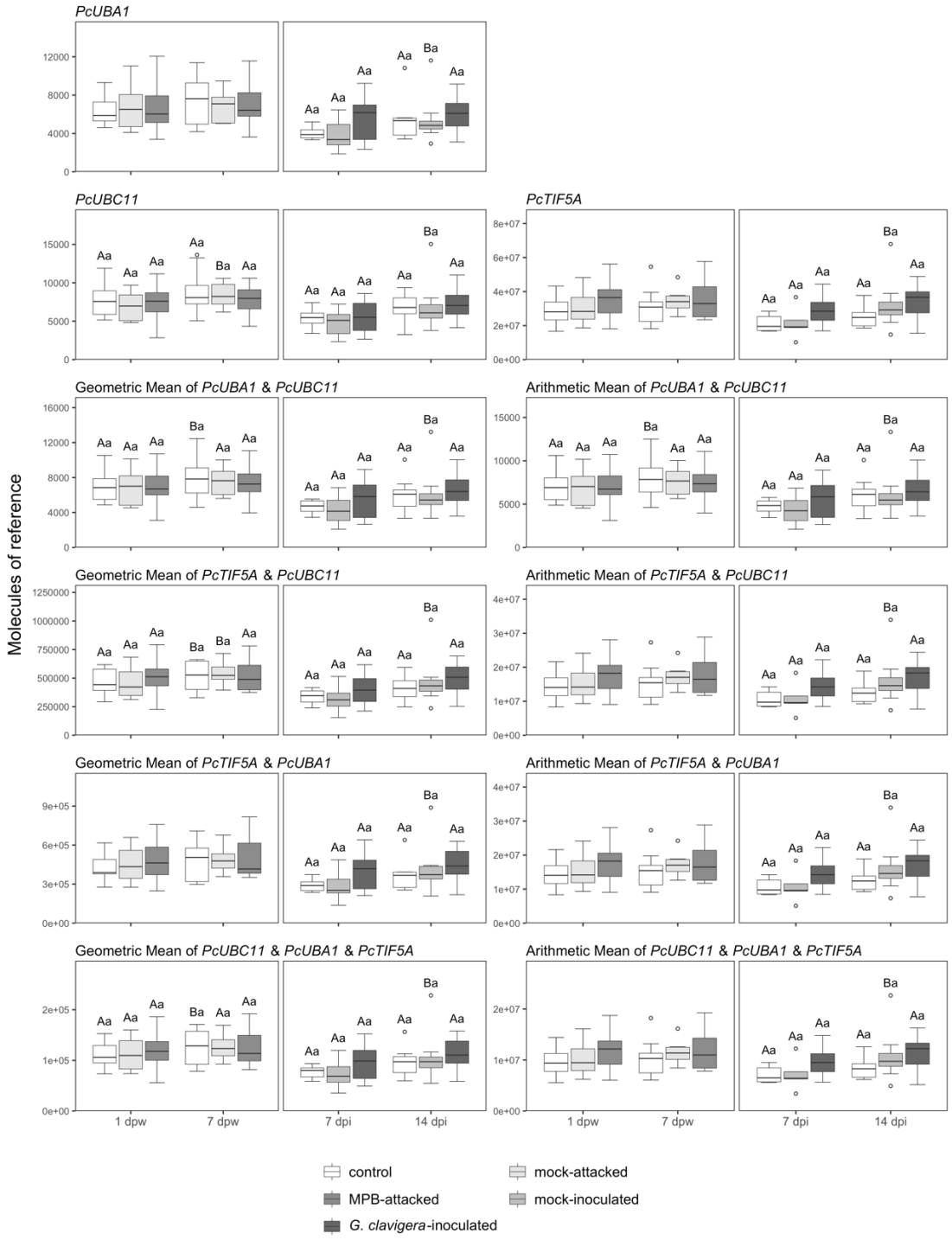

Appendix 3 Figure 8. qRT-PCR transcript profiles of reference genes in secondary xylem of lodgepole pine trees inoculated with *G. clavigera* or attacked by MPB. White, light grey, medium grey, and dark grey boxplots represent control, mock-wounded, *G. clavigera*-inoculated, and mountain pine beetle-attacked trees, respectively. Significant differences between estimated marginal means of treatment groups are indicated by letters (adjusted p-value < 0.05, n = 5-8).

Appendix 3 Table 2. Summary of analysis of deviance of generalized linear mixed models fit to phloem reference gene qRT-PCR expression data. Asterisks (*) indicate interactions between factors. All genes were fit to the following formula: transcript abundance ~ time point * treatment, family = Gamma (link = log).

	MPB attack			*G. clavigera* inoculation		
	df	χ^2	*p*	df	χ^2	*p*
PcUbiquitin-activating enzyme 1 (PcUBA1)						
treatment	2	1.23	5.41×10^{-1}	2	1.69	4.31×10^{-1}
time point	1	3.59	5.83×10^{-2}	1	1.56	2.12×10^{-1}
treatment * time point	2	4.04	1.32×10^{-1}	2	2.32	3.14×10^{-1}
PcEukaryotic translation initiation factor 5A-1 (PcTIF5A)						
treatment	2	2.10	3.50×10^{-1}	2	2.59	2.74×10^{-1}
time point	1	0.74	3.88×10^{-1}	1	1.06	3.03×10^{-1}
treatment * time point	2	2.56	2.79×10^{-1}	2	2.65	2.66×10^{-1}
PcVacuolar ATP synthase subunit A (PcVHA-A)						
treatment	2	3.63	1.63×10^{-1}	2	4.62	9.92×10^{-2}
time point	1	0.66	4.16×10^{-1}	1	0.06	8.02×10^{-1}
treatment * time point	2	0.60	7.40×10^{-1}	2	5.10	7.82×10^{-2}
Arithmetic Mean of PcUBA1 and PcVHA-A						
treatment	2	2.38	3.05×10^{-1}	2	3.39	1.84×10^{-1}
time point	1	2.29	1.30×10^{-1}	1	0.31	5.75×10^{-1}
treatment * time point	2	1.91	3.85×10^{-1}	2	3.47	1.76×10^{-1}
Arithmetic Mean of PcUBA1 and PcTIF5A						
treatment	2	2.10	3.50×10^{-1}	2	2.59	2.74×10^{-1}
time point	1	0.74	3.89×10^{-1}	1	1.06	3.04×10^{-1}
treatment * time point	2	2.56	2.78×10^{-1}	2	2.65	2.66×10^{-1}
Arithmetic Mean of PcTIF5a and PcVHA-A						
treatment	2	2.10	3.50×10^{-1}	2	2.59	2.74×10^{-1}
time point	1	0.74	3.89×10^{-1}	1	1.06	3.03×10^{-1}
treatment * time point	2	2.56	2.79×10^{-1}	2	2.65	2.66×10^{-1}

	MPB attack			*G. clavigera* inoculation		
	df	χ^2	*p*	df	χ^2	*p*
Geometric Mean of PcUBA1 and PcVHA-A						
treatment	2	2.31	3.15×10^{-1}	2	3.34	1.88×10^{-1}
time point	1	2.18	1.40×10^{-1}	1	0.37	5.44×10^{-1}
treatment * time point	2	2.08	3.54×10^{-1}	2	3.42	1.81×10^{-1}
Geometric Mean of PcUBA1 and PcTIF5A						
treatment	2	1.63	4.42×10^{-1}	2	2.29	3.18×10^{-1}
time point	1	0.34	5.60×10^{-1}	1	0.27	6.07×10^{-1}
treatment * time point	2	3.73	1.55×10^{-1}	2	3.08	2.14×10^{-1}
Geometric Mean of PcTIF5A and PcVHA-A						
treatment	2	3.23	1.99×10^{-1}	2	4.16	1.25×10^{-1}
time point	1	0.01	9.33×10^{-1}	1	0.36	5.47×10^{-1}
treatment * time point	2	1.35	5.08×10^{-1}	2	4.62	9.92×10^{-2}
Arithmetic Mean of PcTIF5a, PcVHA-A, and PcUBA1						
treatment	2	2.10	3.50×10^{-1}	2	2.59	2.73×10^{-1}
time point	1	0.74	3.89×10^{-1}	1	1.06	3.04×10^{-1}
treatment * time point	2	2.56	2.78×10^{-1}	2	2.65	2.66×10^{-1}
Geometric Mean of PcTIF5a, PcVHA-A, and PcUBA1						
treatment	2	2.52	2.83×10^{-1}	2	3.40	1.83×10^{-1}
time point	1	0.47	4.93×10^{-1}	1	0.06	7.99×10^{-1}
treatment * time point	2	2.41	3.00×10^{-1}	2	3.78	1.51×10^{-1}

Appendix 3 Table 3. Summary of analysis of deviance of generalized linear mixed models fit to xylem reference gene qRT-PCR expression data. Asterisks (*) indicate interactions between factors. All genes were fit to the following formula: transcript abundance ~ time point * treatment, family = Gamma (link = log).

	MPB attack			*G. clavigera* inoculation		
	df	χ^2	*p*	df	χ^2	*p*
PcUbiquitin-activating enzyme 1 (PcUBA1)						
treatment	2	0.13	9.37×10^{-1}	2	1.05	5.91×10^{-1}
time point	1	1.69	1.93×10^{-1}	1	6.36	$\mathbf{1.17 \times 10^{-2}}$
treatment * time point	2	2.22	3.29×10^{-1}	2	2.27	3.22×10^{-1}
PcEukaryotic translation initiation factor 5A-1 (PcTIF5A)						
treatment	2	1.82	4.02×10^{-1}	2	4.23	1.21×10^{-1}
time point	1	2.05	1.52×10^{-1}	1	6.13	$\mathbf{1.33 \times 10^{-2}}$
treatment * time point	2	5.15	7.63×10^{-2}	2	2.67	2.63×10^{-1}
PcUbiquitin-conjugating enzyme 11 (PcUBC11)						
treatment	2	0.02	9.88×10^{-1}	2	0.29	8.63×10^{-1}
time point	1	6.89	$\mathbf{8.69 \times 10^{-3}}$	1	12.79	$\mathbf{3.48 \times 10^{-4}}$
treatment * time point	2	1.85	3.97×10^{-1}	2	1.04	5.94×10^{-1}
Arithmetic Mean of PcUBA1 and PcUBC11						
treatment	2	0.02	9.92×10^{-1}	2	0.63	7.31×10^{-1}
time point	1	4.11	$\mathbf{4.26 \times 10^{-2}}$	1	9.45	$\mathbf{2.11 \times 10^{-3}}$
treatment * time point	2	2.01	3.66×10^{-1}	2	1.48	4.78×10^{-1}
Arithmetic Mean of PcUBA1 and PcTIF5A						
treatment	2	1.82	4.02×10^{-1}	2	4.23	1.21×10^{-1}
time point	1	2.05	1.52×10^{-1}	1	6.13	$\mathbf{1.33 \times 10^{-2}}$
treatment * time point	2	5.14	7.64×10^{-2}	2	2.67	2.63×10^{-1}
Arithmetic Mean of PcTIF5a and PcUBC11						
treatment	2	1.82	4.02×10^{-1}	2	4.23	1.21×10^{-1}
time point	1	2.05	1.52×10^{-1}	1	6.14	$\mathbf{1.32 \times 10^{-2}}$
treatment * time point	2	5.15	7.63×10^{-2}	2	2.67	2.63×10^{-1}

	MPB attack			*G. clavigera* inoculation		
	df	**χ^2**	***p***	**df**	**χ^2**	***p***
Geometric Mean of PcUBA1 and PcUBC11						
treatment	2	0.02	9.89×10^{-1}	2	0.65	7.22×10^{-1}
time point	1	4.01	$\mathbf{4.54 \times 10^{-2}}$	1	9.32	$\mathbf{2.26 \times 10^{-3}}$
treatment * time point	2	1.91	3.84×10^{-1}	2	1.50	4.71×10^{-1}
Geometric Mean of PcUBA1 and PcTIF5A						
treatment	2	0.79	6.73×10^{-1}	2	2.43	2.97×10^{-1}
time point	1	2.11	1.46×10^{-1}	1	6.52	$\mathbf{1.07 \times 10^{-2}}$
treatment * time point	2	3.31	1.91×10^{-1}	2	2.39	3.02×10^{-1}
Geometric Mean of PcTIF5A and PcUBC11						
treatment	2	0.44	8.02×10^{-1}	2	1.58	4.54×10^{-1}
time point	1	5.55	$\mathbf{1.85 \times 10^{-2}}$	1	9.19	$\mathbf{2.44 \times 10^{-3}}$
treatment * time point	2	4.40	1.11×10^{-1}	2	1.83	4.00×10^{-1}
Arithmetic Mean of PcTIF5a, PcUBC11, and PcUBA1						
treatment	2	1.82	4.02×10^{-1}	2	4.23	1.21×10^{-1}
time point	1	2.05	1.52×10^{-1}	1	6.14	$\mathbf{1.32 \times 10^{-2}}$
treatment * time point	2	5.14	7.64×10^{-2}	2	2.67	2.63×10^{-1}
Geometric Mean of PcTIF5a, PcUBC11, and PcUBA1						
treatment	2	0.32	8.50×10^{-1}	2	1.44	4.87×10^{-1}
time point	1	3.87	$\mathbf{4.93 \times 10^{-2}}$	1	8.34	$\mathbf{3.87 \times 10^{-3}}$
treatment * time point	2	3.09	2.13×10^{-1}	2	1.88	3.90×10^{-1}

Appendix 3 Table 4. Summary of analysis of deviance of generalized linear mixed models fit to phloem phenolic biosynthesis qRT-PCR expression data. Asterisks (*) indicate interactions between factors. All genes were fit to the following formula: normalized transcript abundance ~ time point * treatment, family = Gamma (link = log).

	MPB attack			*G. clavigera* inoculation		
	df	χ^2	*p*	df	χ^2	*p*
PcStilbene Synthase (PcSTS)						
treatment	2	3.89	1.43×10^{-1}	2	66.33	$\mathbf{3.95 \times 10^{-15}}$
time point	1	13.22	$\mathbf{2.77 \times 10^{-4}}$	1	0.56	4.54×10^{-1}
treatment * time point	2	9.37	$\mathbf{9.23 \times 10^{-3}}$	2	0.76	6.85×10^{-1}
PcDihydroflavonol Reductase 1 (PcDFR1)						
treatment	2	21.10	$\mathbf{2.62 \times 10^{-5}}$	2	95.51	$\mathbf{1.82 \times 10^{-21}}$
time point	1	14.46	$\mathbf{1.43 \times 10^{-4}}$	1	1.55	2.13×10^{-1}
treatment * time point	2	7.14	$\mathbf{2.82 \times 10^{-2}}$	2	5.75	5.64×10^{-2}
PcDihydroflavonol Reductase 2 (PcDFR2)						
treatment	2	24.11	$\mathbf{5.82 \times 10^{-6}}$	2	9.03	$\mathbf{1.10 \times 10^{-2}}$
time point	1	10.39	$\mathbf{1.27 \times 10^{-3}}$	1	0.95	3.30×10^{-1}
treatment * time point	2	7.81	$\mathbf{2.02 \times 10^{-2}}$	2	1.15	5.61×10^{-1}
PcStilbene o-Methyltransferase 1 (PcOMT1)						
treatment	2	38.50	$\mathbf{4.36 \times 10^{-9}}$	2	71.56	$\mathbf{2.89 \times 10^{-16}}$
time point	1	22.95	$\mathbf{1.66 \times 10^{-6}}$	1	0.10	7.51×10^{-1}
treatment * time point	2	25.99	$\mathbf{2.27 \times 10^{-6}}$	2	0.80	6.71×10^{-1}
PcStilbene o-Methyltransferase 2 (PcOMT2)						
treatment	2	4.34	1.14×10^{-1}	2	3.40	1.82×10^{-1}
time point	1	11.33	$\mathbf{7.62 \times 10^{-4}}$	1	2.78	9.56×10^{-2}
treatment * time point	2	10.97	$\mathbf{4.16 \times 10^{-3}}$	2	6.09	$\mathbf{4.76 \times 10^{-2}}$
PcChalcone Synthase (PcCHS)						
treatment	2	5.88	$\mathbf{5.28 \times 10^{-2}}$	2	13.21	$\mathbf{1.35 \times 10^{-3}}$
time point	1	3.80	$\mathbf{5.12 \times 10^{-2}}$	1	3.51	6.09×10^{-2}
treatment * time point	2	5.11	7.77×10^{-2}	2	6.13	$\mathbf{4.67 \times 10^{-2}}$

Appendix 3 Table 5. Summary of analysis of deviance of generalized linear mixed models fit to xylem phenolic biosynthesis qRT-PCR expression data. Asterisks (*) indicate interactions between factors. All genes were fit to the following formula: normalized transcript abundance ~ time point * treatment, family = Gamma (link = log).

	MPB attack			*G. clavigera* inoculation		
	df	χ^2	*p*	df	χ^2	*p*
PcStilbene Synthase (PcSTS)						
treatment	2	14.12	$\mathbf{8.60 \times 10^{-4}}$	2	159.84	$\mathbf{1.95 \times 10^{-35}}$
time point	1	95.85	$\mathbf{1.24 \times 10^{-22}}$	1	2.54	1.11×10^{-1}
treatment * time point	2	49.53	$\mathbf{1.75 \times 10^{-11}}$	2	12.27	$\mathbf{2.16 \times 10^{-3}}$
PcDihydroflavonol Reductase 1 (PcDFR1)						
treatment	2	3.75	1.53×10^{-1}	2	22.89	$\mathbf{1.07 \times 10^{-5}}$
time point	1	17.82	$\mathbf{2.43 \times 10^{-5}}$	1	8.56	$\mathbf{3.44 \times 10^{-3}}$
treatment * time point	2	9.47	$\mathbf{8.78 \times 10^{-3}}$	2	0.78	6.76×10^{-1}
PcDihydroflavonol Reductase 2 (PcDFR2)						
treatment	2	7.06	$\mathbf{2.93 \times 10^{-2}}$	2	25.74	$\mathbf{2.58 \times 10^{-6}}$
time point	1	3.16	7.53×10^{-2}	1	7.33	$\mathbf{6.80 \times 10^{-3}}$
treatment * time point	2	0.49	7.84×10^{-1}	2	2.94	2.30×10^{-1}
PcStilbene o-Methyltransferase 1 (PcOMT1)						
treatment	2	3.25	1.97×10^{-1}	2	8.84	$\mathbf{1.20 \times 10^{-2}}$
time point	1	2.67	1.02×10^{-1}	1	4.57	$\mathbf{3.25 \times 10^{-2}}$
treatment * time point	2	7.09	$\mathbf{2.89 \times 10^{-2}}$	2	10.58	$\mathbf{5.05 \times 10^{-3}}$
PcStilbene o-Methyltransferase 2 (PcOMT2)						
treatment	2	0.49	7.81×10^{-1}	2	0.69	7.07×10^{-1}
time point	1	2.57	1.09×10^{-1}	1	2.12	1.45×10^{-1}
treatment * time point	2	0.06	9.72×10^{-1}	2	4.47	1.07×10^{-1}
PcChalcone Synthase (PcCHS)						
treatment	2	3.28	1.94×10^{-1}	2	68.63	$\mathbf{1.25 \times 10^{-15}}$
time point	1	43.96	$\mathbf{3.36 \times 10^{-11}}$	1	13.75	$\mathbf{2.08 \times 10^{-4}}$
treatment * time point	2	11.81	$\mathbf{2.73 \times 10^{-3}}$	2	0.11	9.49×10^{-1}

Appendix 4

List of Figures and Tables

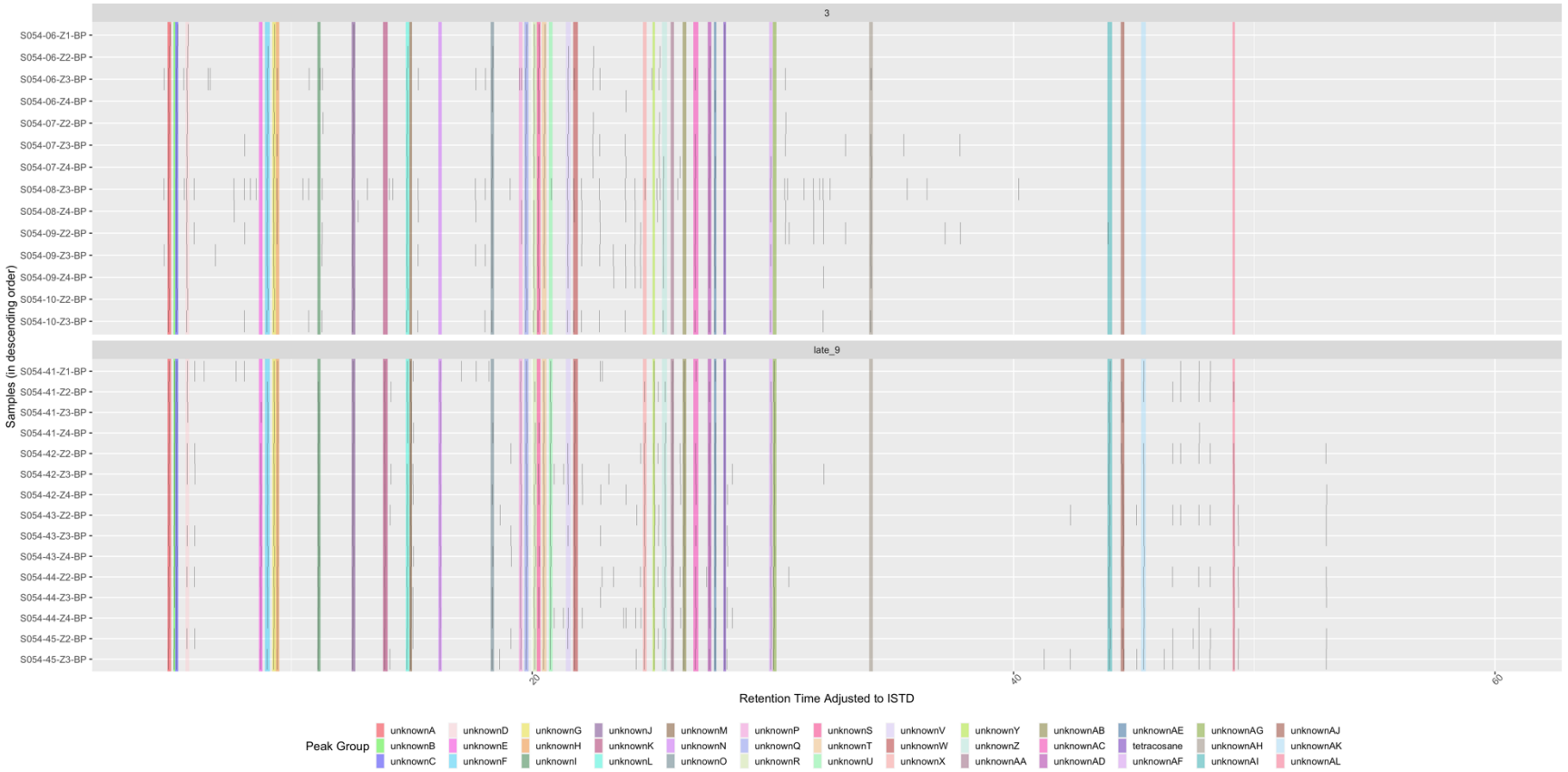

Appendix 4 Figure 1. Annotation of metabolite peaks from seedling wax extracts and selection for NMDS. Black vertical dashes represent peaks detected at specific retention times (x-axis) for each sample (y-axis), separated by bud burst stage (stages 3 and late 9). Colored lines indicate peak assignment to a compound group, based on a range of retention times (i.e. the width of the colored line). Peak retention times were adjusted to imrove alignment across samples and to account for drift between runs. Retention time for each peak has been adjusted to the retention time of the internal standard (Rt_{sample}-Rt_{ISTD}). Peak groups were manually assigned based on the approximate alignment of a single peak across samples, without overlap with other groups, and based on the detection of included peaks in most samples in at least one stage (n = 4). Groups were initially labeled “Unknown_” and assigned a unique letter, and then

MS identification was used to rename groups based on the compounds they included. All labeled groups shown here were included in NMDS analysis; peaks not included within the colored lines for the shown groups were omitted from analysis.

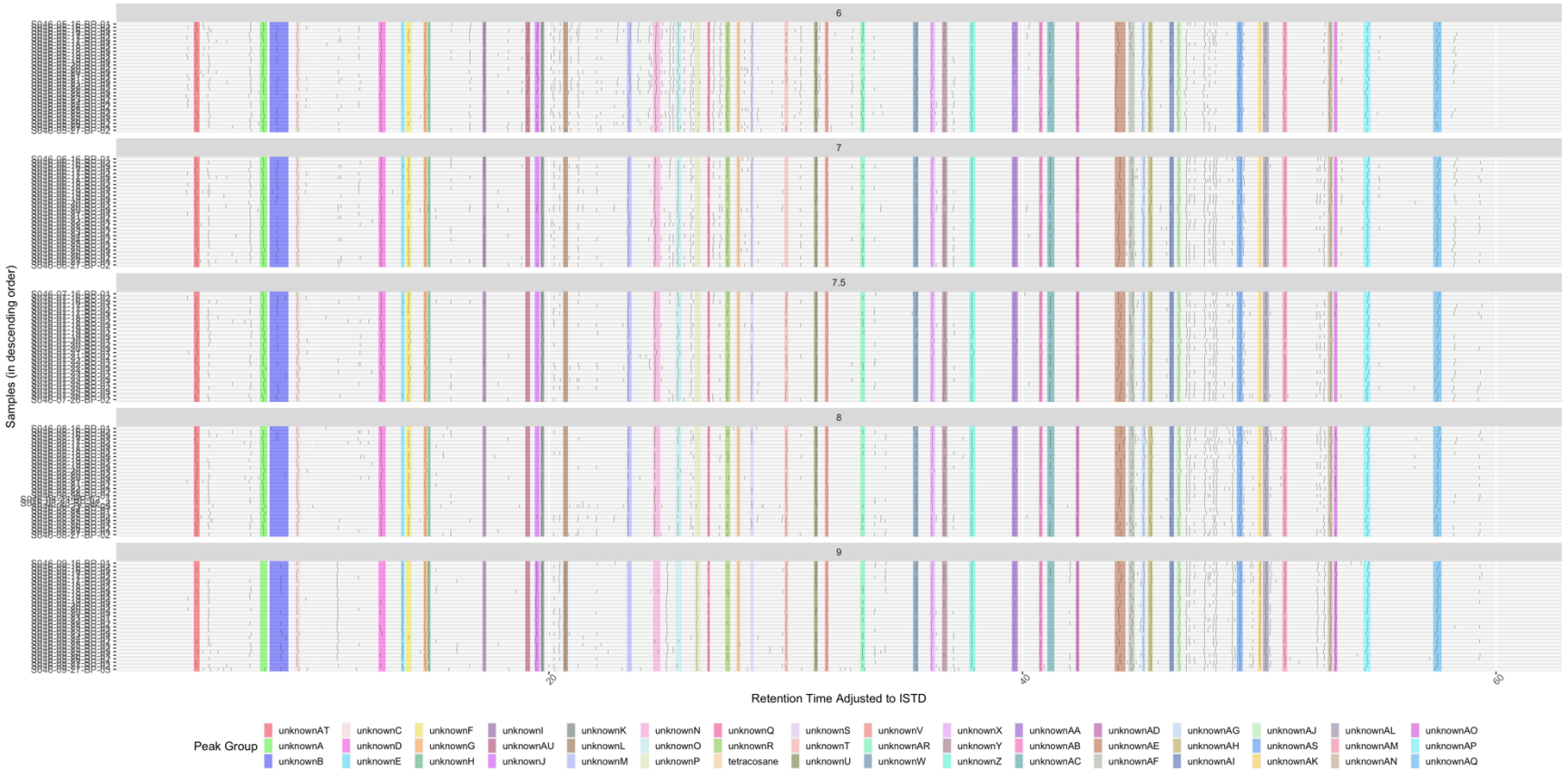

Appendix 4 Figure 2. Annotation of metabolite peaks from mature tree wax extracts and selection for NMDS. Black vertical dashes represent peaks detected at specific retention times (x-axis) for each sample (y-axis), separated by bud burst stage (stages 6 to 9). Colored lines indicate peak assignment to a compound group, based on a range of retention times (i.e. the width of the colored line). Peak retention times were adjusted to imrove alignment across samples and to account for drift between runs. Retention time for each peak has been adjusted to the retention time of the internal standard (Rt_{sample}-Rt_{ISTD}). Peak groups were manually assigned based on the approximate alignment of a single peak across samples, without overlap with other groups, and based on the detection of included peaks in most samples in at least one stage (n = 10-12). Groups were initially labeled “Unknown_” and assigned a unique

letter, and then MS identification was used to rename groups based on the compounds they included. All labeled groups shown here were included in NMDS analysis; peaks not included within the colored lines for the shown groups were omitted from analysis.

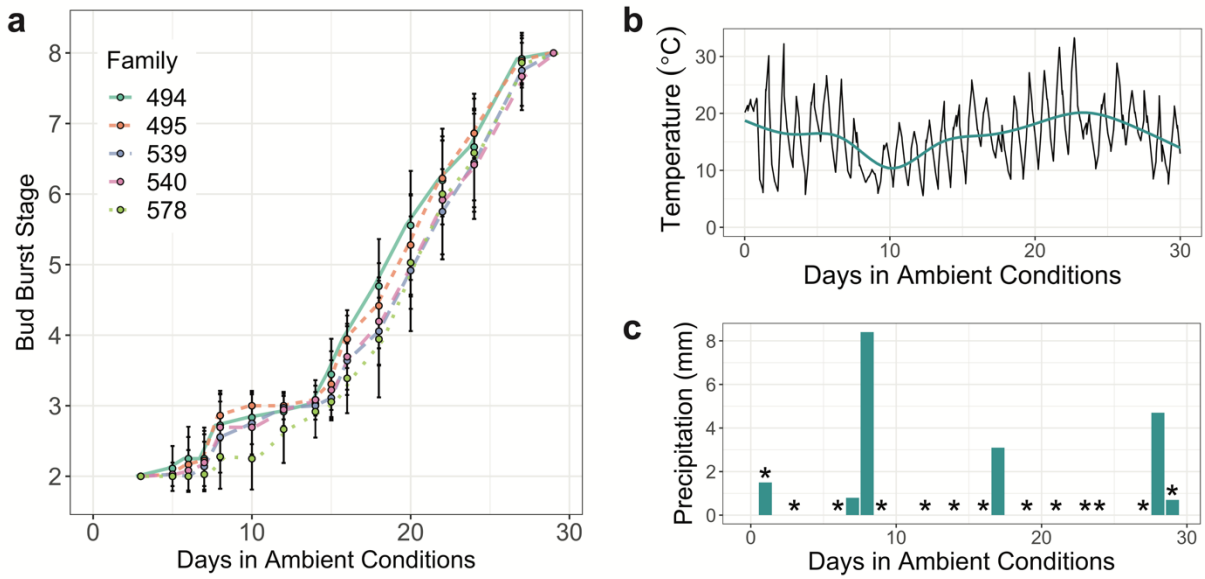

Appendix 4 Figure 3. Bud burst phenology of white spruce seedlings grown in ambient conditions at the University of Alberta in Edmonton, Alberta in May-June 2019. a Differences in bud burst phenology between seedling families under ambient (natural) conditions; points represent the mean bud burst stage ± standard deviation (n = 36). **b** Temperature profile during bud burst; blue line represents the average daily temperature. **(c)** Precipitation during bud burst (bar graph); asterisks indicate dates when trees were watered manually.

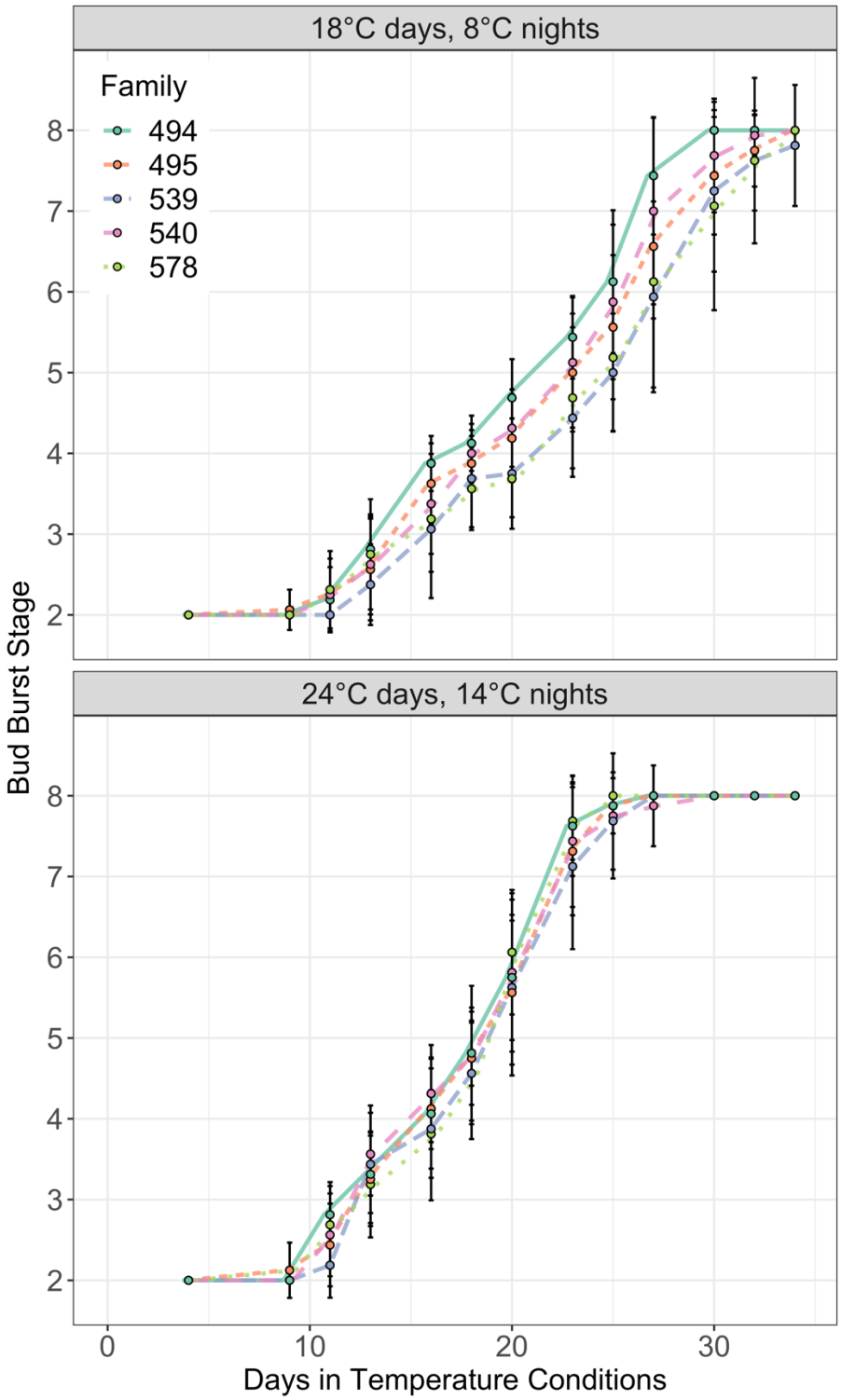

Appendix 4 Figure 4. Differences in bud burst phenology of seedlings across families grown under seasonally average conditions (18ºC days, 8ºC nights) compared to warmer conditions (24ºC days, 14ºC nights). Points represent the average bud burst stage ± standard deviation (n = 16).

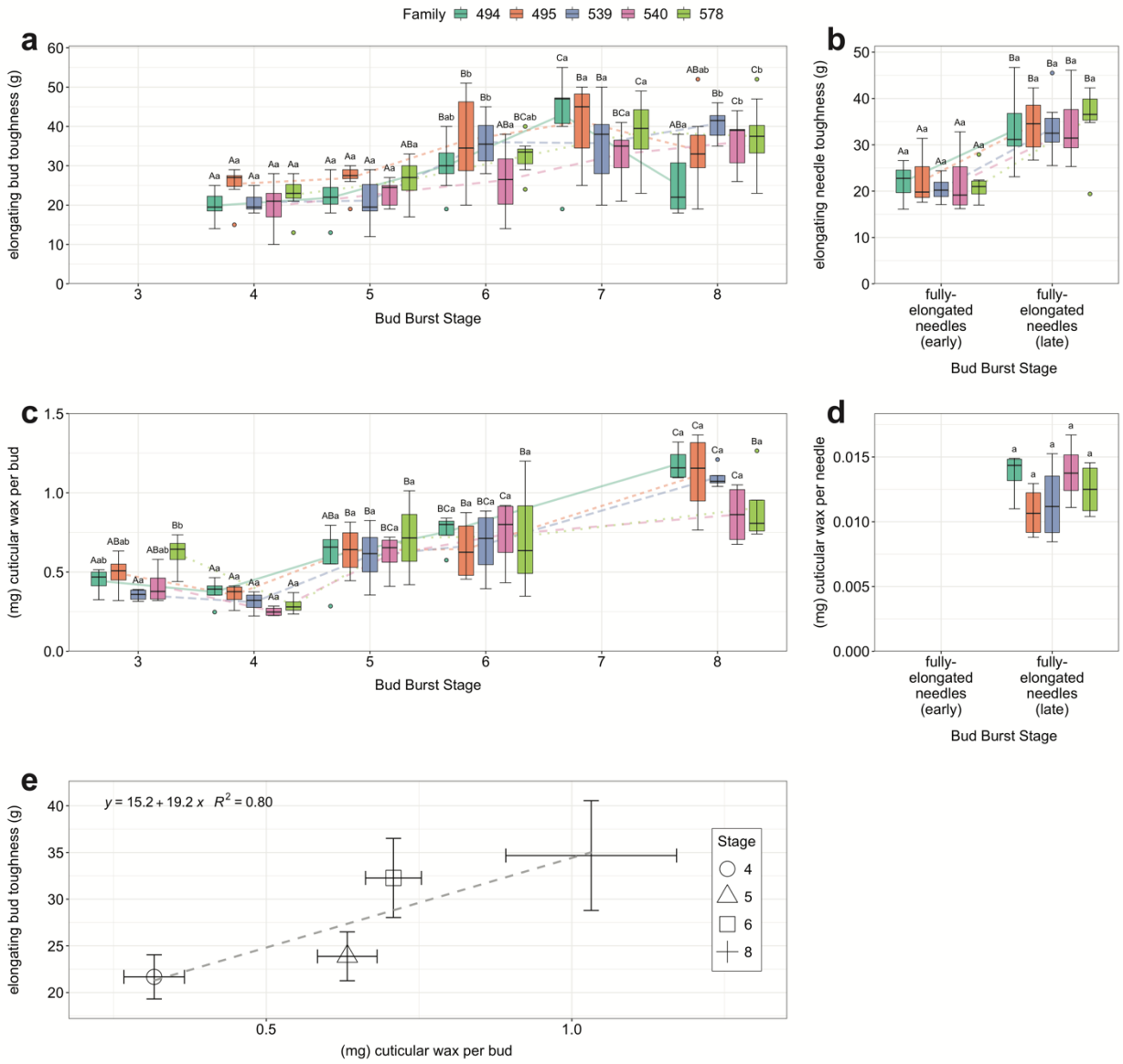

Appendix 4 Figure 5. Bud toughness and cuticular wax deposition during bud burst are positively correlated in seedlings in additional years of measurement. Measurements were taken during bud burst in 2019. **a,b** Toughness of **(a)** intact buds (n = 8) or **(b)** elongated needles (n = 8). **c,d** Cuticular wax extracted from **(c)** intact buds (n = 4) or **(d)** elongated needles (n = 4). For (**a-d)**, capitalized letters represent significant differences (Tukey-adjusted $p < 0.05$) between stages with a family, lower case letters represent differences within a stage between families. **e** Correlation of toughness and cuticular wax weights of intact buds across shared bud burst stages. Points represent the mean across families ± standard deviation (n= 20-40).

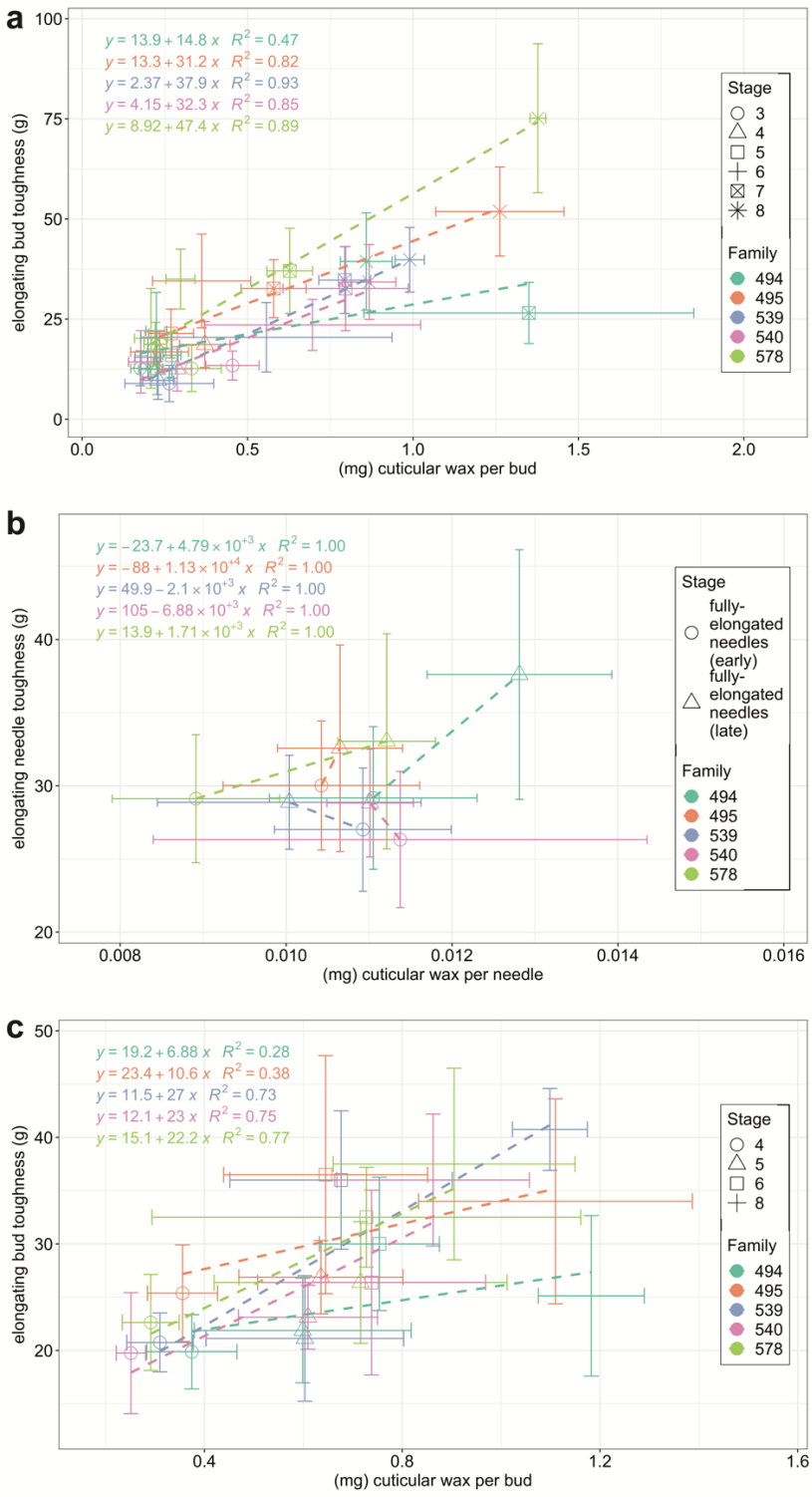

Appendix 4 Figure 6. Correlation of toughness and cuticular wax weights across shared bud burst stages by family for **(a)** intact buds of seedlings grown in 2020 (n = 4-8), **(b)** elongated needles of seedlings grown in 2020 (n = 4-8), or **(c)** intact buds of seedlings grown in 2019 (n = 4-8). Points represent the mean within a family ± standard deviation.

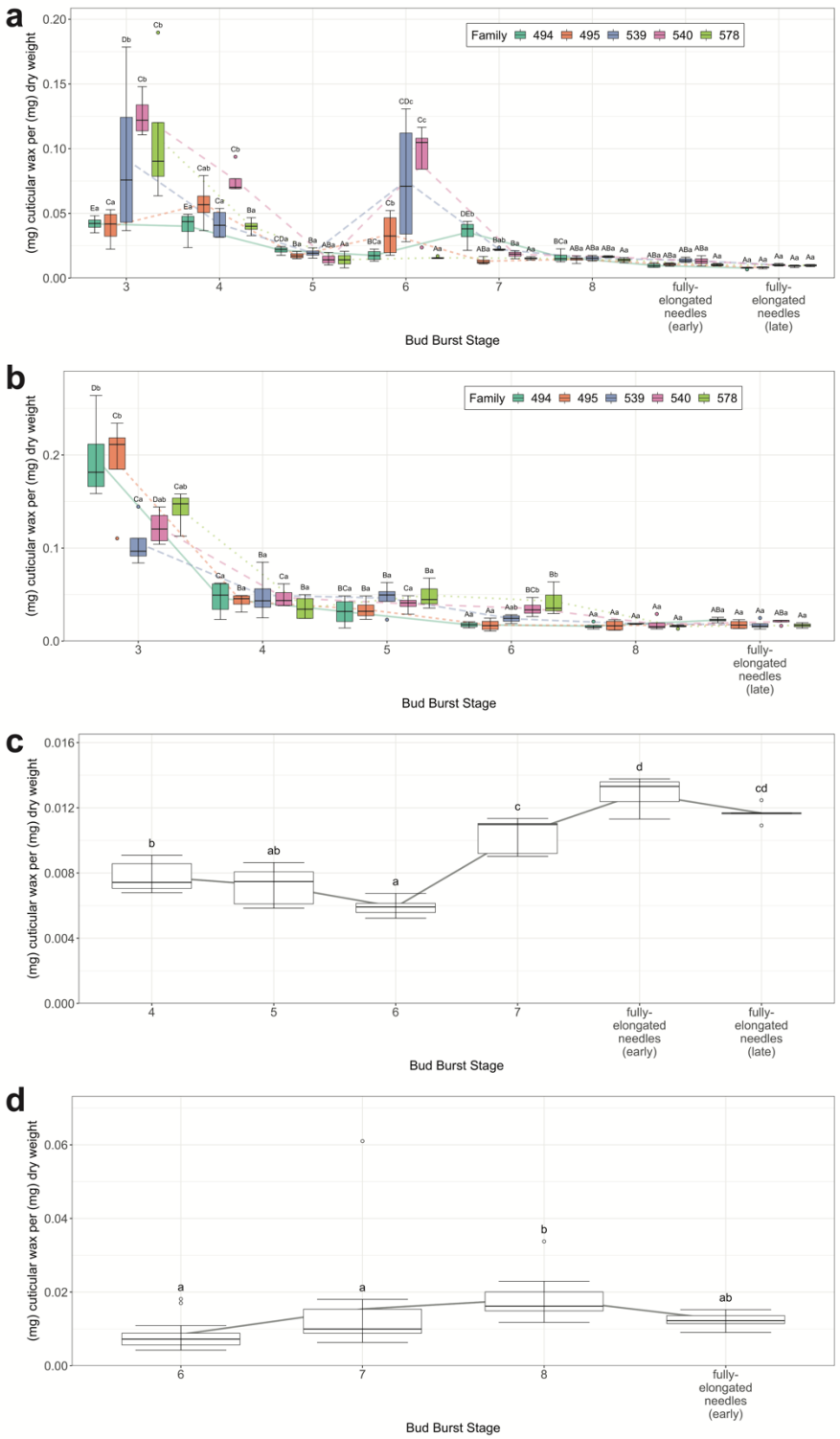

Appendix 4 Figure 7. Changes in cuticular wax extracts of buds relative to tissue dry weight over bud burst. a,b Cuticular wax of seedling apical buds and elongated needles in **(a)** 2020 (n = 4) and **(b)** 2019 (n = 4). For seedlings **(a,b)**, upper case letters represent significant

differences (Tukey-adjusted $p < 0.05$) between stages within families, lower case letters represent differences within a stage between families. **c,d** Cuticular wax of buds and elongated needles from lateral branches of mature trees in **(c)** 2020 (n = 5) and **(d)** 2017 (n = 10-12). For mature trees **(c,d)**, letters denote significant differences between stages (Tukey-adjusted $p < 0.05$).